IDENTIFICATION OF BIOACTIVE MOLECULES IN THE CONTROL OF FLOWERING TIME

Author:

Jesús Praena Tamayo

Supervisors:

Reyes Benlloch Ortiz

Francisco Madueño Albi

UNIVERSITAT POLITÈCNICA DE VALÈNCIA

Valencia, Spain

June 2022

Agradecimientos / Acknowledgments

La ciencia, si algo tiene que me gusta, es su indudable parte colaborativa. Esta tesis lleva muchos nombres de aquellos que han participado de una manera directa o indirectamente. En especial, hay un grupo de personas esenciales quienes han sido mis guías en el laberinto científico en lo que supone plantearse una pregunta y ser capaz de formular respuestas adecuadas. Gracias por la oportunidad y la fe que habéis puesto en mí.

Durante aquellas clases del máster en las que ese profesor simpático hizo que me interesara por otras ramas de la biotecnología vegetal y que desde que empecé la tesis ha estado siempre disponible para discutir, hipotetizar, celebrar pequeñas alegrías y por plantearme otros puntos de vista a mis hipótesis. Gracias, Paco.

Por toda mi formación y abrirme un mundo de posibilidades, por descubrirme nuevas áreas de la biología molecular, enseñarme a trabajar en el laboratorio y dar juntos mis primeros pasos en la ciencia, animarme a no conformarme e intentar mejorar, por saber escuchar cuando lo he necesitado y por confiar en mí. Gracias, Reyes.

A todos mis compañeros del laboratorio 1.07 y 1.09. Todos vosotros habéis participado en el día a día y año tras año, habéis hecho que tengamos un ambiente excelente en el que hemos disfrutado el tiempo juntos y que trabajar sea muy fácil. Es un lujo contar con compañeros como vosotros. Especialmente a Cristina por toda la ayuda, asesoramiento, consejos y la inspiradora pasión que transmite al discutir proyectos o ideas. Gracias.

A special thanks to Thomas for hosting me in his lab. He was very welcoming with his kindness, humility and closeness with which he treated me from day one, and without his support during and after my research stay, this work would have been very different. I also thank Ilara for her patience, constant support and willingness to help me wherever I needed it. From her I have received more of a friendship than a collaborator.

A mi familia, por el continuo apoyo durante toda mi vida. A Mar, por ser un ancla en la tormenta, enseñarme y compartir el mismo sendero. A Simba y Pumba, mis compañeros de vida perruna, quienes con un paseo me quitaban todas las preocupaciones.

Sois muchos y lo siento si olvido algún nombre: Ana B, Majo, Marcos, Rick, Marina, Rubén, Anamarija, Jorge H, Josito, Zeta, Jorge L, Ana A, Ludo, Vicente, Edu, Paz, Carol, Irene, Mari Ángeles, Vero, Clara, Pepe, Antoñele, Carmen, Alfredo, Fran, Ricardo, Pablo, Joan… a todos, esta tesis es también vuestra. Gracias.

Abstract

Flowering time is one of the most important traits affecting crop productivity and yield. The identification of natural or synthetic bioactive compounds for the control of flowering induction is of great interest. The identification of compounds with the potential to regulate flowering could allow us to fine-tune flowering responses in crops and adapt them to the changing environmental conditions. To identify these compounds, we have taken two different approaches: a chemical genetic screening and the characterization of the metabolome of floral transition.

First, we performed a chemical genetic screening to identify small molecules that have the potential to control the expression of the florigen *FLOWERING LOCUS T* (*FT*) or FT activity or signaling in Arabidopsis. We used transgenic plants expressing the β-*GLUCURONIDASE* gene (*GUS*) under the control of the *FT* promoter to test a preselected library of 360 molecules. Positive hits were retested by a secondary screening based on the expression of the *LUCIFERASE* (*LUC*) reporter gene under the control of the *FT* promoter. Using this approach, we have identified one molecule that successfully induces flowering under *in vitro* culture conditions.

Secondly, we have characterized the function of pipecolic acid (Pip), a molecule previously identified as a candidate to regulate flowering time. We have confirmed that mutations in enzymes responsible for Pip biosynthesis display an altered flowering response. A new role for Pip in rosette growth is also revealed in this work.

Finally, we used an inducible system based on the promoter of *CONSTANS* (*CO*) driving the expression of *CO* fused to the rat glucocorticoid receptor (*CO::GR*). Such a construction provides a tool to induce flowering with a single dexamethasone treatment. We then performed a comprehensive metabolomic study of the shoot apex and leaf samples that included targeted metabolomics, lipidomics, hormone quantification, and transcriptomics. Integration of these *omic* datasets has allowed us to point out metabolic pathways that are altered during floral induction. Characterization of loss-of-function mutants coding key enzymes of those metabolic pathways revealed that some of these mutants showed a flowering time phenotype. Among them, we focused on the characterization of the contribution of the raffinose metabolism, a storage oligosaccharide, to the determination of flowering time. Mutants affecting *RAFFINOSE SYNTHASE 5* (*RS5*) exhibit an early flowering phenotype and reduced fertility. We

propose a model in which the balance between simple and storage carbohydrates in the apex changes during floral induction. This change could be modulated by ABA and flowering-related genes, and it triggers changes in trehalose metabolism, promoting flowering by an early *FT* upregulation.

Resumen

El tiempo de floración es uno de los caracteres más importantes que influyen en la productividad y el rendimiento de los cultivos. La identificación de compuestos sintéticos que sean bioactivos en el control de la inducción floral es de gran interés. Su identificación podría permitirnos ajustar el tiempo de floración en los cultivos, adaptándolos a las condiciones ambientales más favorables. Para identificar estos compuestos, hemos tomado dos enfoques diferentes: un cribado genético químico y la caracterización del metaboloma de transición floral.

En primer lugar, realizamos un rastreo de genética química para identificar moléculas pequeñas que tengan el potencial de controlar la expresión del florígeno, *FLOWERING LOCUS* T (*FT*) o la actividad o señalización de FT en Arabidopsis. Para ello, hemos utilizado plantas transgénicas que expresan el gen *β-GLUCURONIDASE* (*GUS*) bajo el control del promotor *FT* para probar una librería de 360 moléculas preseleccionadas. Los resultados positivos obtenidos se volvieron a analizar mediante un cribado secundario basado en la expresión del gen reportero *LUCIFERASE* (*LUC*) bajo el control del promotor *FT*. Utilizando este enfoque, hemos identificado una molécula que induce con éxito la floración en condiciones de cultivo *in vitro*.

En segundo lugar, hemos caracterizado la función del ácido pipecólico (Pip), una molécula previamente identificada como candidata a regular la floración. Hemos confirmado que las mutaciones en las enzimas responsables de la biosíntesis de Pip muestran una alteración en la respuesta del tiempo de floración. Además, hemos identificado un nuevo papel del Pip relacionado con el crecimiento y el tamaño de la roseta de Arabidopsis.

Finalmente, utilizamos un sistema inducible basado en el promotor de *CONSTANS* (*CO*) que controla la expresión del gen endógeno de *CO* fusionado con el receptor de glucocorticoides de rata (*CO::GR*). De manera que con un solo tratamiento con dexametasona podemos inducir la floración. Con este sistema, realizamos un estudio del metaboloma de muestras de ápices y hojas mediante técnicas de metabolómica dirigida, lipidómica, cuantificación hormonal y transcriptómica. La integración de estos conjuntos de datos ómicos nos ha permitido identificar rutas metabólicas que se encuentran alteradas durante la transición floral. A su vez, la caracterización de mutantes de pérdida de función que codifican enzimas clave de esas vías metabólicas, reveló que algunos de

estos mutantes mostraban un fenotipo afectado para el tiempo de floración. Entre ellos, nos enfocamos en la caracterización de los genes relacionados con el metabolismo de la rafinosa, un oligosacárido de reserva. Mutantes afectados en el gen *RAFFINOSE SYNTHASE 5* (*RS5*) presentan un fenotipo de floración temprana y fertilidad reducida. En base a los resultados obtenidos, proponemos un modelo en el que, durante la transición floral, se produce una reestructuración de las ratios entre carbohidratos sencillos (monosacáridos y disacáridos) y de reserva, como la rafinosa. Estos cambios podrían ser modulados por el ácido abscísico (ABA) y por genes relacionados con la floración, desencadenando cambios en el metabolismo de la trehalosa y promoviendo una expresión temprana de *FT*.

Resum

El temps de floració és un dels caràcters amb més influència en la productivitat i el rendiment dels cultius. La identificació de compostos sintètics bioactius per al control de la inducció floral és de gran interés, ja que la seua identificació podria permetre ajustar el temps de floració dels cultius, aspecte que podria contribuir a l'adaptació a condicions ambientals més favorables. Per a identificar aquests compostos, hem portat a terme dues aproximacions diferents: un garbellat genètic químic i la caracterització del metaboloma de la transició floral.

En primer lloc, hem realitzat un cribratge genètic-químicper a identificar xicotetes molècules amb potencial per a controlar l'expressió del florígen, *FLOWERING LOCUS T* (*FT*) o l'activitat o la senyalització de FT a Arabidopsis. Per a portar a terme aquest cribratge, hem utilitzat plantes transgèniques que expressen el gen *β-GLUCURONIDASE* (*GUS*) sota el control del promotor de *FT* amb les quals hem assajat una llibreria de 360 molècules preseleccionades de manera prèvia. Els resultats positius obtinguts en aquest cribratge t s'han sotmés a un cribratge secundari basat en l'expressió del gen reporter *LUCIFERASE* (*LUC*) sota el control del promotor *FT*. La utilització d'aquesta primera aproximació ha permés la idenfiticació d'una molècula que indueix amb èxit la floració en condicions de cultiu in vitro.

En En segon lloc, hem caracteritzat la funció de l'àcid pipecòlic (Pip), una molècula prèviament identificada com a candidata a regular la floració. Aquesta aproximació ens ha permet confirmar que mutacions als enzims responsables de la biosíntesi de Pip comporten una alteració al temps de floració. A més, en aquest treball hem identificat un nou paper del Pip relacionat amb el creixement i la grandària de la roseta d'Arabidopsis.

Finalment, hem utilitzat un sistema induïble basat en el promotor de *CONSTANS* (*CO*) que controla l'expressió del gen endogen de *CO* fusionat al receptor de glucocorticoides de rata (*CO::GR*). Aquesta construcció ens proporciona una ferramenta amb la qual induir la floració amb un sol tractament amb dexametasona. A continuació, hem realitzat un estudi del metaboloma de mostres d'àpexs i fulles mitjançant tècniques de metabolòmica dirigida, lipidómica, quantificació hormonal i transcriptòmica. La integració d'aquest conjunt de dades ómiques ens ha permés identificar les rutes metabòliques que es troben alterades durant la transició floral. Al mateix temps, la caracterització de mutants de pèrdua de funció que codifiquen enzims clau per a aquestes rutes metabòliques, ha revelat

que alguns d'aquests mutants mostren un fenotip afectat pel que fa al temps de floració. Dintre dels mutants analitzats, ens hem centrat en la caracterització dels gens relacionats amb el metabolisme de la rafinosa, un oligosacàrid de reserva. Els mutants del gen *RAFFINOSE SYNTHASE 5* (*RS5*) presenten un fenotip de floració primerenca i fertilitat reduïda. Sobre la base dels resultats obtinguts, proposem un model en el qual, durant la transició floral, es produeix una reestructuració de les ràtios entre carbohidrats senzills (monosacàrids i disacàrids) i de reserva, com la rafinosa. Aquests canvis podrien ser modulats per l'àcid abscísic (ABA) i per gens relacionats amb la floració, i desencadenariencanvis al metabolisme de la trehalosa, així com la generació de l'expressió primerenca de *FT*.

Hypotheses and goals

The main goal of this thesis is to identify novel components of the genetic network controlling flowering time or novel mechanisms in which known factors of this network are regulated. To reach that objective we performed a screening to isolate bioactive molecules with the potential to regulate flowering. Alternatively, we characterize metabolic changes associated with floral induction by an integrative omic approach.

The specific objectives of the dissertation are:

1. Isolate small molecules that have the potential to control flowering time by means of a chemical genetic screening using the model plant *Arabidopsis thaliana.* To do so, we aim to identify molecules that alter the expression pattern of the florigen (*FT*).

2. Evaluate the potential of Pip as a candidate to control flowering time.

3. Identify endogenous metabolites that contribute to the control of flowering time and characterize their mechanisms of action. To this end, an analysis of the metabolome and transcriptome of plant apices and leaves during floral transition was performed.

INDEX

INTRODUCTION

MATHERIAL AND METHODS

RESULTS

Chapter 1: The search for new candidates to regulate flowering time by chemical genetics.

Chapter 2: Effect of Pipecolic acid on plant development.

Chapter 3: A multi-omics approach to decipher the metabolic changes during the floral transition in Arabidopsis.

INTRODUCTION

1. The use of *Arabidopsis thaliana* as a model to study complex biological processes.

From all species of flowering plants, *Arabidopsis thaliana* (from now on Arabidopsis) has been thoroughly studied and used as a model species during the last two decades. Arabidopsis show characteristic that make it a good model organism, such as short generation time (7 weeks), its small genome size, its small size that reduces the requirements in term of growth facilities, ease of crossing, high seed production, self-pollination and the availability of stablished protocols for mutant generation and screening, using different methodologies from classical chemical mutagenesis to more recent gene editing techniques (Miki et al., 2021; Woodward & Bartel, 2018). Arabidopsis belongs to the Brasicaceae, a family of annual herbaceous dicotyledonous plants native to Europe, Northwest Africa and Central Asia (Nordborg & Weigel, 2008). Currently, it is distributed worldwide, with a large number of described natural accessions. This wide distribution of the genus is responsible for observed differences in its life cycle, which are due to genetic variations (Koornneef et al., 2004). This variability affects important traits like flowering time and seed dormancy, which are crucial to determine the timing and length of its natural life cycle (Pigliucci, 2002). This genetic diversity has been often exploited to uncover complex gene networks controlling the plant responses to changes in its environment and the evolution of morphological traits (Carneiro et al., 2015).

The shape of a plant depends on the activity and identity of its meristems, small groups of undifferentiated totipotent cells. Shoot meristems are responsible for the formation of all the aerial organs of the plant, and their growth activity, whether determined or undetermined, defines the architecture of the plant. In the case of crops, plant architecture will in tur determine their productivity (McGarry & Ayre, 2012). All organs from the aerial part of a plant originate from different meristems responsible for the formation of the main axis or stem (apical meristems) and the lateral axes or branches (axillary meristems) (Périlleux et al., 2019). During their life cycle, plants go through different developmental stages. After the initial germination and seedling establishment, the plant develops through a phase of vegetative growth. This stage is again divided into two phases, an initial juvenile phase in which the plant is not capable of flowering and is characterized by the production of vegetative organs, followed by an adult phase in which

the plant maintains its vegetative state but is already capable of responding to the signals that trigger flowering. When endogenous and exogenous conditions are appropriate, the transition from the vegetative phase to the reproductive phase occurs, known as the floral transition, in which the plant stops producing vegetative organs and starts producing flowers (Bäurle & Dean, 2006).

In Arabidopsis, the shoot apical meristem (SAM) during the vegetative phase forms leaf primordia on its flanks, with the stem barely elongating to form a rosette. The duration of this phase is variable and depends on several factors, such as genetic background and environmental conditions, especially temperature and photoperiod (Huijser & Schmid, 2011). The vegetative juvenile phase is characterized by the production of round, smooth leaves without trichomes in the abaxial part, compared to the adult vegetative phase, in which the leaves are elongated and toothed and have trichomes on both sides (Fouracre & Poethig, 2019). After the transition to flowering, the apical meristem becomes a flower-forming meristem, producing floral meristems on its flanks that give rise to flowers.

Arabidopsis was the first plant whose genome was sequenced entirely (The Arabidopsis Genome Initiative, 2000). Together with its previously mentioned characteristics as a model species, this fact explains why Arabidopsis has been widely used in biological and physiological approaches to understand fundamental questions dealing with plant growth, signaling and development (Miki et al., 2021). With the development of modern omic technologies that allow the characterization of global changes in protein (proteomics), genome sequence or gene expression (genomics/transcriptomics) or metabolite abundance (metabolomics), characterization of complex responses has become affordable in plant-like Arabidopsis, where a good amount of molecular tools are also available. Because of the canonical relationship between genes, transcripts, and proteins, these omic technologies are inherently complementary and allow for the detection and identification of many molecules expressed in different organisms (Myrold & Nannipieri, 2013). The combination of different omics approaches can be used to analyze biological processes in a highly complex context where reductionist approaches do not provide sufficient information by measuring DNA, RNA, proteins, peptides, lipids, and metabolites under the same conditions.

2. Genetic control of flowering

One of the most critical moments for the plant is the transition from the vegetative phase to the reproductive phase. In Arabidopsis, this transition is a fundamental and irreversible developmental event (Tessadori et al., 2007). Therefore, choosing the ideal time for flowering is one of the most critical decisions in the life cycle of plants since their correct adaptation to the environment and their reproductive success depend on it (Andrés & Coupland, 2012; Song et al., 2013). To determine the optimal time for flowering, plants have evolved various mechanisms to integrate environmental and endogenous signals. A tightly regulated genetic network ensures that this integration trigger floral transition under optimal conditions. Genes acting in that network have been classified over time in different pathways, depending on the signals they perceive and transduce. In this way, we can talk about the photoperiod pathway, the temperature pathway, hormonal pathways, the autonomous pathway, and finally the age and sugar pathways. Broadly, can classify those pathways in three major categories. The first includes those regulated by light, integrating information on light quality, intensity and length (Thomas, 2006). Secondly, we have those pathways involved in integrating temperature cues, differentiating between exposure to cold (vernalization) and fluctuation in ambient temperatures (Susila et al., 2018). Finally, we have several pathways that integrate different types of endogenous signals: hormones (gibberellins, brassinosteroids, salicylic acid, abscisic acid, ethylene, jasmonic acid, cytokinins and auxins) (Davis, 2009), age (Wang, 2014), the carbohydrate status (Cho et al., 2018) and autonomous signals (Cheng et al., 2017).

The information from the different pathways is collected by a group of genes and converges in the so-called integrating genes, such as *FLOWERING LOCUS T* (*FT*) in the leaf and *SUPPRESSOR OF OVEEXPRESSION OF CO 1* (*SOC1*) in the apex. These genes are responsible for controlling the expression of the flower meristem identity genes (Parcy, 2005). An overview of the main pathways involved in flowering time is in Figure I-1, and in the following sections, I will describe the pathways that are most relevant to the present work.

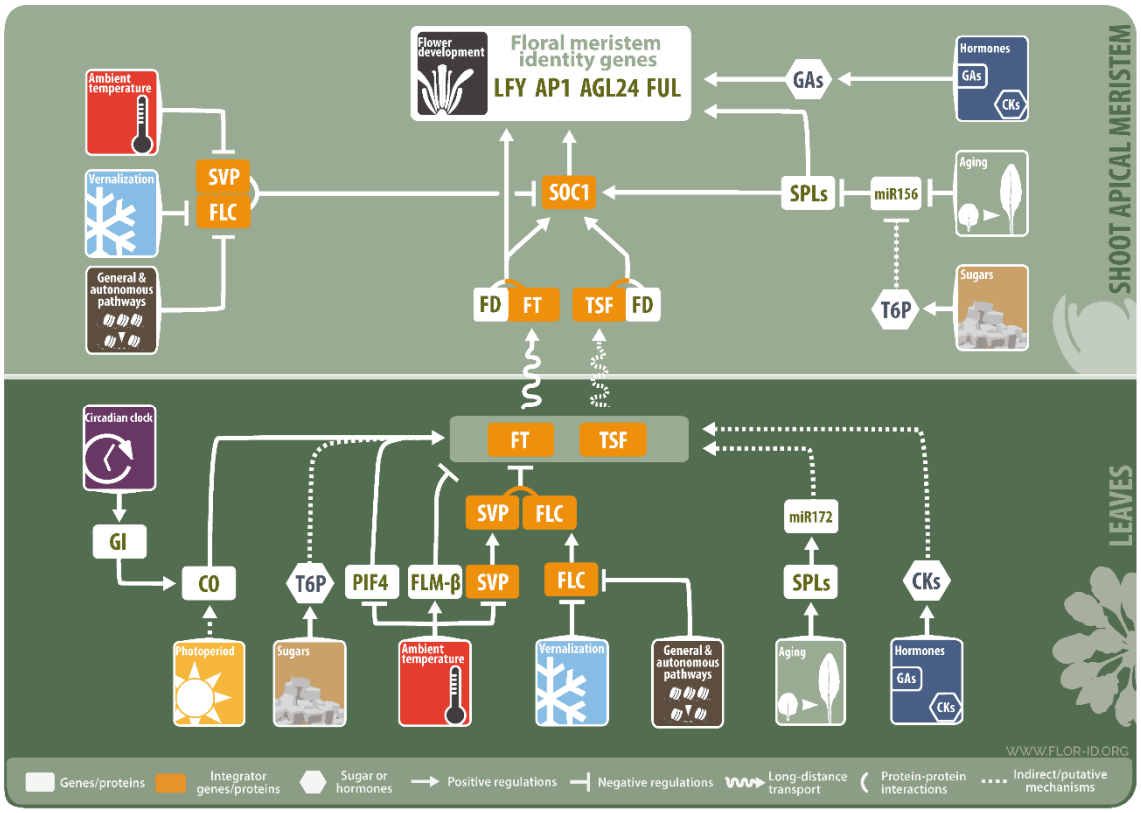

Figure I-1. Integration of genetic pathways controlling flowering in Arabidopsis. Genetic pathways controlling flowering in Arabidopsis perceive exogenous signals, such as temperature, light quality, and the length of the light phase of the day, and endogenous signals such as hormone status or age and transduce these signals to the floral integrators. Floral integrator genes are responsible for coordinating all the information from different pathways so that, when the right conditions are met, activation of floral transition and flower formation occurs. Image from FLOR-ID, Bouché et al., 2016.

Flowering time is not only controlled by different genetic pathways, but each of those pathways is itself regulated at several levels, often including transcriptional, translational and epigenetic mechanisms. Such a tight regulation provides robustness to the system and highlights the functional relevance of the flowering process and its extensive implications on reproductive success.

3. The photoperiod pathway

In many species, the length of the light phase of the day, or photoperiod, is one of the main factors affecting flowering. Plants have evolved intricated mechanisms for measuring variations in day length to accurately determine the onset of flowering over the seasons, especially at higher latitudes and this phenomenon is known as photoperiodism (Garner & Allard, 1925). Based on their responses to photoperiod, plants are divided into three main groups: short-day plants begin flowering when the night exceeds a critical length; long-day (LD) plants flower when the night falls below a critical length or short-day (SD); and day-neutral (ND) plants flower after they reach a certain stage of development regardless of day length (Andrés & Coupland, 2012).

Plants carefully time the onset of flowering to the appropriate season to ensure reproductive success. Flowering too early restricts vegetative growth and thus the accumulation of sufficient resources, while flowering too late exposes developing seeds or flowers to the risk of damaging environmental conditions, such as frost (Johansson & Staiger, 2015).

An important factor in the floral transition is the relative duration of light and darkness, because the change in day length during the year is a reliable indicator of the passage of the seasons (Andrés & Coupland, 2012; Srikanth & Schmid, 2011). For this reason, plants must be able to measure day length, and they do so by means of an endogenous clock, the circadian clock, that synchronizes physiological and molecular processes to the day-night cycle. The core clockwork of the 'circadian' (meaning about a day) timing system operates at the level of individual cells. It involves molecular feedback loops through which clock proteins generate their own 24-hour rhythms (Johansson & Staiger, 2015). In the current model of the Arabidopsis circadian clock, most components function as repressors and are classified in the morning, midday, evening and night genes (Drakakaki et al., 2009a). During the morning, two MYB transcription factors, *LATE ELONGATED HYPOCOTYL* (*LHY*) and *CIRCADIAN CLOCK ASSOCIATED* (*CCA1*), raise their maximum expression level and repress evening and night genes (Kamioka et al., 2016; Nagel et al., 2015). Next, the *PSEUDO RESPONSE REGULATOR* genes *PRR9*, *PRR7*, and *PRR5*, redundantly repress the *CCA1* and *LHY* transcription at the midday (Kamioka et al., 2016; Liu et al., 2016; Nakamichi et al., 2010, 2012). This repression allows the induction of the evening genes, *EARLY FLOWERING 3* (*ELF3*) and *ELF4* and *LUX ARRYTHMO* (*LUX*), whose proteins form a complex that represses *PRR9* and *LUX*

(Drakakaki et al., 2009a). During the night, the expression of *TIMING OF CAB EXPRESSION 1* (*TOC1)*, which is also known as *PRR1*, increases its expression and represses *CCA1* and *LHY* (Gendron et al., 2012; Huang et al., 2012).

A series of studies characterizing mutants displaying altered phenotypes in different photoperiods allowed the identification of three important regulators of this pathway*:* *CONSTANS* (*CO*), *GIGANTEA* (*GI*), and *FT*. Mutations in the *FT* gene cause a significant delay in flowering time, whereas its constitutive expression leads to a significant advance in flowering, meaning that FT is the florigen (Kardailsky et al., 1999; Kobayashi et al., 1999). On the one hand, CO and GI are key regulators of *FT* expression (Kobayashi & Weigel, 2007; Song et al., 2014). Moreover, the central mechanism of photoperiodic measurement is the regulation of *CO*, which occurs in the phloem in companion cells of leaves, and a specific circadian timing mechanism in vascular tissues is essential for photoperiodic flowering (Drakakaki et al., 2009a). CO is an important transcriptional activator of the photoperiodic pathway and is regulated by the circadian clock and light signaling pathways (Putterill et al., 1995; Samach et al., 2000; Suárez-López et al., 2001). On the other hand, the GI protein acts over *CO* and *FT* by binding and stabilizing FLAVIN-BINDING, KELCH REPEAT, F- BOX PROTEIN1 (FKF1), which promotes the stability of the CO protein on long-day conditions and facilitates the degradation of members from the family of CYCLING DOF FACTOR (CDFs) family of transcription factors, repressors of *FT* on long days (Song et al., 2012, 2014). For an overview of the clock converging on *CO*, *GI*, and *FT*, see Figure I-2.

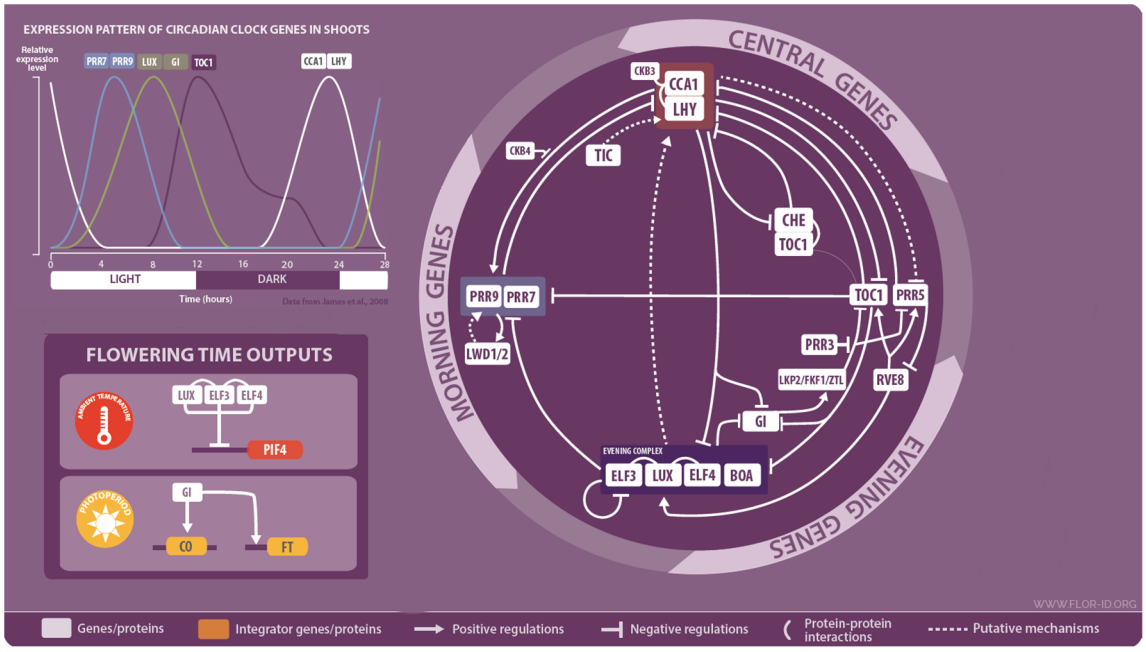

Figure I-2. Summary model of the circadian clock and its association with genes related to flowering time, CO and GI. On the right is a summary of some circadian clock components and their regulation. The top left shows the PRR7, PRR9, LUX, GI, TOC1, CCA1 and LHY expression pattern under neutral day conditions (12h light/12h dark) (James et al., 2008). The bottom left shows results with flowering time. Image modified from FLOR-ID (Bouché et al., 2016).

In Arabidopsis, light is perceived in leaves by photoreceptors phytochromes and cryptochromes, and this information is integrated by the circadian clock that regulates the expression of *CO*. Its mRNA levels oscillate due to the control of the circadian clock, and under SD conditions, the presence of the mRNA did not concur with light, but at LD it does with the peak of the *CO* mRNA cycle (Suárez-López et al., 2001; Yanovsky & Kay, 2002). The light perception by phytochromes and cryptochromes at LD is translated into a stabilization of the CO protein and prevents its degradation by the proteasome complex (Song et al., 2012; Valverde et al., 2004). Then CO protein activates the expression of *FT* in phloem companion cells, and the FT protein travels through the phloem to the shoot apical meristem (Corbesier et al., 2007; Pin & Nilsson, 2012). There, FT protein interacts with the bZIP transcription factor FLOWERING LOCUS D (FD) and proteins from the 14-3-3 family, forming the so-called florigen activating complex (Abe et al., 2005; Kaneko-Suzuki et al., 2018; Taoka et al., 2011; Wigge et al., 2005). Finally, in the SAM, the florigen activating complex induces the expression of key floral genes, such as *SOC1*, *LEAFY* (*LFY*), and *APETALA 1* (*AP1*).

In agreement with the central role of FT in flower induction, its expression is regulated by a complex network of activating and repressive signals acting at different levels and causing changes in transcription, chromatin remodeling, or over *FT* accessibility. For example, the RAV-type transcription factors, *TEMPRANILLO 1 (TEM1)* and *TEMPRANILLO 2* (*TEM2*), bind to the *FT* promoter and repress its expression (Castillejo & Pelaz, 2008) or *POLYCOMB REPRESSIVE COMPLEX 2* (*PRC2*) complex, which acts repressing the expression of *FT* during vegetative growth (Yoshida et al., 2001). Another example of regulation of FT is transport. In the same companion cells where FT is synthesized, the expression of *FT* is also controlled by *ALTERED PHLOEM DEVELOPMENT* (*APL*), which also controls the transport of FT by regulating the expression of *FLOWERING LOCUS T INTERACTIN PROTEIN* (*FTIP1*), which interacts with the protein FT and mediates its transport from the companion cells to the sieve elements of the phloem (Abe et al., 2015; L. Liu et al., 2012). In addition, the regulation of FT transport was recently shown to be temperature-dependent (Liu et al., 2020). The regulation of FT as a central integrator of many signals is very complex and is influenced by a variety of factors (Freytes et al., 2021). For a summary of the photoperiod pathway affecting flowering, see Figure I-3.

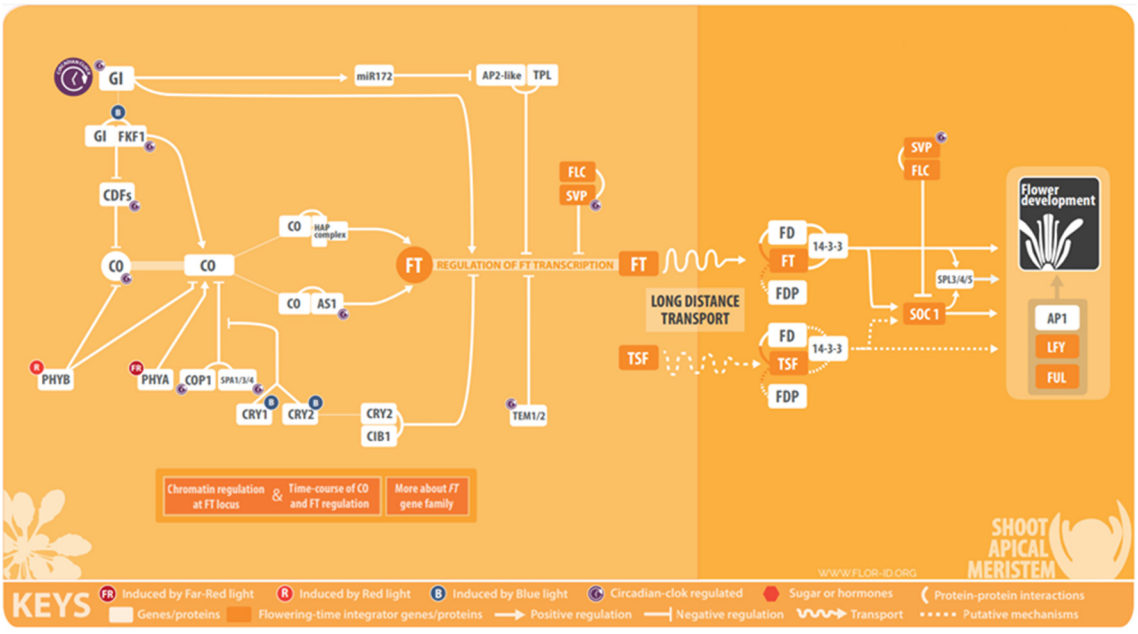

Figure I-3. Genetic control of flowering by the photoperiod signaling pathway. The circadian clock regulates the expression of *GI*, which acts by directly modifying the expression of *FT*. GI forms a complex with FKF1 that promotes the degradation of CDFs, thus indirectly activating *CO*. The transcription factors *TEM1* and *TEM2* bind to the promoter of *FT* and activate its expression. FT protein is transported from the leaves to the SAM, where it interacts with the

transcription factor *FD* to regulate the expression of the floral integrator *SOC1* and the floral meristem identity genes *AP1* and *LFY*, among others. Image taken from FLOR-ID, (Bouché et al., 2016).

3.1. Hormonal control of flowering time

In the context of hormones involved in flowering, gibberellins have traditionally been the most relevant studied and described signaling pathways. Higher-order mutants with loss-of-function in GA biosynthesis have shown a delay in flowering under long-day conditions (Blázquez, Green, et al., 1998; Nilsson et al., 1998; Wilson et al., 1992), and the *ga1-3* mutant that is affected in an early step in the synthesis of GA, do not flower even under short-day conditions (Michaels & Amasino, 1999), suggesting a central role for GAs in the absence of the photoperiod stimulus (Galvão et al., 2012). GA homeostasis is mainly maintained by a fine-tuned regulation of both synthesis enzymes, including GA20-oxidase and GA3-oxidase, which catalyze the final steps of bioactive GAs (Mutasa-Göttgens & Hedden, 2009; Plackett et al., 2012), and inactivation enzymes such as GA2-oxidases, which contribute to the turnover of GAs (Bao et al., 2020; Rieu et al., 2008).

There are different mechanisms that describe how GAs induce flowering. On the one hand, it has been described that GAs (Eriksson et al., 2006) can induce the expression of key floral genes such as *SOC1* (Bonhomme et al., 2000; Moon et al., 2003) and *LFY* (Blázquez, Green, et al., 1998), and on the other hand, GAs have shown to induce *FT* expression under LD and SD conditions, although under short-day conditions *FT* expression level was very low (Hisamatsu & King, 2008; Moon et al., 2003; Wigge et al., 2005). In addition, GA promotes flowering independent of photoperiod by regulating *SQUAMOSA PROMOTER BINDING PROTEIN-LIKE* (*SPL*) genes in leaves and shoot meristem (Galvão et al., 2012).

On the other hand, there is tight crosstalk between GA and other phytohormones that affects floral transition (Bao et al., 2020). Studies on the role of abscisic acid (ABA) in floral transitions are currently gaining importance (Shu, Luo, et al., 2018). In addition to the known roles of GAs and ABA, which antagonistically regulate some biological processes, floral transitions under stress conditions have recently been shown to be affected by ABA. The exact effects of ABA on floral transitions are currently unclear, as

both positive and negative effects have been reported (Izawa, 2021). It has been shown that ABA has positive effects on flowering under stress conditions such as drought. Drought stress leads to early flowering in several plant species, known as drought response (DE) (Verslues & Juenger, 2011). In addition, the ABA deficient mutant, *aba1*, showed reduced early flowering under stress conditions, suggesting that ABA has a positive effect on flowering transitions in DE, but only under long-day conditions. In addition, *GI* and downstream genes such as *FT* are involved in DE under long-day conditions. Interestingly, DE was not observed under short-day conditions in Arabidopsis, suggesting that DE is associated with photoperiod signaling pathways (Izawa, 2021). In contrast, ABA was found to repress flowering by simultaneously affecting *SOC1* expression at the apex (Riboni et al., 2013, 2016). In addition, *SOC1* is also positively influenced by GAs, and because ABA and GAs appear to play opposing roles in flowering by differentially regulating the expression of SOC1 or its signaling. It is suggested that ABA antagonizes GAs in the SAM (Conti, 2017).

3.2. The age pathway

Choosing the right time for flowering depends on many factors, including the stage of development of the plant. A very early start of flowering in the juvenile stage can seriously affect the survival of the plant and its progeny. The age pathway is controlled by microRNAs (miRNAs), small molecules of 21-24 nucleotides of non-coding RNA, of which miRNA156 and miRNA172 play a central role. During the juvenile phase, the concentration of miRNA156 is high in leaves and suppresses the expression of its target genes, members of the *SPL*s family. In turn, the absence of miRNA172 allows AP2-like proteins, AP2, TARGET OF EAT1 (TOE1), TOE2, SCHLAFMUTZE (SMZ), and SCHNARCHZAPFEN (SNZ), together with TOPLESS (TPL), to repress the expression of *FT* (Silvestre Vañó, 2020). As floral transition approaches, the expression of miRNA156 in leaves decreases, which triggers an increase in the expression of miRNA172 and, among others, *SQUAMOSA PROMOTER BINDING PROTEIN-LIKE 3* (*SPL3)*, and *SQUAMOSA PROMOTER BINDING PROTEIN-LIKE 9* (*SPL9)*, which, together with *TPL*, promote flowering by activating the *AP1*, *FUL* and *SOC1* and also *LFY* (Wang et al., 2009; Yamaguchi et al., 2009).

3.3. The sugar/carbohydrate pathway

Sugars provide energy and carbon skeletons required for plant growth and development, and also function as signaling molecules that regulate different developmental stages and help plants acclimate to environmental changes (Cho et al., 2018; Wingler, 2018). The relevance of these types of metabolites and their biosynthetic processes has increased in recent years with the discovery of flowering time phenotypes associated with altered expression of genes for chlorophyll synthesis and thus photosynthesis in different species such as sweet potato (Jiang et al., 2019), tomato (Fantini et al., 2019) and rice (Peng et al., 2019).

Starch is the final storage product of photosynthesis and its metabolism is upregulated differently during the floral transition in response to photoperiods. Moreover, it has been shown that changes in starch metabolism affects flowering time in Arabidopsis (Ortiz-Marchena et al., 2014, 2015). Arabidopsis is a plant with apoplastic transport of photoassimilates and has a higher requirement for glucose and fructose than sucrose during the reproductive phase; however, sucrose was required to form more leaves during the vegetative phase (Duplat-Bermúdez et al., 2016). In addition, plants misexpressing *FT* in the SAM had an early flowering phenotype under SD conditions, and transcriptome analyses showed that monosaccharide transporter genes were upregulated. Therefore, misexpression of *FT* in SAM leads to flowering and may accelerate the high requirement of hexoses for plant growth and flowering (Duplat-Bermúdez et al., 2016).

Mobilization of carbohydrates is important for a proper transition to flowering. For example, overexpression of *SUCROSE TRANSPORTER 4* from sweet potato in Arabidopsis resulted in increased *FT* expression and lower sucrose content in leaves (Wang et al., 2020). Another sugar transport recently described to affect flowering time is *SWEET10*, a sucrose transporter gene induced by *FT* and *SOC*1 in response to photoperiod. Its overexpression results in an early flowering phenotype, low miRNA156 expression, and also higher expression levels of *FD*, *SPL4*, and *SPL9* at the apex (Andrés et al., 2020).

In addition to sucrose, trehalose-6-phosphate (T6P) has been shown to contribute to the control of flowering time. Its synthesis is controlled by *TREHALOSE PHOSPHATE SYNTHASE 1* (*TPS1)* (Blázquez et al., 1998), and the regulation of T6P amount are induced by sucrose (Kolbe et al., 2005). The control of flowering by sugar is controlled

by two different pathways acting upstream and downstream of *FT*. On the one hand, the T6P signaling system regulates the floral transition by controlling the transcript levels of *SPL3*, *SPL4*, and *SPL5* in the SAM (Wahl et al., 2013). On the other hand, *TPS1* is responsible for the induction of *FT* and *TWIN SISTER OF FT* (*TSF*) in response to photoperiod in the leaf. These results show that T6P signaling plays a role in flowering transition in two different tissues. In contrast, the T6P pathway controls the expression of flowering transition and flower patterning genes through the age pathway in SAM, independent of the photoperiod pathway (Gawarecka & Ahn, 2021).

4. Omics tools to investigate plant development and signaling

4.1. Metabolomic studies

The metabolome is the collection of all metabolites in a cell, tissue, organ, or organism that are considered end products of cellular processes (Sumner et al., 2003). Metabolomic approaches intend to characterize chemical processes involved in metabolism, as well as substrates, reactions, intermediates and final products. All molecules involved in these steps are called metabolites and tend to have a low molecular weight (<1500 Da) (Deborde et al., 2017). They are usually classified as primary metabolites if they are present in larger amounts in cells or are essential for survival and are involved in important processes such as growth, development, or reproduction (Kumar et al., 2017). On the other hand, secondary metabolites are not individually found in greatest abundance in the metabolome and their absence does not lead to death of the organism, but they still affect its long-term. The plant kingdom contains a huge diversity of metabolites of about 200,000 compounds, the vast majority of which are still unknown. It is estimated that around 10000 secondary metabolites have been discovered in different plant species. The discovered metabolites differ structurally in their biochemical properties and functions and are considered very important for plant biology (Razzaq et al., 2019). Metabolomics holds enormous potential in the context of plant research and is one of the fastest developing and most attractive technique among the omics technologies. Current metabolomics platforms play a critical role in exploring unknown regulatory networks that control plant growth and development (Patel et al., 2021).

Plants produce and accumulate a variety of primary and secondary metabolites via processes in which precursor structures are modeled by biochemical steps driven by

different enzyme classes. Changes in the metabolome across independent plants, plants growing under different conditions, or changes triggered by different treatments can provide information about the structure of a metabolic network underlying the physiological response. In this way, metabolomics has been used to study plant metabolism and identify unknown gene functions by comparing the profiles of wild type and genetically modified plants, as well as plants at different stages of development (Carneiro et al., 2015). These studies have demonstrated the robustness of these techniques when applied to design metabolic engineering strategies, process engineering, biomarker discovery or functional characterization of novel molecules.

Physical and chemical properties of metabolites are highly variable because the term metabolites include many different types of compounds, such as carbohydrates, lipids, amino acids, short peptides, nucleic acids, alcohols and organic acids produced by anabolism or catabolism (Fiehn, 2016). Lipidomics involves the analysis of lipids in a biological system. It has also been reported that changes in lipid metabolism lead to changes in plant growth, development and response to a variety of environmental signals (Li et al., 2015; Macabuhay et al., 2022). Lipids serve as major building blocks of cell membranes, but they also have relevant roles as energy storage compounds and contribute to cell communication by modulating transport, intracellular and extracellular cell signalling and membrane anchoring (Rupasinghe & Roessner, 2018). Lipids can be classified into eight main classes that include fatty acids (FA), glycerolipids (GL), glycerophospholipids (GP), sphingolipids (SP), sterol lipids (ST), prenol lipids (PR), saccharolipids (SL), and polyketides (PK) (Fahy et al., 2009) and the most studied in plants are GL, GP and SP.

Glycerolipids consist of glycerol backbones with varying numbers of fatty acids, such as monoacylglycerides, diacylglycerides, and triacylglycerides. Glycerophospholipids are the major building blocks of cell membranes involved in cell signaling, membrane anchoring, and substrate transport. These are derived from phosphatidic acid (PA) and consist of different molecular species with varying fatty acid chain length and degree of unsaturation (Narasimhan et al., 2013). In plants, the major glycerophospholipids are phosphatidylcholine (PC), phosphatidylethanolamine (PE), phosphatidylglycerol (PG), phosphatidylinositol (PI), phosphatidylserine (PS), and lysophosphatidylcholine (LPC), which are important components for the formation of lipid bilayers as part of cell membranes (van Meer, 2005). Sphingolipids are derivatives of ceramides and consist of

amide groups attached to long-chain fatty acids with sphingoid backbones. Compared to sphingolipids in animals, sphingomyelin, globosides, sulfatides, or gangliosides are not present in plants, but glycosyl-inositol phosphorylceramides (GIPCs), glycosyl-CERamides (gluCER), and ceramides account for about 64%, 34%, and 2%, respectively, of the total sphingolipids in Arabidopsis (Markham & Jaworski, 2007). Therefore, due to the large biomass of plants and fungi, GIPCs are the most abundant sphingolipids in the biosphere (Rupasinghe & Roessner, 2018).

The application of analytical methods using Arabidopsis as a model plant has mainly focused on genetic studies, elucidation of gene functions, and, in most cases, understanding the extension of metabolite correlation with gene expression (Carneiro et al., 2015). The components of the metabolome can be considered the end product of gene expression that defines the biochemical phenotype of a cell or tissue (Figure I-4). Therefore, quantitative and qualitative measurement of metabolites in different tissues or under different conditions provides a comprehensive view of biochemical status that can be used to monitor or evaluate gene function (Fiehn, 2002; Weckwerth, 2003). The transcriptome represents mRNA changes in the cellular machinery required for protein synthesis, but increases in mRNA levels do not always correlate with protein levels or translated proteins may not be enzymatically active. For these reasons, changes in the transcriptome or proteome do not necessarily correspond to a change in biochemical phenotype (Ghatak et al., 2018). Metabolomics-based screenings have been shown to be useful for rapidly characterizing novel function genes in both Arabidopsis and and rice (Albinsky et al., 2010).

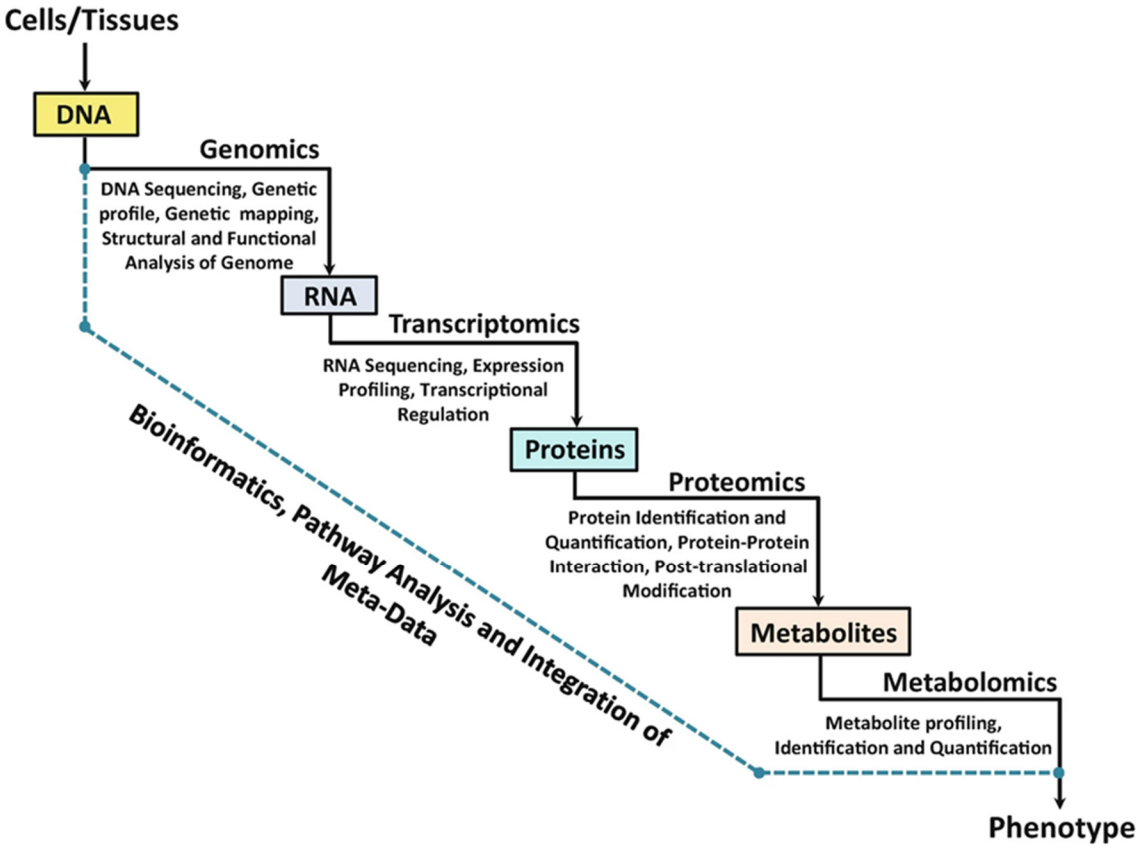

Figure I-4. Flow of biological information from the genome to the metabolome of a particular cell, tissue, or developmental stage to study phenotypes or processes. Metabolomics is a complementary tool for functional genomics and systems biology**.** Figure from Ghatak et al., 2018.

4.2. Chemical genetics

The identification of small molecules that could affect biological function requires of a large number of compounds to perform screening. One of the most important requirements for this type of analysis is those candidate molecules should be of low molecular weight. Chemical genetics is commonly used to study how small molecules affect protein-protein, protein-peptide, or metabolite-enzyme interactions. This technique allows dose-dependent responses that lead to concentration-dependent phenotypes (Amos, 2021). Chemical genetics is an experimental approach based on the screening of biological material for a target phenotype when exposed to a library of known molecules. Chemical libraries can consist of different types of compounds, and they can be synthetic or natural. Ideally, selected compounds should be bioactive, have low molecular weight, and be able to penetrate plant membranes to reach their target.

The oldest form of forward genetics was a technique based solely on observing random mutations in nature and identifying the responsible mutation. However, classical genetic approaches are limited when genes are functionally redundant, when they are essential for plant growth and/or development, or when the mutations affecting those genes have pleiotropic effects, having multiple phenotypic expressions (Hicks & Raikhel, 2012; Serrano et al., 2015). Chemical genetic approaches have proven to be efficient alternatives to overcome these problems. Small molecules can act as agonists or antagonists, meaning that they can modulate the function of a protein directly (by binding the protein and modulating its structure, function or its ability to form complexes) or indirectly (by modulating the expression of a regulatory gene). In this context, the application of small molecules to a biological system has clear advantages since they can alter protein function rapidly, conditionally and reversibly (Tóth & Van der Hoorn, 2010). Chemical genetics can be used to address the problem of redundancy since small molecules can target proteins that belong to the same family or have the same function (Nowak et al., 1997). Likewise, they can overcome problems when analyzing the function of genes with pleiotropic effects since small molecules can affect specific protein domains, opening the possibility to uncouple different functions performed by the same protein. Finally, studies performed in plants with different genetic backgrounds have shown that small molecules can alter the same biological process in different plants, provided that the regulatory gene/protein network is conserved among them (Serrano et al., 2015).

Given the advantages that chemical genetics offer compared to more classical forward genetic approaches, its application to dissect complex plant processes has increased in the last decade (Tóth & Van der Hoorn, 2010). Chemical genetics has substantially contributed to the understanding of plant hormone signaling (Rigal et al., 2014), circadian clock function (Chen et al., 2012), or plant immunity (Pieterse et al., 2009), among others.

Arabidopsis has been used in chemical genetic screenings since it can be grown in microplates. Alternatively, screenings can be performed using cell cultures to explore metabolic pathways specific to a particular cell type (McCourt & Desveaux, 2010). Two types of chemical screenings have been performed in plants. Phenotypic or forward chemical screening is the most commonly used and consists of identifying a bioactive compound that causes a phenotypic change (Figure I-5A). The second type of screening is called target-based or reverse chemical screening. The goal of this strategy is first to identify a compound that affects the function or activity of a specific protein. Once

potential candidate molecules are selected, they are applied to the plant to observe a possible phenotypic change (Figure I-5B).

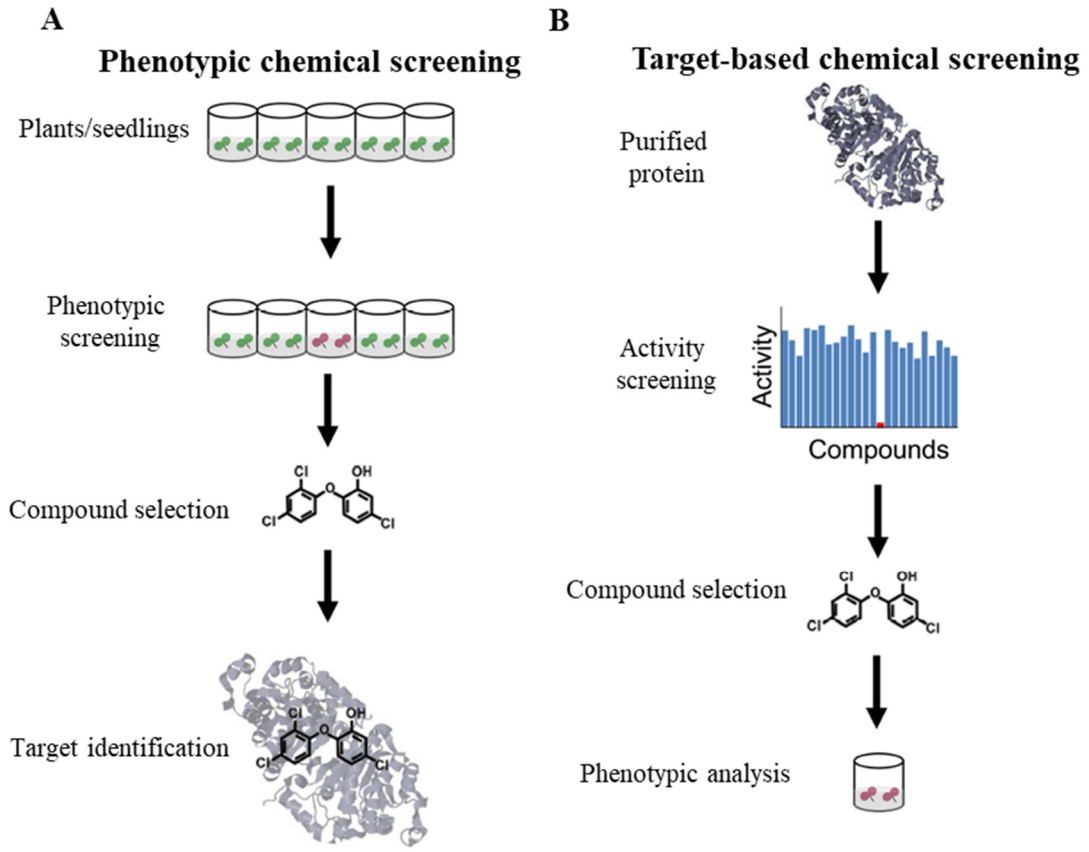

Figure I-5. Comparison of forward and reverse chemical screening. In **A,** the goal of phenotypic or forward chemical screening is to identify a (selective) bioactive compound from a set of chemicals that produces a phenotypic change, usually in a microplate format. Once a selective compound is found, the molecular target is identified, either by a genetic approach or by a biochemical purification strategy. In **B**, the goal of targeted or reverse chemical screening is to identify a compound that modulates the activity of a selected protein. The chemical is then used to determine the phenotypic consequences of its application to plants. Figure from Serrano et al., 2015.

To analyze the effect of small molecules on the plant, gene reporters can be used to detect changes in the expression of a gene of interest. In plants, two of the commonly used reporter genes are the *UidA(β-GLUCURONIDASE*; *GUS*) and the *LUCIFERASE* (*LUC*) genes (Koo et al., 2007). A transcriptional fusion is performed in which the reporter gene is expressed under the control of the promoter of the gene of interest so that a signal appears when the gene is expressed. In this way, the activity of the gene reporter product,

the GUS or LUC enzymes, will depend on the expression level of the promoter. In the case of GUS, its activity can be visualized by the conversion of the X-Gluc substrate (5-brom-4-chloro-3-indolyl- *β-D*-glucoronide) into the insoluble compound 5,5´-dichloro-4,4´-dibromo-indigo that forms a blue precipitate (Jefferson et al., 1987). GUS reporters also offer several advantages, such as their sensitivity, but the detection procedure is time-consuming and often implies the destruction of the plant (Velten et al., 2008). On the other hand, LUCs area a wide range of enzymes that can generate oxygen and a light signal in the presence of luciferin, an enzyme-specific substrate (Contag & Bachmann, 2002). Luciferase reporters have proven to be sensitive markers and effective tools for discovering gene function in plants (Velten et al., 2008).

Once screening has been performed and the molecules of interest that trigger the response have been identified, classical genetic, biochemical, and purification methods can be used to identify the target protein and its contribution to the observed phenotype (Hicks & Raikhel, 2012; Robert et al., 2009; Serrano et al., 2015). Chemical plant genetics is a relatively young field, but it has proven to be very useful for the discovery and characterization of metabolic pathways through drug discovery and protein targeting. Most of the screenings already performed in Arabidopsis have focused on hormone signaling pathways (Drakakaki et al., 2011). In this way, newly natural or small synthetic molecules have been discovered to play a role in these metabolic pathways by mimicking the activity of a hormone or competing with its targets (Serrano et al., 2015; Stokes & McCourt, 2014). Although the study of hormones is obviously beneficial because they play a critical role in plant development, other important processes can also be studied using chemical genetics. With the development of new libraries and different protocols and tools for chemical genetic screening, this type of approach has become increasingly relevant (Serrano et al., 2015).

5. Pipecolic acid as a signaling molecule involved in the control of plant development

Plants have developed a complex and dynamic innate immune system that relies on sensing and signaling using small molecules for defense against pathogens (Pieterse et al., 2009; Spoel & Dong, 2012). While local defense is critical for limiting pathogen growth, plants also possess the ability to prime and amplify immune responses at distal sites. This global response is termed systemic acquired resistance (SAR) (Fu & Dong, 2013). Pipecolic acid (Pip) is a non-proteinogenic amino acid widely distributed in plants, animals and microorganisms. It is an important precursor of many secondary metabolites (He, 2006). Its biosynthesis has been extensively studied in animals and plants mainly because of its close relationship with lysine metabolism (Broquist, 1991; Gupta & Spenser, 1969).

Pip, and its derivative N-hydroxypipecolic acid (NHP), have been proposed to act as signalings molecules (Návarová et al., 2012) (Hartmann & Zeier, 2018). Pip is synthesize in the plastids from lysine, by the consecutive action of AGD2-LIKE DEFENSE RESPONSE PROTEIN 1 (ALD1) and SAR DEFICIENT 4 (SARD4) enzymes. Pip is then exported to the cytosol, where it is converted into NHP by the FLAVIN-DEPENDENT MONOOXYGENASE 1 (FOM1) enzyme (Figure I-6A). NHP has emerged as the most likely long-distance signal, as mutants defective in the biosynthesis of NHP have been shown to exhibit a severely impaired SAR response (Huang et al., 2020; Sun & Zhang, 2021; Yildiz et al., 2021) (Figure I-6B).

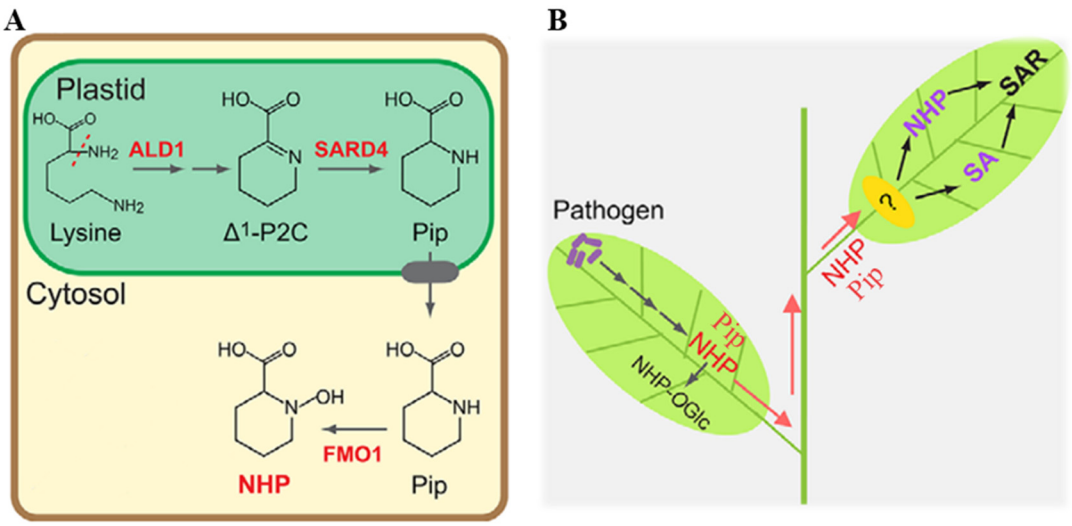

Figure I-6. Pipecolic acid (Pip) and N-Hydroxypipecolic acid (NHP) biosynthesis and downstream signaling. In **A**, the biosynthetic pathway of NHP. In plastids, the aminotransferase

ALD1 removes the a-amino group from lysine to form -amino-a-keto-caproic acid, which spontaneously cycles to Δ^1-piperideine-2-carboxylic acid (Δ^1-P2C). The reductase SARD4 converts Δ^1-P2C to pipecolic acid (Pip), which is exported to the cytosol via unknown transporters. Pip can travel or be catalyzed by FMO1, which catalyzes the N-hydroxylation of Pip to produce NHP. In **B**, infection with a pathogen triggers the biosynthesis of NHP and Pip, which are transferred to distal leaves. NHP or Pip may be sensed by one or more receptors yet to be determined and activate SAR by promoting biosynthesis of NHP and SA in distal leaves. Figure modified from Sun & Zhang, 2021.

Pipecolic acid has been detected in various plant species and organs, including seeds, roots, tubers, leaves, shoots, flowers, and fruits (Vranova et al., 2013), and its concentrations vary within plants, being highest in shoot tissue (Aldag & Young, 1970). One of the biological functions of Pip is to act as an osmoprotectant via the osmoregulated catabolism of L-lysine and proline in halophytic plants (Galili et al., 2001; Moulin et al., 2006). In addition, Pip was found to increase in tissues whose growth was affected by ectopic treatments, either to promote growth in fruits by gibberellins or to inhibit it by maleic hydrazide in leaves (Vranova et al., 2013). As for its effect on development, contradictory effects have been described in relation to flowering. On the one hand, Pip was reported to strongly induce flowering in *Lemna gibba* and *L. paucicostata*. However, this induction was much less with the D-enantiomer than with L-Pip (Fujioka & Sakurai, 1992). On the other hand, in orchids, Pip does not have the effect observed in *Lemna* (Kostenyuk et al., 1999).

MATERIALS AND METHODS

1. Plant material and growth conditions

All *Arabidopsis thaliana* mutants used in this work are insertion mutants (T-DNA or transposon) and appear in Table M1, summarizing the allele, the type of mutant, the position of the insertion in the gene, the genetic background, the code of the mutant, and the reference. If the mutant has not yet been described, the code appears in NASC (Eurasian Arabidopsis Stock Center) format.

Table M1. Mutant lines used classified by chapters in this work.

CHAPTER 2						
Locus	**Line**	**Type**	**Insertion**	**Ecotipe**	**Code**	**Ref**
AT2G13810	*ald1-1*	T-DNA	1st exon	Col-0	SALK_007673	(Song et al., 2004)
AT5G52810	*sard4-5*	T-DNA	exon	Col-0	GABI_428E01	(Ding et al., 2016)
AT1G19240	*fmo1-1*	T-DNA	4th exon	Col-0	SALK_026163	(Bartsch et al., 2006)
AT2G13810	*ald1-2*	Transposon (Gene trap)	Pomoter and 1st exon	Ler-0	CSHL_GT542 (Sundaresan et al., 1995)	*N27064
CHAPTER 3						
Locus	**Line**	**Type**	**Insertion**	**Ecotype**	**Code**	**Ref**
AT5G15840	*co-10*	T-DNA	1st exon	Col-0	SAIL_24_H04	(Jang et al., 2008; Laubinger et al., 2006)
AT1G65480	*ft-10*	T-DNA	1st intron	Col-0	GK-290E08	(Yoo et al., 2005)
AT5G08380	*agal1-1*	T-DNA	5th intron	Col-0	SALK_083934	(Imaizumi et al., 2017)
AT3G56310	*agal3-1*	T-DNA	1st exon	Col-0	SALK_012366C	(Imaizumi et al., 2017)
AT3G26380	*apse-1*	T-DNA	1st exon	Col-0	SALK_016141C	(Imaizumi et al., 2017)

AT3G06580	*galk*	T-DNA	4th exon	Col-0	GK-489D10	(Egert et al., 2012)
AT2G47180	*gs1-1*	T-DNA	4th exon	Col-0	SALK_121059C	(Jing et al., 2018)
AT1G56600	*gs2-1*	T-DNA	Promoter	Col-0	SALK_101144C	(Jing et al., 2018)
AT2G47180 AT1G56600	*gs1-1,gs2-1*	Double	4th exon Promoter	Col-0	This work	This work
AT1G09350	*gs3-1*	T-DNA	1st intron	Col-0	SALK_201770C	*N689428
AT1G60470	*gs4-1*	T-DNA	2nd intron	Col-0	SALK_029719C	*N661987
AT3G57520	*rs2-2*	T-DNA	8th exon	Col-0	GK-024G04	*N402284
AT4G01970	*rs4-1*	T-DNA	1st exon	Col-0	SALK_045237C	(Gangl et al., 2015)
AT5G40390	*rs5-2*	T-DNA	2nd Exon	Col-0	SALK_085989C	(Egert et al., 2013)
AT5G40390	*rs5-3*	T-DNA	1st exon	Col-0	GK-106F01	(Zuther et al., 2004)
Double	*rs4-1,rs5-2*	T-DNA	1st exon 1st exon	Col-0	This work	This work
Double	*rs5-2,rs6-1*	T-DNA	1st exon 1st exon	Col-0	This work	This work
AT5G20250	*rs6-1*	T-DNA	1st exon	Col-0		N653138
AT4G34135	*ugt73b2*	T-DNA	Promoter	Col-0	SALK_043888C	N679594
AT4G34131	**ugt73b3*	T-DNA	Promoter	Col-0	SALK_040058C	N655461
AT1G06000	*ugt89c1*	T-DNA	Exon	Col-0	SALK_068559C	(Yonekura-Sakakibara et al., 2007)
AT1G30530	*ugt78d1*	T-DNA	2nd exon	Col-0	SAIL_568_F08	(Jones et al., 2003)
AT4G19230	*cyp707a1-1*	T-DNA	3th exon	Col-0	SALK_069127	(Okamoto et al., 2006)
AT2G29090	*cyp707a2-1*	T-DNA	5th intron	Col-0	SALK_072410	(Kushiro et al., 2004)

AT5G45340	*cyp707a3 -1*	T-DNA	1st exon	Col-0	SALK_078170	(Kushiro et al., 2004)
Double	*a1-1,a3-1*	T-DNA	3rd exon 1st exon	Col-0	SALK_069127 SALK_078170	(Okamoto et al., 2006)
Double	*a2-1,a3-1*	T-DNA	5th intron 1st exon	Col-0	SALK_072410 SALK_078170	(Okamoto et al., 2006)
AT1G28130	*vas2-2*	T-DNA	1st exon	Col-0	SALK_094646C	(Zheng et al., 2016)
AT4G27260	*wes1*	T-DNA	3rd exon	Col-0	SALK_151766C	(Park et al., 2007; Zhang et al., 2007)
AT1G59500	*gh3.4*	T-DNA	3rd exon	Col-0	SALK_102549C	(Porco et al., 2016)

All constructs used in this work are listed in Table M2, as well as the destiny vectors used, the genetic background, and the resistance of the plants/bacteria used in the selection.

Table M2. Genetic constructs used for genetic transformation in the different genetic backgrounds used in this work.

Construction	**[a] Promoter**	**Destination vector**	**Background**	**[b] Resistance**	
				Bacteria	**Plant**
pCO::LUC	3 kb	pGWB635	Col-0	Spec	Basta
pFT::LUC	6 kb				
pAP1::LUC	3 kb				
pSUC2::CO-GR [c]	2.1 kb	pGWB601	Col-0 *co-10* *ft-10*	Spec	Basta
pFT::FT-GR	6 kb				
pCO::FT-GR	3 kb	pGWB401	Col-0 *co-10*	Spec	Kan

			ft-10		
pCO::GUS-GFP	3 kb	pBGWFS7	Col-0	Spec	Basta
pFT::GUS-GFP	6 kb				

[a] All promoters were introduced into plasmid pUC57 with attL1 and attL2 recombination sites for GATEWAY. [b] Spec and kan are abbreviations for streptomycin and kanamycin, respectively. Basta is the commercial name for the herbicide containing phosphinothricin. [c] The entry vector with the *SUC2* promoter was kindly obtained from Coupland laboratory in a binary Gateway system.

Sequencing of DNA fragments amplified by PCR for their subsequent cloning was performed at the Sequencing Service of the Institute of Plant Molecular and Cell Biology (IBMCP) (Valencia) using the capillary sequencer "ABI 3130 XL" (Applied Biosystems).

1.1. Arabidopsis growth in the greenhouse or growth chambers

Arabidopsis plants were grown in a 2:1:1 mixture of black peat:perlite:vermiculite in 6.5 x 6.5 x 5 cm or 4.1 x 4.5 x 5 cm pots. After sowing, seeds were stratified in the dark at 4°C for 3-4 days and plants were grown in greenhouse cabins with natural light supplemented with cold white light (4600lm) to achieve a photoperiod of 16h, and the temperature was kept constant between 21ºC and 23ºC. Alternatively, plants were grown in culture chambers with cool white fluorescent light (4600lm) under a long-day photoperiod of 16h light and 8h dark at 21ºC or a short-day photoperiod of 8h light and 16h dark. Irrigation was carried out twice weekly with Hoagland No. 1 solution enriched with trace elements (Hoagland & Arnon, 1950).

1.2. Arabidopsis crosses.

To generate the double mutants listed in Table M1, flowers of the recipient plant were emasculated with dissecting forceps until only the pistil remained. Then, the stamens of the donor plant were collected and the pollen was deposited on the stigma of the recipient plant. The stamens for pollination were collected as soon as the flowers opened.

1.3. *In vitro* growth conditions

For *in vitro* culture used to select transgenic plants, *A. thaliana* seeds were sterilized with an aqueous solution of 70% (v/v) ethanol and 0.005% (v/v) Triton-X-100 for 3 min with agitation, washed with 96% (v/v) ethanol for 1 min with agitation and dried. Plants were cultured in Petri dishes sealed with Micropore^{TM} 3M surgical tape to facilitate gas exchange in a solid culture medium (pH 5.9) consisting of 2.2 g/L MS salts (Duchefa), 20 g/L sucrose, 0.1 g/L MES, and 6.0 g/L agar. Hygromycin (40µg/mL), glufosinate-ammonium (Basta, 15µg/mL) or kanamycin (50µg/mL) were used as selective agents, as appropriate. Seeds were stratified after sowing in Petri dishes for 3-4 days at 4ºC in the dark and then transferred to *in vitro* culture cabinets with a long-day photoperiod of 16h and a constant temperature of 24ºC. Illumination was provided by Sylvania Gro Lux 36W fluorescent tubes emitting cool white light (850 lm).

For the experiments in Chapter 1 and the growth in 24- and 96-multiwell plates, we used MS1 medium containing 2.2 g/L MS vit (Murashige & Skoog medium with vitamins), 0.1 g/L MES hydrate, 10 g/L sucrose, and 6.8 g/L bacterial agar dissolved in distilled water. For the experiments in Chapter 2 to characterize the effect of pipecolic acid on Arabidopsis development, we used the MS1 medium. For the experiments to quantify the sugar in the apex and leaf samples in Chapter 3, we used a variation of the MS1 medium, that contained less sucrose, 5 g/L.

2. Bacterial cultures

Bacteria were cultured in LB medium (Luria-Bertani medium) consisting of: tryptone 10 g/L, yeast extract 5.0 g/L and NaCl 1.0 g/L, pH 7.0. Liquid cultures of *E. coli* and *Agrobacterium tumefaciens* (*A. tumefaciens*) were incubated overnight at 37ºC and 28ºC, respectively, and shaken at 200 rpm. The bacteria strains used in this work are in Table M3. The solid medium was prepared by adding agar 15 g/L and the cultures were incubated at 37ºC overnight for *E. coli* or at 28ºC for 2 days for *A. tumefaciens.*

Table M3. Different bacterial strains used in this work.

Strain	Purpose	Reference

Escherichia coli DH5α	Cloning and bacteria transformation	(Hanahan, 1983)
Escherichia coli Supercharge EZ10	Cloning and bacteria transformation	Clontech
Agrobacterium tumefaciens C58 pMP90	Arabidopsis transformation	(Koncz & Schell, 1986)

For the selection of transformed bacteria, culture media were supplemented with the following list of antibiotics as needed: spectinomycin (100µg/mL), chloramphenicol (33µg/mL), gentamicin (100µg/mL), ampicillin (100µg/mL). mL), kanamycin (50µg/mL) or rifampicin (100µg/mL).

2.1. Long-term preservation of microorganisms

For long-term preservation of bacterial cultures, glycerinated cultures were prepared in cryovials from exponential phase cultures of *E.coli* or *A. tumefaciens* to which pure glycerol was added until a final concentration of 25%. Once the glycerinates were prepared, they were quickly frozen in liquid nitrogen and stored in freezer boxes at -80ºC.

3. Molecular Biology Methods

3.1. Bacterial DNA extraction

Commercial kits were used for the extraction of plasmid DNA from *E. coli*. For standard extractions, 4 mL of a stationary culture of *E. coli* cultured in LB medium with the appropriate antibiotics was used using the GeneJET Plasmid Miniprep Kit (Fermentas). For medium and large extractions, the Plasmid Midi Kit (Qiagen) system was used, starting with 100 mL of a saturated culture of *E. coli* in LB medium supplemented with the appropriate antibiotics.

For isolation of plasmid DNA from cultures of *A. tumefaciens*, we start from 5mL of a stationary phase culture of the bacterium previously grown for 48h at 20ºC in LB medium supplemented with rifampicin 100µg/mL and the required antibiotics. Next, the resulting DNA was used only for re-transformation of *E. coli* cells and the plasmid was repurified.

The constructs were then retested by Sanger sequencing (IBMCP sequencing services) or enzymatic digestion.

3.2. Arabidopsis total RNA and genomic DNA extraction

For the extraction of genomic DNA from Arabidopsis, young leaves of approximately 1 cm in length were collected on ice. Genomic DNA was extracted following the "Quick DNA prep for PCR" (Weigel & Glazebrook, 2009). Finally, the extracted genomic DNA was resuspended in 90 µL of Milli-Q water.

Arabidopsis RNA extraction for analysis of the expression level of a gene by RT-qPCR was performed using the "E.Z.N.A. Plant RNA kit" with the DNase treatment on the column (Omega) according to the manufacturer's instructions. The obtained RNA was quantified in a Nanodrop ND1000 system (Applied Biosystems), and its integrity was determined by 1.5% agarose gel electrophoresis.

3.3. cDNA synthesis

For cDNA synthesis, we started with 3 µg of Arabidopsis RNA previously isolated and treated with DNase. The transcription was performed using the "SuperScript IV" system and "Oligo dT12-18" (Thermo) according to the manufacturer's instructions.

3.4. Polymerase chain reaction (PCR) and amplicon amplification

PCR was used to amplify DNA fragments for various purposes, such as cloning, genotyping of mutant lines, or quantification of gene expression. In each case, different combinations of specific primers, DNA templates of different types such as cDNA, genomic DNA, plasmid DNA, or PCR fragments, and different types of DNA polymerases were used. For amplification of DNA fragments for subsequent cloning, the high-fidelity polymerase HF Phusion (Thermo) was used, whereas for genotyping of mutant lines, the commercial polymerase GoTaq (Fermentas) was used, following the protocol described by the manufacturer for both polymerases.

Some of the procedures performed after PCR, such as cloning or sequencing, require the use of high-quality and pure DNA amplicons, so an additional purification step was often performed after amplification. In cases where PCR amplification generated a single fragment, primer, buffer, and polymerase residues were purified using the "NucleoSpin PCR cleanup" system (MachereyNagel) according to the manufacturer's instructions. In cases where PCR generated several large fragments of different sizes, they were separated by electrophoresis in a 1.5% agarose gel. The fragment of interest was cut from the gel using a blade, and the DNA contained in the fragment was recovered using the "NucleoSpin Gel Cleanup" system (MachereyNagel) according to the manufacturer's instructions. In both cases, the clean DNA was eluted in 15 µl of sterile Milli-Q water.

3.5. Reverse Transcription-Quantitative Real-Time PCR (RT-qPCR) conditions

Real-time quantitative PCR (RT-qPCR) was used for relative quantification of gene expression. To perform RT-qPCR, specific primers for the gene to be analyzed were first designed using Primer 3 Plus software (http://www.bioinformatics.nl/cgi-bin/primer3plus/primer3plus.cgi), trying to match them as closely as possible to the following parameters: Hybridization temperature between 58-62ºC, content in GC between 40-60%, amplicons generated between 180-300pb. Each of the designed primer pairs was tested in qPCR with serial dilutions of cDNA (1, 1/10, 1/100 and 1/1000) to test their amplification efficiency and to analyze possible amplification problems, such as the generation of non-specific amplicons or primer dimers. All primer pairs that showed efficiency values lower than 90 or higher than 110 were discarded.

The RT-qPCR reactions, for both quantification and calculation of primer efficiencies, were performed in a final volume of 10µL containing 2µL of cDNA (0.02ng/µL), 2µL of "Premix PyroTaq Eva Green qPCR Mix Plus" (GMC) (5X) and 0.4 µL of each of the primers (5 µM). All reactions were performed in triplicate and in a "7500 Fast PCR System" thermal cycler (Applied). The cDNA of the gene of interest was quantified during the exponential phase of the PCR reaction based on the number of cycles required to exceed the established threshold of fluorescence (Ct). From this value, the relative expression of the gene of interest with respect to the constitutive *TAP42 INTERACTING PROTEIN OF 41 KDA (TIP4)1* or *ISOPENTENYL-DIPHOSPHATE DELTA-*

ISOMERASE II (*IPP2*) gene was calculated by the $2^{-\Delta\Delta CT}$ method (Livak & Schmittgen, 2001).

3.6. Analysis of DNA by digestion with restriction enzymes

Digestion of DNA with restriction enzymes was performed according to standard protocols (Maniatis & Fritsch, 1982), using the manufacturer's recommended buffers and conditions for each enzyme. Analysis of DNA fragments generated during digestion was performed by electrophoresis in agarose gels at 1% concentration in 1X TBE buffer [Tris 44.5mM (pH 8.0), boric acid 44.5mM, EDTA 1.25mM].

4. Generation of genetically modified organisms

4.1. Bacterial transformation

Bacterial transformation was performed by electroporation with a "GenePulserTM" (Bio-Rad) device according to the manufacturer's recommendations, using electrocompetent *E.coli* or *A. tumefacins* cells obtained according to the protocol described in "Pulse controller, operation instructions and applications guide, accessory for bacterial and fungal electro-transformation" (Bio-Rad Laboratories, 1992) in the case of *E. coli* and Wen-Jun and Forde (1989) in the case of *A. tumefaciens*. An electrical pulse of 200Ω, 25µF, 1.8kV was applied for *E.coli* and 400Ω, 25µF, 1.8kV for *A.tumefaciens.*

4.2. Arabidopsis transformation

The transformation of *A. thaliana* with the different constructs generated in this work was carried out according to the agroinfiltration protocol described by Clough & Bent, 1998.

5. Histological sections and RNA *in situ* hybridization

To investigate tissue-specific expression of the *RS5* gene by RNA *in situ* hybridization, we collected tips at different developmental stages on days 7 (vegetative), 12 (transition), and 15 (inflorescence). Samples were collected in a FAE solution (50% ethanol, 3.7%

(v/v) formaldehyde, 5% glacial acetic acid) and placed under vacuum according to the procedure described in (Ferrandiz et al., 2000). FAE was then replaced with a fresh solution and incubated for 2 hours at room temperature. After fixation, samples were washed several times with 70% ethanol. The eosin staining and subsequent paraffin embedding of the samples was performed in the microcopy service at IBMCP by an automated tissue processor (LEICA TP 1020). Paraffin blocks were mounted using a LEICA EG1150H embedding device. Next, a LEICA RM-2005 microtome was used to obtain histological sections of 8 µm thick sections of the apices.

To design a specific *RS5* RNA probe, we first obtained the cDNA sequences of the *RS1*, we downloaded mRNA sequences from *RS2*, *RS4*, *RS5* and *RS6* genes from the Phytozome Web Service (Goodstein et al., 2012) and performed an alignment of their sequences using the BioEdit tool. We identified a region located between 805-1179 bp from the ATG codon as highly *RS5* specific. The synthesized sense and antisense probe were quantified. For this, the probes were precipitated with a mixture of 1µg/mL yeast tRNA (Roche), 0.6M ammonium acetate and absolute ethanol and centrifuged at 4ºC and 13000 rpm for 15 minutes. The precipitate was then washed with 70% ethanol and air-dried to resuspend the precipitated probe in 10µl RNase-free water finally. For quantification, 1 µl was taken from each probe and 1/20, 1/250, 1/1000 and 1/2500 dilutions were prepared from them. Then, 1 µl of each of the dilutions was applied to a Hybond XL nylon membrane (Amersham) and the probe was fixed to the membrane using a UV light oven. Next, the membrane with the probes was first incubated in 1X TBS (50 mM Tris-Cl, pH 7.5) for 2 minutes and replaced with a solution of 1X TBS with Blocking Reagent at 0.5% (Roche) and incubated for 10 minutes. The membrane was then added to a 1/3000 solution of Anti DIG-ab antibody (Roche) in 1X TBS and incubated for 15 minutes at room temperature. The washing was done with detection buffer (1M Tris, 1M NaCl, 0.5M MgCl2) without substrate, followed by incubation with detection buffer with the substrate (BCIP, Nitro Blue Tetrazolium) (Roche) until the signal was visible. The remaining 9 µl of the probe was diluted with 91 µl of hybridization solution: 6X SSC, 3% SDS, 50% formamide, 100 µg/mL tRNA and stored at -20ºC until use. The hybridization temperature with the sense and antisense probes for *RS5* was 53ºC for 12 hours. The Leica DMS1000 microscope and Leica Application Suite (Leica) image analysis software was used to visualize and obtain the images shown in this work.

6. Phenotypic analysis of plants.

Statistical analysis of flowering experiments, rosette area and leaf size measurements, cell number and cell size, number of fruits and seeds, expression level by RT-qPCR, and luminescence signal was performed using a Student's t-test or ANOVA by the Astatsa (2016, Navendu Vasavada) virtual platform (https://astatsa.com/OneWay_ANOVA_with_TukeyHSD/) as described in each figure or table.

6.1. Flowering time evaluation

Flowering time measurements are described in detail in each section and experiment, following the guidelines provided in Praena et al., 2022.

6.2. Evaluation of the number of fruits and seeds

The total number of fruits produced by the main inflorescence until its arrest was scored. For this purpose, weekly measurements of newly produced fruits were made in Col-0, *rs5-2* and *rs5-3*. To count the number of seeds per fruit, we collected mature fruits between the floral nodes 6 to 15 in two batches and performed measurements using an Olympus SZ60 magnifying glass.

6.3. Estimation of Arabidopsis rosette area

The easy leaf area mobile application was used to measure the rosette area. All measurements were taken at the same height of the plant, as described in the protocol (Easlon & Bloom, 2014). Average leaf size was estimated by dividing the total area by the total number of rosette leaves.

6.4. Estimation of cell size and cell number in Arabidopsis leaves

Experiments to count cell size and cell number were performed according to the protocol described in (De Veylder et al., 2001). Plants were grown in the greenhouse under LD

condition and collected 10 days after germination. They were incubated overnight in methanol to remove chlorophylls and pigments. Then, seedlings were incubated in lactic acid for 10 hours, then washed with methanol and stored until visualization. Visualization was performed using a Leica DMS1000 microscope by opening the shutter completely to facilitate visualization of the epidermal cells and using Leica Application Suite (Leica) image analysis software. Each leaf was photographed in 4 quadrants located 25% and 75% from the distance between the tip and base of the leaf blade of the abaxial epidermis of each leaf (De Veylder et al., 2001) and the total number of cells was estimated by dividing the area of the leaf blade by the average cell area of each leaf.

7. Plant treatments

7.1. Dexamethasone treatment

To activate the CO::GR fusion protein, plants were treated with a solution of dexamethasone 30μM, and Tween 20 0.01% by spraying the rosette.

7.2. Abscisic acid (ABA) treatments.

The ABA treatment on the apices was performed for 4 days between ZT8 and ZT10 by applying a drop of ABA solution (30 μM ABA in Mili-Q water), while the mock treatment contained only Mili-Q water.

7.3. Pipecolic acid treatment

The different treatments with pipecolic acid (Sigma-Aldrich, Ref: 60618) were performed as described in each section. For the irrigation experiments, we prepared the solutions by dissolving them directly in tap water. For the *in vitro* culture experiments, we prepared stocks of 1 M and 100 mM Pip in Mili-Q water and filtering the solutions using sterile Millex syringe filters with a membrane diameter of 4 mm and a pore size of 0.45 μm. Six seeds of the Col-0, *ald1-1* and *sard4-5* lines were sown in glass vessels (10.5 cm high x 9.8 cm in diameter) containing approximately 50 mL of MS0.5 medium supplemented or not with Pip at various concentrations. Seeds were then stratified in a cold chamber for 4 days before transferring to an *in vitro* growth chamber in LD conditions.

8. Chemical genetic screenings

8.1. Conditions and experimental design for the primary chemical genetic screening.

The tested the library of 360 molecules that comes from an original library of 2016 chemicals with known biological activity from www.msdiscovery.com. The original Stocks were in 100% DMSO at a concentration range of 10-20 mM (Robert et al., 2008). The 24-well plates with MS1 media with molecules or DMSO were prepared by adding 2 µl of the concentrated library of each molecule in the wells, and then 400 mL of media was added by pipetting and ensuring it was mixed well before solidifying. Next, we sterilized seeds from the p*FT*::*GUS* line and sowed 6 seeds per well. After 4 days of stratification in a cold chamber at 4 ºC, plates were transferred to an *in vitro* chamber under LD conditions. Due to the range of concentrations of the original stocks in the library, the final concentrations tested for the molecules varied between 25 µM and 50 µM. For this initial experiment, we performed two technical replicates corresponding to 12 plants. The second screening to confirm positive results was performed as described for the first but increased the number of technical replicates to three, corresponding to 18 plants analyzed.

8.2. Conditions and experimental design for the secondary chemical genetic screening.

We purchased the selected molecules from ChemBridge and named them as described in Section 1.1.2. The stocks were prepared at 10 mM in DMSO. Next, to test the CF1, CF2, CF3, CF4, CF5 and CF11 molecules, we followed the same procedure as for the primary and secondary screening described in the previous section, but increased the number of concentrations tested to 100 µM, 75 µM, 50 µM, 25 µM, and 12.5 µM. In the case of the CF11 molecule, we additionally increased the number of concentrations tested to 20 µM, 10 µM, 5 µM, and 2.5 µM. The growth conditions for the screenings using p*FT::LUC* reporter line were the same as for the screening using the p*FT::GUS* line. We performed this experiment using 96-well sterile plates with 100 mL of medium per well. The medium was MS1 supplemented with the molecules at different concentrations for the experimental test or with the same amount of DMSO for the controls.

9. Reporter gene analysis techniques

9.1. β-glucuronidase (GUS) activity assay

We thank Dr. Turck (Max Planck Institute for Plant Breeding Research, Cologne, Germany) for kindly providing the *pFT::GUS* line. For analysis of β-glucuronidase activity in *GUS* gene fusion reporter line, samples were immersed in 90% (v/v) acetone fixative solution and incubated at 4ºC for 15 minutes. Then, samples were immersed overnight in a developing solution (50mM sodium phosphate buffer, 10mM potassium ferrocyanide, 10mM potassium ferricyanide, 0.2% (v/v) Triton-X-100, 1mM X-Gluc). A 5-minute vacuum pulse was applied to facilitate penetration. Next day, samples were washed with increasing concentrations of ethanol (v/v) (30 minutes each, room temperature): 20%, 30%, 50%, FAE (absolute ethanol 50% (v /v), glacial acetic acid 10% (v/v), formaldehyde 5% (v/v)) and ethanol 70%. Finally, we observed the samples, directly or after rinsing the tissue with chloral hydrate. The protocol of S. Christensen in Weigel and Glazebrook (2002) was followed.

9.2. Luciferase (LUC) activity assay

To evaluate the LUC signal in *pFT:: LUC* and *pAP1:: LUC* plants, we grew the plants in soil on SD conditions and transferred them to the LD chamber. Plants were treated with a luciferin solution (D-luciferin 30 µM + Tween 0.05% + Mili Q-water) or mock (Tween 0.05% + Mili Q-water). Plants were placed between two transparent films and treated with the solutions 30 minutes before images were taken using the LAS3000 instrument with an exposure time of 15 minutes. Quantification of luciferase signal was performed in white sterile 96-well microplates (Promega, Ref: E5650) for luciferase assay by adding the luciferin solution (D-luciferin 30 µM + Mili Q-water) and mock solutions (Mili Q-water) to each well. Each sample was immersed in individualized wells with the luciferin or mock solutions for the measurement. Luminescence was read using the GloMax-Multi Detection System-Promega (Model:9301-062) according to the Luminometer Quick Protocol at www.promega.es. In all experiments performed, the signal detected in the mock treatments was never higher than that detected in the control Col-0 with luciferin treatment.

For the luciferase experiment with molecules CF1, CF2, CF3, CF4, CF5 and CF11, we use the system described in (García-Maquilón et al., 2021) with some modifications.

Instead of adding 20 seeds per well, we sowed only 1 seed per well. In this way, we reduce the error resulting from the shading effect and the availability of nutrients when many plants grow together in a small space. For luminescence measurement, we added 150 µl of luciferin solution (D-luciferin 100 µM + MS1 liquid (without agar)) per well to completely cover the plant. Then, plates were left in the growth chamber for 1 hour before we started the measurement with LAS-3000 with an exposure time of 10 minutes. We followed the specification and settings described in (García-Maquilón et al., 2021) for image acquisition and analysis for quantification using the ReadPlate 2.1 plugin from Fiji/Image J. The different time points of bioluminescence measurement were described in detail in the corresponding figure. At least 12 biological replicates were tested for each concentration and for each molecule.

10. Bioinformatic analysis

10.1. Sequence analysis

Benchling (https://www.benchling.com/) was used to analyze sequences from Sanger sequencing and to design primers for PCR or to analyze restriction maps.

10.2. Statistical analysis (Student's t-test/ANOVA).

For statistical analysis of all experiments related to the metabolome and lipidome of apices and leaves, we used the MetaboAnalyst 5.0 online platform with the Statistical Analysis module. Normalization was by pooled sample from the group (group PQN) set to day 0, data transformation was "log transformation (base 10)", and data scaling was "auto-scaling" (mean-centered and divided by standard deviation of each variable). The sPLS-DA for the analysis of the number of components was performed using the validation method "5-fold CV". The heat map was made considering all time points with the normalized data as the data source and the standardization of the "autoscale features" using the Ward cluster method. The main representative metabolites were identified by applying ANOVA. For more information, see FAQ from https://www.MetaboAnalyst.ca/ or (Pang et al., 2021).

For the remaining statistical analyzes using Student's t-test/ ANOVA, which are not given in each section, we use the online platform Astatsa www.astatsa.com/

11. Treatment and sampling for metabolomics, lipidomics, transcriptomics and hormone profiling.

We stratified the seeds in sterile water at 4ºC for 3-4 days, then sowed them and placed them under long-day conditions (16h light/8h dark). After 3 days we opened the trays (all germinated plants) and on the 4th day we removed the covers completely. The plants grew for another 10 days (14 in total) under long-day conditions. After that, we started treatment with dexamethasone 30 µM + Tween (0.01%) and mock (water + Tween 0.01%) by spraying the rosette with 3 sprays per plant (≈260 µl). At this time, the plants had 4-5 leaves. The treatment was always done at ZT13 (three hours before lights off). After the treatments, the trays were again covered with a transparent cover for 12 hours. At this time, the first openings were made to re-acclimatize the plants one hour after the lights were turned on (corresponding to ZT1), and finally the cover was completely removed 9 hours later (ZT10) (at this time, no moisture was observed on the leaves as a result of the treatment). All apex and leaf samples were collected between ZT14-16. Leaf samples were collected by cutting the petiole of the youngest fully expanded leaf with fine tweezers and immediately freezing it in liquid nitrogen. The apex of the corresponding plant was then harvested, removing all visible petioles, leaflets (small leaves), root, hypocotyl and stem. The apex was immediately frozen in liquid nitrogen. All samples were stored at -80 ºC until processing for metabolites extractions.

11.1. Extraction of metabolites and preparation of samples

For each treatment (Dexa and Mock) and time point (days), 10-11 mg fresh weight of frozen sample from the apices and 16-17 mg from the leaves were used for metabolite extraction and analysis by targeted metabolomics (GC-TOF-MS and LC-QTOF-MS) and untargeted metabolomics (LC-QTOF-MS). Metabolites were extracted according to the procedure described in (Gullberg et al., 2004), using 1 mL of the extraction mixture (chloroform: methanol:water v/v (1:3:1) , from which we obtained 900 ul of supernatant. Subsequently, 166 µl of the apex and 100 µl of the leaf extractions were dried in SpeedVac and prepared for metabolomics analysis using GC-TOF-MS and LC-QTOF-MS. Quality control (QC) samples were prepared by pipetting 50 µl of each sample, each time and each condition up to a stock of 400 µl. The remainder of the extraction volume was stored at -80°C (518 µl for apices and 650 µl for leaves) and used for hormonal

quantifications essays. For lipidomics, we perform chloroform/methanol-based extractions using the same procedure as in Melo et al., 2021.

11.2. Targeted metabolomics by GC-MS

Samples were derivatized overnight at room temperature by adding 30 µL methoxyamine (15 ng/µL pyridine), followed by 30 µL MSTFA with 1% TMCS for 1 hour, and finally 30 µL methyl stearate (15 ng/µL in heptane) was added before injection into the instrument. The internal standards (IS) were added as described in (Gullberg et al., 2004).The GC-TOF-MS instrument used was an Agilent 7890B gas chromatograph equipped with a 10 m × 0.18 mm fused silica capillary column with a 0.18 µm Rxi-5 Sil MS stationary phase (Restek Corporation, U.S.) and connected to a Pegasus BT time-of-flight mass spectrometer, GC-TOF-MS (Leco Corp., St Joseph, MI, USA). Splitless injections were performed using an L-PAL3 autosampler (CTC Analytics AG, Switzerland). The temperature of the injector was 270 ºC, the purge flow rate was 20 mL min^{-1} and the column temperature was held at 70ºC for 2 minutes, then raised by 40 ºC min^{-1} until 320 ºC and remained there for 2 minutes. The transfer line temperature was 250 °C and the ion source was 200 °C. Ions were generated with a 70 eV electron beam at an ionization current of 2.0 mA, and 30 spectra/s were recorded in the mass range m/z 50-800. The accelerating voltage was turned on after a solvent delay of 150 s. All generated spectra files were converted to NetCDF file format and peak alignment, integration and feature identification files were processed using in-house scripts for MATLAB ver. 8.1. To determine the retention time index of the detected compounds, an alkane mixture (C12 - C40) was analyzed (Schauer et al., 2005). Metabolite identification was performed manually by comparing mass spectra and retention indexes using NIST MS Search v. 2.0 with in-house libraries and NIST98 spectral database.

11.3. Targeted and untargeted metabolomics and lipidomics by LC-MS.

For untargeted and targeted metabolomics analysis, the LC-QTOF-MS instruments used was an Agilent 1290 Infinity UHPLC system (Agilent Technologies, Waldbronn, Germany) for chromatographic separation with an Acquity UPLC HSS T3, 2.1 × 50 mm, 1.8 µm C18 column in combination with a 2.1 mm × 5 mm, 1.8 µm VanGuard precolumn

(Waters Corporation, Milford, MA, USA). 2 µl of the resuspended samples (methanol: water 50%) containing internal standards (Gullberg et al., 2004). Mobile phases A (water containing 0.1% formic acid) and B (75/25 acetonitrile: 2-propanol, 0.1% formic acid) were used as elution buffers for the gradient. For each injection, the initial flow rate was 0-5 mL min^{-1} and the compounds were eluted with a linear gradient of 0.1-10% of B for 2 minutes. The gradient was increased to 99% over 5 minutes and held at 99% for 2 minutes. Then B was gradually reduced until the next injection at a flow rate of 0-5 mL min^{-1}. The mass spectrometer was an Aligent 6550 Q-TOF with jet stream electrospray ionization in positive or negative ion mode. The same settings were used for both modes, with a capillary voltage of 4000 V in positive or negative mode. For more information on the procedures, please refer to (Abreu et al., 2020).

Lipidomics was performed in the positive mode. The instrument was the same as previously described, but the pre-columns and columns were changed. The precolumn was 2.1 mm × 5 mm, 1.7 µm VanGuard (Waters Corporation, Milford, MA, USA) and the column was Acquity UPLC CSH, 2.1 × 50 mm, 1.7 µm C18. The gradient elution buffers were A (60:40 acetonitrile:water, 10 mM ammonium formate, 0.1% formic acid) and B (89.1:10.5:0.4 2-propanol:acetonitrile:water, 10 mM ammonium formate, 0.1% formic acid) at a flow rate of 0.5 mL/min.

All the generated files for targeted metabolomics and lipidomics were processed using MassHunter Profinder B.08.00 (Agilent Technologies).

11.4. Hormone quantification

For hormone quantification, we added an IS mix containing 80 pg/µl of the deuterated hormones SA-D6, IAA-13C6, JA-D6 and ABA-D6 (Olchemim Ltd., Olomouc, Czech Republic) to each sample. The samples were evaporated using a SpeedVac concentrator (Savant Instrument, Framing-dale, NY, USA) until approximately 100 µl of solvent was left, and a small aliquot of the remaining supernatants were pooled and used to create quality control (QC) samples. After evaporation, 5 µl of 1M HCl was added prior to solid phase extraction (SPE) analysis. SPE was performed using a Biotage Pressure +48 manifold (Biotage, Uppsala, Sweden). All samples were purified using a reversed-phase HLB Oasis® column (1 cc/30 mg, Waters). The SPE sorbent was activated and

equilibrated according to the manufacture's instructions (Waters). Prior to analysis, samples were resuspended in methanol (16 µl): water (24 µl). A 9-level calibration of curve IAA; ABA; JA and SA was prepared by serial dilution (ranging: 62.5 fg/µl - 400 pg/µl) and spiked with internal standards (0.1 ng/µl). The analysis was conducted using an Agilent UHPLC system (Infinity 1290) coupled with an electrospray ionization source (ESI) to an Agilent 6495 triple quadrupole system equipped with iFunnel Technology (Agilent Technologies, Santa Clara, CA, USA). Chromatographic separation was performed on a Waters UPLC HSS T3 column (2.1 mm × 50 mm, 1.8-µm particle size), the mobile phase consisted of 0.1% acetic acid in MQ-water (A) and ACN (B). The gradient was 15% B for 5 min followed by a linear gradient from 15 to 50% over 2.5 minutes, then increased from 50 to 99% B in one minute, hold at 99% B from 8.5-9.5 min, and thereafter returned to initial conditions and re-equilibrated for 2 minutes. The flow rate was set of 600 µL/min and the column was heated to 40 °C. Prior to analysis the samples were dissolved in 40 µl 40 % MeOH containing internal standards (0.1ng/µL), injection volumes were 10 µL. The mass spectrometer was operated in positive/ negative switching ESI mode with gas temperature set at 150°C; gas flow 12 L min-1; nebulizer pressure 20 psi; sheath gas temperature 400°C; sheath gas flow 12 L min-1; capillary voltage 4000 V (neg), 3500 V (pos); nozzle voltage 1500V (pos), 500 V (neg); iFunnel high pressure RF 150 V; iFunnel low pressure RF 60 V. The fragmentor voltage 380 V and cell acceleration voltage 5 V. Data were processed using MassHunter Qualitative Analysis and Quantitative Analysis (QqQ; Agilent Technologies, Atlanta, GA, USA) and Excel (Microsoft, Redmond, Washington, USA) software. Different extract volumes and mg of starting material were compensated for during calculations.

11.5. Transcriptome analysis

RNA extraction and DNAse treatment for transcriptome analysis were performed using the RNeasy Plant Mini Kit and RNase-Free DNase Set from Qiagen. Extracted RNA was quantified using NanoDrop ND1000 and its quality was determined in a Bioanalyzer 2100 (Agilent). Samples were sequenced on NovaSeq6000 (NovaSeq Control Software 1.6.0/RTA v3.4.4) with a 151nt(Read1)-10nt(Index1)-10nt(Index2)-151nt(Read2) setup using 'NovaSeqXp' workflow in 'S4' mode flowcell. The Bcl to FastQ conversion was

performed using bcl2fastq_v2.20.0.422 from the CASAVA software suite. The quality scale used is Sanger / phred33 / Illumina 1.8.

Pre-processing of the data was performed according to the guidelines described here: http://franklin.upsc.se:3000/materials/materials/Guidelines-for-RNA-Seq-data-analysis.pdf. Briefly, the quality of the raw sequence data was assessed using FastQC (http://www.bioinformatics.babraham.ac.uk/projects/fastqc/) v0.11.4. Residual ribosomal RNA (rRNA) contamination was assessed and filtered using SortMeRNA (v2.1; Kopylova et al. 2012; settings --log --paired_in --fastx--sam --num_alignments 1) using the rRNA sequences provided with SortMeRNA (rfam-5s-database-id98.fasta, rfam-5.8s-database-id98.fasta, silva-arc-16s-database-id95.fasta, silva-bac-16s-database-id85.fasta, silva-euk-18s-database-id95.fasta, silva-arc-23s-database-id98.fasta, silva-bac-23s-database-id98.fasta and silva-euk-28s-database-id98.fasta). Data were then filtered to remove adapters and trimmed for quality using Trimmomatic (v0.39; Bolger et al., 2014); settings TruSeq3-PE-2.fa:2:30:10 SLIDINGWINDOW:5:20 MINLEN:50). After both filtering steps, FastQC was run again to ensure that no technical artefacts were introduced. Read counts were determined using salmon (v0.14.1, Patro et al., 2017) with non-default parameters --gcBias –seqBias and using the ARAPORT11 cDNA sequences as a reference (retrieved from the TAIR resource; (Berardini et al., 2015; Cheng et al., 2017). Salmon abundance values were imported into R (v3.6.2; R Core Team 2019) using the Bioconductor (v3.10; Gentleman et al., 2004) tximport package (v.1.12.3; (Soneson et al., 2015). For data quality assessment (QA) and visualisation, read counts were normalized using a variance stabilizing transformation as implemented in DESeq2. The biological relevance of the data - e.g. biological replicates similarity - was assessed using Principal Component Analysis (PCA) and other visualizations (e.g. heatmaps), using custom R scripts, available at https://github.com/nicolasDelhomme/arabidopsis-floral-induction. Statistical analysis of differential expression (DE) of genes and transcripts between conditions was performed in R using the Bioconductor DESeq2 package (v1.26.0; Love et al., 2014), with the following model: ~ MGenotype * MDay to account for both the genotype and the day of harvesting. FDR-adjusted p-values were used to assess significance, with a common threshold of 1% used throughout. All expression results were generated using custom scripts in R. Differentially expressed genes (DEGs) determined in the previous step were used for Gene Ontology (GO) enrichment analyses using custom R scripts.

12. Pathway enrichment analysis

12.1. Pathway enrichment analysis for targeted metabolomics and lipid classification.

This type of analysis was performed only for the apex samples. For the targeted metabolome results, after performing the statistical analysis, we selected the "Pathway Analysis" option and the same data normalization, transformation, and scaling as described in the "Statistical Analysis (T-Test/ ANOVA)" section. The enrichment method chosen was the global test > Relative-betweemess Centrality > Reference Metabolome > Arabidopsis thaliana (KEGG).

For the lipidomics results, after performing the statistical analysis, we selected the "Enrichment Analysis" option and the same data normalization, transformation, and scaling as described in the "Statistical Analysis (T-Test/ ANOVA)" section. The metabolite set library was "Main-class" and "Sub-class" for lipid sets. For more information, see FAQ from https://www.MetaboAnalyst.ca/ or (Pang et al., 2021).

12.2. Processing files and pathway enrichment analysis by MetaboAnalyst (untargeted metabolomic data).

The raw spectra files were uploaded to the MetaboAnalyst platform in mzML file format to perform LC-MS spectra processing including QC samples. The LC-MS platform was selected as HPLC-Q/TOF with the default parameters. The polarity selected was negative, and the only abducts selected were [M-H]- and [M+Cl]-. The results were then uploaded for "Functional Analysis" in the "Global Metabolomics" section, and the categories of Dexa and Mock were assigned to each file accordingly. Samples were normalized by the median, "log transformation (base 10)" was selected as the data transformation, and data scaling was "auto-scaling" (mean-centered and divided by the standard deviation of each variable).

To perform the pathway analysis, we selected the GSEA (uses total rank based on t.score) and Mummichog (version 2.0) algorithms and set a p-value cutoff of 0.05. The abducts selected were the same as described previously. Finally, we selected the Plants Pathway Library > Arabidopsis thaliana (KEGG) and identified pathways that contained at least 3 entries.

12.3. Pathway enrichment analysis by Plant Metabolomic Network (targeted metabolomic, lipidomic and transcriptomic data).

For the results of targeted metabolomics and lipidomics in the apex, we performed an analysis of the enrichment of metabolic pathways with those metabolites that showed a significant difference in abundance with a p-value < 0.05 (t-test) for each of the analysis time points (days 1, 3, and 5) and the comparison of conditions (Dexa vs. Mock). For the results from the transcriptome, we selected the DEGs with a fold change > 0.5 and < -0.5 for days 1 and 3. The parameters selected were those reported in (Hawkins et al., 2021).

13. Extraction and analysis of sugar content by GC-MS.

The analysis of sugars in Col-0 and *rs5-2* mutant was performed in the Metabolomics Platform of the Institute of Plant Molecular and Cell Biology (UPV-CSIC) by derivatization followed by gas chromatography-mass spectrometry. All the samples were collected at ZT14- ZT16 from plants grown in vitro under LD conditions. For extraction, Col-0 and *rs5-2* apices and leaves samples (40 mg fresh weight) were homogenized in liquid nitrogen, and 1400 µL 100% methanol with 60 µL internal standard was added to each sample (Ribitol to 0.2 mg/mL in water). The sample was then incubated at 70 ºC for 15 minutes and centrifuged at 14,000 rpm for 10 minutes. The supernatant was transferred to a glass vial, and 750 mL of CHCl3 and 1500 mL of H_2O were added. The mixture was shaken for 15 seconds and centrifuged at 14,000 rpm for 15 minutes. 150 µL of the supernatant (aqueous phase, methanol/water) was dried under vacuum for 3 hours. For derivatization, the dried residues were resuspended in 40 µL of 20 mg/mL methoxyamine hydrochloride in pyridine and incubated at 37°C for 90 minutes. Next, 70 µL of MSTFA (N-methyl-N-[trimethylsilyl]trifluoroacetamide) and 6 µL of a standard mixture for adjusting retention times were added to each sample (mixture of fatty acid methyl esters with 8 to 24 carbons at 3.7% [w/v]) and incubated for 30 minutes at 37ºC. 100 µL of each sample was transferred to a chromatography vial and gas chromatography was performed. Gas chromatography and mass spectrometry: 2 µL of each sample was injected in splitless and split 1:10 mode into a 6890N gas chromatograph (Agilent Technologies Inc. Santa Clara, CA) coupled to a Pegasus 4D TOF mass spectrometer (LECO, St. Joseph, MI). Gas chromatography was performed using a BPX35 column (30 m × 0.32 mm × 0.25 µm) (SGE Analytical Science Pty Ltd., Australia) with helium as the carrier gas at a constant

flow rate of 2 mL/minute. The liner was set at 230°C. The oven program was set at 85°C for 2 minutes and increased to 360°C with a ramp of 8°C per minute. Mass spectra were recorded at 6.25 spectra per second in the range of m/z 35-900 and an ionization energy of 70 eV. Chromatograms and mass spectra were analyzed using CHROMATOF software (LECO, St. Joseph, MI). Compounds of interest were identified by comparison with the spectra of previously traced standards.

RESULTS

Chapter 1: The search for new candidates to regulate flowering time by chemical genetics.

Flowering time is one of the most relevant traits influencing crop productivity and yield. Floral transition is a strictly regulated process in which environmental signals, such as temperature or photoperiod, and endogenous biological cues, like hormonal levels and energy status, are integrated. Furthermore, there is an extensive functional redundancy in flowering regulatory pathways that contributes to a robust floral transition response (Andrés & Coupland, 2012). This extensive redundancy often represents a difficulty when studying the regulation of flowering time through forward genetic approaches. (Serrano et al., 2015). These problems can be circumvented by the use of chemical genetic approaches, which exploit the potential of small molecules to modify biological processes by specifically binding to components of the corresponding pathways (Serrano et al., 2015). Chemical genomics is also a good tool for studying processes regulated by multiple genes, or when a gene product is critical for survival, or when a single gene is responsible for multiple phenotypes. (Serrano et al., 2015). The phenotypes caused by small molecules are mostly reversible and tunable and can act as a general antagonist inhibiting multiple network components or, conversely, they can be specific agonists activating only one of the network components, opening the possibility of identifying specific responses (Tóth & Van der Hoorn, 2010). The use of chemical genetics to search for new regulatory components of the floral pathways or to understand the activity of their modifiers can provide a deeper understanding of the floral regulatory network. Identifying bioactive compounds in the control of floral induction represents an opportunity to identify unknown mechanisms involved in the regulation of this relevant agricultural trait. In this chapter, we describe a chemical genetic screening performed to isolate molecules that modulate the expression of *FT,* a master regulator of floral induction/transition.

1.1. A small library of bioactive molecules to screen for regulators of floral transition.

We performed a chemical-genetic screening in collaboration with Dr. Stéphanie Robert (UPSC, Umea, Sweden), using a library of 360 small molecules. Although 360 molecules might seem small library, this library is especially useful because all these molecules had

been carefully tested and it was confirmed that they can be absorbed by the plant and produce a response in development, therefore behaving as bioactive molecules. This library was selected from a combination of five chemical libraries containing in total 46418 compounds (20000 from Chembridge Diverset library, 10000 from Chembridge Novacore library, 10000 from Sigma TimTec Myria library, 3650 from LATCA library and 2768 compounds from CLICKables library), which were tested in Arabidopsis and tobacco pollen (Drakakaki et al., 2011). The library used in this work was generated in Robert's laboratory by an initial pre-selection using an automated chemical screening system that assesses the effect in vesicle trafficking and ultimately on the plasma membrane via endosomes and associated signal transduction pathways (Drakakaki et al., 2009b; Robert et al., 2008). In the context of our research, this is of great interest because *FT* is a PEBP protein that has been shown to bind to the PC, whose availability in the plant affects flowering time (Nakamura et al., 2014). In addition, there are reports that *FTIP1*, a membrane protein of the endoplasmic reticulum, interacts with FT and is essential for flowering by affecting its transport to SAM (Liu et al., 2012, 2013; Romera-Branchat et al., 2014). In summary, we believe that this library, previously evaluated for vesicular transport, may provide interesting results in the study and identification of novel regulators of floral transition via *FT*.

1.1.1. Characterization of the expression of floral marker genes under *in vitro* culture conditions by RT-qPCR.

The use of *in vitro* chemical genetic screening makes it possible to test the effect of many molecules on the trait of interest in a short time, minimizing space requirements. We aimed to identify molecules that modulate *FT* expression. Since the screening needs to be done with *in vitro* culture grown plants, we tested the expression of *FT* in plants grown under those conditions, as well as the expression of a marker gene for floral transition (*SOC1*) and a floral meristem marker gene (*AP1*). The objective of this first experiment was to characterize the timing of floral transition in seedlings grown under the same condition needed for the screening, to determine the optimal time to perform the screening. For that, we grew Col-0 plants *in vitro* culture under LD and took samples every day (whole seedlings) to determine the time at which a significant increase in the expression of *FT* occurred, associated with an increase in *SOC1* expression and a later upregulation of *AP1* (Figure 1).

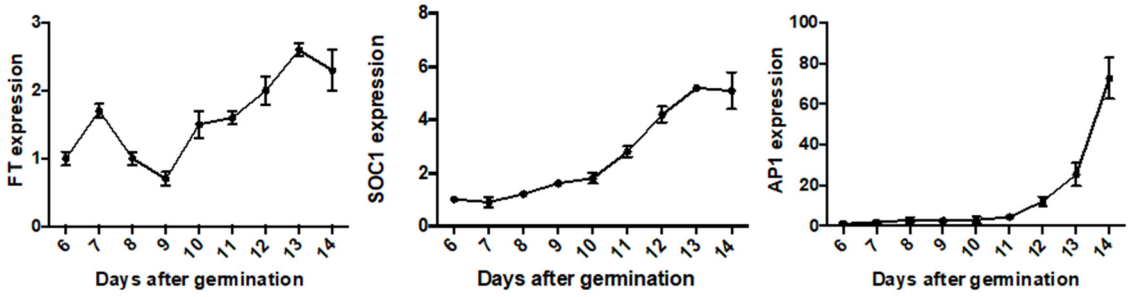

Figure 1. Time-course expression of *FT*, *SOC1* and *AP1* in seedlings grown *in vitro* in long-day. 12 seedlings were collected at ZT10 per biological replicate. *TIP41* was used as reference gene. Error bars indicate the standard error of the mean (SEM) of three biological replicates.

Under these conditions, expression of *FT* increased steadily from day 10 after germination. *SOC1* was consequently up-regulated from day 11 and *AP1* expression was observed from day 12. From these data, we can infer that under these experimental conditions, the floral transition occurs between day 9 and 11 after germination since *AP1* expression on day 12 marks the appearance of the first floral meristems at the shoot apical inflorescence meristem. Therefore, we decided to perform our chemical screening on day 10 after germination in order to be able to identify significant changes in the level of *FT* expression or its spatial expression pattern.

1.1.2. Screening for induction of β-glucuronidase expressed under the *FT* promotor.

To analyze the effect of small molecules on a plant, gene reporters such as *β-GLUCURONIDASE* (*GUS*) and *LUCIFERASE* (*LUC*) can be used to detect the expression of the promoter of the gene of interest (Ruijter et al., 2003). The expression pattern of *FT* has been extensively studied (Cho et al., 2017; Jin et al., 2021; Song et al., 2013). Plants expressing the *GUS* reporter gene under the *FT* promoter display GUS activity in the vascular tissue of cotyledons and leaves (Takada & Goto, 2003). Moreover, it has been shown that mutations in *FT* regulators can cause an increase or a decrease in the reporter signal (Takada & Goto, 2003). Thus, in our experimental approach, we used a reporter line expressing the *GUS* gene under the control of the *FT* promoter (p*FT*::*GUS*).

To perform the first screening, a different molecule was tested in each well, of a 24-wells plate, with 6 seedlings per well and one control (DMSO) per raw. A total of 20 molecules and 4 controls per plate were evaluated and this was repeated twice to obtain two different

technical replicates. A total of 36 plates and 5184 plants were analyzed based on the different signal patterns of *FT* expression detected and categorized into the four GUS expression pattern scenarios compared to controls, as described in Figure 2: no change, increased, decreased, or ectopic expression.

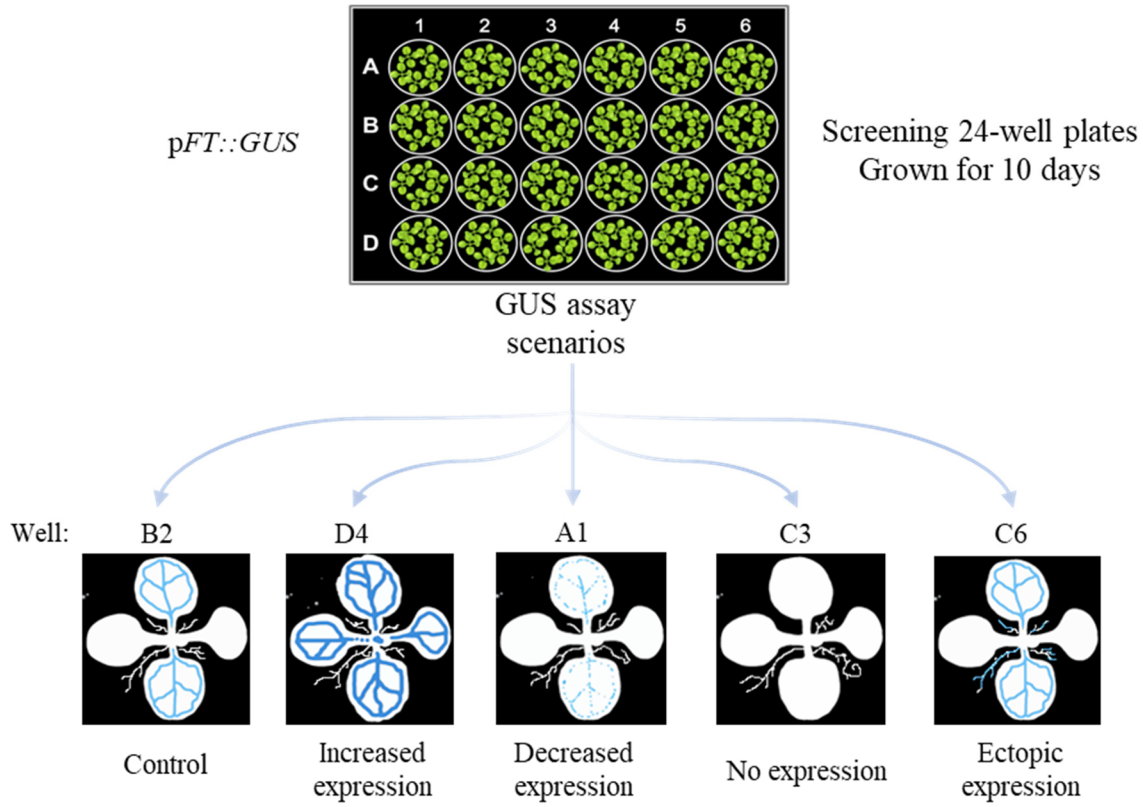

Figure 2. Experimental setup for the p*FT*::*GUS* primary screening of the 360 library bioactive molecules. p*FT*::*GUS* plants were grown *in vitro* culture in 24-well plates under LD conditions, and seedlings were harvested after 10 days. Six seedlings were sown per well. Four control wells (DMSO, mock treatment) were randomly distributed in each plate. A total of 20 molecules were tested per plate. Upper panel shows the experimental design. Lower panel shows the predicted outcomes of the screening.

A second screening was performed to confirm the positive results among the molecules that showed a change in the expression of the *GUS* gene driven by the *FT* promoter. For this purpose, the same setup as described in Figure 2 was used for a total of 3 replicates so that a total of 18 plants were evaluated per molecule. In this way, we found that 12% of the molecules evaluated affected *pFT:GUS* expression, confirming 43 potential hits that were classified into three categories according to their effect: 25 molecules (corresponding to 7% of the molecules tested) caused an increase in *GUS* expression, 7 molecules caused a decrease (2%) and 11 molecules triggered ectopic *GUS* expression

(3%). It should be noted that the ectopic signal detected was found in the roots (Figure 3).

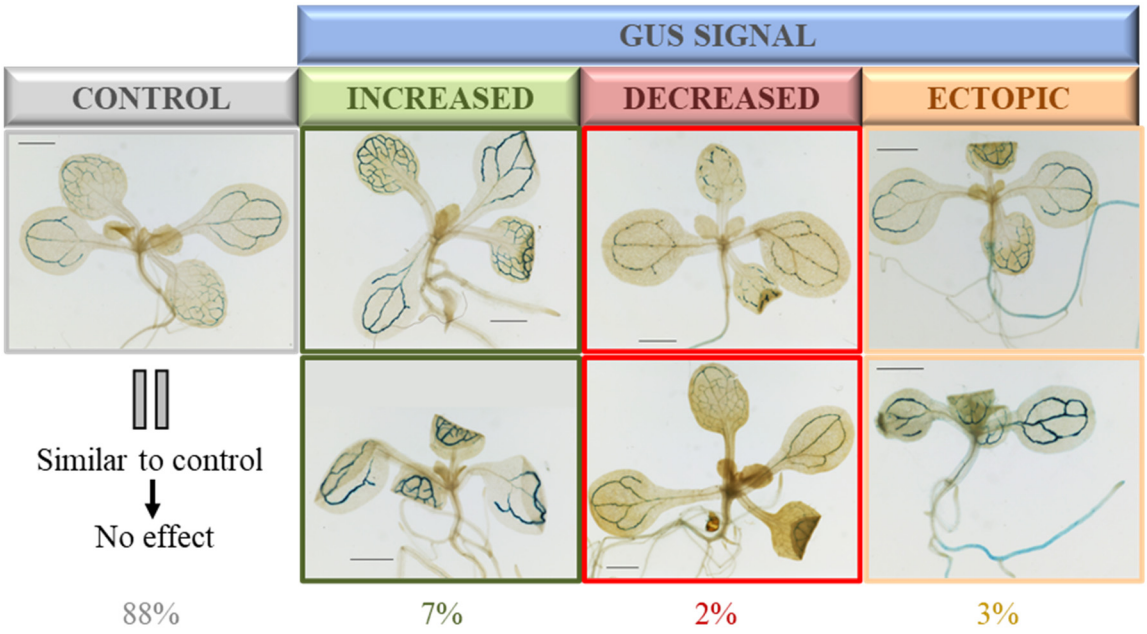

Figure 3. Representative image of the results of the secondary screening after testing the library of molecules for their effect on *pFT:GUS* expression. After the screening, tested molecules were grouped into four categories depending on the change of GUS signal that they caused. Similar to control (grey), increased (green), decrease (red) and ectopic signal (orange). The scale bars indicate 1mm.

Among the molecules that caused changes in expression of p*FT::GUS* line (Figure 3), we selected six molecules for further analysis based on several criteria, including the stability of the response across the screenings, the degree of change in *GUS* expression and the price of the synthetic molecules in the market. Selected molecules are shown/indicated in Table 1.

Table 1. Molecules identified as positive hits in the chemical screening and selected for further analysis.

ID[a]	Molecule	Formula	MW[b]	Abr[c]
5528790	4-tert-butyl-N'-(2-pyridinylmethylene)benzohydrazide	$C_{17}H_{19}N_3O$	281	CF1
5532951	N'-[(2-methyl-1H-indol-3-yl)methylene]-2-(2-methylphenoxy)acetohydrazide	$C_{19}H_{19}N_3O_2$	321	CF2

5556103	3-chloro-N'-(2-pyridinylmethylene)-1-benzothiophene-2-carbohydrazide	C_{15} H_{10} Cl N_3 O S	316	CF3
5845432	2,4,6-trimethyl-N-(5-methyl-1,3,4-thiadiazol-2-yl)benzenesulfonamide	C_{12} H_{15} N_3 O_2 S_2	297	CF4
7658085	1-(2-chloro-6-fluorobenzyl)-2-methyl-1H-benzimidazole	C_{15} H_{12} Cl F N_2	275	CF5
7493237	3-[(4-chloro-1H-pyrazol-1-yl)methyl]-N-(pentafluorophenyl)benzamide	C_{17} H_9 Cl F_5 N_3 O	402	CF11

[a] ID: identification number in the ChemBridge database.
[b] MW: molecular weight.
[c] Abr: abbreviated name used in the text for the molecule.

Among the molecules that affect the GUS signal, increasing it, it was pipecolic acid (Pip). This metabolite is of importance in the context of our research and we will discuss this molecule in more detail in Chapter 2. For now, it is worth noting that we previously identified Pip as a molecule differentially accumulating when comparing the metabolome of plants induced to flower by photoperiod with that from non-induced plants (Chapter 2). Treatment of *pFT:GUS* seedling with Pip caused an increase in the GUS signal that can be observed in Figure 4.

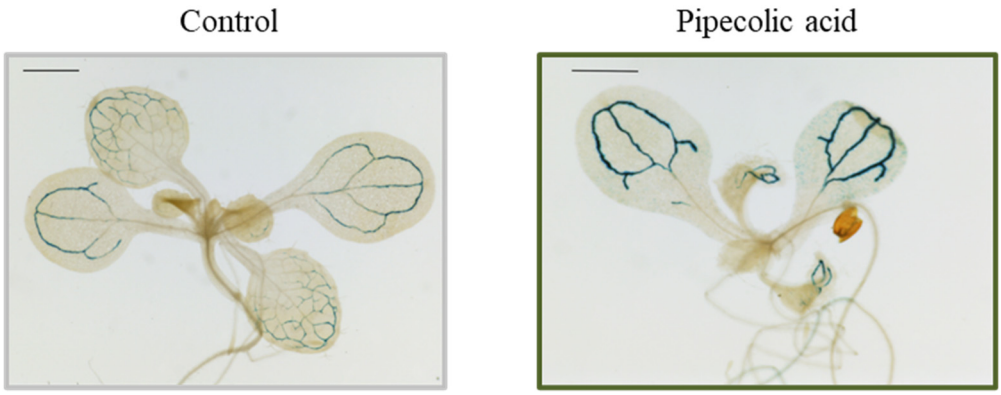

Figure 4. Effect of pipecolic acid expression on p*FT::GUS* expression pattern. 10-days-old p*FT::GUS* plants grown *in vitro*, under LD conditions, on MS media supplemented or not with pipecolic acid. Scale bars represent 1 mm.

1.2. Developing tools for a secondary screening with a luciferase reporter system.

Primary chemical genetic screenings must be followed by a robust secondary screening that allows to discard effects that are not related to the analyzed/studied pathway. For example, a molecule could cause non-specific activation of GUS activity or could activate the expression of a particular gene but blocking the activation of downstream targets. The design of robust secondary screenings are therefore crucial to choose among promising positive hits and identify useful bioactive molecules. With this aim, we have designed two tools to evaluate positive hits from the primary screening. First, we set up a system to evaluate the effect of the molecules on *FT* expression level using an alternative reporter system (to discard unspecific effects of the molecules selected on the basis of GUS activity). Second, we designed a tool to evaluate the effect of the selected molecules based on the expression of *AP1*, a well-known *FT* target gene. If a molecule is specifically activating endogenous *FT* expression, expression of FT target genes (FT signaling) should also be modulated by treating plants with that molecule.

We generated a reporter line expressing the *LUC* gene under the control of the *FT* promoter (p*FT*:*LUC)*. The *LUC* reporter gene is a tool that allows the quantification of changes in its expression measured as a luminescent signal. In order to evaluate if the reporter line replicated the expression of the *FT* gene, we generated a transgenic homozygous line and measured *LUC* expression after a SD-to-LD shift, a treatment known to activate *FT* expression. Figure 5 shows the results of one of the transgenic *pFT::LUC* lines (#4), displaying expression of *LUC* in the vascular tissue in response to the change in photoperiod conditions, as expected. We, therefore, concluded that we could use this line as a tool to perform a secondary screening to evaluate the potential of the selected molecules.

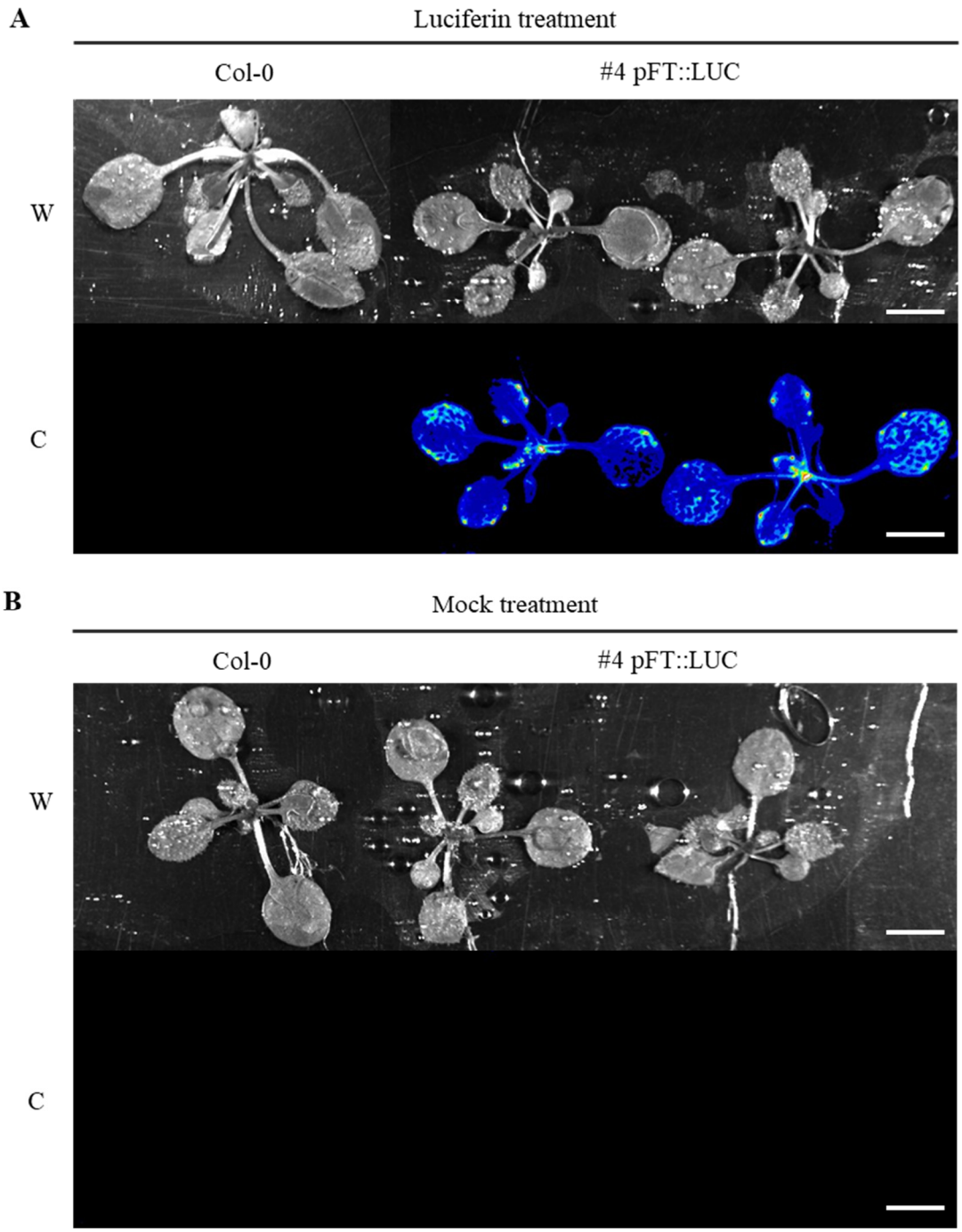

Figure 5. *In vivo* luciferase assay of p*FT::LUC* #4 line. Homozygous p*FT:LUC* #4 plants and Col-0 plants were grown for 20 days in SD and then transferred to LD conditions. After 1 day in LD, luciferin (30µM) was sprayed on the plants and luminescence signal was captured at ZT14 - ZT16. W, white light and C, chemiluminescence. In **A** and **B,** plants were treated with luciferin and the mock solution, respectively. The scale bars indicate 1 cm.

Our second approach to evaluate the effect of the selected molecules of *FT* signaling consisted of using a reporter line where *LUC* expression was driven by *AP1* promoter. With this aim, we generated a batch of p*AP1::LUC* lines and, after isolating two

homozygous lines with an insertion, we evaluated the behavior of these two lines (p*AP1::LUC* #7 and #16) to test whether *LUC* signal mimicked that of endogenous *AP1* expression. For that, we grew p*AP1*::*LUC* plants under SD and transferred them to LD. We analyzed the images in vivo by spraying the plants with luciferin solution (Figure 6A) and in parallel, we collected the shoot apices to quantify the luminescence signal over time (Figure 6B). Activation of *AP1* after the SD-to-LD shift was observed in both lines, but in p*AP1::LUC* #16 line, luciferase activity levels in the apex were significantly higher than in p*AP1::LUC* #7. Thus, we concluded that p*AP1::LUC* #16 line displayed a better response to photoperiodic induction and is more suitable for detecting variations of *FT* signaling as it has a higher response than line #7.

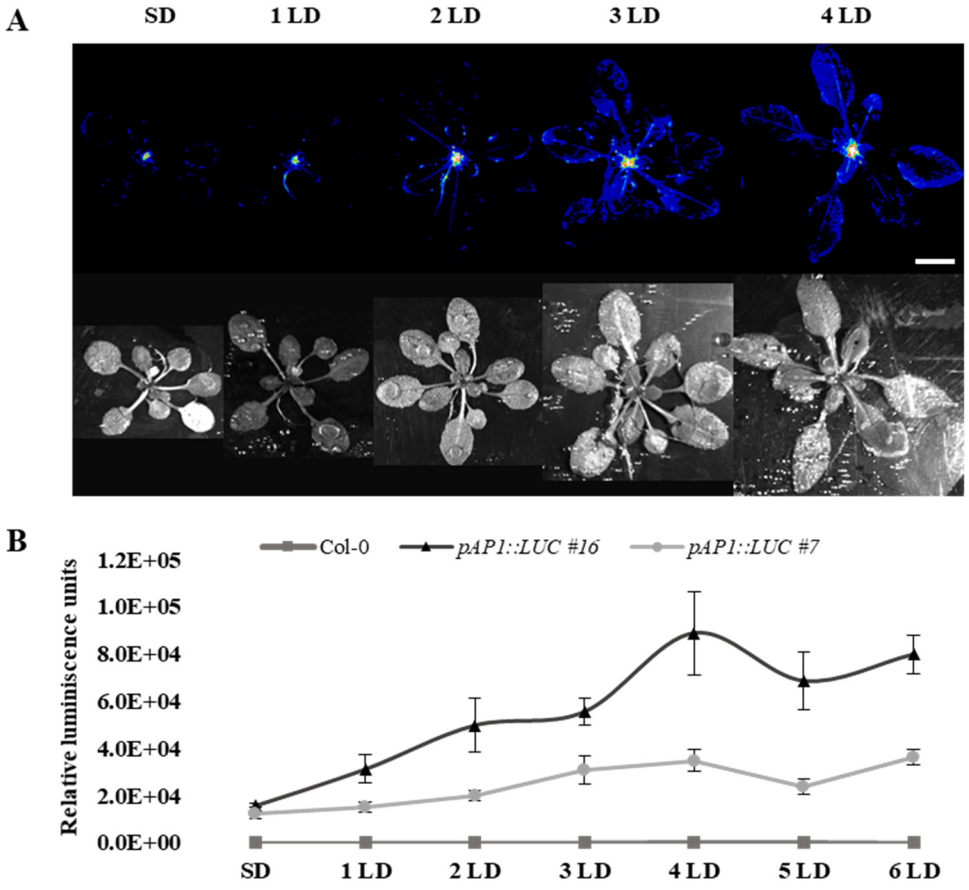

Figure 6. Evaluation of homozygous p*AP1::LUC* reporter lines. Plants were grown for 20 days under SD conditions and then transferred to LD. **A,** Visualization of *in vivo* luciferase activity in line p*AP1::LUC* #16. Luciferin (30µM) was applied one day after transfer to LD by spraying the plants. Images were captured at ZT14 - ZT16 with LAS-3000. Scale bar indicates 1 cm. **B,** Time-course of luciferase activity in the apex of plants from *pAP1::LUC* #7 and *pAP1::LUC*#16 lines during a SD-to-LD shift. Apices were collected at ZT15. Error bars indicate the standard error of the mean (SEM) of six biological replicates. The scale bar indicates 1 cm.

In summary, we have generated two transgenic lines, p*FT*::*LUC* and p*AP1*::*LUC*, as tools to perform a robust secondary screening and evaluation of the selected molecules, discarding possible unspecific effects and fine-tuning the selection of the most promising candidate molecule with the potential to modulate *FT* expression and signaling.

1.2.1. Re-testing the molecules selected among the positive hits in the first and second screenings.

Once selected the candidate molecules, we obtained new stocks from those (Chembridge) and proceeded to test their effect on seedling development at different concentrations, as done in section 1.1.2. Since the concentration range of molecules in the library varied between 25 and 50 μM, we decided to initially test the effect of concentrations ranging from 12.5μM to 100 μM for each molecule. As described for the first and second screenings, seeds from the p*FT*::*GUS* reporter line were sown in MS media and grown *in vitro* in the presence of each of the six selected molecules at the concentrations indicated in Table 2. The effect of the molecules on the growth of seedlings was assessed at day 10.

Table 2. Effect of different concentrations of the six selected molecules on the growth of p*FT*::*GUS* seedlings.

	Concentration (μM)				
Molecule	**100**	**75**	**50**	**25**	**12.5**
CF1	No germination	No germination	No germination	Chlorotic seedlings	Healthy seedlings
CF2	No germination	No germination	Chlorotic seedlings	Chlorotic seedlings	Healthy seedlings
CF3	No germination	No germination	Chlorotic seedlings	Healthy seedlings	Healthy seedlings
CF4	No germination	No germination	Dwarf	Healthy seedlings	Healthy seedlings
CF5	No germination	No germination	No germination	No germination	Healthy seedlings
CF11	No germination	No germination	No germination	No germination	Withe seedlings

	Concentration (µM)			
	20	**10**	**5**	**2.5**
***CF11**	No germination	White seedlings	Pink seedlings	Healthy seedlings

*****Additional experiment to determine the non-toxic concentration of CF11. Seeds were sown on MS media supplemented with the indicated concentrations of the molecules and grown under *in vitro* culture conditions. The response of the seedlings to the different concentrations is described below. No germination means that no plant germinated. Chlorotic means that cotyledons and leaves were yellow. Dwarf means that the growth of all tissues of the seedling is reduced. White and pink refers to the color of the entire seedling, cotyledons and leaves. Healthy means that no phenotype was observed compared to the controls in DMSO.

Surprisingly, almost all tested concentrations showed some degree of toxicity effect on the growth or development of the seedlings (germination inhibition, chlorosis or other developmental defects, such as coloration or size as described in Table 2). We found that CF1 and CF2 caused seedling toxicity at concentrations between 50 and 25 µM, but a healthy growth at 12.5 µM compared with the controls. Treatment with CF3 and CF4 at a concentration of 50µM resulted in chlorosis and dwarfism, respectively. Meanwhile, a concentration of 25µM showed no apparent effect on seedling growth or development. The CF5 molecules inhibited germination at all concentrations except at 12.5µM, where the seedlings grew as control seedlings. Finally, for the CF11 molecule, all concentrations tested showed adverse effects on germination, or the seedlings exhibited a pigment deficiency. For CF11, we performed an additional experiment expanding the range of concentrations tested (Table 2, Additional experiment). As a result, we found that the seedlings that grew at the lowest CF11 concentration, 2.5 µM, were the only ones in which no developmental alterations were detected and were similar to the control seedlings to which only DMSO was added. Based on the results obtained, we determined that the concentrations to be used to assess/study the effect of the molecules on the expression of *FT* should be less than 25 µM for CF1, CF2 and CF5, less than 50 µM for CF3 and CF4, and less than 5 µM for CF11.

1.3. An additional screening based on the *LUC* reporter gene to analyze the effect of the molecules on *FT* expression.

A secondary screening was conducted with the selected molecules to discard the possibility of an unspecific effect of the molecules on the reporter system used in the primary screening (p*FT::GUS*). To do so, we used the p*FT::LUC* lines described in section 1.2, with a new system that allowed us to analyze a larger number of plants while reducing the amount of medium and molecules required. In addition, the use of LUC reporter systems instead of GUS has the advantage of allowing quantification of the signal, which makes these reporters more suitable for the generation of dose-response curves.

Thus, we used 96-well plates with a semiautomatic quantification system of the *LUC* reporter by image analysis (García-Maquilón et al., 2021), and we adapted it to analyze the variation of *FT* expression. This system is a good choice for studying *Arabidopsis* because the seedlings are small and fit in the microwells. As there was/is no need to grow the plants for a long time to measure *FT* expression, we could screen a large number of plants and, therefore, replicates. In this way, for each concentration evaluated in this screening, we tested at least 12 biological replicates. We grew the plants for eight days in MS1 medium supplemented with the CF molecules at different concentrations under LD conditions and measured the bioluminescence through the day. Luciferin was added to the microwell plates at ZT2, and then the plates were returned to the growth chamber for one hour until we started measuring luciferase activity from ZT3 and every two hours for the following 8 hours (Figure 7).

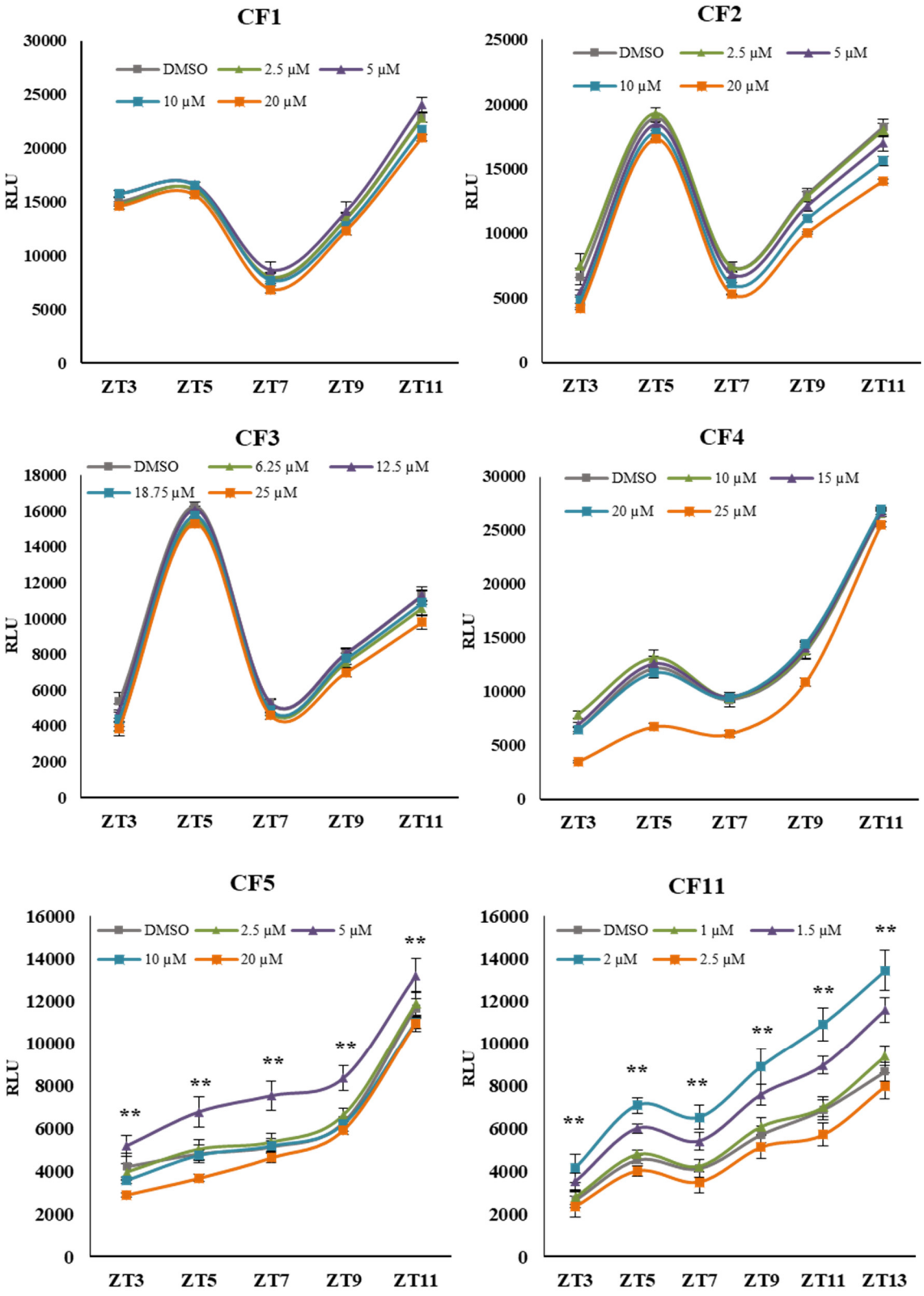

Figure 7. Luciferase activity in p*FT:LUC* plants grown in medium supplemented with the six different molecules. For each molecule concentration, twelve plants were measured. Twelve control plants were placed in the next row of the plate. No differences were detected between

controls in the different plates, so we analyzed the data of all control plants per plate together as a group (n =48). Error bars indicate the standard error of the mean (SEM). Plants were grown under long-day conditions in an *in vitro* growing chamber. RLU means relative luminescence units. Statistical differences were detected in CF5 at 5 µM and CF11 at 1.5 and 2 µM in all time-points analyzed. ** indicates P-value < 0.01.

The highest concentration had a growth inhibitory effect for all the molecules studied, with seedlings smaller than those at the other concentrations and to those from the DMSO control. The concentrations of 20 µM for CF1 and CF2, 25 µM for CF3 and CF4, and 2.5 µM for CF11 were at the toxicity limit to the plants. In the case of CF5, plants grew smaller at both 20 µM and 10 µM. In contrast, the other concentrations did not lead to any change in development compared to the control plants grown in DMSO. Analyzing the global effect of each molecule, we can conclude that CF1, CF2, CF3, and CF4 did not cause any changes in luciferase activity, as we could not detect significant differences at any time point in the other three concentrations analyzed. In contrast, CF5 and CF11 showed a change in the luminescence signal. At 5 µM, plants growing in the presence of the CF5 molecule showed an increase in luminescence signal of *pFT:LUC* over time. Finally, at 2 µM and 1.5 µM, the incubation with CF11 resulted in an increase in the *pFT:LUC* signal that was more significant the higher the molecule concentration in the culture medium. Based on the results obtained, we selected the molecules CF5 and CF11 to evaluate their effect on flowering time.

1.4. Effect of CF5 and CF11 on flowering.

Plants overexpressing *FT* have an early flowering phenotype (Kardailsky et al., 1999). One of the advantages of using the *LUC* reporter treatment in vivo is that treatment with luciferin can be reversible without killing the plant. To assess whether the enhanced signal from the *pFT:LUC* reporter observed after treatment with the CF5 and CF11 molecules leads to early flowering, we measured flowering time in plants treated with these biomolecules. The results are shown in Figure 8.

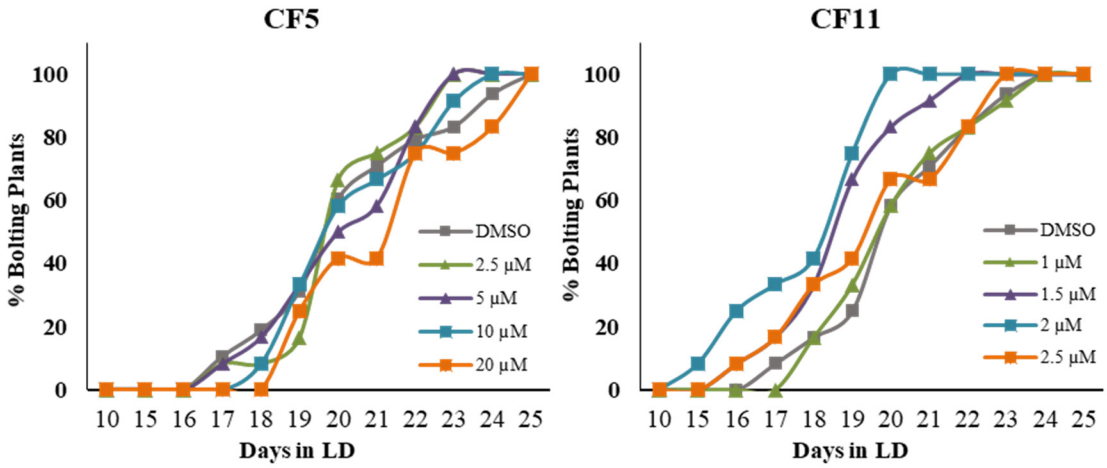

Figure 8. Flowering time of the p*FT*::*LUC* line in response to the CF5 and CF11 molecules. On the left is the percentage of plants that flowered in response to different concentrations of the CF5 and DMSO. On the right is the percentage of plants that flowered in response to different concentrations of the CF11 molecule and DMSO. One plant per well until a total of twelve were measured for each condition (different concentrations or DMSO). Measurements were repeated twice in two different plates per molecule. Plants were grown on MS1 medium, supplemented with different concentrations of CF5 and CF11, under long-day conditions, in an *in vitro* chamber.

We did not observe any alteration in flowering time in the plants grown in medium containing different CF5 concentrations. Regarding CF11, we observed that plants grown in media with a CF11 concentration that led to an increase in the luciferase signal (Figure 7) showed an early flowering phenotype compared with control plants grown with DMSO. Differences were 4 days earlier flowering in plants grown with 2 µM CF11 and 3 days in plants with 1.5 µM CF11. Interestingly, the plants grown at 2.5 µM were smaller than the control plants but still had a similar luminescence signal intensity. This was not expected because since they have less leaf tissue, the activity of the LUC driven by the *FT* promoter should also be lower. Based on these results, we concluded that the CF11 molecule causes an increase in the expression of the p*FT*:*LUC* transgene, which correlates with early flowering.

Chapter 2: Effect of Pipecolic acid on plant development.

With the aim of characterizing metabolic changes associated with the floral transition in Arabidopsis, a preliminary characterization of those changes was performed by comparing metabolic profiles of leaves and shoot apices from plants after a SD to LD transfer, a condition that has shown to induce flowering (Hempel & Feldman, 1995). This pilot experiment identified Pipecolic acid (Pip), a non-protein amino acid, as a metabolite accumulating in leaves during floral induction (increasing between 2 and 3.5 times in plants induced to flower, 2 days after transfer to LD conditions, compared to those growing in non-inductive SD conditions). Moreover, a preliminary experiment with *in vitro* grown *Arabidopsis* plants showed that the addition of Pip in the growth media accelerated bolting compared to non-treated plants. As mentioned in the introduction, Pip was found to have floral promoting effects in duckweed (Fujioka et al., 1987; Fujioka and Sakurai, 1992; Fujioka and Sakurai, 1997).

However, results from this initial Characterization provided us with quite limited results in terms of the number of identifying metabolites with significant changes, possibly due to the fact that microdissection of apices led to an extended sampling time that could have been the cause of a strong variability among replicates masking changes associated with floral transition, Despite this, and due to the fact that a flowering promoting effect of Pip had been previously described in duckweed (Fujioka et al., 1987; Fujioka & Sakurai, 1992, 1997; Kaihara & Takimoto, 1990), we investigated its potential in regulating plant development, focusing on the control of flowering time.

2.1. Studying the effect of Pipecolic acid on flowering time.

2.1.1. Analysis of growth of Arabidopsis under different Pip concentrations *in vitro*.

Plant *in vitro* culture represents an effective procedure for testing the effect of biomolecules on growth and development. Being the plants in permanent contact with the culture media through the roots facilitates absorption of the biomolecule, increasing the chances of causing/leading to a phenotype associated with the biomolecule. Therefore, we analyzed the effect of Pip at different concentrations on plant development *in vitro* culture and under long-day growing conditions.

Table 1. Flowering time of Col-0 plants grown *in vitro* on MS medium supplemented with different Pip concentrations.

Condition	Rosette leaves [a]	Cauline leaves [a]	Total leaf number [a]
MS	8.8 ± 0.7	2.9 ± 0.9	11.7 ± 1.2
MS + Pip 100 mM	9.1 ± 1	3 ± 0.6	12.1 ± 1.2
MS + Pip 1 mM	8.6 ± 1.1	3.2 ± 0.8	11.8 ± 1.6
MS + Pip 0.1 mM	8.3 ± 0.8	2 ± 0.9	***10.3 ± 1.3**[b]

[a] Data shows the average number of leaves +/- standard deviation; n=16.
[b] ANOVA with Tukey correction was performed to calculate the significance differences relative to MS control. In bold, cases where statistical differences were detected, * p value<0.05

We observed that Pip added to *in vitro* MS medium at 0.1 mM slightly promoted flowering. Surprisingly, we did not find any differences in flowering time at higher Pip concentrations.

2.1.2. Flowering time in knock-out mutants of genes involved in pipecolic acid biosynthesis.

The *ALD1* and *SARD4* genes sequentially control Pip biosynthesis. The ALD1 enzyme uses lysine as a substrate to produce Δ^1-P2C. Then, SARD4 catalyzes the production/conversion of Δ^1-P2C to Pip. To further understand the putative role of Pip on flowering, we characterized the flowering time of the knock-out mutants *ald1-1* and *sard4-5*, affecting Pip biosynthesis. It has been reported that the *ald1-1* mutant does not accumulate Pip, but in the *sard4*-5 mutant, accumulation of reduced amounts of Pip has been described (Hartmann et al., 2017). The determination of flowering time of these mutants, measured as total leaf number and days to bolting, is shown in Figure 1.

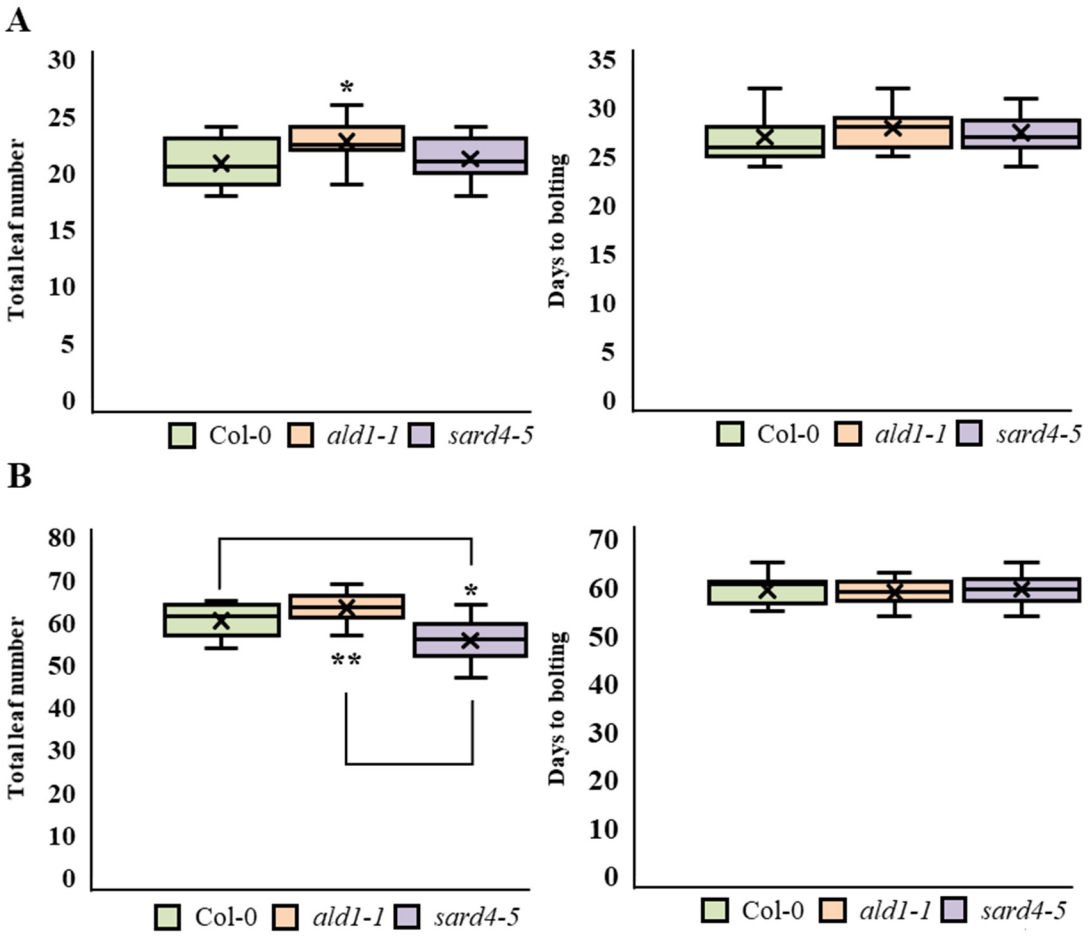

Figure 1. Flowering time characterization of Col-0, *ald1-1* and *sard4-5* mutants. **A,** Determination of flowering time of plants grown under LD conditions. The number of total leaves is shown on the left panel, days to bolting on the right panel. **B,** Determination of flowering tine of plants grown under SD. Boxplots show the first and the third quartile, and the line represents the median. The mean is shown as a cross. Whiskers show the highest and lowest values. Sample size in SD is n =12, sample size in LD is n=16. ANOVA with Tukey correction was performed to calculate the significance differences marked by long lines. ** indicates p-value < 0.01 and * indicates p-value < 0.05.

The result of this experiment showed that the *ald1-1* mutant exhibited a moderate but significant delay in flowering time, producing more leaves than Col-0 under both LD and SD conditions. In contrast, the *sard4-5* mutant flowered with the same number of leaves than Col-0 under LD but flowered with a moderately smaller number of leaves than the wild type under SD. Interestingly, though *ald1-1* and *sard4-5* differed from the wild type in the number of leaves to flowering, no difference in the bolting time was observed

between the mutants and the wild type. This indicates that the formation rate of new leaves at the shoot apical meristem, the plastochrone, is altered in these mutants.

2.2. Characterization of the effect of *ald1-1* and *sard4-5* mutations on the area of the rosette.

In our conditions, we have observed that the plants grown under short days usually produce bigger rosette leaves than the ones grown in long days. In addition, overexpression of *FT* has been reported to cause early flowering and to stop rosette leaf growth, while the wild types continue leaf growth expansion. Probably, and considering that the floral meristems are strong sinks, it has been proposed that stopping leaf expansion could be a strategy to balance the energy needs of the floral meristem (Duplat-Bermúdez et al., 2016). Because of that, differences in leaf size between different genotypes are more noticeable under SD conditions. To study the size of leaves of *ald1-1* and *sadr4-5* plants, we grew plants under SD conditions for 28 days. Then, a fraction of the plants were maintained under SD and the others were transferred to LD, to induce the floral transition and, at the same time, evaluate if there was any relation between defects in flowering time and rosette size.

The rosette area was measured when the bolting inflorescences were 1 cm high. The Figure 2A shows that *ald1-1* and *sard4-5* rosettes look bigger than the wild type. In addition, we observed that both under SD and SD-to-LD conditions, the *ald1-1* and *sard 4-5* mutants showed significant differences in rosette size in comparison to the wild type (Figure 2B, left), with SD and SD-to-LD means of 63.1 ± 5.4 cm^2 and 30.6 ± 6.1 cm^2 for *ald1-1*, 45.4 ± 13.3 cm^2 and 22.4 ± 5.8 cm^2 for *sard4-5* and 36.7 ± 8 cm^2 and 15.8 ± 4 cm^2 for Col-0. The *ald1-1* mutant displayed the most severe rosette size phenotype meanwhile *sard4-5* displayed an intermediate phenotype between *ald1-1* and Col-0.

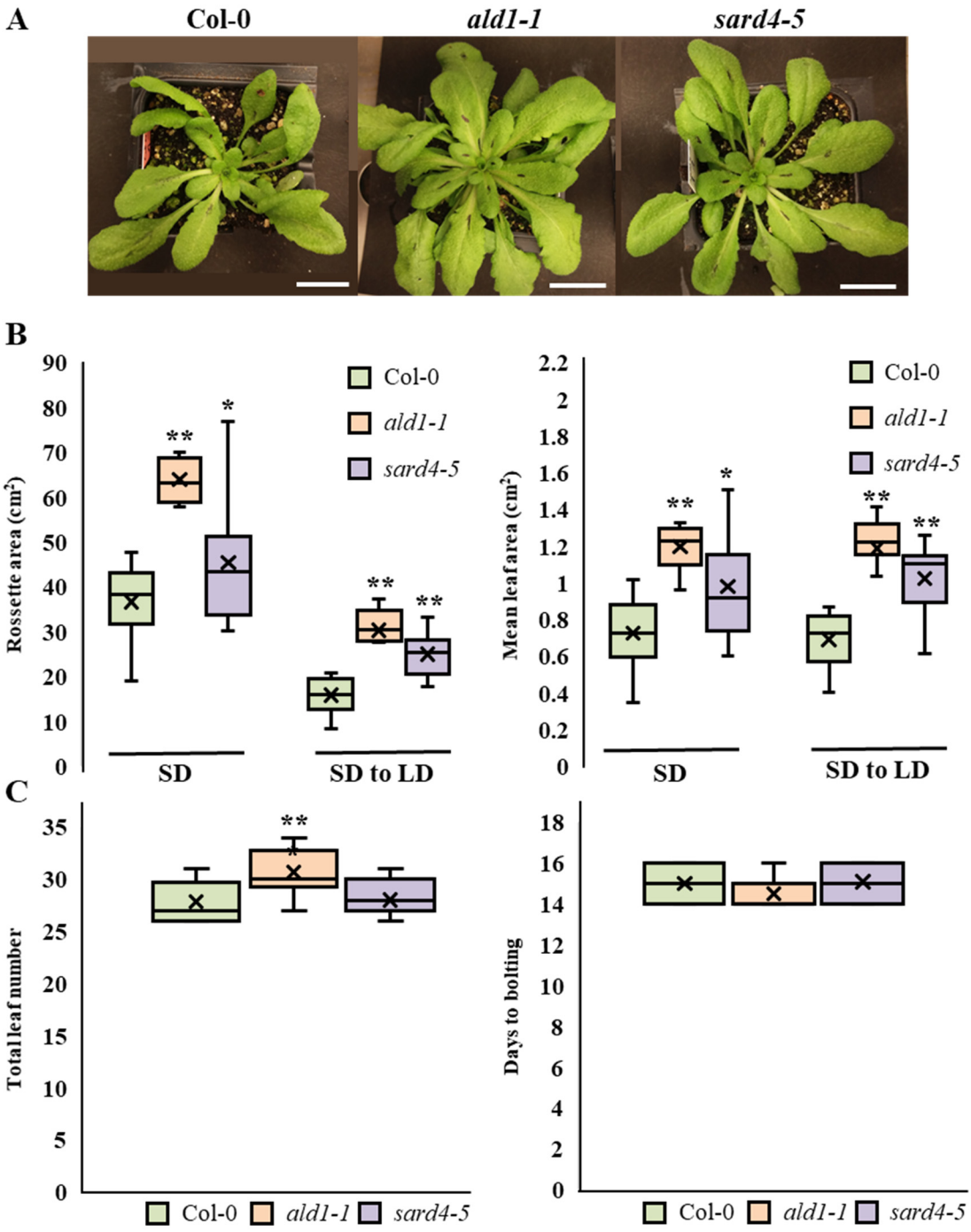

Figure 2. Rosette area characterization of Col-0, *ald1-1* and *sard4-5* mutants. **A,** Image of representative plants grown for 28 days under SD conditions and 7 additional days after transfer to LD. Scale bars represent 1 cm. **B,** Quantification of rosette area and the mean leaf area. A group of plants were grown permanently in short day conditions (**SD**), and another group was grown under short-day conditions for 28 days and then transferred to long-day conditions (**SD to LD**). The rosette area measurement was done with the *"Easy Leaf Area." app* and it was performed when the main inflorescence of the plants had reached a high of 1 cm. The ratio of mean leaf area was calculated by dividing the area of each plant by the number of rosette leaves and removing

the inflorescence to avoid false detection. In SD this occurred synchronously on day 68 from germination, and in the plants grown under SD and transferred to LD, bolting inflorescences reached a 1cm high synchronously at day 16 after shifting to LD. **C**, Flowering time of plants grown 28 days under SD and shifted to LD, measured as total number of leaves or days to bolting. Boxplots show the first and the third quartile, and the line represents the median. The mean is shown as a cross. Whiskers show the highest and lowest values. The size of groups was n=12. ANOVA with Tukey correction was performed to calculate the significant differences marked by long lines. ** indicates p-value < 0.01 and * indicates p-value < 0.05.

We did not detected differences in flowering behavior from what we previously observed (Figure 1A): *ald1-1* produced more leaves than Col-0 and *sard4-5.* Again*,* this difference did not translate into a difference in days to bolting. One possible explanation for the larger rosette area of the *ald1-1* mutant could be that its rosette has a larger number of leaves; because of that, one could think that the rosette size is also larger. Alternatively, the larger rosette size could be due to bigger leaves, as they reach a larger size in *adl1-1* than in Col-0. Therefore, we calculated the ratio of the mean leaf area per cm^2 and the results were similar to those observed previously (Figure 2B, right) in terms of the size of the entire rosette (Figure 2B, left). This supports that both the *ad1-1* and *sard4-5* mutants develop a larger rosette than Col-0, regardless of the total leaf number.

2.3. Study of the effect of Pip on rosette growth

The phenotype displayed by ald*1-1* and *sard4-5* mutants suggested that Pip could play a role in the control of flowering and leaf rosette growth. We wanted to further explore this hypothesis by testing whether exogenous Pip treatment could influence any of those developmental traits in the wild type and the mutant plants. With this aim, we watered plants with Pip (10 mM Pip + tween 0.01%) or mock (water + tween 0.01%) once a week until all the plants had flowered and then measured total leaf number and the days to bolting.

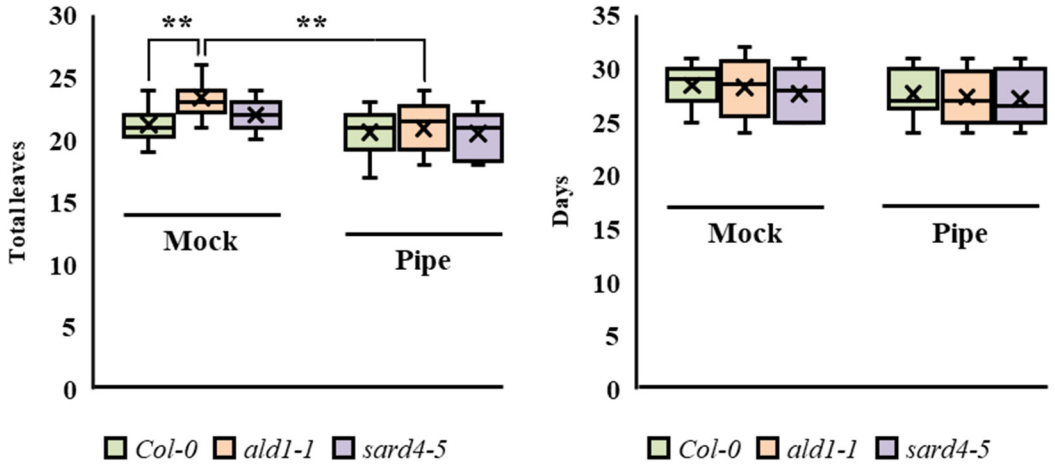

Figure 3. Flowering time of Col-0, *ald1-1* and *sard4-5* mutants treated with Pip. The left panel shows the total leaf number and the right panel shows the days to bolting. Plants were grown under LD conditions. Plants were irrigated with 15 mL of 10 mM Pip + 0-01% of tween20 (Pip) or with tween20 (Mock). Boxplots show the first and the third quartile, and the line represents the median. The mean is shown as a cross. Whiskers show the highest and lowest values. The group size was n=16 for all the genotypes and treatments. ANOVA with Tukey correction was performed to calculate the significant differences marked by long lines. ** indicates p-value<0.01.

The *ald1-1* mutant produced a higher leaf number than the wild-type, agreeing with the previously described results (Figure 1A and Figure 2C). However, these differences disappeared with the Pip treatment: Pip-treated *ald1-1* and Col-0 plants produced a similar number of total leaves. On the other hand, Pip treatment did not alter leaf number in Col-0 or *sard4-5*. These results suggested that exogenous Pip treatment rescues the late flowering phenotype observed in *ald1-1*.

Next, we analyzed the growth of the mutants over time and tested whether the rosette phenotype could be rescued by exogenous Pip treatment, as was the case for the flowering phenotype. With this aim, we grew plants under LD conditions and, from day 7 after germination, watered them with 15 mL of 10 mM Pip or Mock every 3-4 days and measured the rosette area once a week. The results are shown in Figure 4.

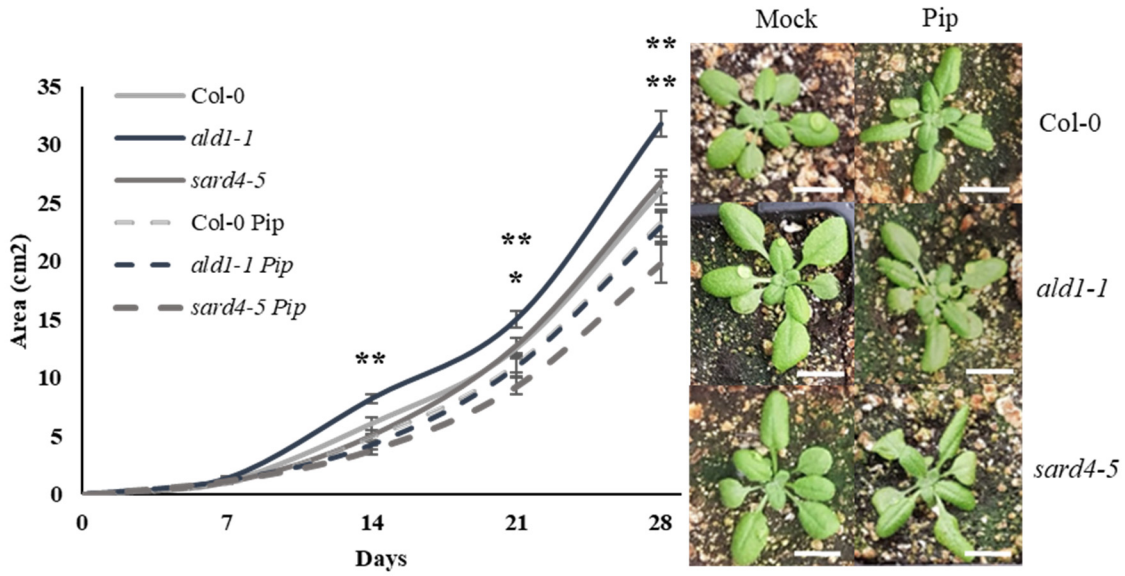

Figure 4. Phenotypic characterization of the rosette area development in response to mock and Pip treatments. Plants were grown under LD conditions. Pip or Mock-treatment was applied every 3-4 days, starting at day 7 after germination. Rosette area was measured every 7 days with the *"Easy Leaf Area"* app. The left panel shows changes in rosette area over time. On day 14, ** refers to significant differences detected between treated or untreated *ald1-1* plants. At day 21, ** marks significant differences between treated or untreated *ald1.1* and * for *sard4-5*. On day 28, ** marks the significant differences between treated or untreated plants of both mutants. ANOVA with Tukey correction was performed to calculate the significant differences. ** indicates p-value<0.05 and * indicates p-value<0.05. Error bars indicate the standard error of the mean (SEM). On the right panel, pictures corresponding to representative plants of the three genotypes, Pip- or mock-treated, 14-days after germination. Scale bars indicate 1 cm.

Our results showed that the greatest differences between treatments were observed with the *ald1-1* mutant, which displayed a significant phenotypic response at day 7 after the first treatment. On the other hand, the *sard4-5* mutant also showed a significant response to the Pip treatment, with a reduction on rosette area over time that was evident from day 14 after the first treatment. In contrast, treatment of Col-0 plants with Pip did not produce any significant change in rosette area. In summary, exogenous Pip treatment rescued the rosette area phenotype of both *ald1-1* and *sard4-5* mutants, as it did for the late flowering phenotype of the *ald1-1* mutant. However, Pip treatment of wild type plants did not cause a reduction of rosette area.

2.4. Cellular basis of the larger rosette phenotype of pipecolic biosynthesis mutants.

Once the phenotype of increased rosette area in pipecolic biosynthesis mutants was confirmed, we wondered whether this phenotype was due to the leaves having a higher number of cells or to increased cell size in the leaves. To identify the cause of the increased rosette size phenotype, we measured cell size and cell number in wild-type, *ald1-1* and *sard4-5* mutants at an early developmental stage (in the first true leaves 7 days after germination), when there are no differences in the leaf size.

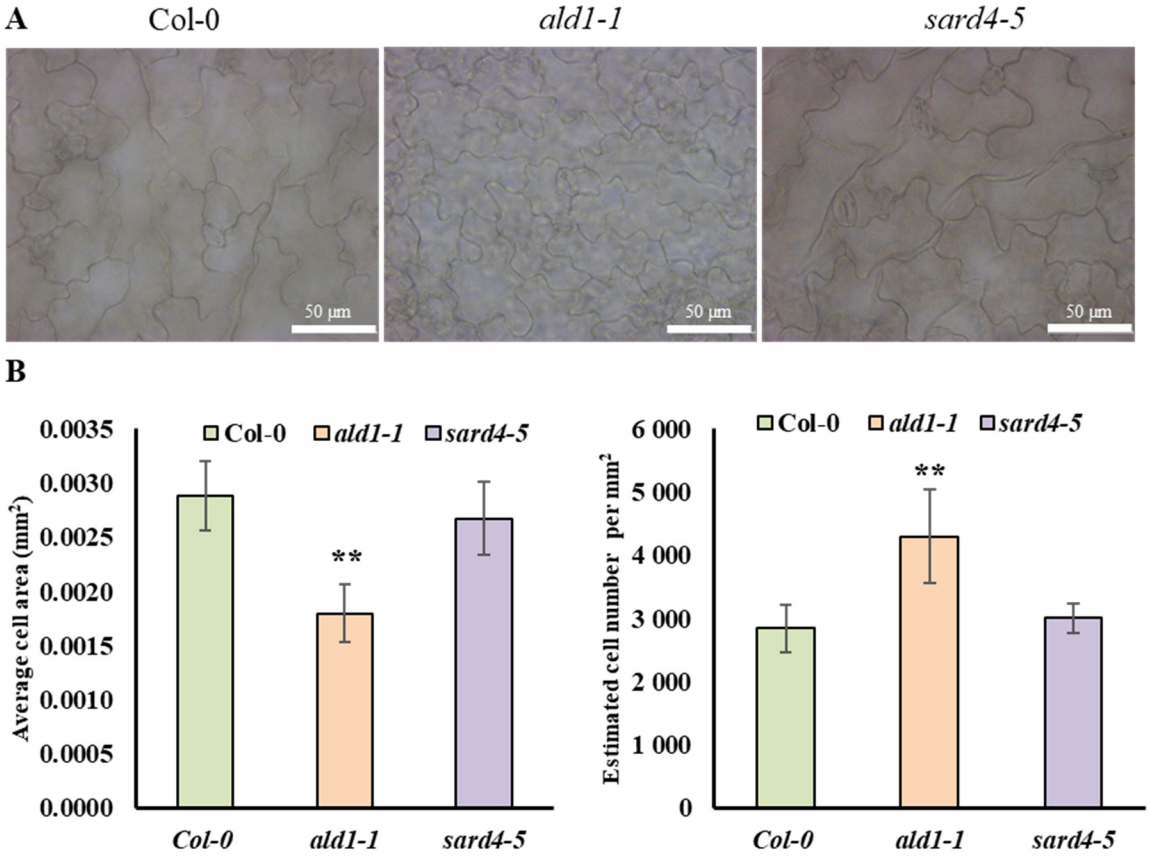

Figure 5. Effect of *ald1-1 and sard4-5* mutations in the cell area and number in seedling leaves. A, representative micrographs of the epidermis of abaxial leaf blade of 7 days after-germination seedlings from the wild type and the *ald1-1 and sard4-5* mutants **B,** At the left side, average cell area of the epidermis of leaves of the different genotypes; at the right side, estimated cell number in the epidermis of the abaxial side of leaves of the different genotypes. Plants were grown under LD conditions and collected on day 7 after germination. The means and standard deviations for the leaves were 8.14 ± 0.69 mm^2 (Col-0), 7.59 ± 0.49 mm^2 (*ald1-1)* and 7.99 ± 0.57 mm^2 (*sard4-5)*. Approximately the size of 80 cells were measured by Fiji analysis software. The total cell number was estimated by dividing the area of the leaf blade by the average cell area of the leaf of each genotype. The graph represents the average of 5 biological replicates, and the

error bars represent the standard deviation of the mean. ANOVA with Tukey correction was performed to calculate the significant differences. ** indicates p-value < 0.01.

Results showed that, at this early developmental stage (7 days after germination), the leaves from the *ald1-1* mutant have smaller cells than those of *sard4-5* or Col-0. The fact that the cell size of leaves from *sard4-5* does not differ from Col-0 at this stage suggests that the difference in rosette size in this mutant must be due to other causes, such as a difference in cell elongation during development. On the other hand, defects in the rosette leaf in the *ald1-1* mutant seem to be complex and might point out to an alteration of the cell division/cell elongation balance during development.

2.5. Characterization of additional mutants affecting genes involved in the biosynthesis of Pip.

During this research and the investigation of Pip as a metabolite possibly involved in flowering, it was discovered that a Pip-derived metabolite, NHP, is involved in the initiation of SAR signaling and that *FMO1*, a key regulator of SAR associated defense priming, is responsible for its biosynthesis, placing NHP downstream of PIP in its known effects (Chen et al., 2018). Thus, we decided to characterize the phenotype of a knock-out mutant of *FMO1*, comparing it with the phenotype of Pip biosynthesis mutant the *ald1-1*. At the same time, we decided to obtain and study a second mutant allele of the *ALD1* gene. For that, we selected and characterized the GT542 line, carrying a transposon insertion in the CDS of the *ALD1* gene in the *Landsberg erecta* (Ler) ecotype, which we will call from now on *ald1-2*, and also the mutant *fmo1-1* (Mishina & Zeier, 2006). Because ALD1, SARD4 and FMO1 act sequentially in the NHP biosynthetic pathway, and the role of Pip at SAR recently was also attributed to the NHP, we decided to investigate whether the phenotype of *fmo1-1* and *ald1-2* was similar to that described for *ald1-1*. To this end, we grew plants from these genotypes under LD conditions and evaluated flowering time based on the total number of leaves and days to bolting, rosette size, and average leaf area (Figure 6).

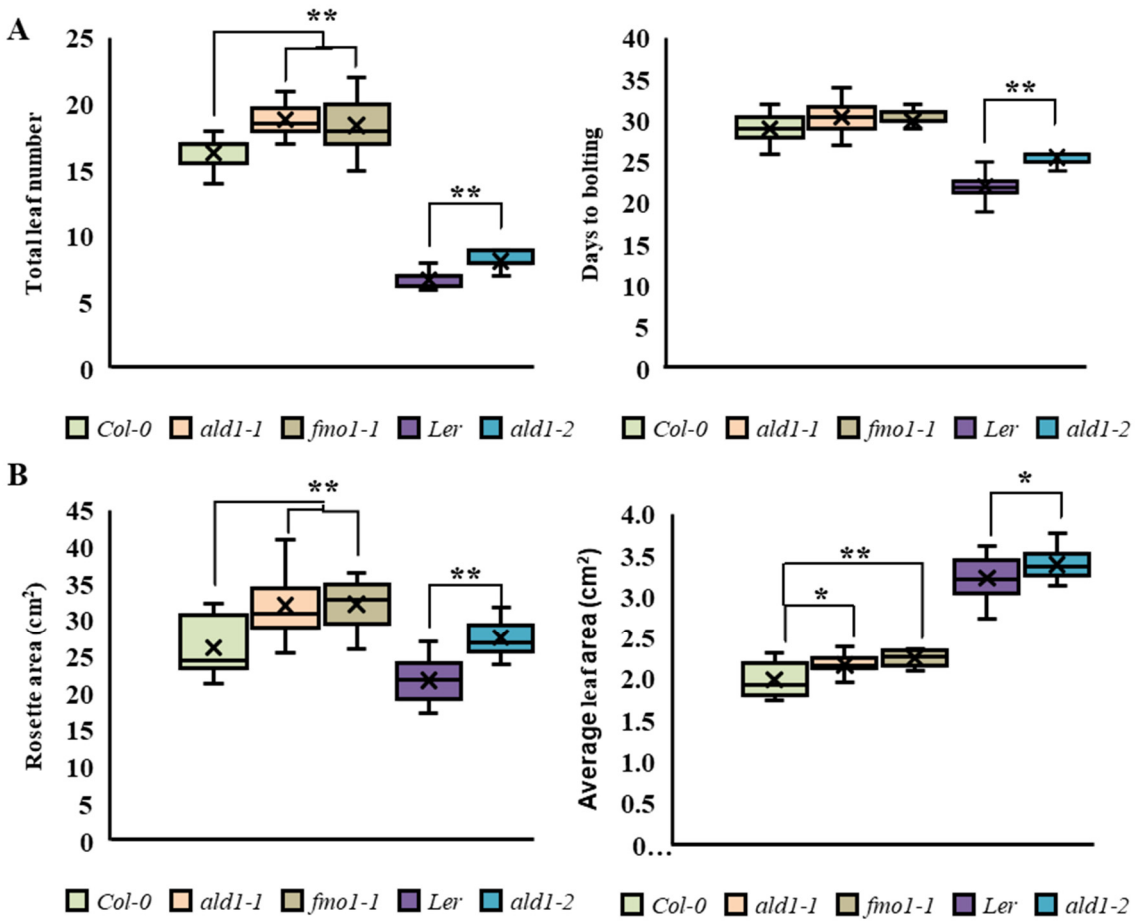

Figure 6. Characterization of flowering time and rosette area of *ALD1* and *FMO1* mutants. **A,** Characterization of flowering time of the Col-0, *ald1-1*, *fmo1-1*, Ler and *ald1-1* genotypes by scoring total leaves (left) and days to bolting (right). **B,** Rosette area measurement by Easy Leaf Area app. The Quantification was made on day 34 after sowing when all the plants had flowered. The floral bud was removed to avoid interference. The average leaf area was estimated by dividing the rosette area by the number of rosette leaves for each plant. Boxplots show the first and the third quartile, and the line represents the median. The mean is shown as a cross. Whiskers show the highest and lowest values. The group size from left to right was n=13, 20, 15, 20, 15. ANOVA with Tukey correction was performed to calculate the significant differences marked by long lines. ** indicates p-value<0.01 and * indicates p-value<0.05.

The results confirmed that the *ald1-1* mutant is slightly late flowering in terms of total leaf number, as previously described. Interestingly, both the *ald1-2* mutant and the *fmo1-1* showed a similar phenotype with an increased number of total leaves, which in the case of the *ald1-2* was accompanied by a difference in days to bolting as well.

Moreover, both the *fmo1-1* and *GT542* displayed an increased rosette area phenotype similar to *ald1-1*, both in terms of rosette area and average leaf area, being in this case

the severity of the phenotypes very similar among the three mutants analyzed. These results show that the flowering-time and leaf-size phenotypes observed in the *ald1-1* mutant are also observed in another independent mutant allele of the *ALD1* gene, *ald1-2*, which demonstrates that these phenotypic defects are associated to the mutations in the *ALD1* gene. They also show that the *fmo1-1* mutant has a very similar phenotype to *ald1-1*, which makes sense since ALD1 acts before FMO1 in the synthesis of NHP. These data suggest that the role attributed to flowering, rosette area size, and cell number and size could be a phenotype controlled by the metabolite NHP rather than Pip.

2.6. Analysis of the effect of Pip on the development in *Marchantia polymorpha*.

We have observed an increase in leaf number and rosette area in the *ald1-1*, *ald1-2* and *fmo1-1* mutants. Moreover, we observed a higher number of cells per area unit in the *ald1-1* mutant. For that reason, we consider the possibility that Pip has a role in the cell cycle so that when it is absent, the plant produces a higher number of cells in the leaves at early developmental stages, and in more advanced stages, a greater number of leaves during its growth until the floral transition occurs. In turn, Pip treatments reversed the rosette area phenotype of the *ald1-1* mutant, leading to a smaller rosette. Pipecolic treatment has a similar effect on the rosette area also in Col-0 for at least 4 weeks of treatment.

We thought that the effect of Pip on growth might be conserved in the plant kingdom and decided to test the response of the liverwort *Marchantia polymorpha* to Pip. To test that, we grew *M polymorpha* in media supplemented with Mock or Pip at 1 µM and 100 µM and evaluated its growth in terms of thallus area.

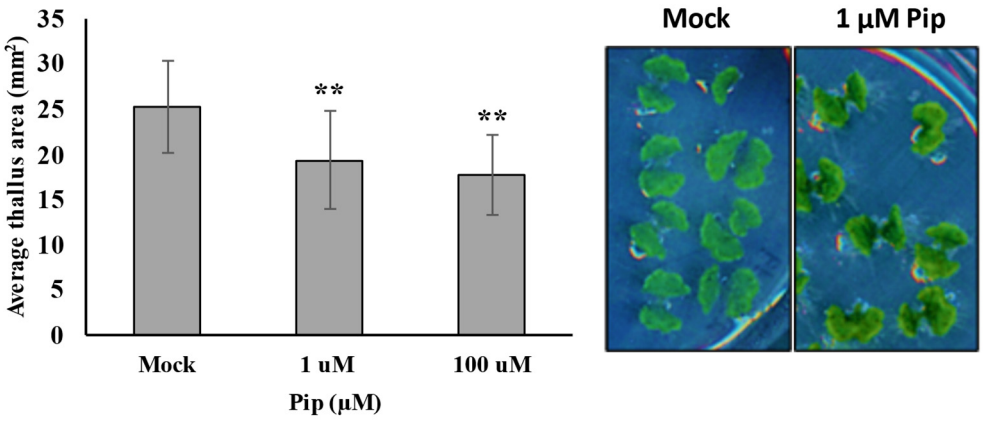

Figure 7. Growth of thallus of *Marchantia polymorpha* grown on *in vitro* medium supplemented with Pip. On the left side, the graph represents the surface of the tallus at different Pip concentrations. On the right side, pictures show *M polymorpha*. The plants were grown for 7 days *in vitro* under LD conditions on media supplemented with mock or Pip at 1 µM and 100 µM. The population size (from left to right) was n= 34, 43 and 12. The error bars represent the standard deviation of the mean. ANOVA with Tukey correction was performed to calculate the significant differences. ** indicates p-value<0.01.

The plants grown at different concentrations of pipecolic developed a smaller thallus than those with no Pip in the medium. Therefore, Pip affected *M. polymorpha* growth and these results suggest that the for rosette and thallus growth might be conserved in both species.

Chapter 3: A multi-omics approach to decipher the metabolic changes during the floral transition in Arabidopsis.

3.1. Generation of dexamethasone-inducible transgenic lines expressing CO or FT proteins under the control of phloem specific promotors (p*SUC2*, p*CO* or p*FT*).

With the aim of generating a system in which we could readily control floral induction in Arabidopsis by inducing *CO* or *FT* expression in the vascular tissue, we generated constructs where the corresponding endogenous promoters drove the expression of a CO or FT protein fusion to the rat glucocorticoid receptor (GR). This system allows a precise, quick, and specific response that triggers the floral induction. Fusion of GR to a nuclear protein, such as CO or FT, makes that protein activatable by dexamethasone (Abe et al., 2005; Simon et al., 1996). Alternatively, to provide phloem-specific expression of the fusion proteins, the promoter of the *SUCROSE-PROTON SYMPORTER 2* (p*SUC2*) was used. To evaluate which combination of promoter and fusion protein provided a robust system to analyze floral transition, we characterized the phenotype caused by p*CO*::*CO-GR*, p*SUC2*::*CO-GR*, p*FT*::*FT-GR* and p*SUC2*::*FT-GR* in the wild type and in the corresponding mutant backgrounds (Table 1).

We selected 12 T1 plants (independent lines with uniform phenotype and no alteration in growth). For each line, approximately 100 seeds (T2 segregating generation) were grown in a medium supplemented with the antibiotic for the resistance gene construction *in vitro*. After 12 days, we phenotype sensitive/resistant plants and chose those with a single copy of the transgene to be acclimated to the greenhouse (n=24). One week after, we treated the plants with dexamethasone solution (30μM dexamethasone; 0.01% Tween-20) or mock solution (0.01% Tween-20) and closed the trays with a transparent cover for 24 hours to maintain high humidity. Next, we measured the flowering time in response to the treatments. Due to the high number of managed plants, the results are shown standardized: S (similar flowering) when there was no significant difference in flowering time with the corresponding background (Col-0, *ft-10* or *co-10*), EF (early flowering) or LF (late flowering) when they flowered earlier or later than the corresponding background, respectively (Table 1).

Table 1. Flowering time response in dexamethasone-inducible transgenic lines in Col-0, *ft-10* and *co-10* mutant backgrounds. Compared to the mutant background, the table shows the flowering response after dexamethasone and mock treatments. S means a response similar to the background. LF refers to a late flowering response, and EF is an early flowering response.

Background	**Construction**	**Response**	
		Dexamethasone	**Mock**
Col-0	*pSUC2::CO-GR*	S	LF
Col-0	*pSUC2::FT-GR*	S	S
Col-0	*pFT::FT-GR*	S	S
Col-0	*pCO::CO-GR*	S	LF
ft-10	*pSUC2::CO-GR*	S	S
ft-10	*pSUC2::FT-GR*	S	S
ft-10	*pFT::FT-GR*	S	S
ft-10	*pCO::CO-GR*	S	S
co-10	*pSUC2::CO-GR*	EF	S
co-10	*pSUC2::FT-GR*	S	S
co-10	*pFT::FT-GR*	S	S
co-10	*pCO::CO-GR*	EF	S

Analysis of the flowering time showed that lines expressing the *CO-GR* transgene in the Col-0 background exhibited an unexpected late-flowering phenotype in response to mock treatment, probably due to the accumulation of CO-GR protein in the cytoplasm. Conversely, the same lines treated with dexamethasone flowered earlier than the mock-treated plants, displaying a response similar to the Col-0 plants. In general, we did not observe any response upon dexamethasone or mock treatment in lines expressing the *FT-GR* transgene in none of the three genetic backgrounds tested. As expected, treatment with dexamethasone of the p*CO*::*CO-GR* or p*SUC2*::*CO-GR* lines in the *ft-10* background did not alter the flowering response compared to the corresponding mock-treated plants, presumably due to the lack of a functional FT protein. Finally, transgenic lines expressing the CO-GR protein under the control of the *CO* or *SUC2* promoter in the *co-10* mutant background displayed a very clear response, flowering early upon dexamethasone treatment compared to mock-treated plants. These lines were selected for further analyses.

3.1.1. Selection of the best inducible system to trigger floral induction.

To assess which of two constructs, p*CO*::*CO-GR* or p*SUC2*::*CO-GR*, represented a better tool to control floral transition, we characterized their flowering time response to dexamethasone treatment in T3 homozygous transgenic lines with one T-DNA insertion in the *co-10* mutant background (Table 2).

Table 2. Flowering time determination in homozygous transgenic lines p*CO*::*CO-GR co-10* and p*SUC2*::*CO-GR co-10* (T3 plants) upon dexamethasone or mock treatment. Data show the average total leaf number (+/- standard deviation; n=25).

Controls	**Construction**	**Total leaf number**	
Col-0	-	18.4 ± 1.6	
co-10	-	46.1 ± 4.4	
Line		**Dexa**	**Mock**
#2	p*CO*::*CO-GR*	29 ± 2.6	44.5 ± 3.6
#3	p*CO*::*CO-GR*	33 ± 2.3	45.5 ± 3.7
#4	p*CO*::*CO-GR*	26.2 ± 2.4	44 ± 3.3
#7	p*CO*::*CO-GR*	29 ± 2.7	44.4 ± 4.3
#9	**p*CO*::*CO-GR***	**25 ± 1.7**	**45.2 ± 3**
#1	p*SUC2*::*CO-GR*	28.6 ± 1.9	46.4 ± 3.8
#2	p*SUC2*::*CO-GR*	35.4 ± 2.8	45.8 ± 2.5
#3	p*SUC2*::*CO-GR*	33.5 ± 2.4	46.3 ± 3.4
#5	p*SUC2*::*CO-GR*	35.9 ± 2.7	46.3 ± 2.7
#8	p*SUC2*::*CO-GR*	32.4 ± 2.4	45.1 ± 3.5

In general, expression of *CO-GR* under the control of the endogenous *CONSTANS* promoter (p*CO*) provided a better response in terms of floral induction compared to CO-GR expression under the p*SUC2* promoter. Moreover, we observed the formation of aberrant fruits in 60% of the transgenic T1 p*SUC2*::*CO-GR co-10* lines analyzed. Among the analyzed p*CO*::*CO-GR co-10* lines, we identified line number #9 as providing an excellent flowering response to dexamethasone, almost fully complementing the *co-10* mutant phenotype (Figure 1A and 1B). This line flowered as late as the *co-10* mutant when treated with mock solution but, upon dexamethasone treatment, plants flowered with 25 leaves, more similar to the wild type Col-0, which produced an average of 18 total leaves (Figure 1).

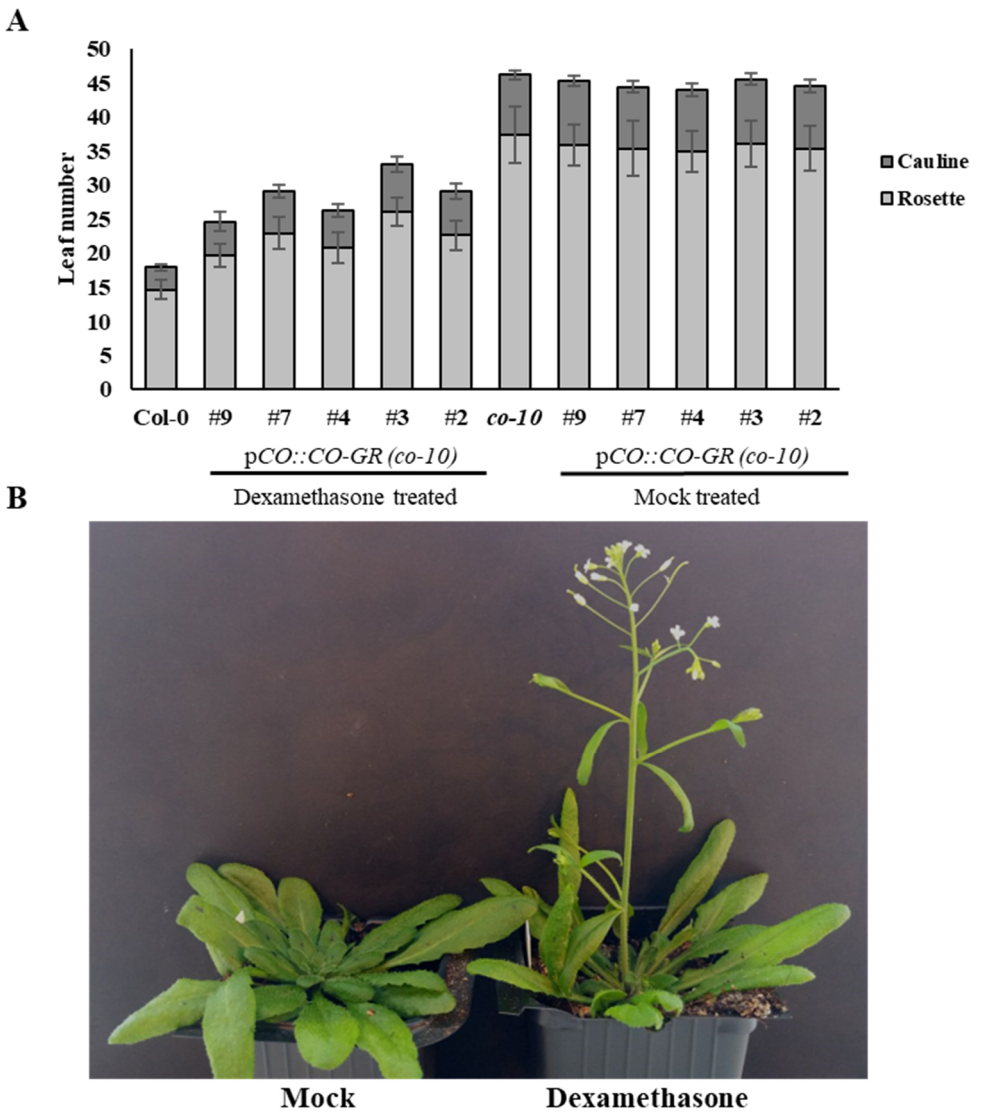

Figure 1. Characterization of flowering time of a set of p*CO*::*CO-GR co-10* lines. **A.** Flowering time determination as total leaf number in Col-0, *co-10* and p*CO*::*CO-GR co-10* lines #2, #3, #4, #7 and #9. The graphs show the average of rosette leaves, cauline leaves, and total leaves (average +/- SD; n=25). **B**. Phenotype of 42-day old mock- and dexamethasone-treated p*CO*::*CO-GR co-10* #9 plants. Plants were grown *in vitro* and LD conditions for 12 days, transferred to the greenhouse, and the rosette was treated with dexamethasone or mock solution.

3.1.2. Characterization of the expression pattern driven by the *CO* promoter used in the inducible p*CO*::*CO-GR* #9.

To assess to what extent the *CO* promoter fragment that we used in the constructs (p*CO*) drives an expression pattern like that of the endogenous *CO* gene, we analyzed the expression pattern driven by that promoter fragment.

The generation of reporter lines using the *β-GLUCURONIDASE* (*GUS*) gene is an effective tool to study specific expression patterns associated with promoters. In this manner, we generated a transgenic line that expressed the *GUS* gene under the control of the promoter used in our selected inducible system (p*CO*::*GUS* line). We could detect specific *GUS* gene expression in the leaf vascular tissue in the p*CO*::*GUS* line, as described in the literature for the *CO* promoter (Figure 2) (Takada & Goto, 2003; An et al., 2004). Moreover, we also performed a time-course experiment to evaluate the diurnal expression of the *CO-GR* transgene in the pCO::*CO-GR co-10* #9 line grown under long-day conditions (16h light/8h dark) *in vitro*.

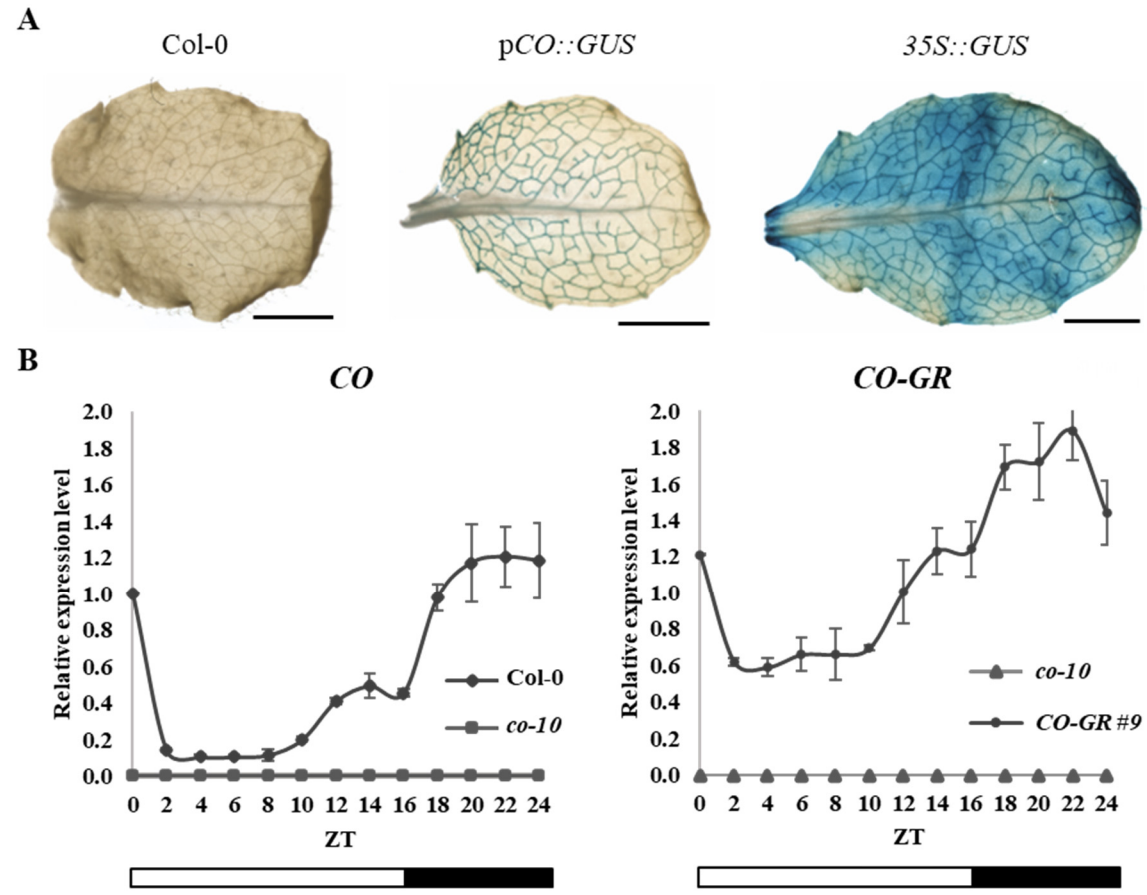

Figure 2. Characterization of the p*CO* and the diurnal expression of the *CO-GR* transgene. **A.** GUS assay showing *GUS* expression in Col-0 leaf (left, negative control)**,** p*CO::GUS* transgenic line (middle) and *35S*::*GUS* transgenic line (right, positive control). **B.** Time-course expression of the *CO-GR* transgene under the *CO* promoter in the selected p*CO*::*CO-GR co-10* #9 line. The results show the average of 3 biological replicates, and the error bars represent the standard deviation. To the left, *CO* expression in Col-0 and to the right, *CO-GR* expression in the #9 line.

These results show that the *CO* promoter used in the inducible system provides phloem-specific expression in the leaves, as expected. Moreover, in the p*CO*::*CO-GR co-10* #9 line, the *CO-GR* transgene displays a similar diurnal expression pattern as that described for the *CO* endogenous gene in Col-0 (Suárez-López et al., 2001; Valverde et al., 2004). In this line, *CO-GR* expression increases from ZT10 until the lights are off at ZT16 and further increases during the dark period until the lights are on when the transgene expression falls. This matches the expected results and mimics *CO* endogenous gene expression.

In summary, the pCO::*CO-GR co-10* #9 line responds appropriately to the dexamethasone treatment, triggering floral induction, and both the tissue specificity and temporal expression pattern of the *CO-GR* transgene matched with that of the endogenous *CO.*

3.2. Assessment of experimental conditions to induce floral transition in Col-0 and *co-10* backgrounds.

3.2.1. Setting up the developmental stage and timing to induce flowering in the CO-GR inducible system.

Different genetic pathways control flowering in plants and long photoperiods have an activator effect, mediating CO. *CO* expression is localized in the phloem and is influenced by circadian rhythms. The coincidence of light with *CO* diurnal peak expression in the evening stabilizes the CO protein, inducing *FT* expression (Valverde et al., 2004). Subsequently, FT travels through the phloem to the shoot apex meristem, where it triggers flowering (Corbesier et al., 2007).

The knock-out mutant *co-10* displays a marginal response to the photoperiodic signal: its development under LD conditions is similar to wild type plants grown under SD. A well-described method to induce flowering in Arabidopsis is to apply a SD-to-LD shift, where plants are grown in SD for 21 days and then shifted to LD. Our inducible system acts in a similar way as a SD-to-LD shift, since the dexa treatment activates the CO-FT module and results in floral transition. To decipher the correct developmental stage to induce flowering, we characterize the *co-10* growth under SD, LD and SD-to-LD shift conditions (Figure 3).

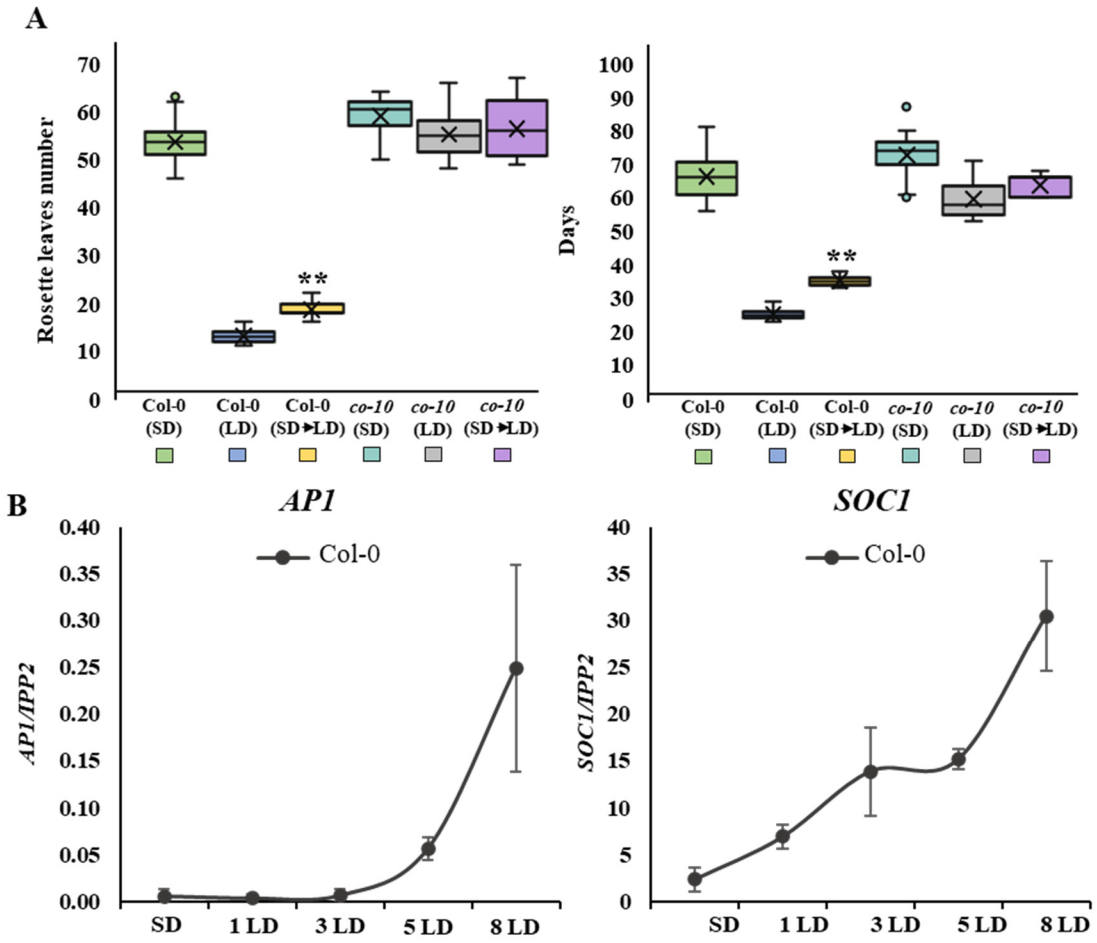

Figure 3. Characterization of Col-0 and *co-10* in response to a shift from SD to LD conditions. A. Flowering time characterization of *co-10* and Col-0 in LD, SD and SD-to-LD conditions. Boxplots show the first and the third quartile and the line represent the median. The mean is shown as a cross. Whiskers show the highest and lowest values and outliers are shown as dots. The population size per group from left to right is n= 20, 28, 24, 24, 21 and 14. ANOVA with Tukey correction was performed to calculate the significant differences. ** indicates p-value<0.01. **B.** Characterization of *AP1* and *SOC1* expression levels in Col-0 and *co-10* plants after a SD-to-LD shift. The expression of *AP1* and *SOC1* was not detected in *co-10*. *IPP2* was used as a reference gene. Plants were grown for 21 days in SD conditions and then shifted to LD. Apex samples were collected at ZT8. Error bars correspond to the standard deviation of the mean of three biological replicates.

The results show that, as previously described, Col-0 plants shifted from SD to LD flower earlier than those grown in SD, with an average total leaf number of 18.5 ± 1.5 compared to those growing in continuous LD, which flowered after an average of 13.1 ± 1.2 total leaves. These plants had between 4 and 5 leaves when they were transferred to LD, indicating that at this developmental stage the plants are competent to respond to the

photoperiodic signal. Floral transition after SD-to-LD shift was confirmed by upregulation of *SOC1* as soon as one day after the shift, and development of floral meristems occurred after 5 days in LD (indicated by *AP1* expression). We observed a minimal response after the SD-to-LD shift in the co-10 mutant: shifted plants produced an average four leaves less than plant growing in continuous LD. This difference corresponds to the activation of pathways that respond to the photoperiodic signal in a CO-FT independent manner.

3.2.2. Molecular characterization of floral induction in the p*CO*::*CO-GR* line #9 at different time points after Dexamethasone and Mock treatments.

We observed that under our growing conditions, after 14 days in LD, co-10 plants have produced 4-5 leaves and were in a similar developmental stage as Col-0 SD-grown plants analyzed in the previous section. At this point, plants were treated with dexa or mock solution, as described in section 3.3, and leaf and apex material was collected to characterize the expression of a set of flowering-related genes (*AP1*, *SOC1*, *TERMINAL FLOWER 1* (*TFL1), LFY* and *FT*).

Since *CO* directly upregulates *FT*, we measured its expression in the leaves to assess whether the CO-GR fusion protein was able to trigger *FT* expression as the endogenous CO protein. The induction of *FT* expression by the *CO-GR* fusion protein in dexamethasone-treated plants was successful (Figure 4). *FT* levels rise as soon as one day after the dexamethasone treatment when expression reached its maximum level and then decreased until day five, coinciding with comparable levels to those of the mock-treated plants. According to *FT* expression on day 1, we observed an increase in the floral marker genes *SOC1* and *TFL1* on day 3, *LFY* on day 5, and *AP1* on day 8. Since the upregulation of *LFY* and *AP1* marks the formation of floral meristems, we established that the floral transition occurs in p*CO*::*CO-GR* #9 plants between day 1 and 8 after dexamethasone treatment. The dexamethasone leaf treatment was effective from the first day and lasted at least until the third day, although expression of *FT* was very low on that day. Thus, we conclude that under our conditions, activation of *FT* expression for 2-3 days by dexamethasone induction of CO-GR protein in the leaf was sufficient to initiate floral transition.

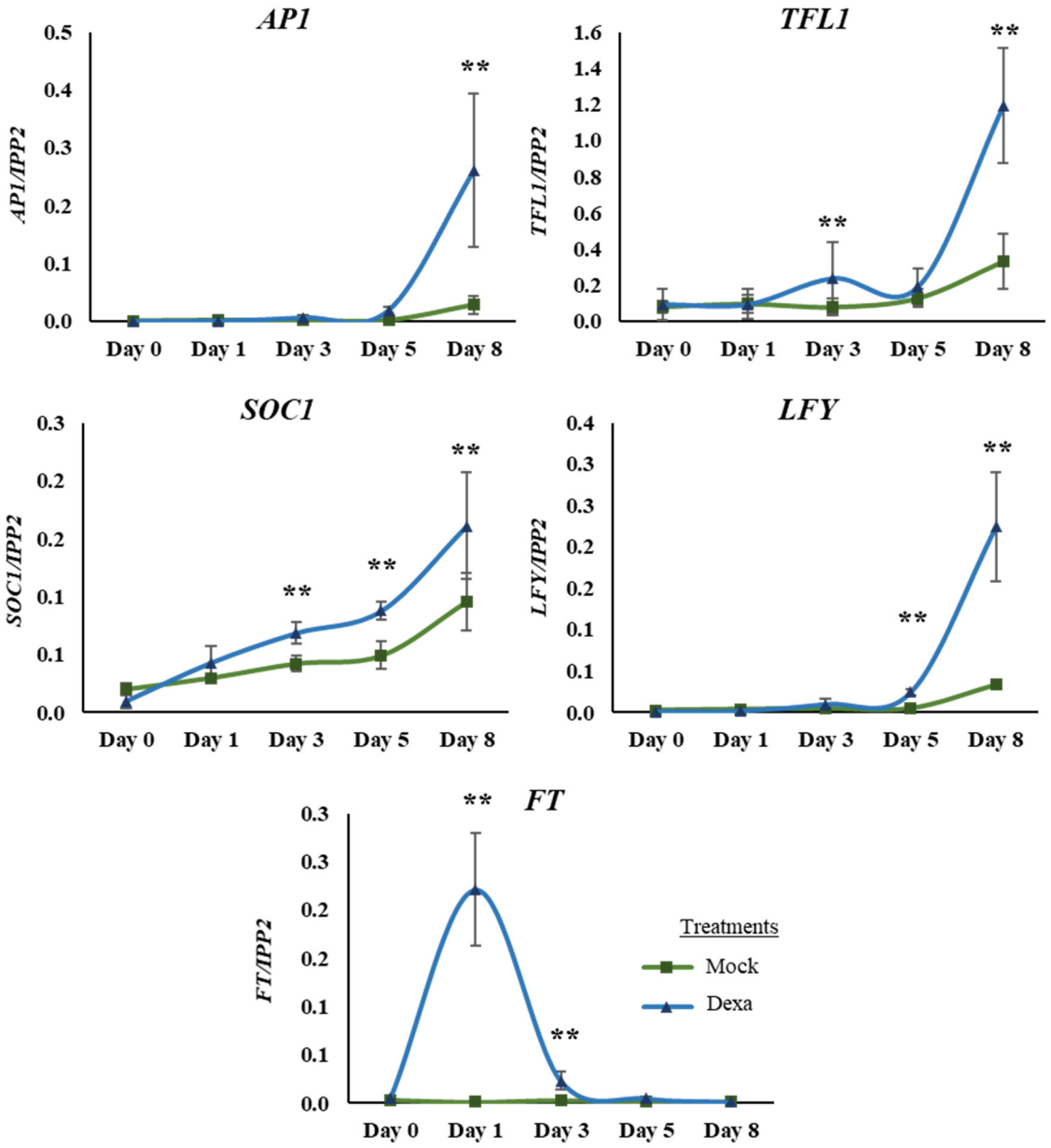

Figure 4. Molecular characterization of the induction by dexamethasone of #9 p*CO*::*CO-GR*. Apices and leaves from dexa- and mock-treated plants were collected on day 0 (before treatment) and 1, 3, 5 and 8 days after treatment application. *IPP2* was used as the reference gene. The results show the average of 3 biological replicates, and the error bars represent the standard deviation. Significance level was measured by ANOVA with Tukey correction compared with the amplification results from mock treatment. ** indicates p-value < 0.01.

3.3. Experimental design for the integrated analysis of changes associated with floral transition: differential metabolomics, lipidomics, hormone quantification and transcriptomics analysis in apices and leaves of induced and non-induced p*CO::CO-GR* plants.

Metabolites are the end products of cellular regulatory processes, and their levels can be regarded as the ultimate response of a biological system to genetic or environmental changes (Fiehn, 2002) . The goal of this study is the identification of metabolic pathways and the corresponding metabolites and regulatory gene networks, with a significant contribution to the control of floral transition in Arabidopsis.With this aim, we collected samples from long-day grown plants of the inducible p*CO*::*CO-GR* #9 line (from now on p*CO*::*CO-GR*), in a time series after mock or dexamethasone treatment. Those samples were used to characterize changes in abundance of metabolites, lipids, hormones and changes in gene expression (transcriptome) (Figure 5).

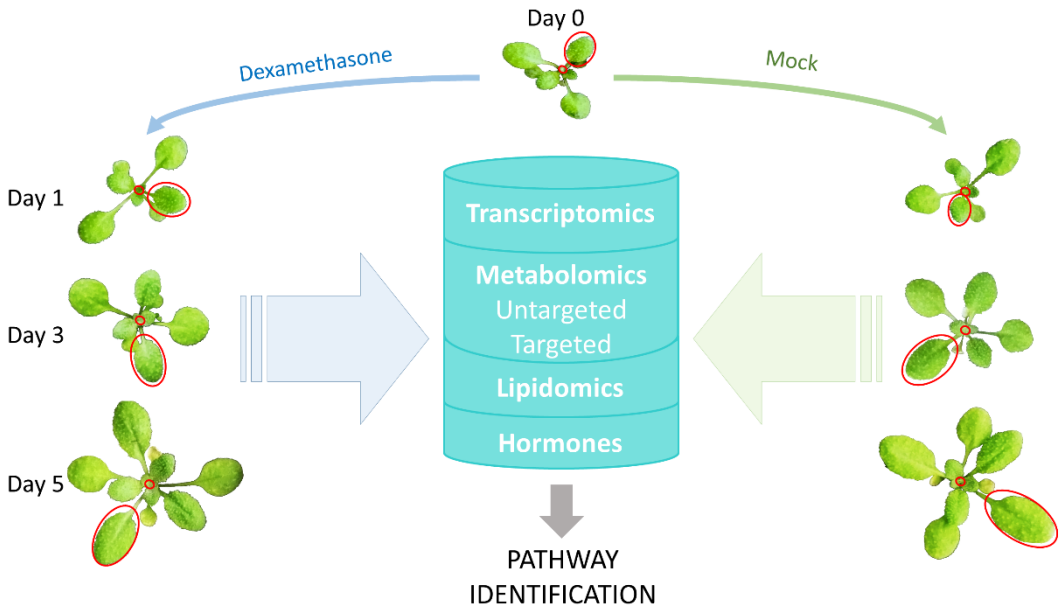

Figure 5. Experimental design for an integrated analysis of changes associated with the floral transition.

The plants grew for 14 days in soil under long-day conditions when they were treated with dexamethasone and mock solutions by spraying the rosette. Tissue samples were collected at day 0 (before the treatment) and 1, 3, and 5 days after the treatment. Optimal sampling times were determined experimentally as described in the next section (3.3.1). All samples were collected two hours before lights off, between *Zeitgeber* time 14 and 16 (ZT14-ZT16). We sampled the apex and the third or fourth corresponding fully-developed leaf per plant (red circles in Figure 5). We collected 8 biological replicates

consisting of a pool of 35-30 apices and leaves per treatment and per analysis. These samples were used to run: we run metabolomics GC-MS data analysis (targeted), LC-MS (targeted and untargeted), lipidomics by LC-MS and hormone profiling. In addition, four additional samples were collected to perform a transcriptomic analysis. In total, more than 9000 plants were grown for these approaches, and tissue samples were collected in a narrow time frame (maximum 2 hours) to study the metabolic and transcriptomic changes that occur during the transition to flowering.

3.3.1. Identification of the optimal timepoints to perform the multi-omic analysis in this experimental system.

Tissue samples were collected during a stay in Prof. Thomas Moritz's laboratory at Umea Plant Science Center (UPSC). Due to the considerable space requirements to handle such a large number of plants, we used an independent growth chamber that differs in light quality and intensity from that used in our pilot experiments (performed at the IBMCP laboratory in Valencia). For this reason, we decided to characterize the flowering response of the inducible system in these conditions, both in terms of flowering time and at the molecular level. We measure the flowering time under the new conditions with a similar method described in section 3.2.2.

Our results showed a faster floral induction in dexamethasone-treated plants (Figure 6) than that previously observed (Figure 4), with an increase of *SOC1* expression already starting one day after dexamethasone treatment. *TFL1* expression increased from day 3, and *LFY* and *AP1* between days 3-5. Additionally, we observed that 39% of the dexamethasone-treated apices collected on day 8 showed visible flower buds, which means that the floral transition most likely happened between day 1 and 3 after dexamethasone treatment. Accordingly, bolting was observed approximately between 12 and 14 days after induction (with plants producing between 5 or 6 additional leaves during this time). The dexamethasone-treated plants flowered with an average and standard deviation of rosette leaves of 18.9 ± 1.5 compared to Col-0 with 14 ± 1.7. In contrast, no differences were detected between the mock-treated plants (34.3 ± 2.3) compared to *co-10 (*35.8± 2.7).

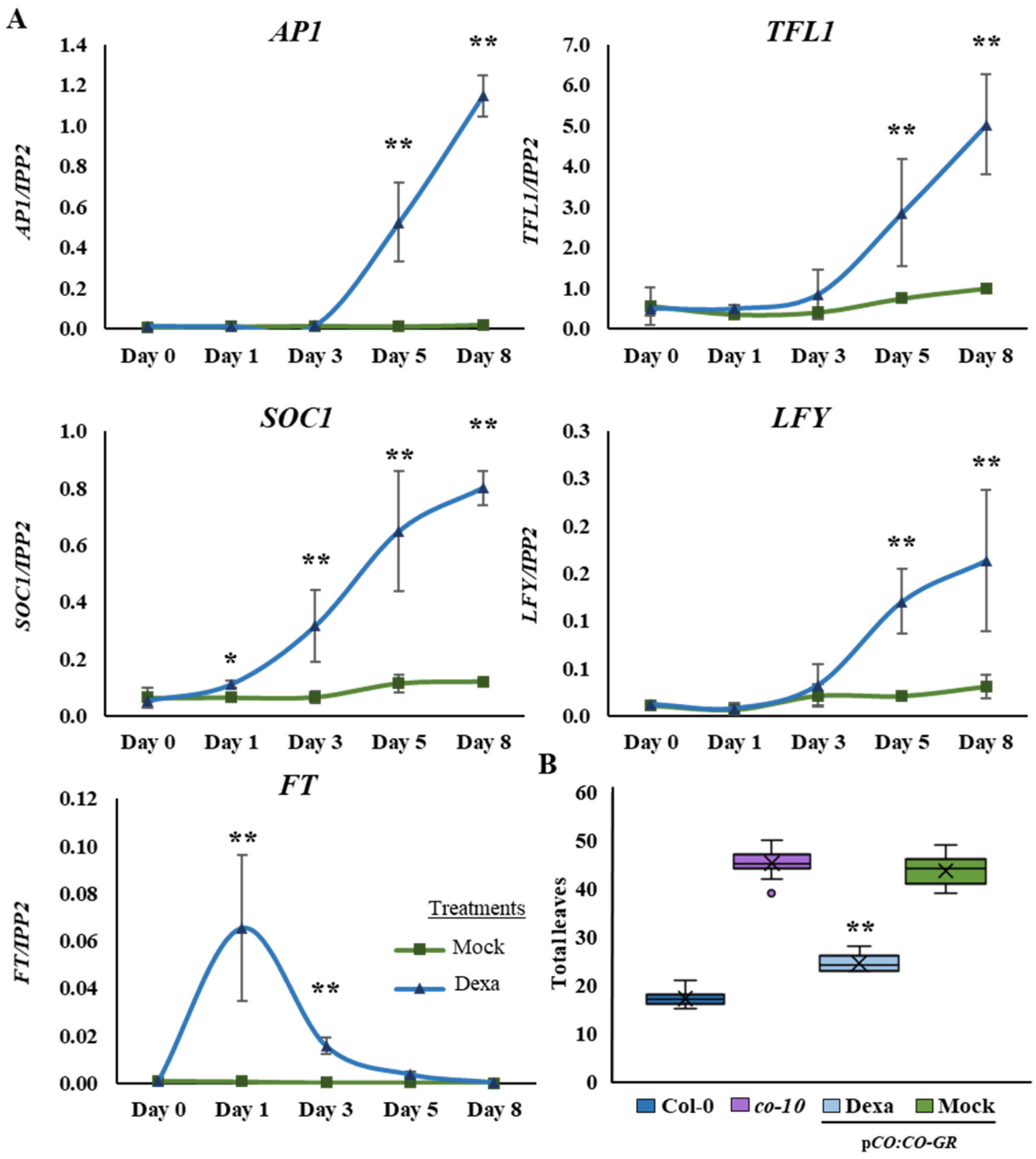

Figure 6. Characterization of the induction by dexamethasone of p*CO*::*CO-GR* in UPSC growth facilities. A. Molecular characterization of the induction by dexamethasone of #9 p*CO*::*CO-GR*. The results show the average of 3 biological replicates, and the error bars represent the standard deviation. **B.** Flowering time measured as total leaf number. Boxplots show the first and the third quartile, and the line represents the median. The mean is shown as a cross. Whiskers show the highest and lowest values and outliers are shown as dots. The population size per group was n= 25. ANOVA with Tukey correction was performed to calculate the significant differences. ** indicates p-value<0.01,* indicates p-value<0.05.

Based on our results, we established that the optimal time points to analyze changes associated with the floral transition by omics approaches was between the day of the

dexamethasone treatment and up to day 5 after treatment, when based on the expression of *AP1* and *LFY* genes, floral meristems had already been initiated at the shoot apical meristem.

3.3.2. Identification of changes in metabolite abundance associated with floral transition.

The study of metabolomics has gained attention in the last decade. Most research laboratories established metabolic profiles for liquid chromatography-mass spectrometry (LC-MS) and gas chromatography-mass spectrometry (GC-MS), which also led to the enrichment of libraries and public metabolite databases as Kyoto Encyclopedia of Genes and Genomes (KEGG) (Sharma et al., 2021). In recent years there have been significant advances in high-throughput analytical chromatography instruments and processing software and online statistical and data analysis tools such as Cytoscape, MetaboAnalyst, and XCMS (Kumar et al., 2017). Also, the introduction of QTOF (Quadrupole Time of Flight) to the GC-MS and LC-MS instruments has improved the separation of coeluting peaks and also facilitated higher sample throughput, increasing peak resolution, mass accuracy and rapid identification of hundreds of metabolites in a short span of time (Chawla & Ranjan, 2016; Ralston-Hooper et al., 2008).

Samples collected as described in the previous section were analyzed by Gas and Liquid Chromatography coupled to Mass Spectrometry (GC-TOF-MS and LC-Q-TOF-MS). The electrospray ionization (ESI) technique selected for LC-MS has a substantial impact on the detection of metabolite profiles and can be performed in positive or negative ion mode to detect different metabolites, offering more comprehensive metabolome coverage than using a single polarity (Lei et al., 2011).

Comparison of mass spectrometry profiles with databases of known Arabidopsis metabolites allowed the identification in leaf tissue of 65 metabolites by GC-MS and 95 by LC-MS (41 in ESI+ and 54 in ESI-). Similarly, 64 metabolites were detected in apex samples by GC-MS and 95 by LC-MS (57 in ESI+ and 53 in ESI-). In a subsequent analysis and after removing duplicate metabolites detected by the different techniques, we identified a total of 136 metabolites in the leaf and 133 in the apex tissues (Supplementary File 1). Surprisingly, we did not observe any significant differences in metabolite abundance in leaves at any of the analyzed time points. However, we did find

significant differences in metabolite abundance in apex samples. For a first exploratory data analysis for multiple groups and to better visualize the data, we performed a heatmap with the top 55 metabolites showing more significant differences between all conditions (Figure 7).

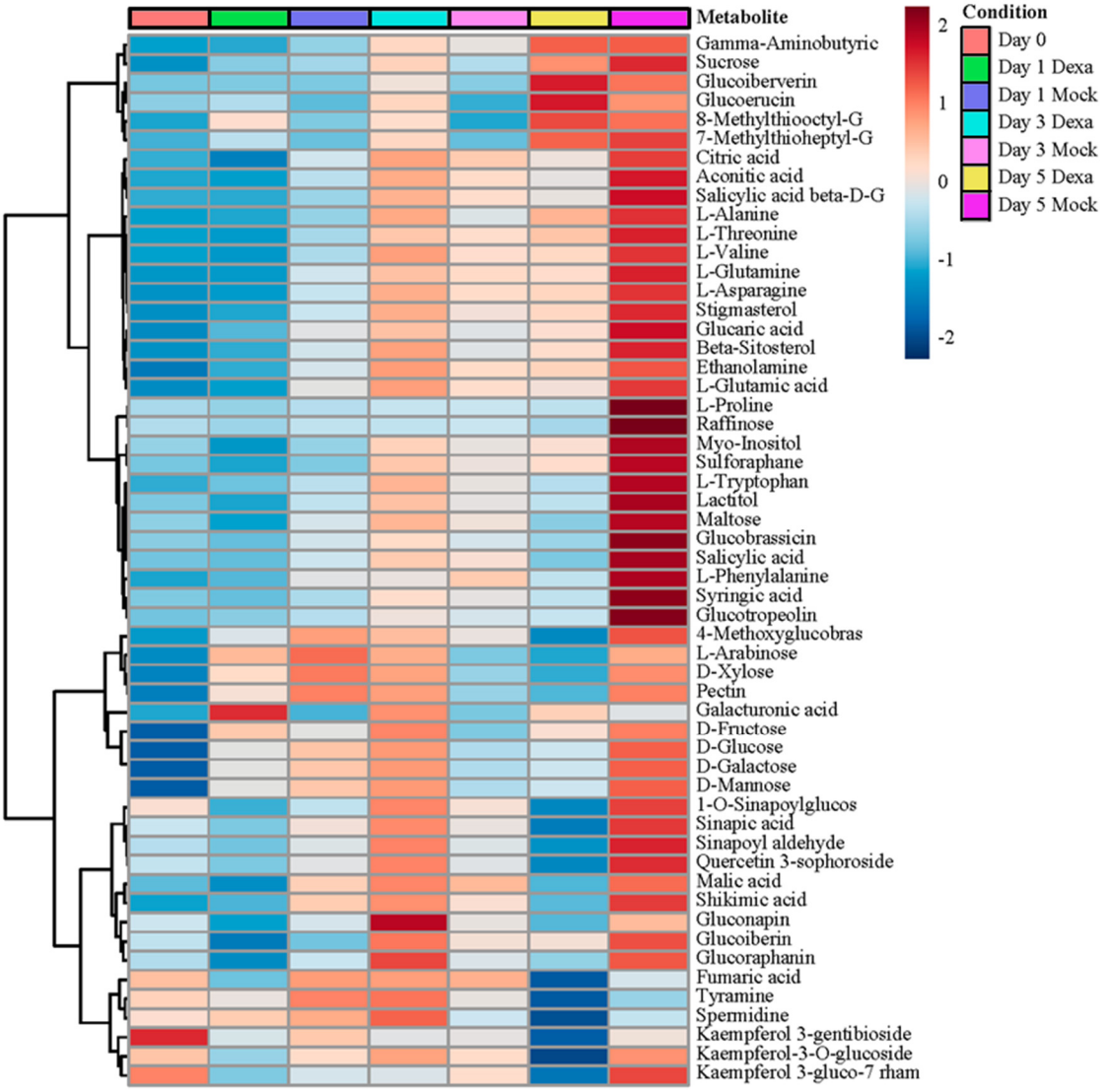

Figure 7. Hierarchical clustering results are shown as a heatmap performed with the top 55 more significant metabolites in all conditions. The ANOVA test with Tukey's Honestly Significant Difference (Tukey's HSD) was performed for the multigroup analysis.

An additional comparative univariate analysis with Fisher's least significant difference method (Fisher's LSD) among treatments in each timepoint displayed two different behaviors regarding the samples at the other time points. On day 1, after dexamethasone treatment, 25 significant metabolites were found (Supplementary File 2). These differences are characterized by a reduction of the abundance of the metabolites in the

induced samples *versus* the non-induced ones. Conversely, on day 3 the induced samples have more metabolite abundance than the mock-treated, with 16 significant features detected (Supplementary File 2).

Finally, we observed profound changes in the metabolite abundance in the apex at day 5, with 115 metabolites displaying significant differences in their abundance (t-test, p-value <0.05) (Supplementary File 2). These results were consistent with what we observed in the expression analysis of flowering marker genes (Figure 6), when on day 8 we could already find floral buds.

The sparse Partial Least Square-Discriminant Analysis (sPLS-DA) algorithm can be used to effectively reduce the number of variables or metabolites in high-dimensional metabolomics data to produce robust and easy-to-interpret models (Cao et al., 2011). Using this algorithm, we identified three major principal components that explain 78.9% of the variance in apex samples and allow a clear separation between groups (Figure 8A).

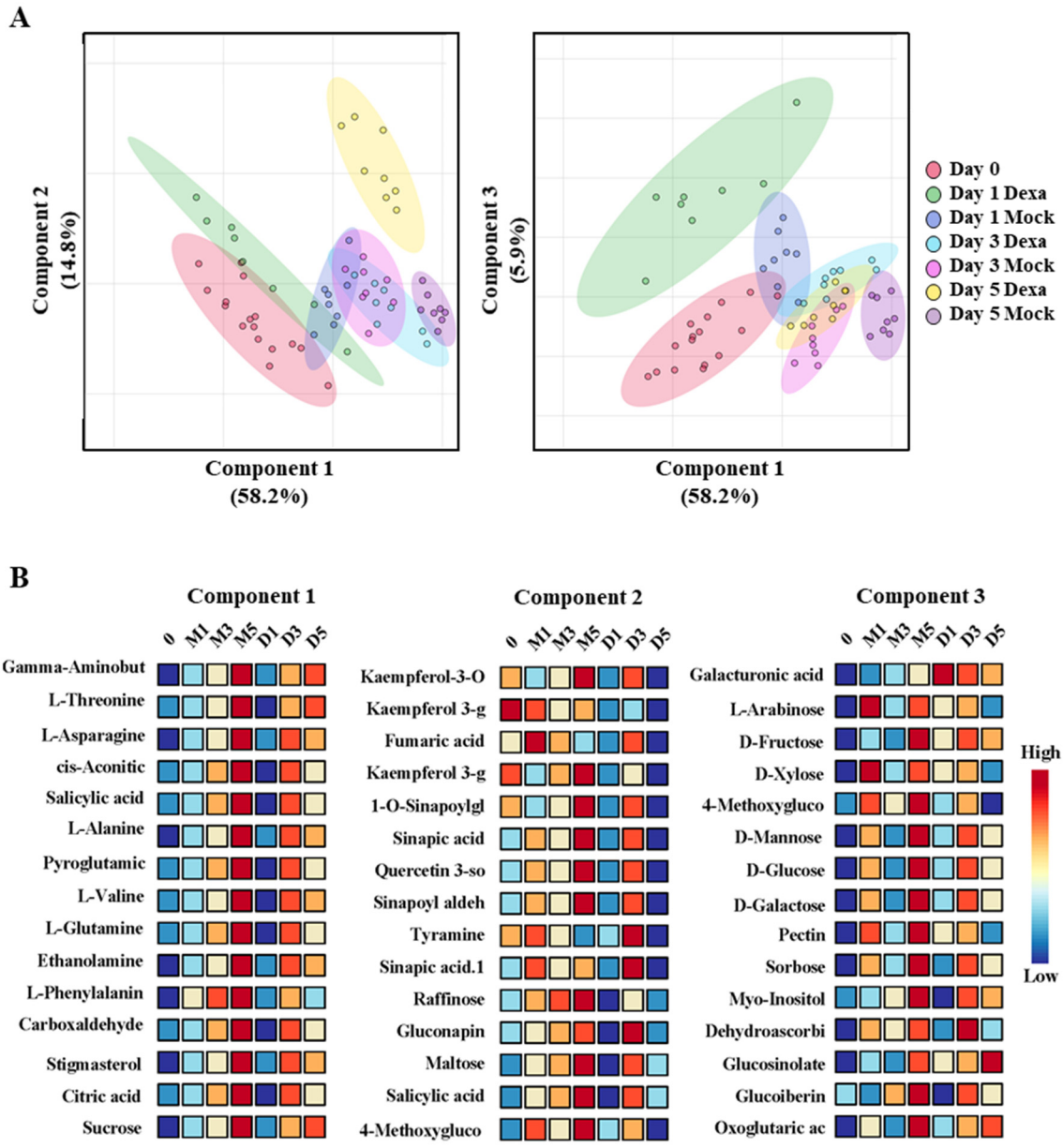

Figure 8. Apex sample treatments representation through days using the first 3 principal components (PCs) from sPLS-DA. A. Score plot between the three major selected PCs. The explained variances are shown in colored brackets assigned per group. **B**. Score plot showing the 15 top variables selected by the sPLS-DA model for a given component. 0, means the samples collected before treatments, M refers to the mock treatment and D refers to dexamethasone treatment. The numbers followed by M and D indicate the sampling day after treatment. The variables are ranked by the absolute values of their loadings.

Analyzing the relative abundance of the different metabolites as a function of treatments over time, we can observe that component 1, responsible for 58.2% of the model variations, seems to refer to growth days since we observe a general tendency for metabolites to increase over time, with amino acids (threonine, asparagine, alanine,

valine, glutamine) being particularly abundant (Figure 8B). On the other hand, components 2 and 3 differ from the pattern observed in component 1, explaining 14.8% and 5.9% of the variance, respectively. Component 2 is characterized by a reduction in the relative abundance of metabolites in dexamethasone-treated apex samples. In this component, we find various glycoside derivatives of phenylpropanoids (kaempferol and quercetin) and carbohydrates (raffinose and maltose). In this case, there is an apparent difference in the abundance of these metabolites when comparing dexa/mock at days 1 and 5. On day 3, however, the opposite happens and we observe an increase in the relative abundance of the metabolites. Finally, component 3 seems to be dominated by carbohydrates (arabinose, fructose, xylose, mannose, glucose, galactose, sorbose) and other glucoside derivatives (galacturonic acid, 4-methoxyglucobrassicin and 8-Methylthiooctyl glucosinolate). In this component, a greater increase in the relative abundance of the metabolites appears to predominate in the dexamethasone-treated samples, with differences at day 3 being particularly relevant. In summary, the results of this model indicate that the first component could be influenced by temporal variation in metabolites as a result of growth. The second and third components could be influenced by changes in metabolites affected by floral induction by dexamethasone.

3.3.2.1. Identification of pathways altered during floral transition based on metabolites detected using a targeted method.

We applied different methods to extract information on the identified metabolites showing a different accumulation in induced and control samples, focusing on day 1 and 3 after induction. First, we used the MetaboAnalyst platform (Pang et al., 2021) to analyze data regarding the relative amount of the identified metabolites and to identify pathways with significant changes during floral transition. This approach allowed us to identify 33 pathways that changed significantly among treatments at day 1 (FDR < 0.05). Surprisingly, by performing the same analysis with the dataset corresponding to day 3 we were only able to identify one pathway. Secondly, we used all metabolites with significant changes to perform a pathway enrichment study by Plant Metabolomic Network (PMN) (Hawkins et al., 2021); a database that comprises a wide range of metabolites from *Arabidopsis thaliana*. In this way, we identified 13 pathways with a p-value <0.01 on day 1 and one pathway on day 3. Due to the large number of annotated and described pathways, we often found some of them redundant. Therefore, to facilitate the

visualization of the obtained results, we grouped all significant pathways identified by both analysis platforms (Supplementary File 3) into common categories.

Table 3. Analysis of metabolic pathway alterations by significant metabolites changes on day 1 in apex. At the left, identified pathways with MetaboAnalyst platform, and on the right identification by enrichment analysis tool from PMN.

Pathways	
MetaboAnalyst	**Plant Metabolomic Network**
Alanine, aspartate and glutamate metabolism	Indole-3-acetate Inactivation
Phenylalanine metabolism	Jasmonate Biosynthesis
Arginine and proline metabolism	Stachyose biosynthesis
Tyrosine metabolism	L-asparagine Biosynthesis
Glycine, serine and threonine metabolism	L-glutamine Biosynthesis
Galactose metabolism	Proteinogenic Amino Acid Biosynthesis
Inositol phosphate metabolism	Superpathway of glyoxylate cycle and fatty acid degradation
Glyoxylate and dicarboxylate metabolism	Glycine Biosynthesis
Butanoate metabolism	Citrate cycle (TCA cycle)

Our results show that several primary metabolism pathways are regulated during floral transition, including carbohydrate metabolism (galactose and stachyose metabolism), several amino acid biosynthesis pathways and fatty acids. Interestingly, we could identify changes in two hormone homeostasis pathways: jasmonate biosynthesis and indole-a3-acetate inactivation.

3.3.3. Untargeted metabolomic analysis by LC-MS (negative).

In parallel, we decided to perform an untargeted analysis with two objectives. First, because the metabolomics approach generates a large amount of data, the use of other omic data layers, in this scenario the untargeted analysis, could help by filtering the results and highlighting relevant putative metabolites or metabolic pathways. In addition, one of the advantages of the untargeted study is the discovery of unknown metabolites, which could allow the identification of new members or regulators of a process through the discovery of unknown metabolites. Because we found no differences in the leaf samples but many in the apex, we decided to focus on studying the metabolic changes in the apex tissue.

For this type of study, we decided to use data from LC-MS in ESI- mode, since the negative mode allows better sensitivity of the compounds and has lower background noise (Liigand et al., 2017). This approach leads us to the detection of more than 5000 mass spectrometry peaks corresponding to putative metabolites in apex samples (Supplementary File 4). To get a better overall view of the data obtained and to check if there were differences between the different apex samples at different times and treatments, we performed an sPLSD-DA analysis. The results showed that the four mayor principal components explained 55.4% of the variation in separation between groups (Figure 9). The most considerable differences seem to be present in the apices at day 5 after induction.

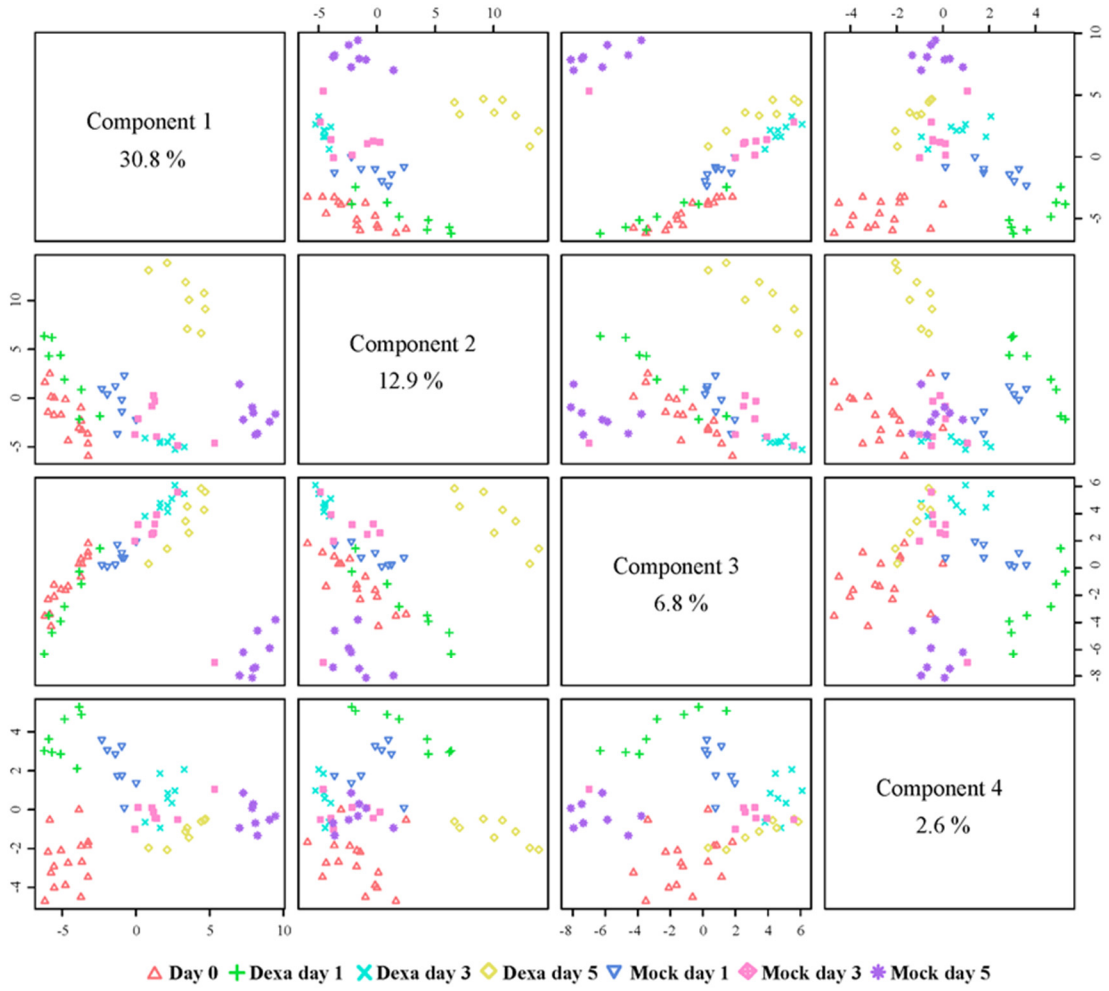

Figure 9. Pairwise score plot between the fourth major components for untargeted approach in apex. The explained variance of each component is shown in the corresponding diagonal cell.

We then performed a univariate analysis using Fisher's LSD between treatment pairs on different days to get an accurate idea of the differences observed at each time point. The number of significant features identified on day 1 was 272 (Supplementary 4), with a predominant reduction of their abundance in the dexamethasone-treated plants, as seen in the heatmap (Figure 10). On days 3 and 5, we identified 68 and 1753 features displaying significant changes in abundance, respectively. The fact that the number of metabolites identified on day 5 was much higher than that of day 3 or day 1 can be attributed to the change of identity of the shoot apical meristem (vegetative to inflorescence) and to the specification of floral tissues in the flank of the shoot apical meristem. On the other hand, as we observe in the data provided by the targeted, the time at which the least significant differences occur is day 3.

Analytical approaches in metabolomics are often referred in two categories: targeted and untargeted. Targeted metabolomics is the measurement of defined groups of chemically characterized and biochemically annotated metabolites (Roberts et al., 2012). In contrast, untargeted metabolomics is the comprehensive analysis of all measurable metabolites in a sample. In addition to a set of identified metabolites, untargeted experiments can yield thousands unidentified features, of which, a fraction may represent unique metabolites (Mahieu & Patti, 2017). The untargeted approach is a global analysis of metabolic changes and is typically carried out for hypothesis generation, followed by targeted profiling for more confident quantification and detection of metabolites (Xiao et al., 2012) or pathways. The metabolite identification is mainly achieved through mass-based search followed by manual verification. First, the *m/z* value of a molecular ion of interest is searched against databases, and the metabolites having molecular weights within a specified tolerance range to the query *m/z* are retrieved from the databases as putative identifications (Xiao et al., 2012) or retention time (RT). Database matching represents only a putative metabolite assignment that must be confirmed by comparing the retention time and/or MS/MS data of a model pure compound to that from the feature of interest in the research sample (Vinaixa et al., 2016). These additional analyses are time-consuming and represent the rate-limiting step of the untargeted metabolomic workflow. Consequently, it is essential to prioritize the list of *m/z* RT features from the raw data that will be subsequently identified by RT and/or MS/MS comparison (Vinaixa et al., 2012). Relevant *m/z*-RT features for MS/MS identification are typically selected based on statistics criteria, either by multivariate data analysis or multiple independent univariate tests (Vinaixa et al., 2012). With the data of the metabolites whose changes in abundance were found to be significant, we performed an analysis of the affected metabolic pathways, the results of which are explained in the following section.

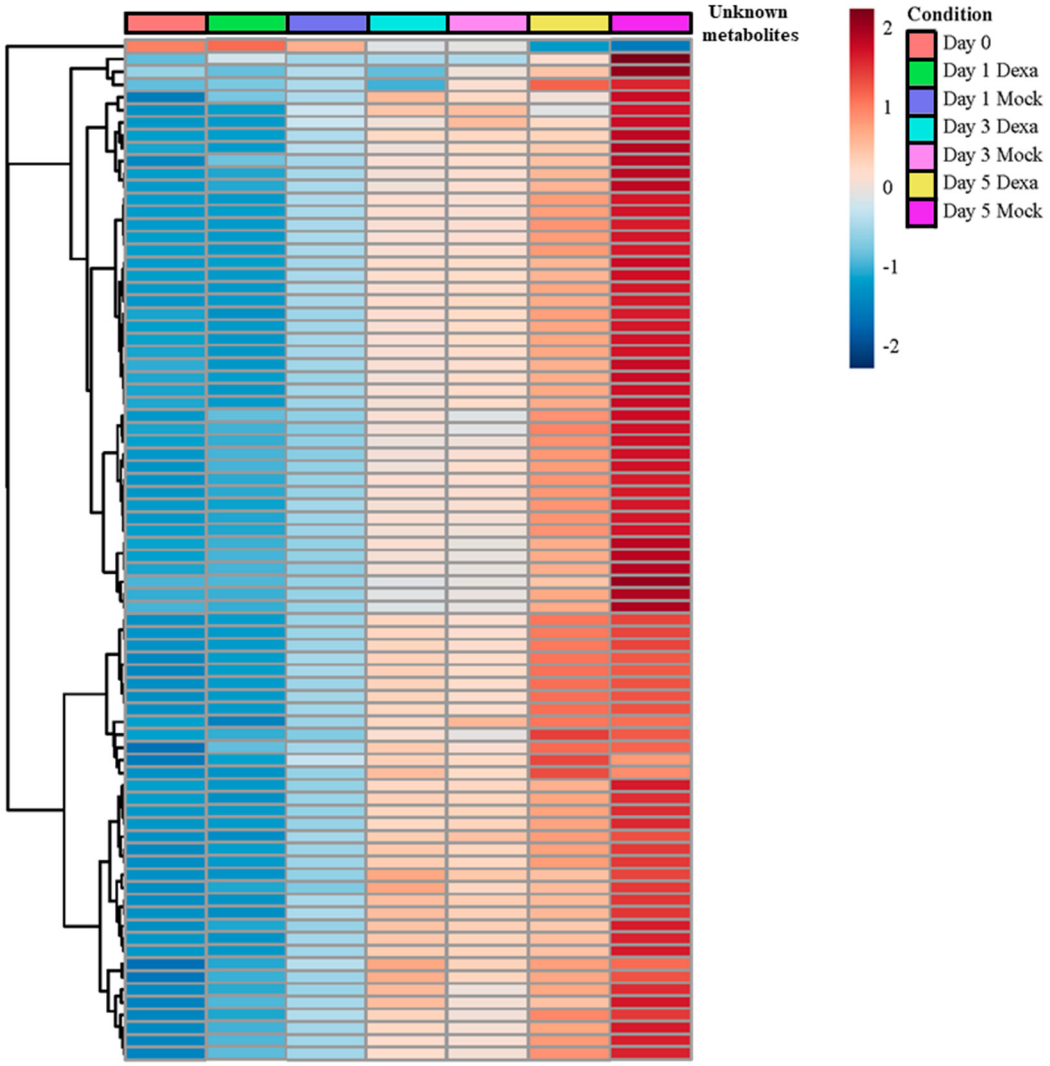

Figure 10. Hierarchical clustering results are shown as a heatmap performed with the top 90 more significant putative metabolites in all conditions. The ANOVA test with Tukey's Honestly Significant Difference (Tukey's HSD) was performed for the multigroup analysis.

3.3.3.1. Identification of pathways altered during floral transition based on metabolites detected using an untargeted method.

Unequivocal identification of metabolites is often difficult following a metabolomic approach and based on the associated mass for each spectrum peak. The advantage of untargeted metabolomics is that as many metabolites as possible can be measured without the need for *a priori* hypothesis. There is no consensus on the best approach for processing and analyzing untargeted metabolomics data. It is reasonable to expect that a

computerized annotation tool will group related features into metabolites and produce a list of metabolites with high-quality annotation (Karnovsky & Li, 2020).

A common mistake in untargeted LC-MS metabolomics is to search each feature in a public database, and use the top or an arbitrary match for pathway analysis. Since the chromatographic information is usually irrelevant in such database search, the top match is usually only one of many possible candidates for the true metabolites. The arbitrary selection of a candidate bears a small probability of finding the true metabolite, and this selection is not necessarily better based on the smallest mass difference between the query and the candidate. When this process is repeated for many metabolites, one ends up using a list of mostly false metabolite identifiers for downstream analysis (Karnovsky & Li, 2020).

An alternative consists of applying the Mummichog algorithm (Li et al., 2013), which analyzes a set of features detected in LC-MS and for each one, a list of possible metabolites as a candidate is computed, being only one valid. First, the algorithm searches for statistically significant features between conditions and then explores pathways using the combination of all candidates and calculates an enrichment p-value for each combination per pathway (Karnovsky & Li, 2020). Thus, we identify features as putative metabolites in the context of individual pathways instead of analyzing individual compounds. Accordingly, we applied the Mummichog algorithm by MetaboAnalyst (Chong et al., 2018) to our dataset from apices on day one after treatment and analyzed a list of significant features considering the potential isotopes and adducts they could correspond to by a Gene Set Enrichment Analysis (GSEA) (Subramanian et al., 2005). These putative compounds were mapped into known *Arabidopsis thaliana* metabolic pathways in the Kyoto Encyclopedia for Genes and Genomes (KEGG) Pathway Database (Kanehisa et al., 2006). As a result, we obtained a list of pathways potentially altered during the floral transition in the apex. On day 1, we identified five pathways with a combined p-value<0.05: galactose metabolism, starch and sucrose metabolism, glycerolipid metabolism, pentose and glucuronate interconversions and ascorbate and aldarate metabolism (Table 4).

Table 4. Meta-Analysis summary of mummichog and GSEA combined results performed by MetaboAnalyst platform on day 1 in the apex.

Pathways	Total size	Significant hits	Mummichog p-value	GSEA p-value	Combined p-value
Galactose metabolism	3	3	2.00E-02	2.00E-02	1.00E-04
Starch and sucrose metabolism	3	3	2.00E-02	2.00E-02	1.00E-04
Glycerolipid metabolism	2	2	9.00E-02	2.00E-02	1.00E-02
Pentose and glucuronate interconversions	2	2	9.00E-02	2.00E-02	1.00E-02
Ascorbate and aldarate metabolism	4	4	1.00E-02	3.40E-01	1.00E-02

Total size indicates the total number of compounds in the KEGG database for a given *Arabidopsis thaliana* pathway. Significant hits refer to the number of significant matches. Mummichog p-value generated from a gamma distribution of significant hits from the Mummichog algorithm. GSEA p-value refers to the p-value from enriched pathways. The combined p-value is the combined p-value from Mummichog and GSEA tests using Fisher's method.

We performed the same kind of analysis to the results obtained with apex samples on day 3 after dexamethasone treatment by the untargeted method. However, in this case, we found much less significant features and only two pathways were depicted: glucosinolate biosynthesis and flavone and flavonol biosynthesis (Table 5).

Table 5. Meta-Analysis summary of mummichog and GSEA combined results performed by MetaboAnalyst platform on day 3 in the apex.

Pathways	Total size	Significate hits	Mummichog p-value	GSEA p-value	Combined p-value
Glucosinolate biosynthesis	3	3	2.00E-02	2.00E-02	1.00E-04
Flavone and flavonol biosynthesis	3	3	2.00E-02	2.00E-02	1.00E-04

Total size indicates the total number of compounds in the KEGG database for a given *Arabidopsis thaliana* pathway. Significant hits refer to the number of significant matches. Mummichog p-value generated from a gamma distribution of significant hits from the Mummichog algorithm. GSEA p-value, refers to the p-value from enriched pathways. Combined p-value are the combined p-value from Mummichog and GSEA test using Fisher's method.

3.3.4. Identification of changes in lipids associated with floral transition.

In plant biology, high-throughput lipid profiling is being used to follow metabolic changes in response to developmental, environmental, and stress-induced physiological changes (Welti, 2007). Identifying the lipid molecular species altered during a process, treatments, or different developmental stages can provide detailed information needed to elucidate the functions of genes involved in lipid metabolism and signaling.

In recent years, great advances have been made in understanding the contribution of lipids to the control of flowering time. FT is a member of a lipid-binding protein family, specifically the phosphatidylethanolamine-binding protein (PEPB) family (Putterill & Varkonyi-Gasic, 2016). These studies discover that, in fact, FT preferentially interacts with the diurnally changing PC in SAM, resulting in increased FT activity and the ability to promote flowering. FT preferentially interacts with PC species containing less unsaturated fatty acids that accumulate predominantly during the light period (Nakamura et al., 2014). This has significantly increased interest in this type of metabolite in the control of flowering. Moreover, a significantly higher resolution crystal structure of FT has recently been resolved, and the putative binding sites for phosphatidylcholine (PC) have been predicted with computational docking simulation (Nakamura et al., 2019).

To improve the available information on lipids and their role in the induction or signaling during floral transition, we decided to perform an exploratory analysis of the major changes in the lipidome in leaves and apices. The samples collected were analyzed by Liquid Chromatography coupled to Mass Spectrometry (LC-Q-TOF-MS) with ESI in negative mode.

The comparison of mass spectrometry profiles with Arabidopsis lipid libraries allowed the identification of a total of 227 lipids in leaf tissue and 190 lipids in apex samples. Surprisingly, we did not observe any significant differences in lipid abundance in leaf samples at any of the analyzed time points. All differences detected over time were concentrated at the apex on day 3 after treatment (Supplementary 5). This result agrees with the observation that there were no significant changes in leaf samples analyzed by targeted metabolomics. However, we found significant differences in lipid abundance in apex samples, although these differences between treatments were limited to day 3 after induction and we did not detect changes at day 1 or day 5. To get a first overview of the

patterns of lipid abundance in the apex, we created a heat map with the 50 lipids that showed the most remarkable differences (Figure 11).

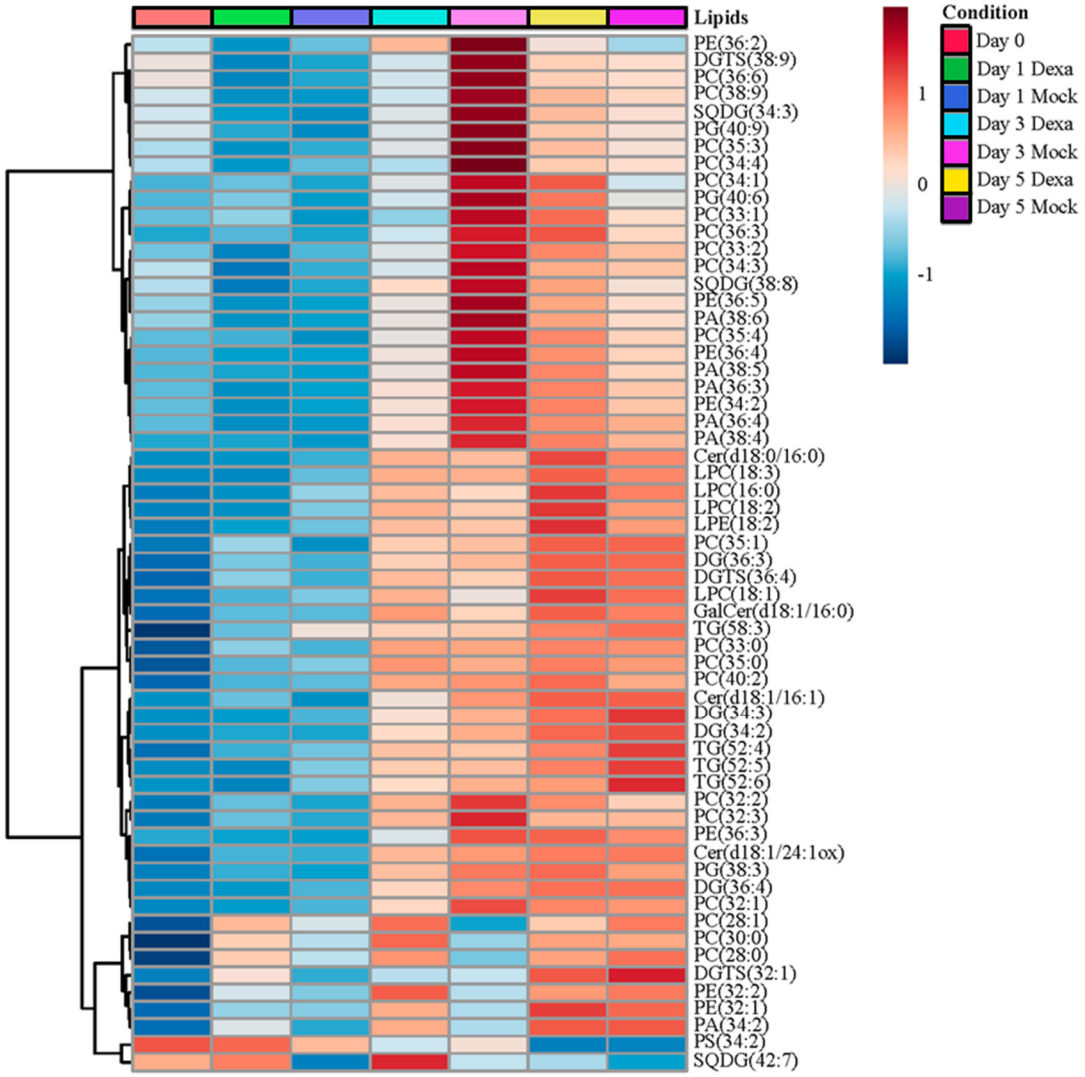

Figure 11. Hierarchical clustering results shown as a heatmap performed with the top 50 more significant lipids in all conditions in apex. The ANOVA test with Tukey's Honestly Significant Difference (Tukey's HSD) was performed for the multigroup analysis.

We identified 48 lipids that displayed a significant change in their abundance in the apex at day 3 (Supplementary File 5). Next, we used these lipids to perform quantitative enrichment analysis (QEA) to identify metabolic pathways (Xia & Wishart, 2010). Through QEA, we can identify meaningful lipid classes that are significantly enriched in the quantitative lipidomics data. This analysis showed that the lipid classes that displayed stronger differences among treatments included glycerophosphoethanolamines, glycerophosphocholines, diacylglycerophosphocholines and diacylglycerophosphates (Table 6).

Table 6. Summary results of the significant lipid class detected by QEA. Quantitative Enrichment Analysis performed with lipid sub-class library from MetaboAnalyst.

Lipid class	Total	Hits	Statistic Q	Holm p	FDR
Diacylglycerophosphocholines	1295	33	41.02	2.59E-02	9.41E-03
Glycerophosphoethanolamines	2423	2	36.52	1.40E-02	8.52E-03
Glycerophosphocholines	485	1	57.10	1.63E-02	8.52E-03
Diacylglycerophosphates	893	2	38.16	7.84E-02	2.24E-02

The Q statistic for a lipid class is the average of the Q statistic for each lipid present in the class. Total indicates the total number of lipids assigned to the sub-class named to the left in the MetaboAnalyst libraries for *Arabidopsis thaliana*. Significant hits refer to the number of significant matches from the total. The lipid classes are ordered by FDR.

3.3.4.1. Identification of lipid pathways altered during floral transition.

In contrast to the described changes identified by the metabolomic approach, which were more intense in samples corresponding to day 1 after treatment, lipidomics analysis on apex and leaf samples showed that most of the changes in lipid abundance were evident on apex samples at day 3 after treatment. Interpretation of lipidomic analysis has been limited due to the complexity and diversity of lipid classes and the lack of information regarding specific biosynthetic and catalytic pathways. Despite these difficulties, we have used the Lipid Pathway Enrichment Analysis (LIPEA) platform, which allows running an Over Representation Analysis (ORA) to identify perturbed lipid pathways provided by the KEGG Database by using exclusively lipid compounds (Acevedo et al., 2018). The significant pathways detected from the analysis among our datasets are in Table 7.

Table 7. Significant lipid pathway changes identified by applying the LIPEA algorithm. The name of the pathways corresponds to the KEGG database.

Pathways	Total size	Significant hits	Raw p-value	Benjamini correction	Bonferroni correction

Glycerophospholipid metabolism	26	5	4.10E-06	4.10E-05	4.10E-05
Glycosylphosphatidylinositol (GPI)-anchor biosynthesis	3	2	3.91E-04	1.30E-03	3.91E-03
Autophagy - other	3	2	3.91E-04	1.30E-03	3.91E-03
Phosphatidylinositol signaling system	11	2	6.82E-03	1.71E-02	6.82E-02

Pathways indicate the name of the significant pathway detected. Total refers to the total number of lipids assigned to the sub-class named to the left in the MetaboAnalyst libraries for *Arabidopsis thaliana*. Significant hits refer to the number of significant matches from the total.

As a result, we identified four lipid pathways with a p-value < 0.05 of significance. The pathway displaying a clearer perturbation was the glycerophospholipid metabolism, which is ubiquitous in nature and is a key component of the lipid bilayer of cells and involved in the metabolism of cell signaling (Bhattacharya, 2019). Phosphatidylinositol metabolism was also perturbed and also is involved in the signaling system.

3.3.5. Characterization of hormone profiles (IAA, jasmonic acid, salicylic acid and abscisic acid) by LC-MS.

Hormones play a relevant role in the regulation of plant development. Besides the well-known role of gibberellins in the control of floral induction in short day conditions (Bao et al., 2020), other hormones have been suggested to contribute to the control of floral induction (Izawa, 2021). We decided to analyze jasmonic acid (JA), abscisic acid (ABA), the auxin indole-3-acetic acid (IAA), and salicylic acid (SA) for several reasons: IAA and JA, because we detected the pathways of indole-3-acetate inactivation and jasmonate biosynthesis using a targeted method (Table 3), SA, because one of the significantly detected metabolites was a glucoside derivative of salicylic acid, and ABA, because we are more interested in the role of ABA in flowering in our laboratory, based on preliminary results of ABA in relation to flowering time. For these reasons, we perform hormone analysis in the apex and leaf samples from day 0 to day 5 after treatment (Figure 12).

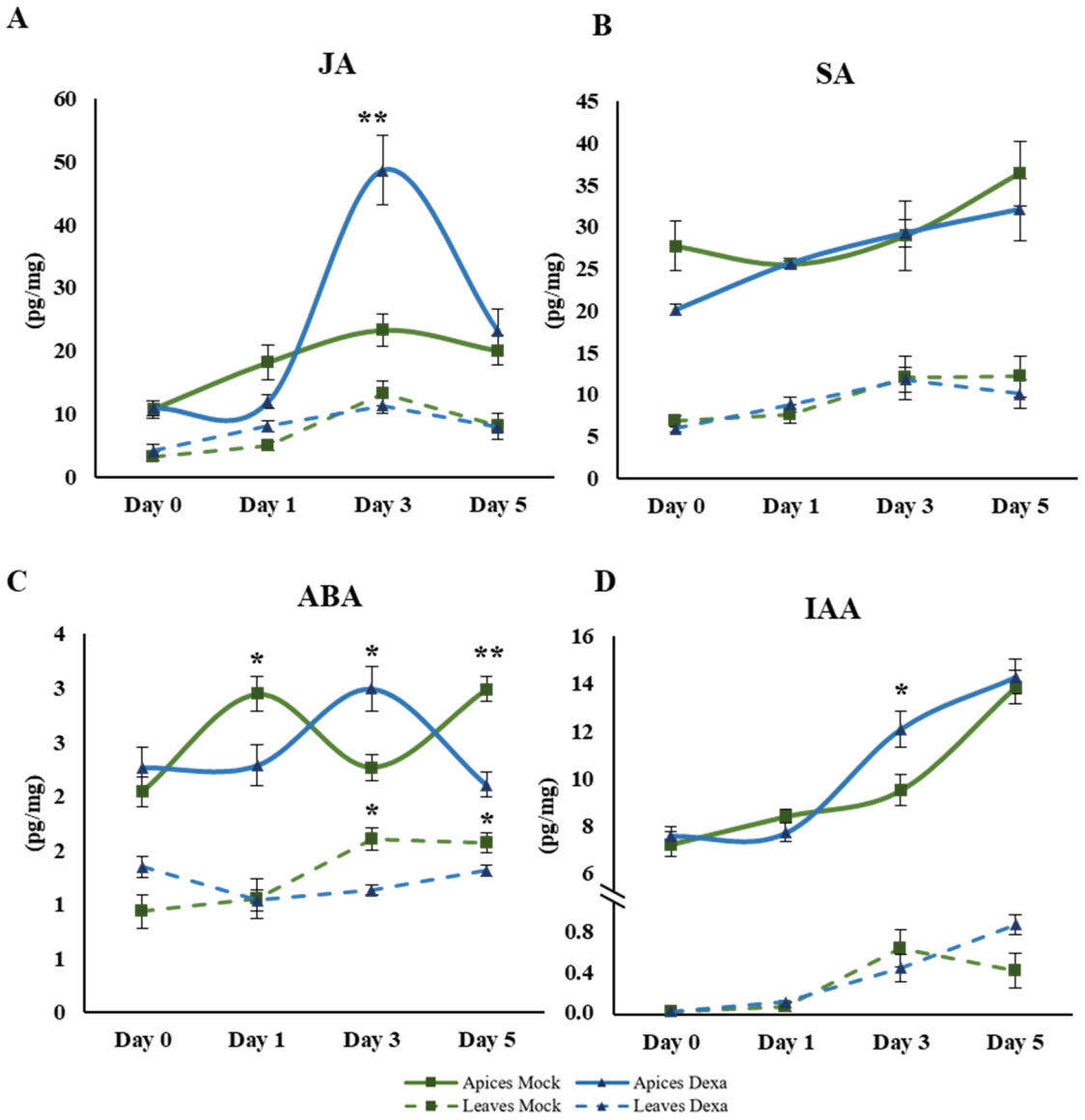

Figure 12. Levels of endogenous hormones in apices and leaves of p*CO*:*CO*:*GR* plants after treatment with dexamethasone. Apex samples in A, B, C and D. Leaf samples in E, F, G and H. Salicylic acid (SA) in A and E. Abscisic acid (ABA) in B and F. Jasmonic acid (JA) in C and G. Indole-3-acetic acid (IAA) in D. Green lines represent the mock treatments and blue the dexamethasone treatment. Error bars indicate the standard error of the mean (SEM) of eight biological replicates. ANOVA with Tukey correction was performed to calculate the significant differences marked by long lines. ** indicates p-value<0.01, * indicates p-value<0.05.

SA values showed no significant change in any of the samples and were constant over time and between treatments (Figure 12B). However, the greatest variation in the abundance of the analyzed hormones was observed in ABA. In the apex, levels decreased on day 1 and 5 after dexamethasone treatment compared with mock-treated plants. Interestingly, this pattern reverses at day 3, when the hormone level in the apex increase

in dexa-treated plants (Figure 12C). The JA and IAA also showed an increase in their levels on day 3 in the apex (Figure 12 A, D) but not in the other time points. On the other hand, ABA was the only hormone that showed variations in the leaf, displaying lower levels in dexa-treated leaves than in mock-treated ones.

In summary, we observed that ABA accumulates in the leaves of plants that remain in the vegetative phase (mock-treated). Also, we observed two different behaviors; in an early stage of floral transition in the apex (corresponding to day 1), we observed a reduction in ABA; in a later stage, an increase in the levels of the hormones analyzed with the exception of SA. This general increase of the IAA, ABA and JA levels in the apex correlates with the increase of the generic metabolite abundance observed at day 3 by the targeted metabolomic approach in the plant apices induced to flower. Finally, it is interesting to highlight that in the cases of the 4 hormones analyzed, the hormone levels, regardless of the treatment, were always higher in the apex than in the leaf.

3.3.6. Changes in the transcriptome associated with the floral transition by RNA-seq analysis.

To gain power of prediction in our omics integrative analysis, we used RNAseq analysis to study the transcriptomic changes in leaves and apices at days 1 and 3 to test whether changes in identified metabolites were correlated with gene expression changes in their biosynthesis or degradation pathways.

We conducted a differential gene expression analysis to characterize transcriptional variations during the floral transition in our experimental system. In leaf samples, we could only identify a few genes with an altered expression when comparing dexamethasone *versus* mock treatments. A total of 24 genes displayed differential expression on day 1 and just one gene on day 3 (log2 fold change > 0.5 and FDR < 0.1) (Supplementary File 6). As expected, *FT* expression was induced in dexamethasone-treated leaves, with a massive fold change of 8, confirming that the inducible system via CO-GR worked. Surprisingly, the only gene upregulated on day 3 was *BROTHER OF FT AND TFL1* (*BFT*), with a massive fold change of 6 (Supplementary File 6). These few changes at the gene expression level are in agreement with results obtained for the leaf metabolome, where we did not identify significant differences between treatments.

In the apex samples, a total of 571 genes on day 1 and 591 on day 3 showed significant differential expression between samples from dexamethasone/mock-treated plants with a $\log_2$ fold change > 0.5 and FDR < 0.05 (Supplementary File 6). Among them, we identified that from the genes coding for enzymes, 59% were downregulated on day 1 and 57% upregulated on day 3 in dexa/mock (Figure 13A).

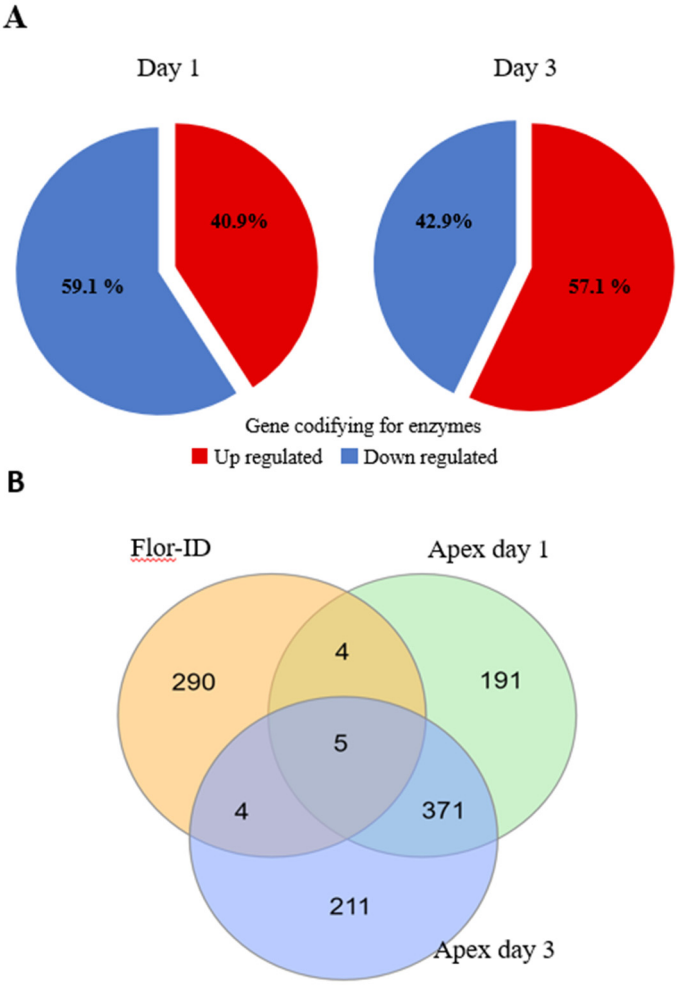

Figure 13. Summary of distribution of genes differentially expressed (DEGs) in apices samples from dexamethasone and mock treated plants. A. Percentage of DEGs codifying for enzymes in apex tissue on days 1 and 3. B. Venn diagram of RNA-seq data compared with Flor-ID gene database.

To investigate whether these transcriptional changes correlate with what has already been described, we compared the DEG list with the Flowering Interactive Database FLOR-ID (Bouché et al., 2016), which contains gene networks with a known function in regulating flowering time (Figure 13B). We detected changes indicating that dexa-treated apices initiated the transition to flowering, such as up-regulation of *SOC1* and *FRUITFULL* (*FUL*) or down-regulation of the flowering repressors *SCHLAFMUTZE* (*SMZ*) and

TARGET OF EAT 3 (*TOE3*). In addition, we identified other flowering-related genes with significant upregulation, including *SQUAMOSA PROMOTER-BINDING-LIKE 4* (*SPL4*), or downregulation, such as *CRYPTOCHROME-INTERACTING BASIC-HELIX-LOOP-HELIX 1* (*CIB1*), *GA INSENSITIVE DWARF 1A* (*GID1A*), *FLOWERING BHLH 4* (*FBH4*), *REVEILLE 2* (*RVE2*), *CONSTANS-LIKE 1* (*COL1*), and *GIBBERELLIN 2-OXIDASE 2* (*GA2OX7*).

We performed a GO enrichment analysis with the DEGs to identify altered putative biological processes and we found multiple categories associated with hormone response and signaling, lipid response, metabolism of small molecules and macromolecules, response to sugars, and metabolite transport, among many other categories (Supplementary File 7).

3.4. Identification of perturbed pathways by integration of transcriptomic data with metabolomic and lipidomic data.

Next, we used the DEGs identified with the inducible system in the apex to determine which metabolic pathways were associated with floral transition at an early-stage (day 1) and a late-stage (day 3) from a gene expression perspective. The metabolic pathway enrichment search and analysis tools from the Plant Metabolomic Network can be used with metabolites (as described in Section 3.3.2.1) or genes. In this scenario, the PMN database includes a list of genes with annotated functions related to metabolism. Among our DEGs gene list, we found 99 at day 1 and 111 at day 3 that were related to metabolic pathways. We performed a pathway enrichment analysis with those and found a total of 47 pathways at day 1 and 51 pathways at day 3 with a p-value < 0.05 and the table 8 summarizes the most significant pathways identified in this analysis.

Table 8. Summary of 21 most significant and non-redundant pathways identified in the apex samples at day 1 and 3 after treatment.

Day 1		Day 3	
Pathway[a]	p-val	**Pathway[a]**	p-val
Proteinogenic Amino Acid Biosynthesis	1.00E-04	Anthocyanin Biosynthesis	1.00E-04
Superpathway of phenylalanine, tyrosine and tryptophan biosynthesis	1.00E-04	Generation of Precursor Metabolites and Energy	1.00E-04

Spermine and Spermidine Degradation	1.00E-04	Flavonoid Biosynthesis	1.00E-04
Generation of Precursor Metabolites and Energy	1.00E-03	Valencene and 7-epi-α-selinene biosynthesis	1.00E-04
Glutathione degradation	1.00E-03	Phenylpropanoid Derivative Biosynthesis	1.00E-04
Stachyose biosynthesis	1.00E-03	Superpathway of phenylalanine, tyrosine and tryptophan biosynthesis	7.00E-03
Sulfur-Containing Secondary Compound Biosynthesis	3.00E-03	Sesquiterpenoid Biosynthesis	1.10E-02
Amine and Polyamine Degradation	4.00E-03	Aliphatic glucosinolate biosynthesis, side chain elongation cycle	1.30E-02
Phytochelatins biosynthesis	5.00E-03	γ-glutamyl cycle	1.60E-02
L-methionine degradation I (to L-homocysteine)	5.00E-03	Syringetin biosynthesis	1.60E-02
UDP-α-D-galacturonate biosynthesis I (from UDP-D-glucuronate)	5.00E-03	Pyridine nucleotide cycling (plants)	1.80E-02
phosphatidate metabolism, as a signaling molecule	6.00E-03	Xylan biosynthesis	2.00E-02
Ethylene Biosynthesis	1.00E-02	Hormone Degradation	2.00E-02
Pyridine nucleotide cycling (plants)	1.10E-02	Lipid-dependent phytate biosynthesis II	2.90E-02
γ-glutamyl cycle	1.20E-02	1D-myo-inositol hexakisphosphate biosynthesis V	2.90E-02
Selenium Metabolism	1.20E-02	Jasmonate Biosynthesis	2.90E-02
Secondary Cell Wall	1.50E-02	Secondary Cell Wall	3.00E-02
Jasmonate Biosynthesis	1.80E-02	Glycolipid desaturation	3.30E-02
L-glutamate biosynthesis IV	1.90E-02	Leucopelargonidin and leucocyanidin biosynthesis	3.30E-02
D-myo-inositol-5-phosphate metabolism	3.10E-02	Fermentation to Short-Chain Fatty Acids	4.50E-02
Gibberellin Inactivation	3.10E-02	Amino Acid Biosynthesis	4.60E-02

[a] The pathway analysis was performed by gene enrichment of DEGs detected at different time points. Fisher's exact test calculated p-value.

Among the 21 most significant pathways identified, we found some metabolic pathways that were also pointed out in the targeted and untargeted metabolomic analysis, such as the amino acid metabolism. Also, carbohydrate metabolism is significantly altered as shown by the numerous pathways identified with the three approaches, including "Stachyose biosynthesis," "UDP-α-D-galacturonate biosynthesis I", "Secondary Cell Wall" and "D-myo-inositol-5-phosphate metabolism". Stachyose belongs to the

Raffinose Family of Oligosaccharides (RFOs) and its biosynthesis uses galactose as a precursor. Galactose metabolism was identified both in the targeted and untargeted approach as one of the most perturbed pathways in our dataset (Table 3 and 4). Moreover, changes in raffinose and myo-inositol abundance in the early floral transition stage on day 1 (Figure 8B and Supplementary File 2) reinforce the role of the stachyose pathway in the metabolic reorganization occurring during floral transition.

Additionally, we observed perturbed pathways related to the synthesis and degradation of hormones in all our analyses. In line with this observation, our transcriptome data showed that there are significant changes in gene expression of several enzymes related to ABA degradation. For example, coinciding with the decrease in ABA in the apex on day 1 shown in the hormone quantification (section 3.3.5), we found a significant increase in expression of *CYTOCHROME P450, FAMILY 707, SUBFAMILY A, POLYPEPTIDE 3 (CYP707A3)* (log_2Fold change of 3.5), a meristem-specific enzyme that catalyzes ABA degradation.

Metabolic changes found on day 3 were quite different from those identified on day 1. Perturbed pathways in a later stage of floral transition included anthocyanin biosynthesis, hormone degradation, flavonoids and phenylpropanoid biosynthesis and lipid metabolism. Regarding the biosynthesis of flavonoid and phenylpropanoid compounds, similar pathways were identified by the untargeted method.

Finally, we could point out perturbations in several lipid-related pathways such as "Lipid-dependent phytate biosynthesis II," "Glycolipid desaturation," and "Fermentation to Short-Chain Fatty Acids." The identification of these pathways with the transcriptome data coincides with what we observed in the lipidomic data, where most of the significant differences appeared on day 3.

3.5. Selection and phenotyping of loss-of-function mutants of the main identified pathways.

As described in the previous section, the integration of omics data pointed out several pathways perturbed during floral transition. Among those, we decided to focus our studies on pathways that appeared recurrently in different omics datasets: galactose metabolism, stachyose biosynthesis and degradation, quercetin/polyphenol or kaempferol glycoside

biosynthesis, abscisic acid degradation and auxin inactivation by conjugation. To assess if any of these pathways have a role in regulating the floral transition, we characterized flowering time in long-day conditions of loss-of-function mutants affecting the synthesis or catabolism of key metabolites for each pathway (Table 9).

Galactose is an abundant sugar in plants, especially in plant cell wall polymers and cytoplasmic metabolites. Its synthesis involves the formation of UDP-glucose, which is epimerized to UDP-galactose (Seifert et al., 2002) and another mechanism to accumulate galactose is the release from cell wall turnover or arabinogalactan protein break-down (Althammer et al., 2020). The α-galactosidase catalyzes the hydrolysis of terminal, non-reducing α-D-galactose residues in α-D-galactosides, including galactose oligosaccharides, galactomannans and galactolipids (Vidershaîn & Beîer, 1976). The members of Glycoside Hydrolase Family 27 (GH27) are enzymes that have α-galactosidase activity as predicted by their amino acid sequence (Naumoff, 2004). Four knock-out mutants have been described in Arabidopsis that affect members of this family: *ALPHA-GALACTOSIDASE 1, 2* and *3* (*AGAL1*, *AGAL2*, *AGAL3*) and *B-L-ARABINOPYRANOSIDASE* (*APSE*). The *apse-1* mutant displays developmental defects, including a significant inhibition of hypocotyl growth (Imaizumi et al., 2017). Since galactose metabolism appeared as an altered pathway by both targeted and untargeted approaches, we decided to evaluate the flowering time phenotype of the mutants *agal1-1*, *agal3-1* and *apse-1* (Imaizumi et al., 2017).

Raffinose and myo-inositol display fluctuation in their abundance among mock and dexa-treated plants. Both metabolites are related to the stachyose pathway and the synthesis of the so-called raffinose oligosaccharides family. RFOs represent a large portion of primary oligosaccharides in plants and it is one of the most widespread sucrosyl oligosaccharide series in flowering plants (Kandler & Hopf, 1982). This series comprises raffinose, stachyose, verbascose and ajugose. These carbohydrates consist of α1,6-linked chains of D-galactose attached to the 6-glucosyl position of sucrose. They are synthesized in leaves, roots and tubers and also can be found in all parts of the plants, including seeds. Stachyose es often the main oligosaccharide in storage organs. Functionally, these carbohydrate soluble are used for carbon transport and storage, although they have been reported to act as protective agents during the maturation of drying seeds (Horbowicz & Obendorf, 1994) and cold stress (Gilmour et al., 2000) and signaling (Sengupta et al., 2015). The first step of RFOs biosynthesis starts with galactinol synthesis catalyzed by GALACTINOL

SYNTHASE (GOLS) enzymes, that transfer galactosyl residues from UDP-galactose to myo-inositol. In a second step, galactosyl units are transferred from galactinol to sucrose to form raffinose, and during this reaction, myo-inositol molecules are recovered. Next, RAFFINOSE SYNTHASE (RS) enzymes add galactosyl units to raffinose to produce stachyose and the following members of the raffinose series. In our targeted approach, we detected a reduction in the amount of raffinose and myo-inositol in the apex on day 1 after treatment or in other words, in the early stage of floral transition. Besides, in our transcriptomic data, we found that several genes related to stachyose synthesis were strongly downregulated in dexa-treated samples at the apex, including *GOLS1*, *GOLS2*, *GOLS4* and *RAFFINOSE SYNTHASE 2/SEED IMBIBITION 2* (*RS2/SIP2*). During seed germination, RFOs are broken down into galactose and sucrose. Galactose must enter a recycling pathway to be converted to UDP-galactose (Gangl & Tenhaken, 2016) but first galactose needs to be phosphorylated to yield galactose-1-phosphate (Egert et al., 2012) by *GALACTOKINASE 1* (*GALK/GAL1*). Taking into account all these data, we decided to characterize the phenotype of loss-of-functions mutants affecting the synthesis of galactinol and raffinose, as well as galactose phosphorylation.

The flavonols such as kaempferol and quercetin glucosidic derivatives are the major flavonoids found in *Arabidopsis thaliana* (Kerhoas et al., 2006; Veit & Pauli, 1999). Their biological function includes ultraviolet protection, defense and resistance against biological and abiotic agents and interacting with plant hormones (Winkel-Shirley, 2002). Glycosylation is one of the most widespread modifications of secondary plant metabolites that can alter properties and functions of the modified compound (Gachon et al., 2005). Several glycosyltransferases are acting in *Arabidopsis thaliana,* but it has been demonstrated to preferentially transport sugars to the 3-OH and 7-OH position of the flavonol (Lim et al., 2004). In our experimental system, we detected the "Flavone and flavonol biosynthesis" by untargeted method, and also this glycoside derivates version was crucial to the separations of the group in apices samples performed by sPLS-DA analysis (Figure 8). For these reasons, we decided to study the flowering time in loss-of-function mutants responsible for adding glycosidation to this type of compounds. Therefore, we selected 2 genes from the UDP-*GLUCOSYL TRANSFERASE 73B* family (*UGT73B2* and *UGT73B3*) as well as the *UDP-GLUCOSYL TRANSFERASE 78C1* (*UGT78C1*) and *UDP-GLUCOSYL TRANSFERASE 89D1* (*UGT89D1*) genes.

Regarding hormones, we have chosen to study them because they recur in different analytical techniques: by direct measurement in the case of ABA, SA and IAA (Figure 12) or as a "hormone degradation" pathway, among others (Table 8). Plant growth and development are controlled by both external cues and intrinsic growth regulators, such as hormones (Santner et al., 2009). Notably, all of these hormones can regulate many processes independently, but cooperation and crosstalk between their signaling pathways appear to exist, as deduced from their overlapping influence on various processes (Depuydt & Hardtke, 2011). The positive effect of gibberellins (GAs) on plant floral transition has been extensively and intensively explored and documented (Shu, Zhou, et al., 2018) and ABA is also involved in the regulation of flowering time as both positive and negative (Riboni et al., 2013; Shu et al., 2016; Wang et al., 2013). The major ABA catabolic pathway is triggered by ABA 8′-hydroxylation catalyzed by the cytochrome P450 CYP707A family (Umezawa et al., 2006). Here, we decided to investigate the possible effects of the *CYP707A3* gene on flowering for two reasons. First, we detected an increase in its expression in the apex on day 1 and second, because we detected a decrease in the ABA total amount in the apex on day 1.

On the other hand, Indole-3-acetic acid (IAA), a prevalent form of auxin, is an important phytohormone that affects many aspects of plant development throughout the whole plant life cycle. IAA also plays a crucial role in allowing plants to respond to the biotic and abiotic stimuli they encounter (Woodward & Bartel, 2005). Besides, synthetic auxins have been used for the synchronization of flowering in horticulture (Sauer et al., 2013). In our data, we detected variations in the IAA in the apex on day 3, and also the "Indole-3-acetate Inactivation" pathway was detected in section 3.3.2.1 (Table 3). IAA is subject to a number of biochemical modifications that regulate its activity and allow plants to fine tune their levels of active auxin (Woodward & Bartel, 2005). The *VAS2/GRETCHEN HAGEN 3.17* (*VAS2*) , *WES1/ GRETCHEN HAGEN 3.5* (*WES1*) and *GRETCHEN HAGEN 3.4* (*GH3.4*) genes encode an IAA-amido synthase that conjugates aspartate and other amino acids to auxin (Woodward & Bartel, 2005). It has been described that *vas2-2, wes1-1* and *gh3.4* have higher free and active IAA levels than wild type (Park et al., 2007; Porco et al., 2016; Zhang et al., 2007; Zheng et al., 2016). Therefore, we decided to evaluate the phenotype for flowering time of the described mutants under long-day conditions (Table 9).

Table 9. Flowering time characterization of homozygous knock-out mutants for the selected metabolic pathways. Data show the total leaf number and days as a measurement of flowering time.

Genotype	Pathway	Rosette[a]	Cauline[b]	Total[c]	Days[d]	n[e]
Col-0	-	12.9 ± 1.1	3.3 ± 0.6	16.2 ± 1.4	28.1 ± 1.3	18
agal1-1	Galactose	13.7 ± 1.6	4 ± 0.7	17.7 ± 1.8	28.2 ± 2.7	12
agal3-1		13 ± 1.8	3.3 ± 0.4	16.3 ± 1.7	28.1 ± 2.9	20
apse-1		12.7 ± 2.1	3.1 ± 0.3	15.8 ± 2.2	29.3 ± 2.7	13
galk	Stachyose biosynthesis/ degradation	12.7 ± 1.6	3.7 ± 0.9	16.4 ± 1.6	26.8 ± 1.8	19
rs2-2		13.4 ± 1.7	3.2 ± 0.5	16.6 ± 1.6	27.9 ± 2	19
gs3-1		13 ± 0.9	3.1 ± 0.2	16.1 ± 0.9	28.2 ± 2.3	18
gs4-1		13.3 ± 1	3.3 ± 0.7	16.6 ± 1.1	26.9 ± 3.2	16
rs5-2		**10.2 ± 1.7**	**2.8 ± 0.6**	**13 ± 1.9**	**23.5 ± 1.9**	**19**
ugt73b2	Quercentin/polyphenol	12.4 ± 1.2	3.9 ± 0.9	16.4 ± 1.8	28.2 ± 1.9	17
ugt73b3		13.1 ± 1.1	3.8 ± 0.7	16.9 ± 1.7	26.3 ± 2.1	15
ugt78c1	Kaempferol glycoside biosynthesis	11.9 ± 1.6	3.6 ± 0.9	15.4 ± 2.1	26.8 ± 2.8	16
ugt89d1		14.8 ± 1.3	3.7 ± 0.6	18.5 ± 1.5	30.2 ± 2	18
cyp707a3	ABA degradation	14.3 ± 1.2	3.4 ± 0.6	17.7 ± 1.5	29.9 ± 2.6	20
vas2-2	Auxin inactivation by conjugation	**10.3 ± 1.8**	**3.2 ± 0.6**	**13.5 ± 1.8**	**25.1 ± 2.1**	**15**
wes1		12.9 ± 1.1	3.2 ± 0.4	16.1 ± 1.1	30 ± 2	20
gh3.4		12.6 ± 1.7	3.1 ± 0.6	15.7 ± 1.8	27.5 ± 2.8	19

Values represent average ± standard deviation. [a] Rosette: number of rosette leaves. [b] Cauline: number of cauline leaves. [c] Total: total number of leaves. [d] Days: number of days until bolting (measured as when the inflorescence stem reaches 1 cm). [e] n= number of plants analyzed.

We found significant differences in flowering time in two mutants, *rs5-2* and *vas2-2*, affecting stachyose synthesis and auxin inactivation, respectively. In contrast, we did not find any significant difference in mutants affecting any of the other analyzed pathways (galactose metabolism, quercetin/polyphenol biosynthesis, kaempferol glycoside biosynthesis or ABA degradation).

In terms of hormones, ABA was the most promising, showing the greatest variation in the dexamethasone induction system used, but on the other hand, we did not obtain a clear phenotype when we analyzed the mutants under long-day conditions. However, our data suggest an obvious importance of ABA in the meristem during the floral transition because, first, the amount of ABA in the induced apices samples was significantly reduced and, second, an enzyme responsible for its degradation increased massively in the apex. On the contrary, the *vas2-2* mutant showed an early flowering phenotype, but since auxin is a hormone involved in an extraordinarily wide variety of biological mechanisms, such as endocytosis, cell polarity, cell cycle, cell elongations, differential growth, light response, embryogenesis, tissue patterning, de novo formation of organs and more (Sauer et al., 2013). In our laboratory, ABA is gaining importance as we have found a linking role from ABA to *TFL1* in different projects (García, 2021.; Martínez, 2022.; Silvestre Vañó, 2020). Therefore, we decided to examine the effect of ABA at the apex during floral transition in more detail before deciding which hormonal pathway (ABA or IAA) to further study for phenotypic characterization of flowering time.

The *rs5-2* mutant is a loss-of-function affecting the *RAFFINOSE SYNTHASE 5* (*RS5*) gene, the only genuine raffinose synthase enzyme catalyzing the synthesis of raffinose from myo-inositol (Egert et al., 2013). The *rs5-2* mutant flowers are early compared to the wild type, both in leaf number and days to bolting under long days conditions. These results agree with the fact that both raffinose and myo-inositol decreased in apices of plants that were induced to flower (Figure 8). Considering these observations, we decided to study further the possible role of those genes and metabolites in the regulation of floral transition.

3.5.1. ABA degradation.

Characterization of hormone profiles (section 3.3.5) showed that ABA decreased at a very early stage after dexamethasone induction (Figure 12C). Accordingly, transcriptomic data in the same type of samples showed that the expression of *CYP707A3* gene increased in dexamethasone-treated compared to mock-treated samples, with a $\log_2$ Fold change of 3.5. *CYP707A3* encodes a protein with ABA 8′-hydroxylase activity, and therefore it is involved in the degradation of ABA. Despite the fact that we did not find any alteration in flowering time in the *cyp707a3* mutant (section 3.5, Table 9), we decided to further investigate the possible role of ABA in early events during floral transition.

Because *CO* integrates photoperiod signals via *GI* (mainly) and the *CO* expression peak does not coincide with light under short-day conditions, the CO protein is not stabilized, preventing activation of *FT* via this pathway. The *co* mutants exhibit expression patterns more similar to those of plants growing in short days than in long days conditions. In this way, our floral induction system, based on the activation of the CO-GR protein by dexamethasone, mimicked the response to the integration of convergent photoperiod signals in *CO* as if plants were growing under short-day conditions but without the other molecular and physical phenotypes associated with growth as a consequence of lower daylight hours. Activation of the CO-GR protein leads to rapid induction of *FT* in the leaf and subsequent activation of *SOC1* in the apex, all within the first 24 hours after dexamethasone treatment (Figure 6 section 3.3.1 and Figure 13 section 3.3.6). In addition, ABA has been described to possibly have a function in the floral transition by inhibiting flowering at the apex by suppressing *SOC1* regardless of photoperiodic conditions (Riboni et al., 2016). For all these reasons, we hypothesize that one of the changes necessary for the onset of floral transition is a reduction in the amount of ABA in the meristem at an early stage. To test this hypothesis, we grew the plants in a short-day chamber to ensure that the meristems remained in the vegetative phase, and we made the switch to the long-day conditions to induce flowering while we treated the apices for four days with an ABA or a mock solution. In agreement with our hypothesis, we would expect a delay in flowering in the plants treated with ABA compared to mock- treated-plants (Figure 14).

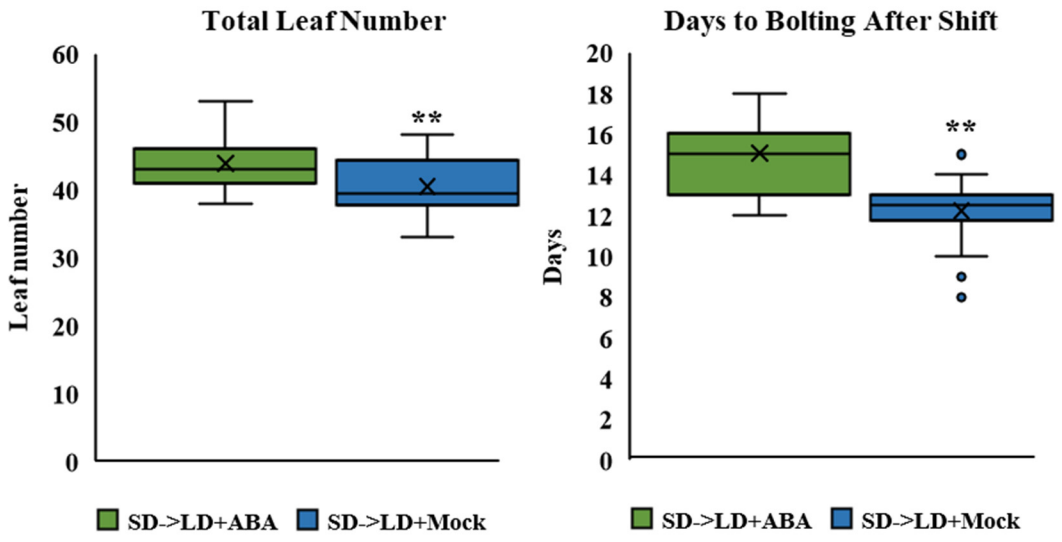

Figure 14. Flowering time characterization, by leaf number and days to bolting, of ABA and mock-treated Col-0 plants. Plants with 22-25 leaves (corresponding to 30-day old plants grown under SD conditions) were shifted to LD conditions and treated with a Mock or ABA solution (30µM, a drop on the shoot apex). The boxplots display the median and the first and third quartile. The mean is represented by a cross and the whiskers indicate maximum and minimum values, excluding outliers. Dots exhibit outlier values. The leaf number and days until bolting was significantly different in both treatments (P-value < 0.01[n_{ABA}=24, n_{Mock}=26]). ANOVA with Tukey correction was performed to calculate the significant differences. ** indicates p-value<0.01, * indicates p-value<0.05.

We found that ABA treatment applied to the meristem delayed flowering both in terms of total leaf number (3 leaves more in ABA-treated plants) and days to bolting (almost three days later in the ABA-treated plants). To investigate whether ABA has an impact on flowering under non-inductive SD conditions, we extended our analysis to include mutants in two more genes encoding ABA hydroxylases: *CYP707a1* and *CYP707a2*. We characterized the flowering time of the three simple mutants and the double mutant combinations under LD and SD conditions.

Table 10. Flowering time characterization of simple and double mutants of the *CYP707A* family under long-day or short-day conditions.

Genotype	Long Day			Short Day		
	Rosette Leaves[a]	Days[b]	n[c]	Rosette Leaves[a]	Days[b]	n[c]
Col-0	15.7 ± 1.1	27.7 ± 1.0	17	60.4 ± 4.3	70.4 ± 6.8	20

cyp707a1-1	15.0 ± 1.4	28.7 ± 2.6	18	65.8 ± 7.2	75.2 ± 8.0	17
cyp707a2-1	13.8 ± 1.0	26.6 ± 2.0	17	65.2 ± 5.8	77.5 ± 9.1	18
cyp707a3-1	16.1 ± 1.8	31.2 ± 2.7	16	**70.2 ± 5.0**	**80.5 ± 7.6**	18
a1-1,a3-1	15.9 ± 1.4	28.0 ± 2.9	20	**68.7 ± 7.2**	**80.0 ± 7.9**	16
a2-1,a3-1	14.3 ± 1.5	29.3 ± 2.1	16	**68.2 ± 6.1**	**78.8 ± 7.9**	17

Values represent average ± standard deviation. [a] Rosette leaves: number of rosette leaves. [b] Days: number of days until bolting (measured as when the inflorescence stem reaches 1 cm). [c] n: number of plants analyzed. ANOVA with Tukey correction was performed to calculate the significant differences which are highlighted in bold and indicate p-value<0.01.

Figure 15. Characterization of flowering time of mutants of three *CYP707A* family genes. Plants were grown under SD. Pictures were made when all plants had produced floral buds.

We confirmed that the *cyp707a3-1* mutant does not display any flowering phenotype when grown in LD conditions, nor do the other simple mutants *cyp707a1-1* and *cyp707a2-1*. However, when plants were grown in SD conditions, the *cyp707a3* mutant flowered significantly later than the wild type, as did all mutant combinations carrying the *cyp707a3-1* allele (Figure 15). Combining the *cyp707a3-1* mutation with *cyp707a1-1* or *cyp707a2-1* did not enhance the late-flowering phenotype.

3.5.2. RFOs biosynthesis and degradation of raffinose oligosaccharides.

Targeted metabolite detection using the metabolomics approach showed that on day 1, after flowering was induced in our system by dexamethasone treatment, the levels of raffinose and myo-inositol decreased compared with the mock (Figure 8, section 3.3.2). Reconstruction of the metabolic pathways with the metabolites showing a significant change in their abundance revealed that stachyose metabolism was affected (Table 3, section 3.3.2.1). In addition, transcriptome analysis showed that several genes involved in raffinose biosynthesis were down-regulated in the apices induced to flower, and the stachyose metabolic pathway was also significantly detected (section 3.3.6 and Table 8, section 3.4). Moreover, the first mutants screening revealed that the *rs5-2* mutant flowers earlier than the wild type (Table 9, section 3.5). Finally, both myo-inositol and raffinose are components of the galactose metabolic pathway that have consistently been found to be significant in both targeted and untargeted approaches (Table 3, section 3.3.2.1 and Table 4, section 3.3.3.1). Figure 16 summarizes the changes in metabolites related to the raffinose metabolism that have been detected by targeted and transcriptomic approaches. Both raffinose and myo-inositol abundance decrease with floral induction, along with an increase in more simple carbohydrates such as fructose or sucrose. At the same time, transcriptomic data showed that *GOLS1*, *GOLS3* and *GOLS4* genes were downregulated upon floral induction, as it was also *RS2*, a member of the *RAFFINOSE SYNTHASE* gene family.

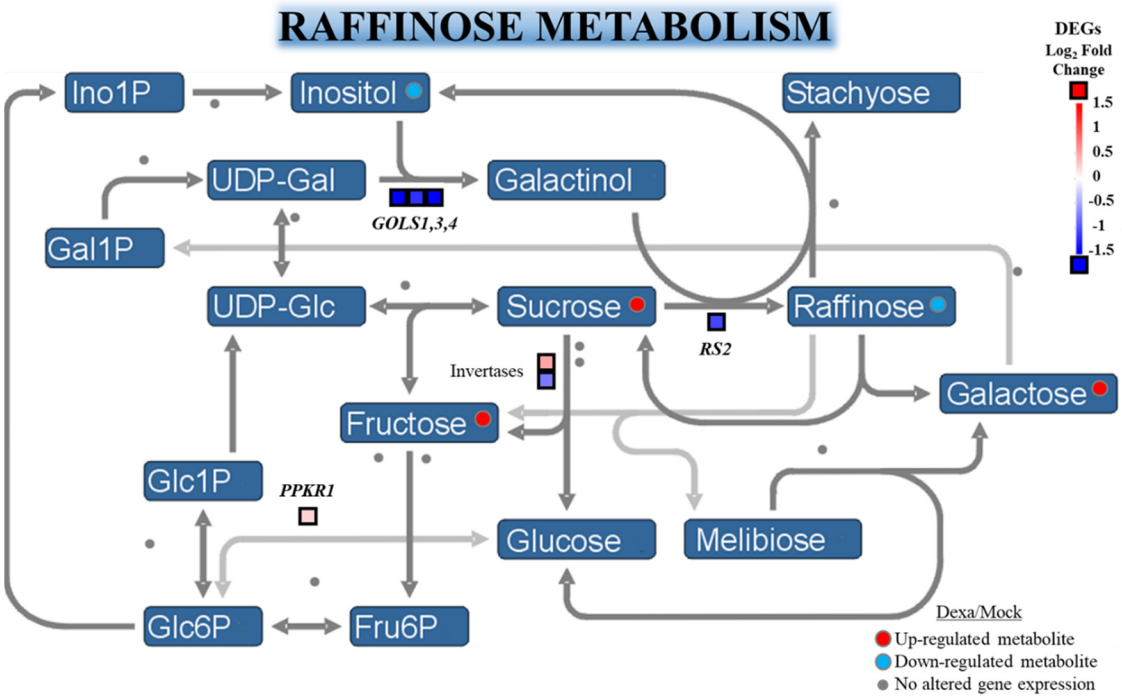

Figure 16. Schematic representation of raffinose metabolism and components of that metabolism detected in the transcriptomic analysis and targeted metabolomic approaches. In an early stage (day 1 after induction), levels of myo-inositol and raffinose decrease and the expression of *GOLS1*, *GOLS2*, *GOLS3* and *RS2* is reduced. We also detected changes in the expression of two invertases. *ALKALINE/NEUTRAL INVERTASE C* (AT3G06500; upregulated) and *ALKALINE/NEUTRAL INVERTASE I* (AT4G09510; down-regulated). In a late-stage (day 3 after induction), the expression of *GOLS4* and *RS2* remained altered and increase the expression of *PEP CARBOXYLASE KINASE-RELATED KINASE 1* (*PPKR1*). Sucrose, fructose and galactose levels increased. The figure is a modification from the raffinose pathway made with MapMan.

To confirm whether mutations in the *RS5* gene had an impact in the control of flowering time we characterized a second loss-of-function mutant allele of *RS5*. The *rs5-3* allele, previously described as *rs14*, corresponds to an insertional mutant from the GABI-Kat collection and the insertion of the T-DNA is located in the first exon. The *rs5-3* plants accumulate high levels of galactinol and defects in raffinose biosynthesis in the leaves (Gangl & Tenhaken, 2016; Knaupp et al., 2011; Zuther et al., 2004).

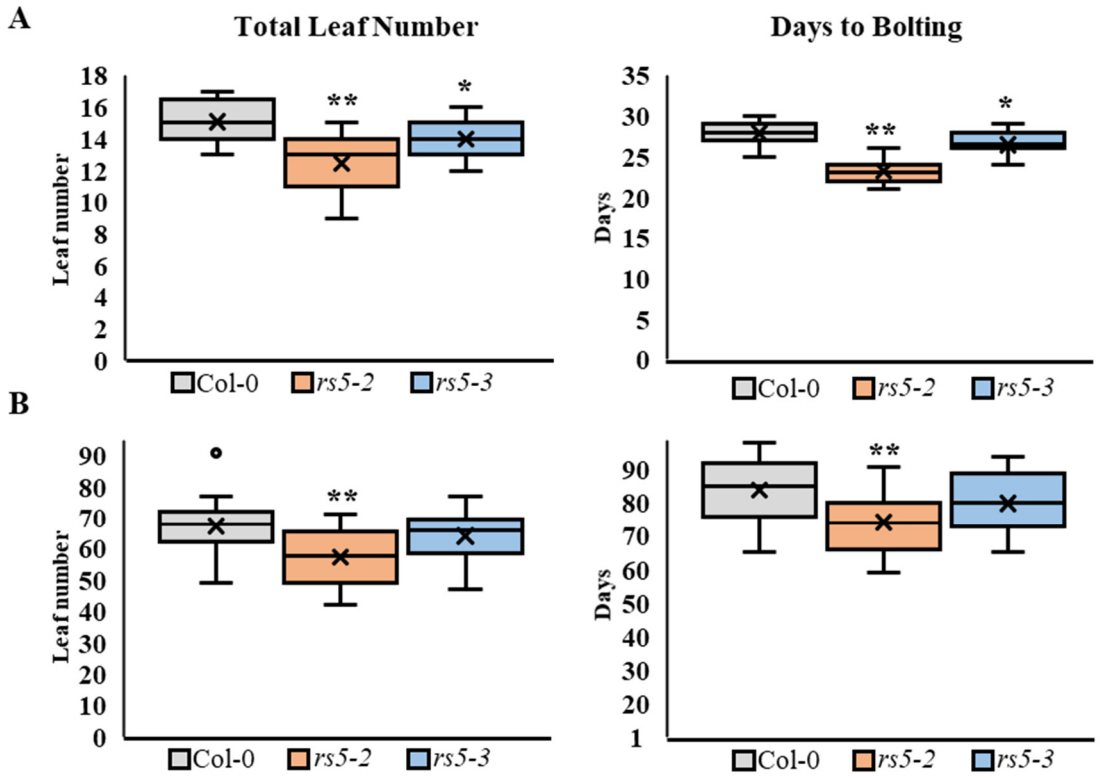

Figure 17. Flowering time characterization of different *rs5* alleles grown under long day (A) and short-day (B) conditions. Boxplots show the first and the third quartile, and the line

represents the median. The mean is shown as a cross. Whiskers show the highest and lowest values and outliers are shown as dots. ANOVA with Tukey correction was performed to calculate the significant differences. ** indicates p-value < 0.01, * indicates p-value < 0.05. LD population sizes for Col-0, *rs5-2, rs5-3*, are 17, 23 and 22 individuals, respectively. SD population size in the same order is 31, 28 and 25 individuals.

We confirmed that both alleles, *rs5-2* and *rs5-3,* exhibit an early flowering behavior in LD conditions (Figure 17). However, the *rs5-2* allele showed a stronger phenotype, flowering with an average of 3 leaves less than Col-0. The *rs5-3* mutant displayed just one leaf of difference in comparison to Col-0. On the other hand, under short days conditions, the *rs5-2* was the only mutant that showed a phenotype, flowering earlier than Col-0 with ten leaves less on average.

Interestingly, we observed that the *rs5-2* mutant produced fewer seeds than the wild type, and the number of fruits per plant and their size was compromised too. However, these additional phenotypes were not present in the *rs5-3* mutant (Figure 18). These data show that the *rs5-2* mutant has a more severe phenotype than *rs5-3 r*egarding reproductive development: flowering time, the number of flowers/fruits, fruit size and the number of seeds.

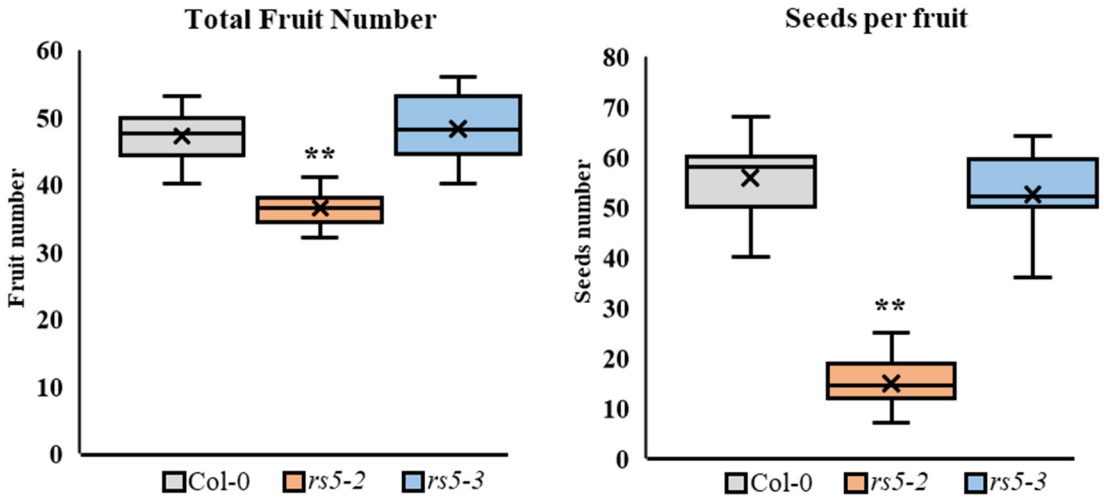

Figure 18. Quantification of fruit and seed number in *rs5* mutants and wild type. To the left, the total fruit number in Col-0, *rs5-2* and *rs5-3*. We scored the number of fruits when the meristem stopped producing flowers (n= 14 plants per genotype). To the right, seed number per fruit. We scored the number of seeds of 10 fruits (floral nodes 6-15). Four replicates per genotype were scored. Boxplots show the first and the third quartile, and the line represents the median. The

mean is shown as a cross. Whiskers show the highest and lowest values. ANOVA with Tukey correction was performed to calculate the significant differences. ** indicates p-value<0.01.

We investigated if mutations in other genes involved in RFO biosynthesis display a flowering time phenotype. We analyzed the flowering time phenotype of simple and double mutant combinations, including: *gs1-1, gs2-1, gs1-1gs2-1, gs3-1, gs4-1, rs2-2, rs4-1, rs5-2, rs5-3, rs6-1, rs2-2 rs5-2, rs4-1 rs5-2 and rs5-2 rs6-1* (Figure 19).

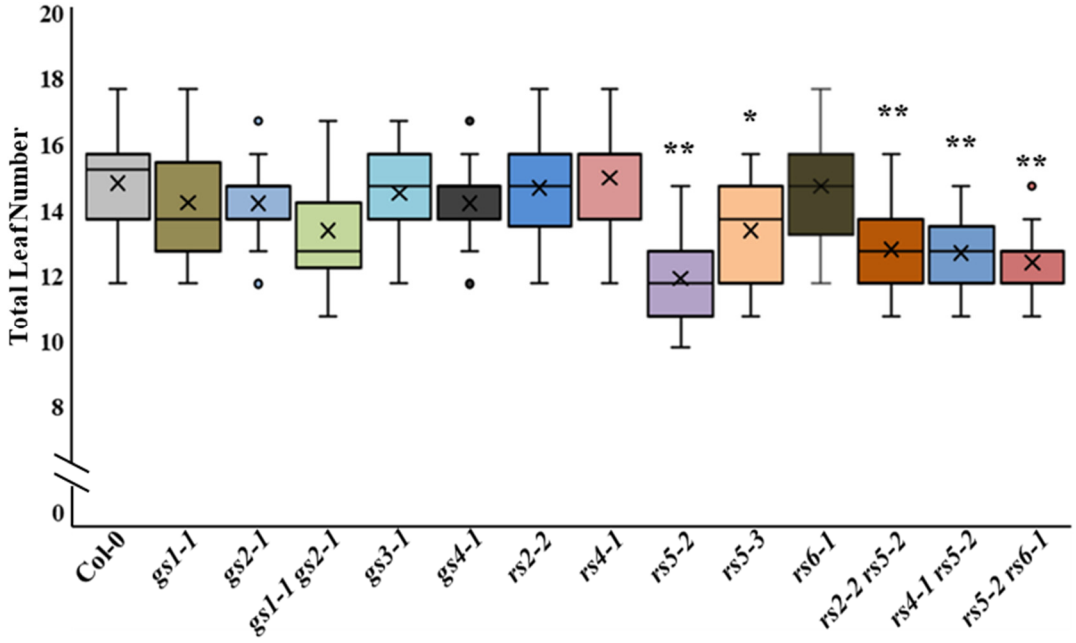

Figure 19. Flowering time phenotype, measured as the total number of leaves produced in the main stem, in Col-0 and simple and double mutants from the *GOLS* and *RS* family members. Boxplots show the first and the third quartile, and the line represents the median. The mean is shown as a cross. Whiskers show the highest and lowest values and outliers are shown as dots. ANOVA with Tukey correction was performed to calculate the significant differences. ** indicates p-value < 0.01, * indicates p-value < 0.05. The size of the populations analyzed, from left to right, is n= 20, 20, 19, 18, 19, 18,19, 24, 24, 22, 17, 20 and 20.

The results show the *rs5-2* allele has an early flowering phenotype with an average of 12.2 ± 1.1 (standard deviation, SD) leaves, *rs5-3* produced 13.5 ± 1.1 leaves and Col-0 produced 15.1 ± 1.6. These results confirm that the *rs5-3* allele has a minor and more moderate effect on flowering time than the *rs5-2* mutation. Additionally, the combination of the *rs5-2* allele with *rs2-2*, *rs4-1* or *rs6-1* did not modify the flowering phenotype. The double mutant *gs1-1gs2-1* did not show any alteration of flowering time as compared to the wild type.

3.6. Characterization of loss-of-function and early flowering phenotype of the *rs5-2* mutant.

3.6.1. Validation of expression changes in *GOLS* and *RS* genes during floral transition.

Transcriptomic data showed that *GOLS1*, *GOLS3*, *GOLS4* and *RS2* genes are downregulated in apex samples of plants induced to flower. According to that, metabolomic data indicate that floral transition is accompanied by a decrease in raffinose in the apex. We validated the transcriptomic data by performing RT-qPCR in apex samples in different developmental stages: vegetative apices, apices in floral transition and inflorescence apices. We extended our study to several members of the *GOLS* and *RS* gene family (Figure 20).

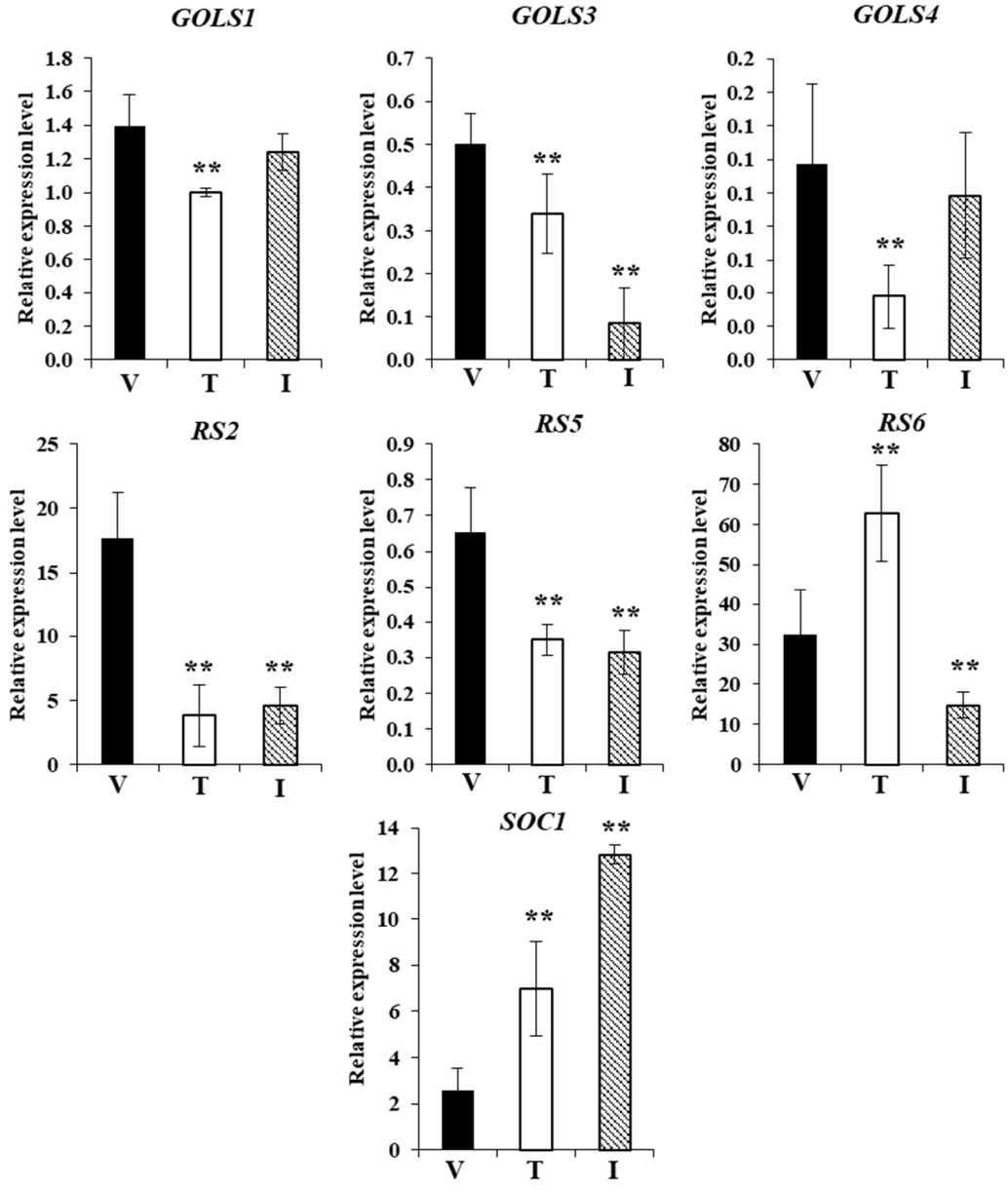

Figure 20. Relative expression level of genes involved in raffinose biosynthesis in vegetative, transition and inflorescence apices. *SOC1* expression was scored as a marker for floral transition. *TIP41* was used as a reference gene. V= vegetative apices on day 7. T= apices in floral transition on day 15. I= inflorescence apices on day 30. The results show the average of 3 biological replicates, and the error bars represent the standard deviation. Significance level measured by ANOVA with Tukey correction compared with the amplification results at day 7 (vegetative). ** indicates p-value<0.01.

Upregulation of *SOC1* confirms that floral transition is initiated at around day 15. We observed that, in agreement with the transcriptome (Figure 13) and RT-qPCR data, the expression of *GOLS1*, *GOLS3*, *GOLS4* and *RS2* decreased as plant switched from the vegetative to the reproductive stage. We also found that *RS5* expression significantly decreased along with phase change. This observation, together with the early flowering phenotype of the *rs5-2* mutant, points out *RS5* as a putative candidate contributing to the control of floral transition via the regulation of raffinose levels in the shoot apical meristem.

3.6.2. Assessment of the effect of exogenous addition of raffinose biosynthesis-related metabolites on flowering time in Col-0 plants.

The RS5 enzyme catalyzes a critical step in raffinose biosynthesis. Loss-of-function mutants affecting this gene accumulate galactinol, one of the substrates of the RS5 enzyme. It has been reported that ectopic treatments with myo-inositol confer protection against drought (Yildizli et al., 2018). Accordingly, we hypothesize that the accumulation of a metabolite related to raffinose metabolism in the meristem, perhaps galactinol or myo-inositol, can act as a flowering-promoting signal. To test this hypothesis, we grew Col-0 plants in media supplemented with different metabolites related to raffinose metabolism, including galactinol, myo-inositol and sucrose, as well as two other carbohydrates (mannitol and lactose). We scored the effect of exogenous addition of those metabolites on the flowering response *in vitro* conditions (Figure 21).

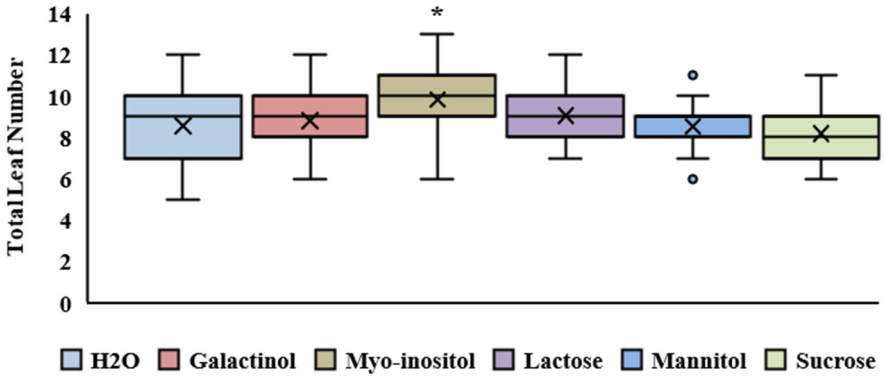

Figure 21. Determination of flowering time in Col-0 plant grown in supplemented media with different metabolites (galactinol, myo-inositol, lactose, mannitol and sucrose). All metabolites were added to the medium at a concentration of 100 µM. The total leaves number refers to the sum of the rosette and cauline leaves. Boxplots show the first and the third quartile, and the line represents the median. The mean is shown as a cross. Whiskers show the highest and lowest values and outliers are shown as dots. Dots exhibit outliers values. ANOVA with Tukey correction was performed to calculate the significance differences. * Indicates p-value<0.05. The population size analyzed from left to right was n= 27 (H_2O), 26 (Galactinol), 25 (Myo-inositol), 20 (Lactose) ,26 (Mannitol), 28 (Sucrose).

Interestingly, we did not observe any effect of exogenous galactinol on the flowering time, nor of any other metabolite assayed with the exception of myo-inositol. Exogenous addition of myo-inositol produced a slight but significant delay in flowering time compared to control plants.

3.6.3. Molecular characterization of *rs5-2*.

To further investigate the mechanism underlying the *rs5-2* early flowering phenotype, we decided to characterize the expression of flowering-related genes such as *FT, SOC1*, *AP1*, and *LFY* in the *rs5-2* mutant background compared to the wild type. To do so, we collected samples in a time-course experiment with *in vitro*-grown plants, collecting entire seedlings every two days, between ZT14 and ZT16. Expression of *AP1*, *SOC1* and *LFY* increased earlier in the *rs5-2* mutant than in the wild type seedlings, in agreement with the early flowering phenotype displayed by the mutant (Figure 22B, C, D). We could

also observe that expression of the florigen *FT* was higher in the *rs5-2* mutant at all time points (Figure 22A).

In Arabidopsis, carbohydrate signaling influences the transition from juvenile to adult phase (Yang et al., 2013; Yu et al., 2013). In leaves, trehalose-6-phosphate (T6P) serves as a signal for sucrose availability and promotes flowering by regulating the expression of *FT* in phloem companion cells in the vasculature (Wahl et al., 2013). In the juvenile phase, the levels of *miR156*-targeted *SPL* genes are low because of high *miR156* levels. As plants age, the amount of *miR156* decreases, leading to an increase in *miR156*-controlled *SPL* genes (Wang, 2014). In addition to induction of *FT* in leaves, the T6P pathway activates *SPL3-5* expression in the SAM, which occurs partly through a *miR156*-dependent pathway and partly via a miR156-independent pathway (Wahl et al., 2013). In plants, trehalose is synthesized from glucose-6-phosphate and UDP-glucose via the intermediate T6P. *TPS1* catalyzes the production of T6P, which is subsequently dephosphorylated to trehalose by *TREHALOSE PHOSPHATE PHOSPHATASES* (*TPP*s) (Paul et al., 2008). There is a correlation between endogenous sucrose content and T6P concentration, both of which increase proportionally (Wahl et al., 2013). To investigate how the defect in raffinose biosynthesis could cause an early upregulation of the florigen and a consequent early floral transition in the *rs5-2* mutant, we measured expression level of *TPS1* and *SPL3* two genes encoding key proteins in the sugar status sensing mechanism in Arabidopsis. The decrease in raffinose levels and the increase in mono and disaccharides (fructose and sucrose) could have an impact on the level of trehalose-6-phosphate (T6P).

These results are consistent with the early flowering phenotype described by overexpression of *FT* in *rs5-2* compared with Col-0 at all-time points examined. Since the expression of *FT* is influenced by the T6P content and this correlates with the endogenous sugar status of the plant. We hypothesize that blocking raffinose metabolism alters sugar balance and increases the amount of T6P. Moreover, trehalose and sugar metabolism also control SOC1 levels. Therefore, we analyze the expression of two genes related to the regulation of trehalose and sugar metabolism in flowering: *TPS1* and *SPL3* (Figure 22E, F).

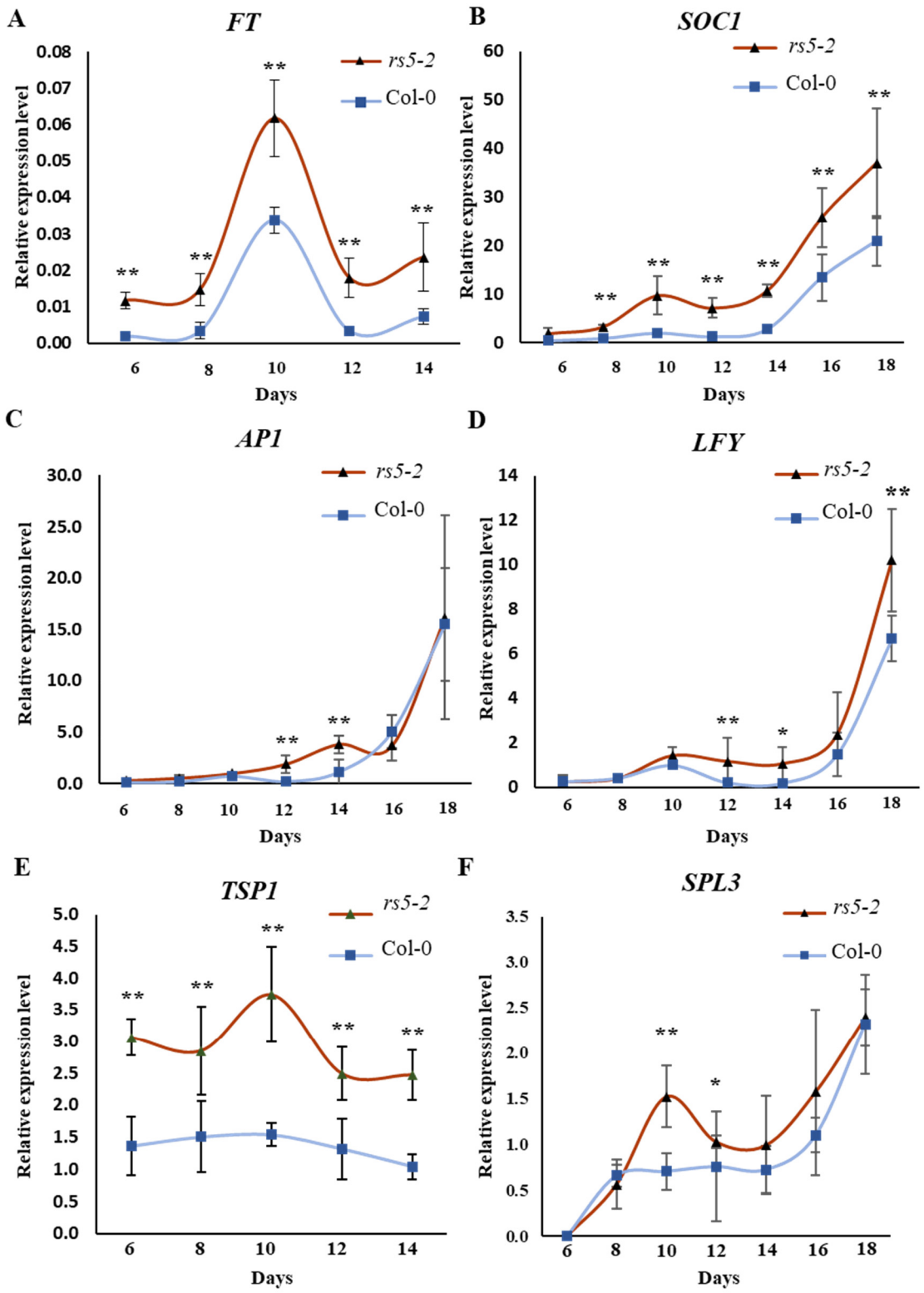

Figure 22. Relative expression level of different genes related with the control of floral transition and floral meristem identity. A, complete seedlings grew *in vitro.* **B**, leaf tissue from seedlings grew in vitro. *TIP41* was used as a reference gene. The results show the average of 3 biological replicates, and the error bars represent the standard deviation. Significance level measured by fisher t-test compared with Col-0. * p-value<0.05, ** p-value<0.01.

The results show that *TPS1* is upregulated in the *rs5-2* mutant background and *SPL3* displays a higher expression in the mutant at day 10, (Figure 21 E, F) around ten days before its expression increases in Col-0 seedlings. These observations support the hypothesis that a deficiency in raffinose synthesis is related to a higher availability of mono and disaccharides, activating the *T6P* signaling pathway that upregulates *FT* and *SPL3* and triggers an early floral transition.

3.6.4. Characterization of the *RS5* expression pattern during floral transition.

To determine the spatial expression pattern of *RS5*, we analyzed its expression by *in situ* hybridization in apices at different developmental stages. Previously, we had observed that *SOC1* expression increases on day 15 after growing in LD conditions in the greenhouse, which means that floral transition has been initiated or is about to occur at that stage. Therefore, we consider that in our growing conditions, floral transition occurs around day 12 to 15 and took samples at day 10 (vegetative stage), day 12 (possibly floral transition) and day 15 (inflorescence stage). Next, we designed specific antisense probes to detect the *RS5* mRNA, trying to avoid conserved regions among the members of the *RS* gene family (Figure 23). The *RS5* expression was observed at a high level in the vegetative stage on day 10 (Figure 23A), both in the meristem and leaf primordia.

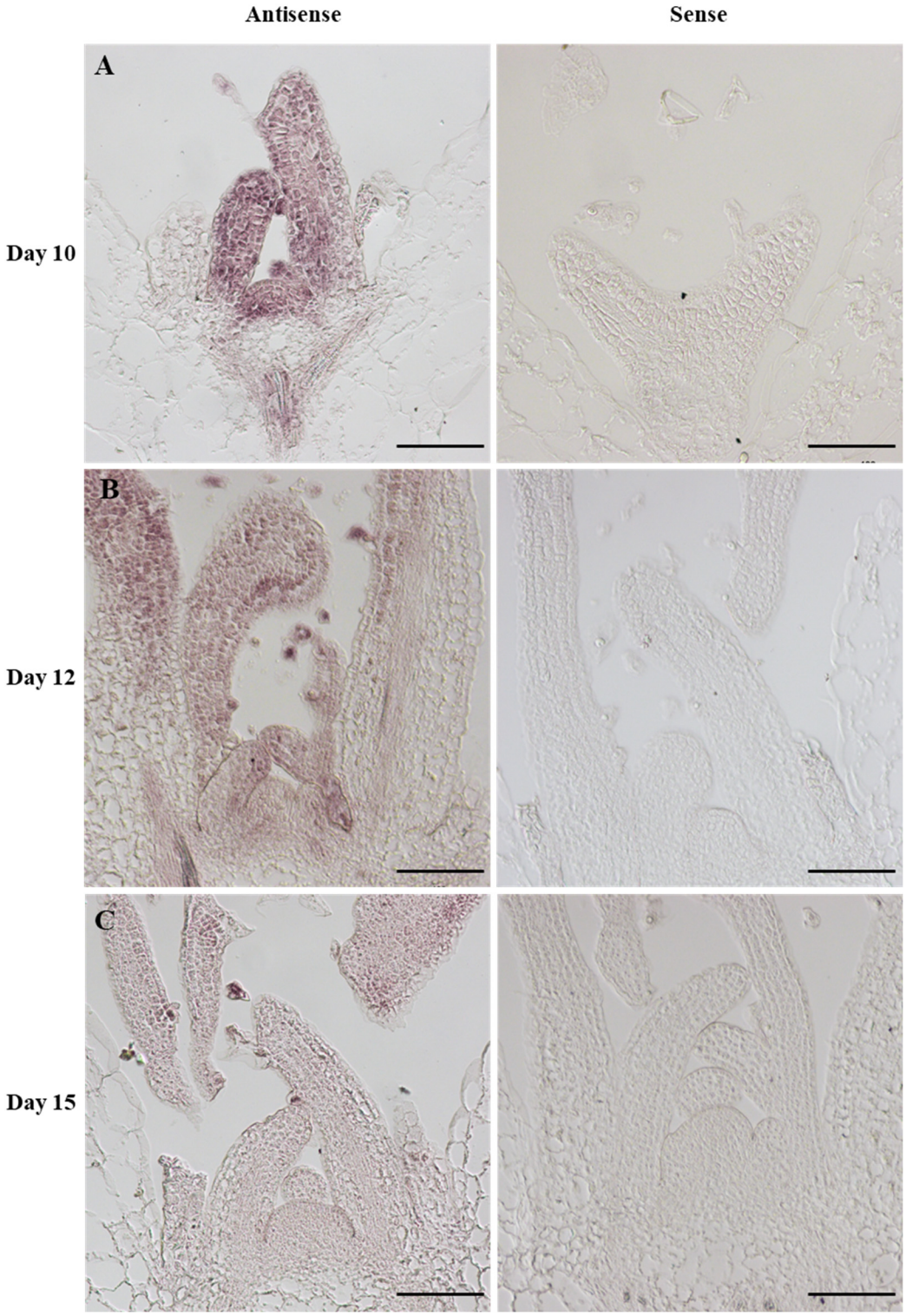

Figure 23. Expression pattern study of *RS5* mRNA by *in situ* hybridization. A, shoot apex sample ten days after germination. **B**, apex sample twelve days after germination. **C**, apex sample fifteen days after germination. In **A**, **B** and **C**, the signal from the antisense probe is shown on the left panel, and the control hybridized with the sense probe is shown on the right panel. Scale bars = 100 µm.

3.6.5. Molecular characterization of floral marker genes in *rs5-2* mutant by RT qPCR.

In previous experiments, we observed that *FT* expression in the *rs5-2* mutant was upregulated at all time points analyzed (Figure 22A). However, since *FT* shows higher expression in the mutant than in the wild type at all developmental stages, we expected to find a stronger flowering phenotype in the *rs5-2* mutant. The expression pattern of *FT* under non-natural light is well described and it is characterized by a first and smaller expression peak in the morning, reaching its highest level during the afternoon, just at the end of the day (Castillejo & Pelaz, 2008; Song et al., 2018). The evidence of higher expression of *FT* could be explained by two different hypotheses. The first was that the circadian expression pattern changed during the day, and the second was that the expression pattern described for *FT* did not change but showed higher expression. Because *CO* is the major activator of *FT* under long-day conditions, we decided to also check the expression of *CO* to confirm whether the increase in *FT* expression was accompanied by an increase in *CO* expression. Therefore, we decided to perform a 24-hour time-course, collecting the entire seedling every 2 hours and compare the expression of *CO* and *FT* in the *rs5-2* mutant and Col-0.

As a result, we found that the circadian expression pattern of *FT* did not change in the *rs5-2* mutant compared with Col-0 (Figure 24). However, *FT* showed higher expression levels from ZT8 to ZT24, but not in the morning (ZT2, ZT4 and ZT6). On the other hand, the expression pattern of *CO* is similar in both Col-0 and *rs5-2*, although there are slight differences in the *CO* expression levels at ZT10, ZT12 and ZT18. Nevertheless, these differences do not explain the higher *FT* expression level in the *rs5-2* mutant.

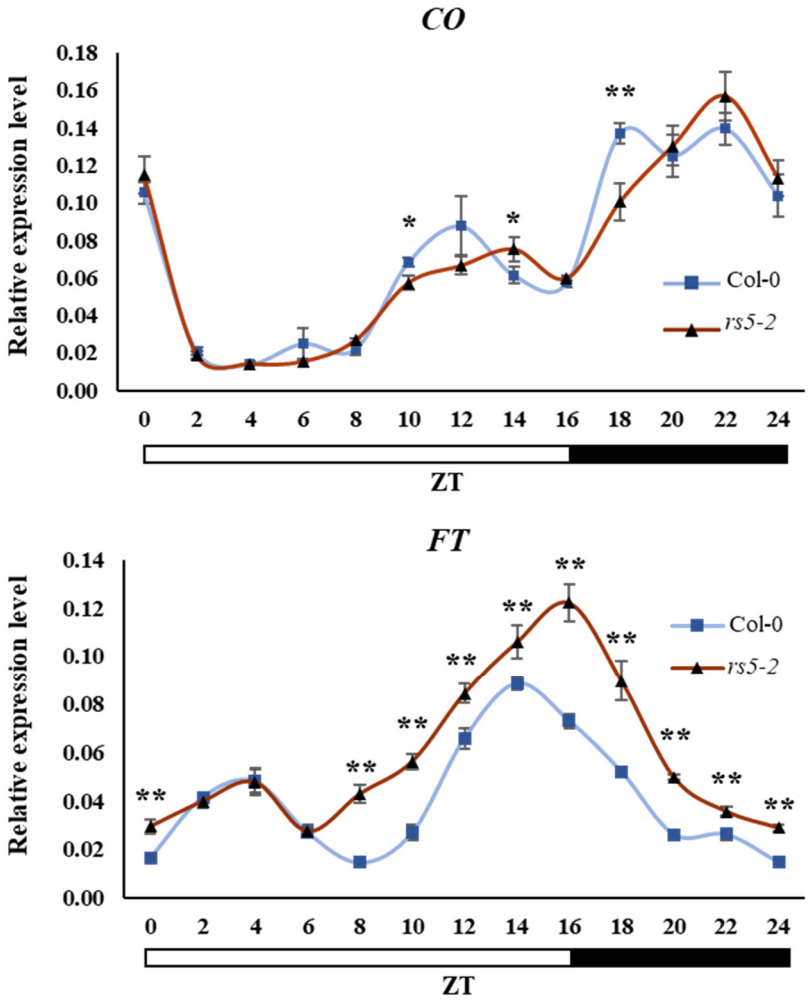

Figure 24. *CO* and *FT* circadian expression in wild type and *rs5-2* mutant under LD. qRT-PCR was performed *in vitro*-grown seedling samples collected 12 days after germination. *IPP2* was used as a reference gene. Error bars are the standard deviation of the mean of three biological replicates.

3.6.6. Endogenous sugars quantification in *rs5-2* mutant by GC-MS.

The variations in sugar levels resulting from a non-functional RS5 protein have been described in several mutants with an alteration of saccharides amount for the plant. For this reason, we decided to quantify some carbohydrates related to the metabolism of galactose to identify the metabolic derivations produced correspondingly of the alteration in the raffinose synthesis during the floral transition. We previously identified that, in the *rs5-2* mutant, floral transition starts between days 10 and 14 under long day conditions, while in wild type Col-0 floral transition starts between days 12-16 (Figure 22). Accordingly, we collected apex and leaf samples on day 12 to quantify carbohydrate content on those tissues (Table 11).

Table 11. Carbohydrates detected by GC-MS in apex and leaf samples from the *rs5-2* mutant and Col-0.

	APICES		LEAVES	
METABOLITE	**Col-0**	***rs5-2***	**Col-0**	***rs5-2***
GLYCEROL	1 ± 0.16	1.09 ± 0.30	1.21 ± 0.14	1.47 ± 0.57
ERYTHRITOL	1 ± 0.19	1.29 ± 0.30	4.31 ± 0.58	**5.71 ± 0.66**
ARABINOSE	1 ± 0.11	**0.75 ± 0.18**	0.70 ± 0.06	0.69 ± 0.10
RHAMNOSE	1 ± 0.18	0.91 ± 0.10	3.76 ± 0.38	**2.44 ± 0.48**
FUCOSE	1 ± 0.18	1.14 ± 0.08	1.90 ± 0.34	1.83 ± 0.41
FRUCTOSE	1 ± 0.09	**0.59 ± 0.11**	0.47 ± 0.04	**0.62 ± 0.12**
GLUCOSE	1 ± 0.16	0.80 ± 0.14	1.00 ± 0.14	**0.64 ± 0.07**
MYO-INOSITOL	1 ± 0.06	1.06 ± 0.15	2.01 ± 0.22	**1.37 ± 0.12**
SUCROSE	1 ± 0.15	**0.66 ± 0.03**	0.53 ± 0.03	0.46 ± 0.07
MALTOSE	1 ± 0.35	0.67 ± 0.08	1.23 ± 0.23	**0.69 ± 0.14**
GALACTINOL	1 ± 0.18	**5.86 ± 1.71**	1.56 ± 0.34	**8.58 ± 1.39**
RAFFINOSE	1 ± 0.20	0.95 ± 0.38	2.21 ± 0.31	**0.99 ± 0.37**

Values represent the average of relative abundance of each metabolite related to Col-0 ± standard deviation. 5 Biological replicates were collected of leaves and apices per Col-0 and *rs5-2*. Each biological replicate consists in a poll of 80-90 apices and leaves. ANOVA with Tukey correction was performed to calculate the significant differences highlighted in bold and indicates p-value<0.01.

We confirmed that raffinose levels were significantly lower in the mutant, although this difference was only apparent in leaf samples and not in apex samples (as we saw in our metabolomic data). Accordingly, we observed a major increase in galactinol, both in leaves and apices. Moreover, we detected an increase in other carbohydrates such as erythritol and fructose in apices of the *rs5-2* mutant. On the contrary, rhamnose, glucose, maltose and myo-inositol showed lower abundance in the *rs5-2* mutant than in Col-0.

3.6.7. Study of the circadian clock in *rs5-2* mutant.

Plants use the circadian clock to internally coordinate various biological processes, such as the perception of day length or the production of carbohydrates derived from photosynthesis. The circadian oscillator in *Arabidopsis thaliana* consists of interlocking transcriptional feedback loops and regulates important processes, such as metabolism and growth (Hsu & Harmer, 2014), and metabolites, such as photosynthetic sugars (Haydon et al., 2013). Recent theoretical studies have revealed the importance of circadian clock entrainment by endogenous sugar on sucrose homeostasis and growth (Ohara et al., 2018). The close relationship between sugars and the regulation of circadian rhythms led us to question whether the alteration in the endogenous levels of specific sugars in the leaves and/or apices could somehow affect the function of the circadian clock, altering the levels of *FT* and leading to the early flowering phenotype observed in the *rs5-2* mutant. Therefore, we performed a circadian clock experiment growing Col-0 and *rs5-2* plants under day-neutral conditions for 10 days (12 h light/12 h dark), after which we switched the plants to continuous light conditions for 3 days and collected samples (entire seedlings) every 3 hours. Next, we quantified the expression of three genes from the central oscillator (*CCA1* and *LHY* as morning genes and *TOC1* as evening gene) and one gene from the morning regulatory loop (*PRR9*).

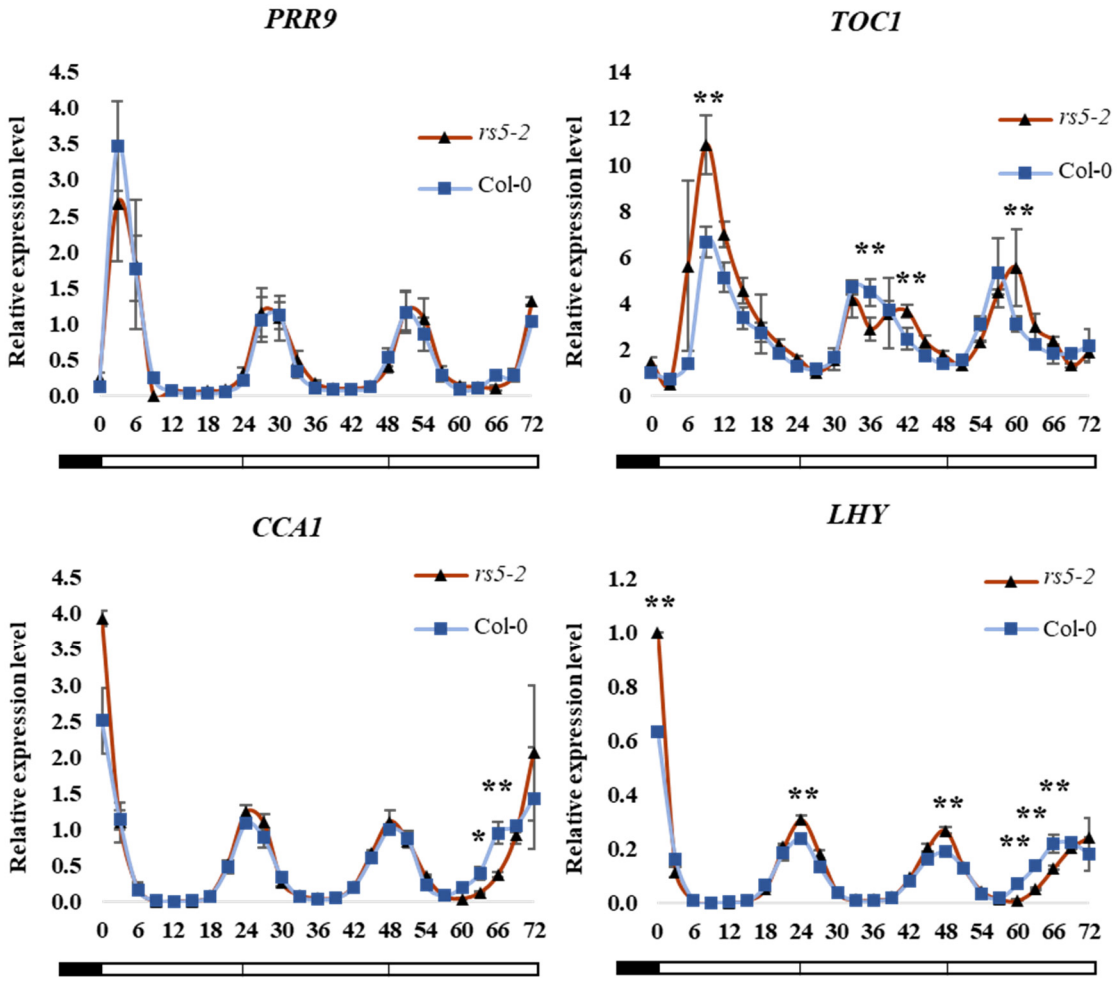

Figure 25. Expression of *PPR9*, *TOC1*, *CCA1* and *LHY* in *rs5-2* and Col-0. Seedlings were entrained in white light/dark cycles of 12 hours for 10 days before being transferred to continuous light. Samples consisting on entire seedlings (16 per biological replicate), were collected every 3 hours during 3 days. qRT-PCR was performed of the whole seedlings collected. IPP2 was used as a reference gene. Error bars are the standard deviation of the mean of three biological replicates.

Examination of the circadian clock in the *rs5-2* mutant showed no major changes, and the expression patterns of the clock genes were similar to those observed in Col-0 (Figure 25). In the case of *PRR9*, we did not detect any significant difference between Col-0 and *rs5-2*. With respect to *CCA1*, the expression pattern in the mutant showed no change from the wild type until 63 and 66 hours of growth in continuous light. The timing of *CCA1* upregulation in the *rs5-2* mutant at those time points was delayed. A similar deviation was observed in the case of the *LHY* expression pattern in the mutant, with a delayed upregulation at the end of the third day. In addition, *LHY* reached a higher peak of expression (ZT0, ZT24, and ZT48). Finally, *TOC1* expression in the *rs5-2* mutant display

a higher peak of expression during the first oscillation (ZT9) and a similar delay in its upregulation on the third day on continuous light conditions. In summary, genes of the central oscillator show a slight delay in their upregulation in the third day in free-running conditions in the mutant, which could imply a longer period of the circadian clock in the *rs5-2* compared to the Col-0.

DISCUSSION

The genetic network that controls flowering is highly conserved in dicotyledonous plants, and many of the critical regulators have been identified in model crop species, such as tomato, pea, and soybean. Knowledge of the genetic networks that control flowering is useful to accelerate plant breeding programs since a large part of the key regulators are conserved between different species. In this context, using Arabidopsis as a model to identify novel regulators or investigate molecular mechanisms underlying flowering, together with different approaches and innovative strategies, has been a useful tool. In this work, we applied two approaches in parallel with the objective of identifying molecules that affect flowering or metabolic pathways affected during the floral transition: chemical genetics and metabolomics. The main difference between the two could be classified according to their origin. Through metabolomics, we can identify endogenous plant molecules and through chemical genetics, we test a library of molecules (natural or synthetic) in a screening-based approach.

Taking some creative license and simplifying the entire context, the process by which a plant acquires the ability to flower would be comparable to climbing a mountain. On the way up to the mountain, climbers find a button that, once pressed, turns the plant into its reproductive phase. In this metaphor, pressing the button would correspond to the activation of *SOC1* expression. Let us now imagine that it is not enough to press the button once, but that it must be pressed thousands of times for the plant to trigger flowering. Only then, the plant will know that it is the optimal time to produce reproductive organs and that "the button" has not been pressed accidentally by a bird that has settled there. All those climbers pushing the button would be molecules of FT on their arrival to the apex. Our mountain has many paths; some are more sophisticated than others, which can be walked faster or slower; some are suitable only for the most skillful climbers; others for those that want a cableway. All these "pathways" to climb the mountain represent all the pathways that control flowering time. From the mechanistic point of view, the base of the mountain will be the genome, which conditions all the possibilities or starting points of the climbing or hiking routes. The hillside will be the transcriptome; the largest slope at the end corresponds to the proteome and at the very top, surrounding the entire environment of our button, is the metabolome.

The identification of small molecules (CF5 and CF11) as regulators of flowering time signals by a chemical genetic screening.

The use of libraries of thousands or hundreds of molecules is a useful tool to identify new candidates affecting flowering time. Such an approach has been previously used to identify regulators of different processes such as hormone signaling and trafficking, avoiding problems derived from functional redundancy on those pathways (Hicks & Raikhel, 2012). In our case, we used a 360-molecule library that may seem small, but each of those molecules has been previously tested and classified as bioactive, affecting vesicular transport in pollen grains (Drakakaki et al., 2011). In this context, lipids play important roles not only as components of cell membranes but also as potential regulators. For example, the florigen FT binds to PC, a phospholipid component of cell membranes (Nakamura et al., 2014). It has also been suggested that the binding of FT in membranes may be a common strategy used by plants to adjust the timing of flowering in response to changing seasonal temperatures (Susila et al., 2021). This fact, which seems to have no apparent connection, becomes very important in the context of our research because two models have been proposed to explain how binding to PC might modulate FT function. One hypothesis suggests that as a component of the nuclear membrane, PC could be important for FT shuttling from the cytosol into the nucleus. A second hypothesis is that vesicles containing PC are responsible for transporting FT to FD (Wickland & Hanzawa, 2015). Moreover, it has been reported that FT protein export from the companion cells to the sieve elements of the phloem is regulated by the endosomal vesicle-mediated trafficking pathway (Liu et al., 2019). The fact that this library specifically affects vesicular transport may increase the chances of finding a positive hit regulating FT signaling and therefore flowering. Tested molecules could affect the expression of *FT* or FT protein transport or interaction with membranes.

Among all tested molecules and after analyzing the library with the p*FT::GUS* line in two different screening rounds, we obtained a positive hit rate of 12% (43 molecules), most of which (7%) caused an increase in the GUS signal. A similar approach using a p*AP1::AP1- LUC* reporter line and the LATCA-library and part of the DIVERSet-CL library, with a total of 8700 molecules, resulted in a hit rate of 3.1% and 2.1%, respectively (Fiers et al., 2017). These hit rates are high as success rates for primary screens in chemical genomics usually vary from less than one to up to a few percent (Drakakaki et al., 2011; Serrano et al., 2015).

When selecting among primary positive hits, we focused in molecules that showed a promoting effect rather than those that repressor activity or produce an ectopic reporter signal. The transition to flowering is controlled by multiple genetic (He et al., 2020; Srikanth & Schmid, 2011), hormonal (Conti, 2017; Izawa, 2021) or chemical (Ionescu et al., 2017; Pfeiffer et al., 2016; Ponnu et al., 2020) pathways that are interrelated to ensure the robustness of the system and generation of offspring. Even null mutants that have no functional *FT* and or grown under SD will eventually flower (Jang et al., 2009; Koornneef et al., 1991).

We observed a discrepancy in the results obtained with the library molecules and with selected positive hits, for which a new batch was bought to investigate further their effect on flowering. Molecules from the new batch showed a cytotoxic effect that was not observed during the primary screening. This effect can be explained by a decay in the activity of the molecules after several rounds of freezing and thawing. The 360-molecule library was generated in the laboratory of Dr. Stéphanie Roberts (UPSC) and it has been tested numerous times in search of molecules modulating a wide range of biological processes. Therefore, it is not unreasonable that these molecules have lost activity over time. Among the 6 selected molecules, only two of them turned out to be promising candidates for triggering flowering, the CF5 and CF11 molecules. The CF5 molecule gave promising results in the primary screening, but later it did not increase the expression of the alternative reporter line p*FT*::*LUC* in the secondary screening and neither caused an early flowering phenotype. There could be several reasons for this, such as nonspecific signals associated with GUS and/or inability to activate endogenous *FT* expression. To test whether this molecule affects *FT* expression, we could quantify the expression of the endogenous *FT* gene in plants treated with this molecule compared to control mock-treated plants.

On the other hand, the treatment of plants with the CF11 molecule caused an increase in the signal of the GUS and LUC reporter genes under the control of p*FT*. In addition, we observed a visible early flowering phenotype, with CF11-treated plants flowered 4 days earlier than the mock-treated plants. Moreover, this effect was dose-dependent: plants flower earlier when using a higher CF11 concentration (being the non-toxic limit 2 μM). However, at the time of this work, we have not further characterized these molecules or their targets. In the future, our group will continue to work with these molecules to characterize their function further, putative targets, and potential as flowering regulators,

not only in Arabidopsis but also in other species of commercial interest such as pea or lupin.

Regarding our experimental design, we have identified some improvements that could lead to more accurate results. In particular, we could adjust the time at which the screening of the luciferase reporter signal measurement was performed. Endogenous *FT* expression peaks at the end of the light period in long days. Therefore, it might be optimal to perform the quantifications of the luciferase signal closer to ZT16. We can not rule out the possibility that the CF1, CF2, CF3, and CF4 molecules actually do affect the expression of the *FT* promoter. A possible solution would be to use the protocol described in Fiers et al. (2017) to perform the signal analysis in which they identified a molecule with flowering-inducing activity. Instead of using the LAS3000 instrument, which requires post-imaging analysis and 10 minutes of integration time for the entire plate, they used the Glomax luminometer, whose output is directly in luminescence units and requires only 2 seconds of integration time per analyzed well.

In the future, we would like to study the effect in flowering time mutants to test for altered sensitivity to the chemical. Identifying mutants that exhibit altered sensitivity to the chemical will allow us to focus on a specific regulatory network. To better characterize the mechanisms of action of the chemical, we have also generated reporter lines that act upstream (*pCO::LUC*) and downstream (*pAP1::LUC*) *FT*. Finally, it would be interesting to determine if an increase in p*FT::LUC* signal increases the signal of the alternative lines we obtained or in different flowering time mutant backgrounds.

Three potential novel functions described for pipecolic acid in Arabidopsis beyond SAR: regulation of flowering time, rosette area and cell cycle.

There are two reasons why we wanted to analyze separately one of the molecules, pipecolic acid (Pip). First, prior to conducting the metabolomics approach described in this work, we conducted a pilot experiment in which we analyzed the metabolome of plants grown in SD and induced to flower by a switch to LD. As a result, we found that pipecolic acid was one of the most promising metabolites whose relative abundance in leaves changed considerably. The sampling and system used in that experiment were very different from the system used in this work, but we decided that it was worthwhile to evaluate the effect of Pip on flowering. In addition, Pip was among the 360 molecules tested in the chemical genomics approach, and treatment of *pFT::GUS* plants with Pip

led to an increased GUS signal. On the other hand, there are several reports for pipecolic acid and its role in triggering flowering in *Lemna spp* (Fujioka et al., 1987; Fujioka & Sakurai, 1992, 1997; Kaihara & Takimoto, 1990; Takimoto et al., 1989). According to our results, the *ald1-1* mutant has a delay in flowering, measured as total leaf number but it showed no phenotype when flowering was scored as days to bolting. However, with another mutant allele (*ald1-2*) in the *Lansberg erecta* (Ler-0) background, which harbors two transposons affecting gene expression (one in the promoter and one in the first exon), showed a late flowering phenotype both in the number of leaves and days to bolting. In addition, during the development of this work, the *FMO1* gene was identified as a new member of the Pip pathway, catalyzing the synthesis of NHP using Pip as a substrate. Moreover, in the last years, it has become clear that NHP has a relevant role as a signaling molecule and trigger of SAR in plants (Hartmann et al., 2018). Therefore, we consider that the effect on flowering that we identified in *ald1* mutants could be due to a decrease in Pip, in NHP, or in both molecules. To further explore this, we re-examined flowering time in *ald1-1, sard4-5 and fmo1-1* and discovered that both *ald1-1* and *sard4-5* exhibited a larger rosette size, whereas *sard4-5* did not exhibit this phenotype. Metabolite quantification studies have shown that *ALD1* catalyzes the first step of Pip synthesis and therefore, knock-out mutants affecting *ALD1* have no Pip. Meanwhile, *SARD4* catalyzes the last step of Pip synthesis but knock-out mutants affecting *SARD4* did contain Pip, which suggests that there must be alternative Pip biosynthesis pathways or genes with redundant function that are still unknown (Ding et al., 2016). The description of NHP as an important signaling molecule derived from Pip implies that functions previously attributed to Pip may actually correspond to NHP. Recent studies suggest that this is indeed the case in SAR (Hartmann & Zeier, 2019; Zeier, 2021), and in our results show that late flowering phenotype and increased rosette area phenotypes are displayed by both *ald1-1* and *fmo1-1*. In this context, it would be interesting to evaluate the response of the *fmo1-1* mutant to Pip treatments. In addition, evaluation of the response of wild type plants and mutants affected in this pathway to NHP treatment would clarify whether the reduced rosette size observed upon Pip treatment is due to Pip or to NHP.

Beyond the effect of Pip on flowering and rosette size, we also observed an effect on plastochron, understanding this as the rate at which the meristem produces new leaves. Our results show that the *ald1-1* plants produce more leaves in a given time period than do Col-0 plants. This could be due to an alteration of the cell cycle in the mutants

explained by a larger rosette size displayed by the mutants and the reversion of that phenotype upon Pip treatments together with a large cell number per mm^2 in the leaf of *ald1-1* mutant.

To explore the possibility that the effect of Pip in leaf area might be conserved in phylogenetically distant species, we evaluated the effect of Pip on the liverwort *Marchantia polymorpha*. Pip caused a reduction of *M. polymorpha* thallus. Undoubtedly, the accidental discovery of this type of phenotype is of great interest from an agronomic point of view. Genes involved on Pip biosynthesis could become candidates for plant breeding programs aimed at increasing the biomass. On the other hand, the identification of new cell cycle regulators is of great interest to research and the pharmaceutical industry.

The floral transition metabolome showed significant changes in the abundance of metabolites in the apex but not in the leaf.

In our work, we were interested in studying the floral transition by considering the metabolome as the final boundary between molecular events and the phenotype and then extending this analysis from the metabolome to the transcriptome. To this end, we used a system to activate the fusion protein CO::GR by dexamethasone, whose expression was controlled by the endogenous *CO* promoter in a *co-10* mutant background, allowing us to revert the late flowering phenotype of the mutant with a treatment with dexamethasone (An et al., 2004; Simon et al., 1996).

Leaf metabolome samples revealed that there were no significant changes in metabolites in response to the activation of the CO::GR protein by dexa treatment, in any of the analyzed time points. These data agreed with the results of the leaf transcriptome, in which only a small number of genes showed differential expression when comparing dexa- and mock-treated plants: we found 24 differential expressed genes on day 1, including *FT*, and only one gene at day 3. On the other hand, we identified significant changes in many metabolites in apex samples from day 1 after treatment, and those differences became massive on day 5. Considering the expression levels of the floral marker genes *LFY* and *AP1* on day 5, the most likely explanation for these large differences at the apex on this day is that the floral transition has already occurred, and therefore we compare the metabolome of the first floral structures in dexa-treated apices

with vegetative apices with leaf primordia in mock-treated plants. Therefore, almost all detected metabolites show significant differences at this time point.

Focusing on the time points previous to floral induction, we were able to distinguish two phases in this process mediated by the photoperiod via activation of the CO-FT module. The action of FT on the meristem implies a metabolic rearrangement in two phases: an early phase corresponding to day 1 and a late phase corresponding to day 3. In the early phase (day 1), we observed a general decrease in metabolites such as amino acids (phenylalanine, tryptophan, proline, glutamine, threonine, valine, asparagine, and alanine) and also raffinose (an important storage carbohydrate) and myo-inositol. Changes in amino acid content during floral transition have been previously reported in leaf exudates of Arabidopsis (Corbesier et al., 2001) and in whole rosettes (Olas et al., 2021) or specifically related to proline metabolism (Trovato et al., 2019). On the other hand, the late transition phase at day 3 is characterized by an increase in metabolite abundance in dexamethasone related to mock treatments with a long representation of mono- and disaccharides such as fructose, galactose, arabinose, glucose, and sucrose, among other metabolites. This increase in small carbohydrates precedes the morphological changes that occur in the apical meristem of the shoot once the transition occurs.

The results of this work presented a challenge in terms of the enormous amount of data generated and its analysis. In this sense, the identification of metabolic pathways using metabolites identified by targeted and untargeted methods, in combination with transcriptomic data, greatly helped us to filter the results and extract functional information. To explore the possible role of the affected metabolic pathways, we characterized the flowering time of knock-out mutants affecting key enzymes of the selected metabolic pathways. In an initial mutant screening, we found that of the six metabolic pathways analyzed, two mutants showed an alteration of flowering time. The affected pathways were the biosynthesis and degradation of stachyose and auxin inactivation by conjugation showed with the *rs5-2* and the *vas2-1* mutant displaying an early flowering phenotype. Next, we evaluated them under SD conditions and the ABA degradation pathway also showed a delay in flowering time.

The role of hormones in flowering is very diverse and among them, auxins are probably the hormone group involved in a wider variety of biological mechanisms such as endocytosis, cell cycle, cell polarity, cell elongation, differential growth, embryogenesis,

tissue patterning and *de novo* formation of organs (Sauer et al., 2013). In our work, the *vas2-1* mutant showed an early flowering time phenotype. This is, of course, an interesting result but due to the time frame of this work, we decided to focus on the pathway related to raffinose synthesis and ABA degradation. Abscisic acid is a hormone whose influence on flowering is controversial, since different studies suggest a activation or a repression effect depending on environmental conditions (Chen et al., 2020; Conti, 2019). Recently, this hormone has been gaining importance and several works have been done in our group linking the role of ABA to *TFL1* (García, 2021.; Martínez, 2022.; Silvestre Vañó, 2020). Under our experimental conditions, in plants grown under SD conditions and shifted to LD, a daily ABA treatment in the apex delayed flowering, which fits the proposed role of ABA as a repressor of *SOC1* (Riboni et al., 2016). In addition, based on transcriptome analysis, we detected an increase in the expression of the *CYP707A3*, a gene involved in ABA degradation that is highly expressed in the shoot apex during the vegetative phase and decreases during floral transition and in the inflorescence meristem. Phenotyping of the *cyp707a3-1* mutant under SD conditions revealed a delayed flowering phenotype. These data suggest a role for ABA as an inhibitor of floral transition at the meristem level that can be abolished by photoperiod under long-day conditions. The role of ABA in regulating flowering is likely to be complex, affecting multiple genetic targets and metabolic pathways. One of these pathways is the RFO synthesis since it has been shown that ABA influences the RFO accumulation and induction of *CaGolS* in chickpea (Salvi et al., 2020), *CsRS* in cucumber (Sui et al., 2012) or *VvGolS1*, *VvGols2* and *VvRS* in grapevine (Wang et al., 2020) among others.

GOLS genes catalyze the first step of RFO biosynthesis by synthesizing galactinol from UDP-galactose and myo-inositol. In Arabidopsis, there are seven members of the *GOLS* family (*GOLS1-GOLS7*) and, interestingly, GOLS, the key enzyme of the RFO biosynthetic pathway, is present only in flowering plants, suggesting that the function of these types of metabolites is a highly specialized in higher plants (Sengupta et al., 2012). Multiple roles have been describe to RFOs, especially as protecting molecules against different types of abiotic stresses, such as heat (Panikulangara et al., 2004), cold and drought (Taji et al., 2002), salinity or osmotic stresses (Sun et al., 2013) or as stabilizing membrane bilayers (Hincha et al., 2003). In addition, the RFOs have been proposed to regulate seed germination (Jang et al., 2018) and seed longevity in different species (de Souza Vidigal et al., 2016) and a dual function in dormant buds (Falavigna et al., 2018).

During dormancy, RFOs provide protection from desiccation and when buds reactivate, they serve as a source of energy (Falavigna et al., 2018). In addition, an effect on flowering time was also observed in rice, with overexpression of the Arabidopsis *GOLS2* gene leading to early flowering and drought tolerance (Selvaraj et al., 2017). The next step in RFOs synthesis is catalyzed by raffinose synthases that produce raffinose from galactinol and sucrose. In Arabidopsis, there are six genes with predicted raffinose synthase activity (*RS1-RS6*). However, raffinose synthase activity has only been biochemically demonstrated for RS4 and RS5 (Nishizawa et al., 2008) and RS2 acts as an alpha-galactosidase and degrading raffinose in sink organs (Peters et al., 2010).

In our experiment, we detected gene expression changes among genes involved in raffinose production. We detected a decrease in the expression of the *GOLS1*, *GOLS3*, *GOLS4*, and *RS2* genes when we analyzed the transcriptome at day 1. On the other hand, we detected a decrease in the expression of *GOLS1*, *GOLS3*, *GOLS4*, *RS2*, and *RS5* genes in Col-0 apices at the floral transition stage when we used the RT-qPCR expression analysis techniques. These data confirm what was observed in the transcriptome and support a possible role of raffinose metabolism in floral transition. RS5 has been described as the major specific raffinose synthase in Arabidopsis (Egert et al., 2013), and its expression analysis by *in situ* hybridization showed a clear expression in vegetative shoot apical meristem and young leaf primordia. This expression decreases when floral transition occurs and the shoot apical meristem becomes an inflorescence meristem. These results prompted us to characterize loss-of-function mutants affecting raffinose metabolism.

Phenotyping of those mutants showed that the *rs5-2* mutant flowered early under LD and SD conditions. However, when we examined the phenotype of another mutant allele described in the literature, we found that the *rs5-3* mutant exhibited a subtle early flowering phenotype under LD but not under SD conditions. These differences could be due to the site of insertion of the transgenes in both lines. The insertion in *rs5-3* is located at the beginning of the gene, 220 base pairs away from the ATG codon, and we identified an alternative in frame ATG 616 bp from the canonical ATG. Despite the T-DNA insertion, this line could express a transcript containing part of the 1st exon and exons 2, 3, 4 and 5, generating a truncated but almost complete protein. On the other hand, the insertion in *rs5-2* is located in the middle of the 2nd exon, in a conserved region among *RS* genes. In addition, the next transcription origin is only at the end of the 3rd exon, and

transcript expression from this ATG would result in a truncated protein containing less than half of the original RS enzyme. These differences could explain the subtle phenotype observed in *rs5-3* compared to the more severe defects detected in the *rs5-2,* in which fertility was also severely affected with a reduction in the number of fruits in the main inflorescence and the number of seeds per silique. In any case, to clarify the different phenotypes of these two mutants, we are currently testing the expression of the *RS5* gene in the different mutant backgrounds, and we will characterize as well alternative mutant alleles affecting the *RS5* gene.

To investigate the possibility of a redundancy effect among members of the *RS* family, we examined flowering time in mutants affecting the *RS2*, *RS4*, and *RS6* genes, and we also generated double mutants with the *rs5-2* allele. Our results showed no alteration of the flowering time in single mutants *rs2-2*, *rs4-1* and *rs6-1* and no change in flowering time in any of the double mutants compared to *rs5-2*. Previously, it was reported that the *din10* mutant, harboring a mutation in the *RS6/ DARK INDUCED 10* gene, exhibited a slightly early flowering phenotype, with upregulation of *FT* expression. In addition, *RS6* expression has been described to be regulated in response to cold by the complex formed by *FLC* and *SVP* (Mateos et al., 2015). Contrary to expectations, we did not observe the phenotype described for *din10* (SAIL-54-G03) in the *rs6-1* (SALK_035336) mutant. Both are T-DNA mutants with the insertions in the first exon. However, the described flowering phenotype for the *din10* mutant is subtle, although significant, differing by less than two leaves from wild type. It is possible that differences in growth conditions account for this phenotypic difference among the two alleles. Increasing the population size in these analyses could help us clarify if the *rs6-1* displays an altered flowering time phenotype.

Several loss-of-function mutants for the *RS5* gene of Arabidopsis have high levels of galactinol as a result of disruption of the raffinose synthesis pathway (Egert et al., 2013; Zuther et al., 2004). To test whether the early flowering effect observed in the *rs5-2* mutant could be mediated by galactinol accumulation, we examined the effect of exogenous addition of galactinol on flowering time *in vitro*. However, we did not observe any change in development in plants growing in galactinol-supplemented medium. We did observe a slight delay in flowering in plants growing in a myo-inositol-supplemented medium compared with controls. There are conflicting reports on the effect of myo-inositol and flowering time. In Arabidopsis, there are 4 different functional genes

involved in the homeostasis of myo-inositol by catalyzing its oxidation to D-glucuronic acid. This reaction is controlled by the *MYO-INOSITOL OXYGENASE* family (*MIOX1, 2, 4* and *5*) (Endres & Tenhaken, 2011) and the four *MIOX* genes are differentially regulated during development (Kanter et al., 2005). Mutations in *MIOX* genes affect flowering time in different ways: under LD conditions *miox2-2* mutants show a delay in flowering, while *miox4-1* shows an early flowering phenotype (Alford et al., 2012).

In general, we found a change in the balance between the accumulation of storage carbohydrates such as raffinose and the release of mono- and disaccharides such as glucose, galactose, mannose, sorbose, and fructose, which have a relevant influence on the needs of the meristem during floral transition before the up-regulation of floral marker genes and the morphological changes at the shoot apical meristem. These changes in the levels of storage oligosaccharides and simple carbohydrates indicate that metabolic reprogramming occurs during the floral transition, consistent with higher energy requirements for the formation of sink tissues such as the reproductive tissues (flowers and fruits) compared with the vegetative leaves, which function as source tissues. In summary, the results of our metabolomics and pathways mutant analysis suggest that a change in the ratio of mono- and disaccharides to raffinose in the apex may play a role in determining flowering time. Similar ideas have been proposed for the role of RFOs in the control of seed vigor in Arabidopsis and maize, where a high RFO/sucrose ratio correlates with increased seed vigor (Li et al., 2017). Similarly, RFOs seem important to control bud dormancy in apple trees, since a decrease in raffinose is also observed during bud reactivation, corresponding to a lower raffinose/sucrose ratio at the time when the bud becomes metabolically active (Falavigna et al., 2018).

In Arabidopsis thaliana, there is a well-known and described sugar pathway involved in flowering that is mainly controlled and integrated via T6P. The T6P signaling system regulates the floral transition by controlling the transcript levels of *SPL*s in SAM and *FT* expression in leaves (Wahl et al., 2013). In this way, T6P acts as a sensor for sugar status and controls the transition from vegetative to reproductive phase. T6P synthesis is catalyzed by *TSP* genes and the relationship between endogenous sucrose and T6P levels have been extensively studied, with a strong correlation found between them in different Arabidopsis tissues such as the apex (Wahl et al., 2013), seedlings and rosettes (Lunn et al., 2006) and also in leaves following fluctuations during the light-dark cycle under a variety of growth conditions (Fichtner & Lunn, 2021). In addition, an exogenous supply

of other hexoses that can be metabolized to sucrose, such as glucose or fructose, have the same effect in seedlings and increases T6P levels (Yadav et al., 2014). In this context, we hypothesize that a reduction in the ratio of raffinose/mono-disaccharides in the apex could lead to an upregulation of *TPS1* and a concomitant increase in T6P, resulting in an early upregulation of *FT* in the leaves of the *rs5-2* mutant and the upregulation of *SPL3* in the apex. These two changes in gene expression could explain the early flowering phenotype of the *rs5-2* mutant. However, the changes in *FT* gene expression could also be explained by the effect of an reduced raffinose/mono-disaccharide ratio on circadian clock function. It is known that sugars modulate the function of the circadian clock in Arabidopsis in a *TPS1*-dependent manner (Frank et al., 2018) or affecting GI stability, a known activator of *FT* (Haydon et al., 2017). In turn, an altered GI stability can affect flowering in different ways, by affecting CO stability or by directing binding to *FT* promoter and interacting with *FT* repressors such as *TEM1* and *TEM2* (Castillejo & Pelaz, 2008; Sawa & Kay, 2011; Song et al., 2014). We found that the *rs5-2* mutant exhibits a slight alteration in the circadian clock that affects the amplitude of *TOC1* and *LHY* and the period at a late stage of *TOC1*, *LHY*, and *CCA1*. These preliminary data must be confirmed by further experiments but alteration in clock function may contribute to the observed *FT* upregulation.

Quantification of sugars in leaves and apices of the *rs5-2* mutant provided contradictory results that did not fully supported our hypothesis derived from the metabolomic data. We did not detect significant differences in raffinose abundance in the *rs5-2* apices compared with wild type. However, we detected very high levels of galactinol, suggesting that indeed RFO metabolism is altered in this tissue. In addition, the bigger differences in sugar content in the *rs5-2* compared to wild type were found in the leaf, with lower amounts of rhamnose, glucose, myo-inositol, maltose, and raffinose. In contrast, only arabinose, fructose, and sucrose had lower levels at the apex. A possible explanation for this phenomenon could be that there are compensatory mechanisms for sugar content in the apex that are not present in the leaf. Interestingly, we observed an opposite pattern of accumulation for erythritol and fructose. Both showed higher abundance in *rs5-2* leaves than in wild type. Erythritol and galactinol are both sugar alcohols whose function is associated with frost tolerance and protection against oxidative damage and osmotic stress (Toubiana et al., 2020). Nevertheless, the metabolism of erythritol in plants is not well studied and has been associated with the postharvest processes of fruits (Bekele et

al., 2016). These unexpected results related to sugar quantification can be explained by the fact that sugar quantification was performed in 12-day-old seedlings, a time when *rs5-2* has already made the transition to flowering, while Col-0 seedlings are still in a vegetative state. In addition, in our first experimental model, we identified molecular events that occur in response to the activation of CO that could be different from what happens when plants are exposed to a natural long day photoperiod.

Based on our results and the described processes related in the literature and in this work, we proposed a model that integrates genetic and metabolomic factors contributing to the control of flowering time downstream of the CO-FT module (Figure D1).

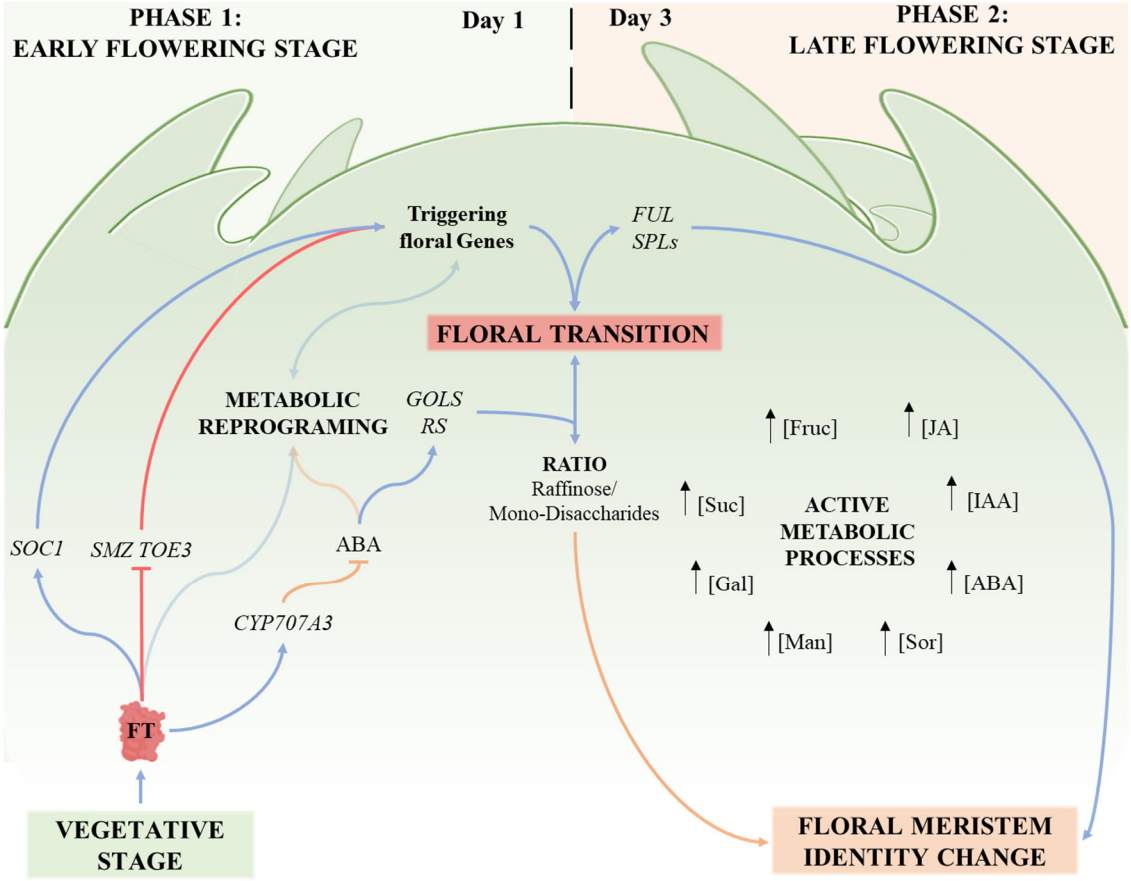

Figure D1. Schematic representation of metabolome and transcriptome changes in an apex during floral transition in the system used in this work. In the proposed model, FT not only induces the expression of *SOC1* triggering the floral transition but also induces the expression of genes responsible for the degradation of abscisic acid, such as *CYP707A3*. Since ABA is an activator for the expression of the *GALACTINOL SYNTHASE* and *RAFFINOSE SYNTHASE* genes, the decrease of ABA would affect this metabolic pathway, decreasing the amount of raffinose available and increasing the content of mono and disaccharides. This would increase the

level of simple sugars at the apex and contribute to the floral transition. The blue and red lines represent a positive (induction) or negative (inhibitor) relation, respectively. The orange lines represent metabolic pathways/reactions. [Fruc], [Suc], [Gal], [Man], [Sor], [ABA], [IAA] and [JA] represent fructose, sucrose, mannose, sorbose, abscisic acid, indole-3-acetic acid and jasmonic acid, respectively.

In conclusion, the results of the metabolomics and transcriptomics approaches, as well as the other experiments resulting from the identification and characterization of metabolic pathways, suggest that the ratio of raffinose to mono and disaccharides changes during floral induction in the apex. These changes are likely integrated by the T6P pathway and the circadian clock function and contribute to the fine-tuning of flowering time in Arabidopsis. Raffinose accumulation might play a role in different organs that undergo changes in developmental stages with different metabolic activity, such as seeds (dormant/germinating), buds (bud initiation/bud burst), or meristems (vegetative/reproductive). Tissue-specific alteration of raffinose content in wild type and mutants from different metabolic pathways controlling flowering could help confirm this and clarify the role of raffinose in controlling flowering.

Summarizing, the most relevant contributions of this work are:

1. The identification by means of a chemical genetic screening of a candidate molecule, CF11, with great potential in the control of flowering time. Targets of CF11 activity and mechanisms of action remain to be elucidated.

2. The characterization of Pip and its derivative NHP as candidate molecules for the regulation of various processes such as flowering time, rosette area, and cell cycle.

3. The description and analysis of the metabolome of floral transition, with the identification of relevant metabolic pathways with a potential contribution to the control of floral transition. Changes in the accumulation of raffinose and mono/disaccharides were observed and a change in the balance between those sugars is propose to contribute to the determination of flowering time.

CONCLUSIONS

First: We have identified CF11, a molecule with potential to control flowering. Treatment of plants with CF11 not only activates the expression of a *FT* reporter construct, but also induces flowering under *in vitro* culture conditions in *Arabidopis thaliana*.

Second: We have described two new roles for Pip in Arabidopsis as a regulator of flowering time and rosette growth. The mechanisms underlying those functions remain to be elucidated. The function of Pip as growth regulator could be conserved, since it also affects the growth of *Marchantia polymorpha* thallus.

Third: We performed an integrative omics study of the floral transition in Arabidopsis leaf and apex tissue, by characterizing changes in metabolites, lipids and transcripts upon activation of floral induction via the photoperiod signaling cascade.

Fourth: The *RAFFINOSE SYNTHASE GENE 5* is expressed in the meristem and leaf primordia and loss-of-function mutations on this gene cause an early flowering phenotype.

Fifth: There is an early decrease in raffinose during floral induction in the apex, followed by an increase in several simple sugars. These changes in sugar availability could contribute to the determination of flowering time in Arabidopsis.

BIBLIOGRAPHY

Abe, M., Kaya, H., Watanabe-Taneda, A., Shibuta, M., Yamaguchi, A., Sakamoto, T., Kurata, T., Ausín, I., Araki, T., & Alonso-Blanco, C. (2015). FE, a phloem-specific Myb-related protein, promotes flowering through transcriptional activation of *FLOWERING LOCUS T* and *FLOWERING LOCUS T INTERACTING PROTEIN 1*. *The Plant Journal*, *83*(6), 1059–1068. https://doi.org/10.1111/tpj.12951

Abe, M., Kobayashi, Y., Yamamoto, S., Daimon, Y., Yamaguchi, A., Ikeda, Y., Ichinoki, H., Notaguchi, M., Goto, K., & Araki, T. (2005). *FD*, a bZIP Protein Mediating Signals from the Floral Pathway Integrator *FT* at the Shoot Apex. *Science*, *309*(5737), 1052–1056. https://doi.org/10.1126/science.1115983

Abreu, I. N., Johansson, A. I., Sokołowska, K., Niittylä, T., Sundberg, B., Hvidsten, T. R., Street, N. R., & Moritz, T. (2020). A metabolite roadmap of the wood-forming tissue in Populus tremula. *New Phytologist*, *228*(5), 1559–1572. https://doi.org/10.1111/nph.16799

Acevedo, A., Durán, C., Ciucci, S., Gerl, M., & Cannistraci, C. V. (2018). *LIPEA: Lipid Pathway Enrichment Analysis* (p. 274969). bioRxiv. https://doi.org/10.1101/274969

Albinsky, D., Kusano, M., Higuchi, M., Hayashi, N., Kobayashi, M., Fukushima, A., Mori, M., Ichikawa, T., Matsui, K., Kuroda, H., Horii, Y., Tsumoto, Y., Sakakibara, H., Hirochika, H., Matsui, M., & Saito, K. (2010). Metabolomic Screening Applied to Rice FOX Arabidopsis Lines Leads to the Identification of a Gene-Changing Nitrogen Metabolism. *Molecular Plant*, *3*(1), 125–142. https://doi.org/10.1093/mp/ssp069

Aldag, R. W., & Young, J. L. (1970). Aspects of D-leucine and D-lysine metabolism in maize and ryegrass seedlings. *Planta*, *95*(3), 187–201. https://doi.org/10.1007/BF00385087

Alford, S., Rangarajan, P., Williams, S., & Gillaspy, G. (2012). Myo-inositol oxygenase is required for responses to low energy conditions in Arabidopsis thaliana. *Frontiers in Plant Science*, *3*. https://www.frontiersin.org/article/10.3389/fpls.2012.00069

Althammer, M., Blöchl, C., Reischl, R., Huber, C. G., & Tenhaken, R. (2020). Phosphoglucomutase Is Not the Target for Galactose Toxicity in Plants. *Frontiers in Plant Science*, *11*. https://www.frontiersin.org/article/10.3389/fpls.2020.00167

Amos, K. (2021). *LEVERAGING CHEMICAL AND COMPUTATIONAL BIOLOGY TO PROBE THE CELLULOSE SYNTHASE COMPLEX* [University of Kentucky Libraries]. https://doi.org/10.13023/ETD.2021.399

An, H., Roussot, C., Suárez-López, P., Corbesier, L., Vincent, C., Piñeiro, M., Hepworth, S., Mouradov, A., Justin, S., Turnbull, C., & Coupland, G. (2004). *CONSTANS* acts in the phloem to regulate a systemic signal that induces photoperiodic flowering of Arabidopsis. *Development*, *131*(15), 3615–3626. https://doi.org/10.1242/dev.01231

Andrés, F., & Coupland, G. (2012). The genetic basis of flowering responses to seasonal cues. *Nature Reviews Genetics*, *13*(9), 627–639.

Andrés, F., Kinoshita, A., Kalluri, N., Fernández, V., Falavigna, V. S., Cruz, T., Jang, S., Chiba, Y., Seo, M., & Mettler-Altmann, T. (2020). The sugar transporter SWEET10 acts downstream of FLOWERING LOCUS T during floral transition of *Arabidopsis thaliana*. *BMC Plant Biology*, *20*(1), 1–14.

Bao, S., Hua, C., Shen, L., & Yu, H. (2020). New insights into gibberellin signaling in regulating flowering in Arabidopsis. *Journal of Integrative Plant Biology*, *62*(1), 118–131.

Bartsch, M., Gobbato, E., Bednarek, P., Debey, S., Schultze, J. L., Bautor, J., & Parker, J. E. (2006). Salicylic Acid–Independent ENHANCED DISEASE SUSCEPTIBILITY1 Signaling in Arabidopsis Immunity and Cell Death Is Regulated by the Monooxygenase *FMO1* and the Nudix Hydrolase NUDT7. *The Plant Cell*, *18*(4), 1038–1051. https://doi.org/10.1105/tpc.105.039982

Bäurle, I., & Dean, C. (2006). The Timing of Developmental Transitions in Plants. *Cell*, *125*(4), 655–664. https://doi.org/10.1016/j.cell.2006.05.005

Bekele, E. A., Ampofo-Asiama, J., Alis, R. R., Hertog, M. L. A. T. M., Nicolai, B. M., & Geeraerd, A. H. (2016). Dynamics of metabolic adaptation during initiation of controlled atmosphere storage of 'Jonagold' apple: Effects of storage gas concentrations and conditioning. *Postharvest Biology and Technology*, *117*, 9–20. https://doi.org/10.1016/j.postharvbio.2016.02.003

Berardini, T. Z., Reiser, L., Li, D., Mezheritsky, Y., Muller, R., Strait, E., & Huala, E. (2015). The Arabidopsis Information Resource: Making and Mining the 'Gold Standard' Annotated Reference Plant Genome. *Genesis (New York, N.Y. : 2000)*, *53*(8), 474–485. https://doi.org/10.1002/dvg.22877

Bhattacharya, A. (2019). Chapter 4—Lipid Metabolism in Plants Under High Temperature. In A. Bhattacharya (Ed.), *Effect of High Temperature on Crop Productivity and Metabolism of Macro Molecules* (pp. 311–389). Academic Press. https://doi.org/10.1016/B978-0-12-817562-0.00004-5

Blázquez, M. A., Green, R., Nilsson, O., Sussman, M. R., & Weigel, D. (1998). Gibberellins Promote Flowering of Arabidopsis by Activating the *LEAFY* Promoter. *The Plant Cell*, *10*(5), 791–800. https://doi.org/10.1105/tpc.10.5.791

Blázquez, M. A., Santos, E., Flores, C., Martínez-Zapater, J. M., Salinas, J., & Gancedo, C. (1998). Isolation and molecular characterization of the Arabidopsis *TPS1* gene, encoding trehalose-6-phosphate synthase. *The Plant Journal*, *13*(5), 685–689. https://doi.org/10.1046/j.1365-313X.1998.00063.x

Bolger, A. M., Lohse, M., & Usadel, B. (2014). Trimmomatic: A flexible trimmer for Illumina sequence data. *Bioinformatics*, *30*(15), 2114–2120. https://doi.org/10.1093/bioinformatics/btu170

Bonhomme, F., Kurz, B., Melzer, S., Bernier, G., & Jacqmard, A. (2000). Cytokinin and gibberellin activate SaMADS A, a gene apparently involved in regulation of the floral transition in *Sinapis alba*. *The Plant Journal*, *24*(1), 103–111. https://doi.org/10.1046/j.1365-313x.2000.00859.x

Bouché, F., Lobet, G., Tocquin, P., & Périlleux, C. (2016). FLOR-ID: An interactive database of flowering-time gene networks in *Arabidopsis thaliana*. *Nucleic Acids Research*, *44*(D1), D1167–D1171. https://doi.org/10.1093/nar/gkv1054

Broquist, H. P. (1991). Lysine-pipecolic acid metabolic relationships in microbes and mammals. *Annual Review of Nutrition*, *11*, 435–448. https://doi.org/10.1146/annurev.nu.11.070191.002251

Carneiro, J. M. T., Madrid, K. C., Maciel, B. C. M., & Arruda, M. A. Z. (2015). *Arabidopsis thaliana* and omics approaches: A review: DOI: 10.5584/jiomics.v5i1.179. *Journal of Integrated OMICS*, *5*(1), 1–16.

Castillejo, C., & Pelaz, S. (2008). The Balance between CONSTANS and TEMPRANILLO Activities Determines *FT* Expression to Trigger Flowering. *Current Biology*, *18*(17), 1338–1343. https://doi.org/10.1016/j.cub.2008.07.075

Chawla, G., & Ranjan, C. (2016). Principle, Instrumentation, and Applications of UPLC: A Novel Technique of Liquid Chromatography. *Open Chemistry Journal*, *3*(1). https://doi.org/10.2174/1874842201603010001

Chen, K., Li, G.-J., Bressan, R. A., Song, C.-P., Zhu, J.-K., & Zhao, Y. (2020). Abscisic acid dynamics, signaling, and functions in plants. *Journal of Integrative Plant Biology*, *62*(1), 25–54. https://doi.org/10.1111/jipb.12899

Chen, Y.-C., Holmes, E. C., Rajniak, J., Kim, J.-G., Tang, S., Fischer, C. R., Mudgett, M. B., & Sattely, E. S. (2018). N-hydroxy-pipecolic acid is a mobile metabolite that induces systemic disease resistance in Arabidopsis. *Proceedings of the National Academy of Sciences*, *115*(21), E4920–E4929. https://doi.org/10.1073/pnas.1805291115

Chen, Z., Yoo, S.-H., Park, Y.-S., Kim, K.-H., Wei, S., Buhr, E., Ye, Z.-Y., Pan, H.-L., & Takahashi, J. S. (2012). Identification of diverse modulators of central and peripheral circadian clocks by high-throughput chemical screening. *Proceedings of the National Academy of Sciences*, *109*(1), 101–106. https://doi.org/10.1073/pnas.1118034108

Cheng, C.-Y., Krishnakumar, V., Chan, A. P., Thibaud-Nissen, F., Schobel, S., & Town, C. D. (2017). Araport11: A complete reannotation of the *Arabidopsis thaliana* reference genome. *The Plant Journal*, *89*(4), 789–804. https://doi.org/10.1111/tpj.13415

Cheng, J.-Z., Zhou, Y.-P., Lv, T.-X., Xie, C.-P., & Tian, C.-E. (2017). Research progress on the autonomous flowering time pathway in Arabidopsis. *Physiology and*

Molecular Biology of Plants, *23*(3), 477–485. https://doi.org/10.1007/s12298-017-0458-3

Cho, L. H., Yoon, J., & An, G. (2017). The control of flowering time by environmental factors. *Plant Journal*, *90*(4), 708–719. https://doi.org/10.1111/tpj.13461

Cho, L.-H., Pasriga, R., Yoon, J., Jeon, J.-S., & An, G. (2018). Roles of Sugars in Controlling Flowering Time. *Journal of Plant Biology*, *61*(3), 121–130. https://doi.org/10.1007/s12374-018-0081-z

Chong, J., Soufan, O., Li, C., Caraus, I., Li, S., Bourque, G., Wishart, D. S., & Xia, J. (2018). MetaboAnalyst 4.0: Towards more transparent and integrative metabolomics analysis. *Nucleic Acids Research*, *46*(W1), W486–W494.

Clough, S. J., & Bent, A. F. (1998). Floral dip: A simplified method for *Agrobacterium*-mediated transformation of *Arabidopsis thaliana*. *The Plant Journal: For Cell and Molecular Biology*, *16*(6), 735–743. https://doi.org/10.1046/j.1365-313x.1998.00343.x

Contag, C. H., & Bachmann, M. H. (2002). Advances in In Vivo Bioluminescence Imaging of Gene Expression. *Annual Review of Biomedical Engineering*, *4*(1), 235–260. https://doi.org/10.1146/annurev.bioeng.4.111901.093336

Conti, L. (2017). Hormonal control of the floral transition: Can one catch them all? *Developmental Biology*, *430*(2), 288–301. https://doi.org/10.1016/j.ydbio.2017.03.024

Conti, L. (2019). The ABA of floral transition: The to do list for perfect escape. *Molecular Plant*, *12*(3), 289–291.

Corbesier, L., Havelange, A., Lejeune, P., Bernier, G., & Périlleux, C. (2001). N content of phloem and xylem exudates during the transition to flowering in *Sinapis alba*

and Arabidopsis thaliana. *Plant, Cell & Environment*, *24*(3), 367–375. https://doi.org/10.1046/j.1365-3040.2001.00683.x

Corbesier, L., Vincent, C., Jang, S., Fornara, F., Fan, Q., Searle, I., Giakountis, A., Farrona, S., Gissot, L., Turnbull, C., & Coupland, G. (2007). FT Protein Movement Contributes to Long-Distance Signaling in Floral Induction of Arabidopsis. *Science*, *316*(5827), 1030–1033. https://doi.org/10.1126/science.1141752

Davis, S. J. (2009). Integrating hormones into the floral-transition pathway of *Arabidopsis thaliana*. *Plant, Cell & Environment*, *32*(9), 1201–1210. https://doi.org/10.1111/j.1365-3040.2009.01968.x

de Souza Vidigal, D., Willems, L., van Arkel, J., Dekkers, B. J. W., Hilhorst, H. W. M., & Bentsink, L. (2016). Galactinol as marker for seed longevity. *Plant Science*, *246*, 112–118. https://doi.org/10.1016/j.plantsci.2016.02.015

De Veylder, L., Beeckman, T., Beemster, G. T. S., Krols, L., Terras, F., Landrieu, I., Van Der Schueren, E., Maes, S., Naudts, M., & Inzé, D. (2001). Functional Analysis of Cyclin-Dependent Kinase Inhibitors of Arabidopsis. *The Plant Cell*, *13*(7), 1653–1668. https://doi.org/10.1105/TPC.010087

Deborde, C., Moing, A., Roch, L., Jacob, D., Rolin, D., & Giraudeau, P. (2017). Plant metabolism as studied by NMR spectroscopy. *Progress in Nuclear Magnetic Resonance Spectroscopy*, *102–103*, 61–97. https://doi.org/10.1016/j.pnmrs.2017.05.001

Depuydt, S., & Hardtke, C. S. (2011). Hormone Signalling Crosstalk in Plant Growth Regulation. *Current Biology*, *21*(9), R365–R373. https://doi.org/10.1016/j.cub.2011.03.013

Ding, P., Rekhter, D., Ding, Y., Feussner, K., Busta, L., Haroth, S., Xu, S., Li, X., Jetter, R., Feussner, I., & Zhang, Y. (2016). Characterization of a Pipecolic Acid Biosynthesis Pathway Required for Systemic Acquired Resistance. *The Plant Cell*, *28*(10), 2603–2615. https://doi.org/10.1105/tpc.16.00486

Drakakaki, G., Robert, S., Raikhel, N. V., & Hicks, G. R. (2009a). Chemical dissection of endosomal pathways. *Plant Signaling & Behavior*, *4*(1), 57–62. https://doi.org/10.4161/psb.4.1.7314

Drakakaki, G., Robert, S., Raikhel, N. V., & Hicks, G. R. (2009b). Chemical dissection of endosomal pathways. *Plant Signaling & Behavior*, *4*(1), 57–62. https://doi.org/10.4161/psb.4.1.7314

Drakakaki, G., Robert, S., Szatmari, A.-M., Brown, M. Q., Nagawa, S., Van Damme, D., Leonard, M., Yang, Z., Girke, T., Schmid, S. L., Russinova, E., Friml, J., Raikhel, N. V., & Hicks, G. R. (2011). Clusters of bioactive compounds target dynamic endomembrane networks in vivo. *Proceedings of the National Academy of Sciences*, *108*(43), 17850–17855. https://doi.org/10.1073/pnas.1108581108

Duplat-Bermúdez, L., Ruiz-Medrano, R., Landsman, D., Mariño-Ramírez, L., & Xoconostle-Cázares, B. (2016). Transcriptomic analysis of Arabidopsis overexpressing flowering locus T driven by a meristem-specific promoter that induces early flowering. *Gene*, *587*(2), 120–131. https://doi.org/10.1016/j.gene.2016.04.060

Easlon, H. M., & Bloom, A. J. (2014). Easy Leaf Area: Automated digital image analysis for rapid and accurate measurement of leaf area. *Applications in Plant Sciences*, *2*(7), 1400033. https://doi.org/10.3732/apps.1400033

Egert, A., Keller, F., & Peters, S. (2013). Abiotic stress-induced accumulation of raffinose in Arabidopsis leaves is mediated by a single raffinose synthase (RS5, At5g40390). *BMC Plant Biology*, *13*(1), 1–9.

Egert, A., Peters, S., Guyot, C., Stieger, B., & Keller, F. (2012). An arabidopsis T-DNA insertion mutant for galactokinase (AtGALK, At3g06580) hyperaccumulates free galactose and is insensitive to exogenous galactose. *Plant and Cell Physiology*, *53*(5), 921–929. https://doi.org/10.1093/pcp/pcs036

Endres, S., & Tenhaken, R. (2011). Down-regulation of the myo-inositol oxygenase gene family has no effect on cell wall composition in Arabidopsis. *Planta*, *234*(1), 157–169. https://doi.org/10.1007/s00425-011-1394-z

Eriksson, S., Böhlenius, H., Moritz, T., & Nilsson, O. (2006). GA4 Is the Active Gibberellin in the Regulation of *LEAFY* Transcription and Arabidopsis Floral Initiation. *The Plant Cell*, *18*(9), 2172–2181. https://doi.org/10.1105/tpc.106.042317

Fahy, E., Subramaniam, S., Murphy, R. C., Nishijima, M., Raetz, C. R. H., Shimizu, T., Spener, F., Meer, G. van, Wakelam, M. J. O., & Dennis, E. A. (2009). Update of the LIPID MAPS comprehensive classification system for lipids1. *Journal of Lipid Research*, *50*, S9–S14. https://doi.org/10.1194/jlr.R800095-JLR200

Falavigna, V. D. S., Porto, D. D., Miotto, Y. E., Santos, H. P. D., Oliveira, P. R. D. D., Margis-Pinheiro, M., Pasquali, G., & Revers, L. F. (2018). Evolutionary diversification of galactinol synthases in Rosaceae: Adaptive roles of galactinol and raffinose during apple bud dormancy. *Journal of Experimental Botany*, *69*(5), 1247–1259. https://doi.org/10.1093/jxb/erx451

Fantini, E., Sulli, M., Zhang, L., Aprea, G., Jiménez-Gómez, J. M., Bendahmane, A., Perrotta, G., Giuliano, G., & Facella, P. (2019). Pivotal Roles of Cryptochromes

1a and 2 in Tomato Development and Physiology. *Plant Physiology*, *179*(2), 732–748. https://doi.org/10.1104/pp.18.00793

Ferrandiz, C., Gu, Q., Martienssen, R., & Yanofsky, M. F. (2000). Redundant regulation of meristem identity and plant architecture by FRUITFULL, APETALA1 and CAULIFLOWER. *Development*, *127*(4), 725–734. https://doi.org/10.1242/dev.127.4.725

Fichtner, F., & Lunn, J. E. (2021). The role of trehalose 6-phosphate (Tre6P) in plant metabolism and development. *Annual Review of Plant Biology*, *72*, 737–760.

Fiehn, O. (2002). Metabolomics—The link between genotypes and phenotypes. In C. Town (Ed.), *Functional Genomics* (pp. 155–171). Springer Netherlands. https://doi.org/10.1007/978-94-010-0448-0_11

Fiehn, O. (2016). Metabolomics by Gas Chromatography-Mass Spectrometry: The combination of targeted and untargeted profiling. *Current Protocols in Molecular Biology / Edited by Frederick M. Ausubel ... [et Al.]*, *114*, 30.4.1-30.4.32. https://doi.org/10.1002/0471142727.mb3004s114

Fiers, M., Hoogenboom, J., Brunazzi, A., Wennekes, T., Angenent, G. C., & Immink, R. G. H. (2017). A plant-based chemical genomics screen for the identification of flowering inducers. *Plant Methods*, *13*(1), 78. https://doi.org/10.1186/s13007-017-0230-2

Fouracre, J. P., & Poethig, R. S. (2019). Role for the shoot apical meristem in the specification of juvenile leaf identity in Arabidopsis. *Proceedings of the National Academy of Sciences*, *116*(20), 10168–10177. https://doi.org/10.1073/pnas.1817853116

Frank, A., Matiolli, C. C., Viana, A. J. C., Hearn, T. J., Kusakina, J., Belbin, F. E., Wells Newman, D., Yochikawa, A., Cano-Ramirez, D. L., Chembath, A., Cragg-Barber,

K., Haydon, M. J., Hotta, C. T., Vincentz, M., Webb, A. A. R., & Dodd, A. N. (2018). Circadian Entrainment in Arabidopsis by the Sugar-Responsive Transcription Factor bZIP63. *Current Biology*, *28*(16), 2597-2606.e6. https://doi.org/10.1016/j.cub.2018.05.092

Freytes, S. N., Canelo, M., & Cerdán, P. D. (2021). Regulation of Flowering Time: When and Where? *Current Opinion in Plant Biology*, *63*, 102049. https://doi.org/10.1016/j.pbi.2021.102049

Fu, Z. Q., & Dong, X. (2013). Systemic Acquired Resistance: Turning Local Infection into Global Defense. *Annual Review of Plant Biology*, *64*(1), 839–863. https://doi.org/10.1146/annurev-arplant-042811-105606

Fujioka, S., & Sakurai, A. (1992). Effect of L-Pipecolic Acid on Flowering in *Lemna paucicostata* and *Lemna gibba*. *Plant and Cell Physiology*, *33*(4), 419–426. https://doi.org/10.1093/oxfordjournals.pcp.a078270

Fujioka, S., & Sakurai, A. (1997). Conversion of Lysine to L-Pipecolic Acid Induces Flowering in *Lemna paucicostata* 151. *Plant and Cell Physiology*, *38*(11), 1278–1280. https://doi.org/10.1093/oxfordjournals.pcp.a029116

Fujioka, S., Sakurai, A., Yamaguchi, I., Murofushi, N., Takahashi, N., Kaihara, S., & Takimoto, A. (1987). Isolation and Identification of L-Pipecolic Acid and Nicotinamide as Flower-Inducing Substances in Lemna. *Plant and Cell Physiology*, *28*(6), 995–1003. https://doi.org/10.1093/oxfordjournals.pcp.a077402

Gachon, C. M. M., Langlois-Meurinne, M., & Saindrenan, P. (2005). Plant secondary metabolism glycosyltransferases: The emerging functional analysis. *Trends in Plant Science*, *10*(11), 542–549. https://doi.org/10.1016/j.tplants.2005.09.007

Galili, G., Tang, G., Zhu, X., & Gakiere, B. (2001). Lysine catabolism: A stress and development super-regulated metabolic pathway. *Current Opinion in Plant Biology*, *4*(3), 261–266. https://doi.org/10.1016/S1369-5266(00)00170-9

Galvão, V. C., Horrer, D., Küttner, F., & Schmid, M. (2012). Spatial control of flowering by DELLA proteins in *Arabidopsis thaliana*. *Development*, *139*(21), 4072–4082.

Gangl, R., Behmüller, R., & Tenhaken, R. (2015). Molecular cloning of *AtRS4*, a seed specific multifunctional RFO synthase/galactosylhydrolase in *Arabidopsis thaliana*. *Frontiers in Plant Science*, *6*. https://www.frontiersin.org/article/10.3389/fpls.2015.00789

Gangl, R., & Tenhaken, R. (2016). Raffinose Family Oligosaccharides Act As Galactose Stores in Seeds and Are Required for Rapid Germination of Arabidopsis in the Dark. *Frontiers in Plant Science*, *7*. https://www.frontiersin.org/article/10.3389/fpls.2016.01115

García, C. G. (2021). *Análisis de la conexión entre la formación de las flores y el estrés abiótico (ABA) a través de TERMINAL FLOWER 1*. 83.

García-Maquilón, I., Rodriguez, P. L., Vaidya, A. S., & Lozano-Juste, J. (2021). A LuciferaseLuciferase ReporterReportersAssay to Identify Chemical Activators of ABAAbscisic acid (ABA)Signaling. In G. R. Hicks & C. Zhang (Eds.), *Plant Chemical Genomics: Methods and Protocols* (pp. 113–121). Springer US. https://doi.org/10.1007/978-1-0716-0954-5_10

Garner, W. W., & Allard, H. A. (1925). *Localization of the Response in Plants to Relative Length of Day and Night*. https://naldc.nal.usda.gov/catalog/IND43967129

Gawarecka, K., & Ahn, J. H. (2021). Isoprenoid-Derived Metabolites and Sugars in the Regulation of Flowering Time: Does Day Length Matter? *Frontiers in Plant Science*, *12*, 765995. https://doi.org/10.3389/fpls.2021.765995

Gendron, J. M., Pruneda-Paz, J. L., Doherty, C. J., Gross, A. M., Kang, S. E., & Kay, S. A. (2012). Arabidopsis circadian clock protein, TOC1, is a DNA-binding transcription factor. *Proceedings of the National Academy of Sciences*, *109*(8), 3167–3172. https://doi.org/10.1073/pnas.1200355109

Gentleman, R. C., Carey, V. J., Bates, D. M., Bolstad, B., Dettling, M., Dudoit, S., Ellis, B., Gautier, L., Ge, Y., Gentry, J., Hornik, K., Hothorn, T., Huber, W., Iacus, S., Irizarry, R., Leisch, F., Li, C., Maechler, M., Rossini, A. J., … Zhang, J. (2004). Bioconductor: Open software development for computational biology and bioinformatics. *Genome Biology*, *5*(10), R80. https://doi.org/10.1186/gb-2004-5-10-r80

Ghatak, A., Chaturvedi, P., & Weckwerth, W. (2018). Metabolomics in Plant Stress Physiology. In R. K. Varshney, M. K. Pandey, & A. Chitikineni (Eds.), *Plant Genetics and Molecular Biology* (pp. 187–236). Springer International Publishing. https://doi.org/10.1007/10_2017_55

Gilmour, S. J., Sebolt, A. M., Salazar, M. P., Everard, J. D., & Thomashow, M. F. (2000). Overexpression of the Arabidopsis CBF3 transcriptional activator mimics multiple biochemical changes associated with cold acclimation. *Plant Physiology*, *124*(4), 1854–1865. https://doi.org/10.1104/pp.124.4.1854

Goodstein, D. M., Shu, S., Howson, R., Neupane, R., Hayes, R. D., Fazo, J., Mitros, T., Dirks, W., Hellsten, U., Putnam, N., & Rokhsar, D. S. (2012). Phytozome: A comparative platform for green plant genomics. *Nucleic Acids Research*, *40*(D1), D1178–D1186. https://doi.org/10.1093/nar/gkr944

Gullberg, J., Jonsson, P., Nordström, A., Sjöström, M., & Moritz, T. (2004). Design of experiments: An efficient strategy to identify factors influencing extraction and derivatization of Arabidopsis thaliana samples in metabolomic studies with gas

chromatography/mass spectrometry. *Analytical Biochemistry*, *331*(2), 283–295. https://doi.org/10.1016/j.ab.2004.04.037

Gupta, R. N., & Spenser, I. D. (1969). Biosynthesis of the piperidine nucleus. The mode of incorporation of lysine into pipecolic acid and into piperidine alkaloids. *The Journal of Biological Chemistry*, *244*(1), 88–94.

Hanahan, D. (1983). Studies on transformation of Escherichia coli with plasmids. *Journal of Molecular Biology*, *166*(4), 557–580. https://doi.org/10.1016/S0022-2836(83)80284-8

Hartmann, M., Kim, D., Bernsdorff, F., Ajami-Rashidi, Z., Scholten, N., Schreiber, S., Zeier, T., Schuck, S., Reichel-Deland, V., & Zeier, J. (2017). Biochemical Principles and Functional Aspects of Pipecolic Acid Biosynthesis in Plant Immunity. *Plant Physiology*, *174*(1), 124–153. https://doi.org/10.1104/pp.17.00222

Hartmann, M., & Zeier, J. (2018). l-lysine metabolism to N-hydroxypipecolic acid: An integral immune-activating pathway in plants. *The Plant Journal*, *96*(1), 5–21. https://doi.org/10.1111/tpj.14037

Hartmann, M., & Zeier, J. (2019). N-hydroxypipecolic acid and salicylic acid: A metabolic duo for systemic acquired resistance. *Current Opinion in Plant Biology*, *50*, 44–57. https://doi.org/10.1016/j.pbi.2019.02.006

Hartmann, M., Zeier, T., Bernsdorff, F., Reichel-Deland, V., Kim, D., Hohmann, M., Scholten, N., Schuck, S., Bräutigam, A., Hölzel, T., Ganter, C., & Zeier, J. (2018). Flavin Monooxygenase-Generated N-Hydroxypipecolic Acid Is a Critical Element of Plant Systemic Immunity. *Cell*, *173*(2), 456-469.e16. https://doi.org/10.1016/j.cell.2018.02.049

Hawkins, C., Ginzburg, D., Zhao, K., Dwyer, W., Xue, B., Xu, A., Rice, S., Cole, B., Paley, S., Karp, P., & Rhee, S. Y. (2021). Plant Metabolic Network 15: A resource of genome-wide metabolism databases for 126 plants and algae. *Journal of Integrative Plant Biology*, *63*(11), 1888–1905. https://doi.org/10.1111/jipb.13163

Haydon, M. J., Mielczarek, O., Frank, A., Román, Á., & Webb, A. A. R. (2017). Sucrose and Ethylene Signaling Interact to Modulate the Circadian Clock. *Plant Physiology*, *175*(2), 947–958. https://doi.org/10.1104/pp.17.00592

Haydon, M. J., Mielczarek, O., Robertson, F. C., Hubbard, K. E., & Webb, A. A. R. (2013). Photosynthetic entrainment of the *Arabidopsis thaliana* circadian clock. *Nature*, *502*(7473), 689–692. https://doi.org/10.1038/nature12603

He, M. (2006). Pipecolic acid in microbes: Biosynthetic routes and enzymes. *Journal of Industrial Microbiology and Biotechnology*, *33*(6), 401–407. https://doi.org/10.1007/s10295-006-0078-3

He, Y., Chen, T., & Zeng, X. (2020). Genetic and Epigenetic Understanding of the Seasonal Timing of Flowering. *Plant Communications*, *1*(1), 100008. https://doi.org/10.1016/j.xplc.2019.100008

Hempel, F. D., & Feldman, L. J. (1995). Specification of chimeric flowering shoots in wild-type Arabidopsis. *The Plant Journal*, *8*(5), 725–731. https://doi.org/10.1046/j.1365-313X.1995.08050725.x

Hicks, G. R., & Raikhel, N. V. (2012). Small Molecules Present Large Opportunities in Plant Biology. *Annual Review of Plant Biology*, *63*(1), 261–282. https://doi.org/10.1146/annurev-arplant-042811-105456

Hincha, D. K., Zuther, E., & Heyer, A. G. (2003). The preservation of liposomes by raffinose family oligosaccharides during drying is mediated by effects on fusion and lipid phase transitions. *Biochimica et Biophysica Acta (BBA)* -

Biomembranes, *1612*(2), 172–177. https://doi.org/10.1016/S0005-2736(03)00116-0

Hisamatsu, T., & King, R. W. (2008). The nature of floral signals in Arabidopsis. II. Roles for FLOWERING LOCUS T (FT) and gibberellin. *Journal of Experimental Botany*, *59*(14), 3821–3829. https://doi.org/10.1093/jxb/ern232

Hoagland, D. R., & Arnon, D. I. (1950). The water-culture method for growing plants without soil. *Circular. California Agricultural Experiment Station*, *347*(2nd edit). https://www.cabdirect.org/cabdirect/abstract/19500302257

Horbowicz, M., & Obendorf, R. L. (1994). Seed desiccation tolerance and storability: Dependence on flatulence-producing oligosaccharides and cyclitols—review and survey. *Seed Science Research*, *4*(4), 385–405. https://doi.org/10.1017/S0960258500002440

Hsu, P. Y., & Harmer, S. L. (2014). Wheels within wheels: The plant circadian system. *Trends in Plant Science*, *19*(4), 240–249. https://doi.org/10.1016/j.tplants.2013.11.007

Huang, W., Pérez-García, P., Pokhilko, A., Millar, A. J., Antoshechkin, I., Riechmann, J. L., & Mas, P. (2012). Mapping the Core of the Arabidopsis Circadian Clock Defines the Network Structure of the Oscillator. *Science*, *336*(6077), 75–79. https://doi.org/10.1126/science.1219075

Huang, W., Wang, Y., Li, X., & Zhang, Y. (2020). Biosynthesis and Regulation of Salicylic Acid and N-Hydroxypipecolic Acid in Plant Immunity. *Molecular Plant*, *13*(1), 31–41. https://doi.org/10.1016/j.molp.2019.12.008

Huijser, P., & Schmid, M. (2011). The control of developmental phase transitions in plants. *Development*, *138*(19), 4117–4129. https://doi.org/10.1242/dev.063511

Imaizumi, C., Tomatsu, H., Kitazawa, K., Yoshimi, Y., Shibano, S., Kikuchi, K., Yamaguchi, M., Kaneko, S., Tsumuraya, Y., & Kotake, T. (2017). Heterologous expression and characterization of an Arabidopsis β-l-arabinopyranosidase and α-d-galactosidases acting on β-l-arabinopyranosyl residues. *Journal of Experimental Botany*, *68*(16), 4651–4661. https://doi.org/10.1093/jxb/erx279

Ionescu, I. A., Møller, B. L., & Sánchez-Pérez, R. (2017). Chemical control of flowering time. *Journal of Experimental Botany*, *68*(3), 369–382.

Izawa, T. (2021). What is going on with the hormonal control of flowering in plants? *The Plant Journal*, *105*(2), 431–445. https://doi.org/10.1111/tpj.15036

James, A. B., Monreal, J. A., Nimmo, G. A., Kelly, C. L., Herzyk, P., Jenkins, G. I., & Nimmo, H. G. (2008). The Circadian Clock in Arabidopsis Roots Is a Simplified Slave Version of the Clock in Shoots. *Science*, *322*(5909), 1832–1835. https://doi.org/10.1126/science.1161403

Jang, J.-H., Shang, Y., Kang, H. K., Kim, S. Y., Kim, B. H., & Nam, K. H. (2018). Arabidopsis *GALACTINOL SYNTHASES 1* (*AtGOLS1*) negatively regulates seed germination. *Plant Science*, *267*, 94–101. https://doi.org/10.1016/j.plantsci.2017.11.010

Jang, S., Marchal, V., Panigrahi, K. C. S., Wenkel, S., Soppe, W., Deng, X.-W., Valverde, F., & Coupland, G. (2008). Arabidopsis COP1 shapes the temporal pattern of CO accumulation conferring a photoperiodic flowering response. *The EMBO Journal*, *27*(8), 1277–1288. https://doi.org/10.1038/emboj.2008.68

Jang, S., Torti, S., & Coupland, G. (2009). Genetic and spatial interactions between FT, TSF and SVP during the early stages of floral induction in Arabidopsis. *The Plant Journal*, *60*(4), 614–625. https://doi.org/10.1111/j.1365-313X.2009.03986.x

Jefferson, R. A., Kavanagh', T. A., & Bevan, M. W. (n.d.). *GUS fusions: ,B-glucuronidase as a sensitive and versatile gene fusion marker in higher plants*. 7.

Jiang, J., Hu, J., Tan, R., Han, Y., & Li, Z. (2019). Expression of *IbVPE1* from sweet potato in Arabidopsis affects leaf development, flowering time and chlorophyll catabolism. *BMC Plant Biology*, *19*(1), 184. https://doi.org/10.1186/s12870-019-1789-8

Jin, S., Nasim, Z., Susila, H., & Ahn, J. H. (2021). Evolution and functional diversification of *FLOWERING LOCUS T/TERMINAL FLOWER 1* family genes in plants. *Seminars in Cell & Developmental Biology*, *109*, 20–30. https://doi.org/10.1016/j.semcdb.2020.05.007

Jing, Y., Lang, S., Wang, D., Xue, H., & Wang, X. F. (2018). Functional characterization of galactinol synthase and raffinose synthase in desiccation tolerance acquisition in developing Arabidopsis seeds. *Journal of Plant Physiology*, *230*, 109–121. https://doi.org/10.1016/j.jplph.2018.10.011

Johansson, M., & Staiger, D. (2015). Time to flower: Interplay between photoperiod and the circadian clock. *Journal of Experimental Botany*, *66*(3), 719–730. https://doi.org/10.1093/jxb/eru441

Jones, P., Messner, B., Nakajima, J.-I., Schäffner, A. R., & Saito, K. (2003). UGT73C6 and UGT78D1, Glycosyltransferases Involved in Flavonol Glycoside Biosynthesis in Arabidopsis thaliana *. *Journal of Biological Chemistry*, *278*(45), 43910–43918. https://doi.org/10.1074/jbc.M303523200

Kaihara, S., & Takimoto, A. (1990). Interaction between L-Pipecolic Acid and Water Extracts of Various Plant Species in Floral Induction of *Lemna paucicostata*. *Plant and Cell Physiology*, *31*(7), 1059–1061. https://doi.org/10.1093/oxfordjournals.pcp.a078003

Kamioka, M., Takao, S., Suzuki, T., Taki, K., Higashiyama, T., Kinoshita, T., & Nakamichi, N. (2016). Direct Repression of Evening Genes by *CIRCADIAN CLOCK-ASSOCIATED1* in the Arabidopsis Circadian Clock. *The Plant Cell*, *28*(3), 696–711. https://doi.org/10.1105/tpc.15.00737

Kandler, O., & Hopf, H. (1982). Oligosaccharides Based on Sucrose (Sucrosyl Oligosaccharides). In F. A. Loewus & W. Tanner (Eds.), *Plant Carbohydrates I: Intracellular Carbohydrates* (pp. 348–383). Springer. https://doi.org/10.1007/978-3-642-68275-9_8

Kanehisa, M., Goto, S., Hattori, M., Aoki-Kinoshita, K. F., Itoh, M., Kawashima, S., Katayama, T., Araki, M., & Hirakawa, M. (2006). From genomics to chemical genomics: New developments in KEGG. *Nucleic Acids Research*, *34*(suppl_1), D354–D357. https://doi.org/10.1093/nar/gkj102

Kaneko-Suzuki, M., Kurihara-Ishikawa, R., Okushita-Terakawa, C., Kojima, C., Nagano-Fujiwara, M., Ohki, I., Tsuji, H., Shimamoto, K., & Taoka, K.-I. (2018). TFL1-Like Proteins in Rice Antagonize Rice FT-Like Protein in Inflorescence Development by Competition for Complex Formation with 14-3-3 and FD. *Plant and Cell Physiology*, *59*(3), 458–468. https://doi.org/10.1093/pcp/pcy021

Kanter, U., Usadel, B., Guerineau, F., Li, Y., Pauly, M., & Tenhaken, R. (2005). The inositol oxygenase gene family of Arabidopsis is involved in the biosynthesis of nucleotide sugar precursors for cell-wall matrix polysaccharides. *Planta*, *221*(2), 243–254. https://doi.org/10.1007/s00425-004-1441-0

Kardailsky, I., Shukla, V. K., Ahn, J. H., Dagenais, N., Christensen, S. K., Nguyen, J. T., Chory, J., Harrison, M. J., & Weigel, D. (1999). Activation Tagging of the Floral Inducer *FT*. *Science*, *286*(5446), 1962–1965. https://doi.org/10.1126/science.286.5446.1962

Karnovsky, A., & Li, S. (2020). Pathway analysis for targeted and untargeted metabolomics. *Computational Methods and Data Analysis for Metabolomics*, 387–400.

Kerhoas, L., Aouak, D., Cingöz, A., Routaboul, J.-M., Lepiniec, L., Einhorn, J., & Birlirakis, N. (2006). Structural characterization of the major flavonoid glycosides from Arabidopsis thaliana seeds. *Journal of Agricultural and Food Chemistry*, *54*(18), 6603–6612. https://doi.org/10.1021/jf061043n

Knaupp, M., Mishra, K. B., Nedbal, L., & Heyer, A. G. (2011). Evidence for a role of raffinose in stabilizing photosystem II during freeze-thaw cycles. *Planta*, *234*(3), 477–486. https://doi.org/10.1007/s00425-011-1413-0

Kobayashi, Y., Kaya, H., Goto, K., Iwabuchi, M., & Araki, T. (1999). A Pair of Related Genes with Antagonistic Roles in Mediating Flowering Signals. *Science*, *286*(5446), 1960–1962. https://doi.org/10.1126/science.286.5446.1960

Kobayashi, Y., & Weigel, D. (2007). Move on up, it's time for change—Mobile signals controlling photoperiod-dependent flowering. *Genes & Development*, *21*(19), 2371–2384. https://doi.org/10.1101/gad.1589007

Kolbe, A., Tiessen, A., Schluepmann, H., Paul, M., Ulrich, S., & Geigenberger, P. (2005). Trehalose 6-phosphate regulates starch synthesis via posttranslational redox activation of ADP-glucose pyrophosphorylase. *Proceedings of the National Academy of Sciences*, *102*(31), 11118–11123. https://doi.org/10.1073/pnas.0503410102

Koncz, C., & Schell, J. (1986). The promoter of TL-DNA gene 5 controls the tissue-specific expression of chimaeric genes carried by a novel type of Agrobacterium binary vector. *Molecular and General Genetics MGG*, *204*(3), 383–396. https://doi.org/10.1007/BF00331014

Koo, J., Kim, Y., Kim, J., Yeom, M., Lee, I. C., & Nam, H. G. (2007). A GUS/Luciferase Fusion Reporter for Plant Gene Trapping and for Assay of Promoter Activity with Luciferin-Dependent Control of the Reporter Protein Stability. *Plant and Cell Physiology*, *48*(8), 1121–1131. https://doi.org/10.1093/pcp/pcm081

Koornneef, M., Alonso-Blanco, C., & Vreugdenhil, D. (2004). Naturally Occurring Genetic Variation in Arabidopsis Thaliana. *Annual Review of Plant Biology*, *55*(1), 141–172. https://doi.org/10.1146/annurev.arplant.55.031903.141605

Koornneef, M., Hanhart, C. J., & van der Veen, J. H. (1991). A genetic and physiological analysis of late flowering mutants in *Arabidopsis thaliana*. *Molecular and General Genetics MGG*, *229*(1), 57–66. https://doi.org/10.1007/BF00264213

Kostenyuk, I., Oh, B. J., & So, I. S. (1999). Induction of early flowering in Cymbidium niveo-marginatum Mak in vitro. *Plant Cell Reports*, *19*(1), 1–5. https://doi.org/10.1007/s002990050701

Kumar, R., Bohra, A., Pandey, A. K., Pandey, M. K., & Kumar, A. (2017). Metabolomics for Plant Improvement: Status and Prospects. *Frontiers in Plant Science*, *8*. https://www.frontiersin.org/article/10.3389/fpls.2017.01302

Kushiro, T., Okamoto, M., Nakabayashi, K., Yamagishi, K., Kitamura, S., Asami, T., Hirai, N., Koshiba, T., Kamiya, Y., & Nambara, E. (2004). The Arabidopsis cytochrome P450 CYP707A encodes ABA 8'-hydroxylases: Key enzymes in ABA catabolism. *The EMBO Journal*, *23*(7), 1647–1656. https://doi.org/10.1038/sj.emboj.7600121

Laubinger, S., Marchal, V., Gentilhomme, J., Wenkel, S., Adrian, J., Jang, S., Kulajta, C., Braun, H., Coupland, G., & Hoecker, U. (2006). Arabidopsis SPA proteins regulate photoperiodic flowering and interact with the floral inducer CONSTANS

to regulate its stability. *Development*, *133*(16), 3213–3222. https://doi.org/10.1242/dev.02481

Lê Cao, K.-A., Boitard, S., & Besse, P. (2011). Sparse PLS discriminant analysis: Biologically relevant feature selection and graphical displays for multiclass problems. *BMC Bioinformatics*, *12*(1), 253. https://doi.org/10.1186/1471-2105-12-253

Lei, Z., Huhman, D. V., & Sumner, L. W. (2011). Mass Spectrometry Strategies in Metabolomics. *The Journal of Biological Chemistry*, *286*(29), 25435–25442. https://doi.org/10.1074/jbc.R111.238691

Li, R., Sun, R., Hicks, G. R., & Raikhel, N. V. (2015). Arabidopsis ribosomal proteins control vacuole trafficking and developmental programs through the regulation of lipid metabolism. *Proceedings of the National Academy of Sciences*, *112*(1), E89–E98. https://doi.org/10.1073/pnas.1422656112

Li, T., Zhang, Y., Wang, D., Liu, Y., Dirk, L. M. A., Goodman, J., Downie, A. B., Wang, J., Wang, G., & Zhao, T. (2017). Regulation of Seed Vigor by Manipulation of Raffinose Family Oligosaccharides in Maize and Arabidopsis thaliana. *Molecular Plant*, *10*(12), 1540–1555. https://doi.org/10.1016/j.molp.2017.10.014

Liigand, P., Kaupmees, K., Haav, K., Liigand, J., Leito, I., Girod, M., Antoine, R., & Kruve, A. (2017). Think Negative: Finding the Best Electrospray Ionization/MS Mode for Your Analyte. *Analytical Chemistry*, *89*(11), 5665–5668. https://doi.org/10.1021/acs.analchem.7b00096

Lim, E.-K., Ashford, D. A., Hou, B., Jackson, R. G., & Bowles, D. J. (2004). Arabidopsis glycosyltransferases as biocatalysts in fermentation for regioselective synthesis of diverse quercetin glucosides. *Biotechnology and Bioengineering*, *87*(5), 623–631. https://doi.org/10.1002/bit.20154

Liu, L., Li, C., Teo, Z. W. N., Zhang, B., & Yu, H. (2019). The MCTP-SNARE Complex Regulates Florigen Transport in Arabidopsis. *The Plant Cell*, *31*(10), 2475–2490. https://doi.org/10.1105/tpc.18.00960

Liu, L., Liu, C., Hou, X., Xi, W., Shen, L., Tao, Z., Wang, Y., & Yu, H. (2012). FTIP1 Is an Essential Regulator Required for Florigen Transport. *PLOS Biology*, *10*(4), e1001313. https://doi.org/10.1371/journal.pbio.1001313

Liu, L., Zhang, Y., & Yu, H. (2020). Florigen trafficking integrates photoperiod and temperature signals in Arabidopsis. *Journal of Integrative Plant Biology*, *62*(9), 1385–1398. https://doi.org/10.1111/jipb.13000

Liu, L., Zhu, Y., Shen, L., & Yu, H. (2013). Emerging insights into florigen transport. *Current Opinion in Plant Biology*, *16*(5), 607–613. https://doi.org/10.1016/j.pbi.2013.06.001

Liu, T. L., Newton, L., Liu, M.-J., Shiu, S.-H., & Farré, E. M. (2016). A G-Box-Like Motif Is Necessary for Transcriptional Regulation by Circadian Pseudo-Response Regulators in Arabidopsis. *Plant Physiology*, *170*(1), 528–539. https://doi.org/10.1104/pp.15.01562

Livak, K. J., & Schmittgen, T. D. (2001). Analysis of Relative Gene Expression Data Using Real-Time Quantitative PCR and the 2−ΔΔCT Method. *Methods*, *25*(4), 402–408. https://doi.org/10.1006/meth.2001.1262

Love, M. I., Huber, W., & Anders, S. (2014). Moderated estimation of fold change and dispersion for RNA-seq data with DESeq2. *Genome Biology*, *15*(12), 550. https://doi.org/10.1186/s13059-014-0550-8

Lunn, J. E., Feil, R., Hendriks, J. H. M., Gibon, Y., Morcuende, R., Osuna, D., Scheible, W.-R., Carillo, P., Hajirezaei, M.-R., & Stitt, M. (2006). Sugar-induced increases in trehalose 6-phosphate are correlated with redox activation of ADPglucose

pyrophosphorylase and higher rates of starch synthesis in Arabidopsis thaliana. *Biochemical Journal*, *397*(1), 139–148. https://doi.org/10.1042/BJ20060083

Macabuhay, A., Arsova, B., Walker, R., Johnson, A., Watt, M., & Roessner, U. (2022). Modulators or facilitators? Roles of lipids in plant root–microbe interactions. *Trends in Plant Science*, *27*(2), 180–190. https://doi.org/10.1016/j.tplants.2021.08.004

Mahieu, N. G., & Patti, G. J. (2017). Systems-Level Annotation of a Metabolomics Data Set Reduces 25 000 Features to Fewer than 1000 Unique Metabolites. *Analytical Chemistry*, *89*(19), 10397–10406. https://doi.org/10.1021/acs.analchem.7b02380

Maniatis, T., & Fritsch, E. F. (1982). *andJ. Sambrook. 1982. Molecular cloning: A laboratory manual*. Cold Spring Harbor Laboratory, Cold Spring Harbor, NY.

Markham, J. E., & Jaworski, J. G. (2007). Rapid measurement of sphingolipids from Arabidopsis thaliana by reversed-phase high-performance liquid chromatography coupled to electrospray ionization tandem mass spectrometry. *Rapid Communications in Mass Spectrometry*, *21*(7), 1304–1314. https://doi.org/10.1002/rcm.2962

Martínez, I. P. (n.d.). *Estudio del posible papel de la señalización del ABA mediando el control de la floración y la inflorescencia por TERMINAL FLOWER 1*. 114.

Mateos, J. L., Madrigal, P., Tsuda, K., Rawat, V., Richter, R., Romera-Branchat, M., Fornara, F., Schneeberger, K., Krajewski, P., & Coupland, G. (2015). Combinatorial activities of SHORT VEGETATIVE PHASE and FLOWERING LOCUS C define distinct modes of flowering regulation in Arabidopsis. *Genome Biology*, *16*(1), 1–23.

McCourt, P., & Desveaux, D. (2010). Plant chemical genetics. *New Phytologist*, *185*(1), 15–26. https://doi.org/10.1111/j.1469-8137.2009.03045.x

McGarry, R. C., & Ayre, B. G. (2012). Manipulating plant architecture with members of the CETS gene family. *Plant Science*, *188–189*, 71–81. https://doi.org/10.1016/j.plantsci.2012.03.002

Melo, G. A., Abreu, I. N., de Oliveira, M. B., Budzinski, I. G. F., Silva, L. V., Pimenta, M. A. S., & Moritz, T. (2021). A metabolomic study of *Gomphrena agrestis* in Brazilian Cerrado suggests drought-adaptive strategies on metabolism. *Scientific Reports*, *11*, 12933. https://doi.org/10.1038/s41598-021-92449-9

Michaels, S. D., & Amasino, R. M. (1999). The gibberellic acid biosynthesis mutant ga1-3 of Arabidopsis thaliana is responsive to vernalization. *Developmental Genetics*, *25*(3), 194–198. https://doi.org/10.1002/(SICI)1520-6408(1999)25:3<194::AID-DVG2>3.0.CO;2-2

Miki, D., Zinta, G., Zhang, W., Peng, F., Feng, Z., & Zhu, J.-K. (2021). CRISPR/Cas9-Based Genome Editing Toolbox for Arabidopsis thaliana. In J. J. Sanchez-Serrano & J. Salinas (Eds.), *Arabidopsis Protocols* (pp. 121–146). Springer US. https://doi.org/10.1007/978-1-0716-0880-7_5

Mishina, T. E., & Zeier, J. (2006). The Arabidopsis Flavin-Dependent Monooxygenase FMO1 Is an Essential Component of Biologically Induced Systemic Acquired Resistance. *Plant Physiology*, *141*(4), 1666–1675. https://doi.org/10.1104/pp.106.081257

Moon, J., Suh, S.-S., Lee, H., Choi, K.-R., Hong, C. B., Paek, N.-C., Kim, S.-G., & Lee, I. (2003). The *SOC1* MADS-box gene integrates vernalization and gibberellin signals for flowering in Arabidopsis. *The Plant Journal*, *35*(5), 613–623. https://doi.org/10.1046/j.1365-313X.2003.01833.x

Moulin, M., Deleu, C., Larher, F., & Bouchereau, A. (2006). The lysine-ketoglutarate reductase–saccharopine dehydrogenase is involved in the osmo-induced synthesis

of pipecolic acid in rapeseed leaf tissues. *Plant Physiology and Biochemistry*, *44*(7), 474–482. https://doi.org/10.1016/j.plaphy.2006.08.005

Mutasa-Göttgens, E., & Hedden, P. (2009). Gibberellin as a factor in floral regulatory networks. *Journal of Experimental Botany*, *60*(7), 1979–1989. https://doi.org/10.1093/jxb/erp040

Myrold, D. D., & Nannipieri, P. (2013). *File: Omics in Soil Science 1P 10Classical Techniques Versus Omics Approaches*.

Nagel, D. H., Doherty, C. J., Pruneda-Paz, J. L., Schmitz, R. J., Ecker, J. R., & Kay, S. A. (2015). Genome-wide identification of CCA1 targets uncovers an expanded clock network in Arabidopsis. *Proceedings of the National Academy of Sciences*, *112*(34), E4802–E4810. https://doi.org/10.1073/pnas.1513609112

Nakamichi, N., Kiba, T., Henriques, R., Mizuno, T., Chua, N.-H., & Sakakibara, H. (2010). PSEUDO-RESPONSE REGULATORS 9, 7, and 5 Are Transcriptional Repressors in the Arabidopsis Circadian Clock. *The Plant Cell*, *22*(3), 594–605. https://doi.org/10.1105/tpc.109.072892

Nakamichi, N., Kiba, T., Kamioka, M., Suzuki, T., Yamashino, T., Higashiyama, T., Sakakibara, H., & Mizuno, T. (2012). Transcriptional repressor PRR5 directly regulates clock-output pathways. *Proceedings of the National Academy of Sciences*, *109*(42), 17123–17128. https://doi.org/10.1073/pnas.1205156109

Nakamura, Y., Andrés, F., Kanehara, K., Liu, Y., Dörmann, P., & Coupland, G. (2014). Arabidopsis florigen FT binds to diurnally oscillating phospholipids that accelerate flowering. *Nature Communications*, *5*(1), 1–7.

Nakamura, Y., Lin, Y.-C., Watanabe, S., Liu, Y., Katsuyama, K., Kanehara, K., & Inaba, K. (2019). High-resolution crystal structure of Arabidopsis FLOWERING

LOCUS T illuminates its phospholipid-binding site in flowering. *IScience*, *21*, 577–586.

Narasimhan, R., Wang, G., Li, M., Roth, M., Welti, R., & Wang, X. (2013). Differential changes in galactolipid and phospholipid species in soybean leaves and roots under nitrogen deficiency and after nodulation. *Phytochemistry*, *96*, 81–91. https://doi.org/10.1016/j.phytochem.2013.09.026

Naumoff, D. G. (2004). Phylogenetic Analysis of α-Galactosidases of the GH27 Family. *Molecular Biology*, *38*(3), 388–400. https://doi.org/10.1023/B:MBIL.0000032210.97006.de

Návarová, H., Bernsdorff, F., Döring, A.-C., & Zeier, J. (2012). Pipecolic acid, an endogenous mediator of defense amplification and priming, is a critical regulator of inducible plant immunity. *The Plant Cell*, *24*(12), 5123–5141. https://doi.org/10.1105/tpc.112.103564

Nilsson, O., Lee, I., Blázquez, M. A., & Weigel, D. (1998). Flowering-Time Genes Modulate the Response to LEAFY Activity. *Genetics*, *150*(1), 403–410. https://doi.org/10.1093/genetics/150.1.403

Nishizawa, A., Yabuta, Y., & Shigeoka, S. (2008). Galactinol and Raffinose Constitute a Novel Function to Protect Plants from Oxidative Damage. *Plant Physiology*, *147*(3), 1251–1263. https://doi.org/10.1104/pp.108.122465

Nordborg, M., & Weigel, D. (2008). Next-generation genetics in plants. *Nature*, *456*(7223), 720–723. https://doi.org/10.1038/nature07629

Nowak, M. A., Boerlijst, M. C., Cooke, J., & Smith, J. M. (1997). Evolution of genetic redundancy. *Nature*, *388*(6638), 167–171. https://doi.org/10.1038/40618

Ohara, T., Hearn, T. J., Webb, A. A. R., & Satake, A. (2018). Gene regulatory network models in response to sugars in the plant circadian system. *Journal of Theoretical Biology*, *457*, 137–151. https://doi.org/10.1016/j.jtbi.2018.08.020

Okamoto, M., Kuwahara, A., Seo, M., Kushiro, T., Asami, T., Hirai, N., Kamiya, Y., Koshiba, T., & Nambara, E. (2006). CYP707A1 and CYP707A2, Which Encode Abscisic Acid 8′-Hydroxylases, Are Indispensable for Proper Control of Seed Dormancy and Germination in Arabidopsis. *Plant Physiology*, *141*(1), 97–107. https://doi.org/10.1104/pp.106.079475

Olas, J. J., Apelt, F., Watanabe, M., Hoefgen, R., & Wahl, V. (2021). Developmental stage-specific metabolite signatures in *Arabidopsis thaliana* under optimal and mild nitrogen limitation. *Plant Science*, *303*, 110746. https://doi.org/10.1016/j.plantsci.2020.110746

Ortiz-Marchena, M. I., Albi, T., Lucas-Reina, E., Said, F. E., Romero-Campero, F. J., Cano, B., Ruiz, M. T., Romero, J. M., & Valverde, F. (2014). Photoperiodic Control of Carbon Distribution during the Floral Transition in Arabidopsis. *The Plant Cell*, *26*(2), 565–584. https://doi.org/10.1105/tpc.114.122721

Ortiz-Marchena, M. I., Romero, J. M., & Valverde, F. (2015). Photoperiodic control of sugar release during the floral transition: What is the role of sugars in the florigenic signal? *Plant Signaling & Behavior*, *10*(5), e1017168.

Pang, Z., Chong, J., Zhou, G., de Lima Morais, D. A., Chang, L., Barrette, M., Gauthier, C., Jacques, P.-É., Li, S., & Xia, J. (2021). MetaboAnalyst 5.0: Narrowing the gap between raw spectra and functional insights. *Nucleic Acids Research*, *49*(W1), W388–W396.

Panikulangara, T. J., Eggers-Schumacher, G., Wunderlich, M., Stransky, H., & Schöffl, F. (2004). *GALACTINOL SYNTHASE1*. A Novel Heat Shock Factor Target Gene

Responsible for Heat-Induced Synthesis of Raffinose Family Oligosaccharides in Arabidopsis. *Plant Physiology*, *136*(2), 3148–3158. https://doi.org/10.1104/pp.104.042606

Parcy, F. (2005). Flowering: A time for integration. *The International Journal of Developmental Biology*, *49*(5–6), 585–593. https://doi.org/10.1387/ijdb.041930fp

Park, J.-E., Park, J.-Y., Kim, Y.-S., Staswick, P. E., Jeon, J., Yun, J., Kim, S.-Y., Kim, J., Lee, Y.-H., & Park, C.-M. (2007). GH3-mediated Auxin Homeostasis Links Growth Regulation with Stress Adaptation Response in Arabidopsis*. *Journal of Biological Chemistry*, *282*(13), 10036–10046. https://doi.org/10.1074/jbc.M610524200

Patel, M., Pandey, S., Kumar, M., Haque, M., Pal, S., & Yadav, N. (2021). Plants Metabolome Study: Emerging Tools and Techniques. *Plants*, *10*(11), 2409. https://doi.org/10.3390/plants10112409

Patro, R., Duggal, G., Love, M. I., Irizarry, R. A., & Kingsford, C. (2017). Salmon provides fast and bias-aware quantification of transcript expression. *Nature Methods*, *14*(4), 417–419. https://doi.org/10.1038/nmeth.4197

Paul, M. J., Primavesi, L. F., Jhurreea, D., & Zhang, Y. (2008). Trehalose Metabolism and Signaling. *Annual Review of Plant Biology*, *59*(1), 417–441. https://doi.org/10.1146/annurev.arplant.59.032607.092945

Peng, Y., Zou, T., Li, L., Tang, S., Li, Q., Zhang, J., Chen, Y., Wang, X., Yang, G., & Hu, Y. (2019). Map-Based Cloning and Functional Analysis of YE1 in Rice, Which Is Involved in Light-Dependent Chlorophyll Biogenesis and Photoperiodic Flowering Pathway. *International Journal of Molecular Sciences*, *20*(3), 758. https://doi.org/10.3390/ijms20030758

Périlleux, C., Bouché, F., Randoux, M., & Orman-Ligeza, B. (2019). Turning Meristems into Fortresses. *Trends in Plant Science*, *24*(5), 431–442. https://doi.org/10.1016/j.tplants.2019.02.004

Peters, S., Egert, A., Stieger, B., & Keller, F. (2010). Functional identification of Arabidopsis *ATSIP2* (At3g57520) as an alkaline α-galactosidase with a substrate specificity for raffinose and an apparent sink-specific expression pattern. *Plant and Cell Physiology*, *51*(10), 1815–1819. https://doi.org/10.1093/pcp/pcq127

Pfeiffer, A., Janocha, D., Dong, Y., Medzihradszky, A., Schöne, S., Daum, G., Suzaki, T., Forner, J., Langenecker, T., Rempel, E., Schmid, M., Wirtz, M., Hell, R., & Lohmann, J. U. (2016). Integration of light and metabolic signals for stem cell activation at the shoot apical meristem. *ELife*, *5*, e17023. https://doi.org/10.7554/eLife.17023

Pieterse, C. M. J., Leon-Reyes, A., Does, D. V. D., Verhage, A., Koornneef, A., Pelt, J. A. V., & Wees, S. C. M. V. (2009). Networking by small-molecules hormones in plant immunity. *Nature Chem. Biol.*, 308–316.

Pigliucci, M. (2002). Ecology and Evolutionary Biology of Arabidopsis. *The Arabidopsis Book / American Society of Plant Biologists*, *1*, e0003. https://doi.org/10.1199/tab.0003

Pin, P. A., & Nilsson, O. (2012). The multifaceted roles of FLOWERING LOCUS T in plant development. *Plant, Cell & Environment*, *35*(10), 1742–1755. https://doi.org/10.1111/j.1365-3040.2012.02558.x

Plackett, A. R. G., Powers, S. J., Fernandez-Garcia, N., Urbanova, T., Takebayashi, Y., Seo, M., Jikumaru, Y., Benlloch, R., Nilsson, O., Ruiz-Rivero, O., Phillips, A. L., Wilson, Z. A., Thomas, S. G., & Hedden, P. (2012). Analysis of the Developmental Roles of the Arabidopsis Gibberellin 20-Oxidases Demonstrates

That GA20ox1, -2, and -3 Are the Dominant Paralogs. *The Plant Cell*, *24*(3), 941–960. https://doi.org/10.1105/tpc.111.095109

Ponnu, J., Schlereth, A., Zacharaki, V., Działo, M. A., Abel, C., Feil, R., Schmid, M., & Wahl, V. (2020). The trehalose 6-phosphate pathway impacts vegetative phase change in Arabidopsis thaliana. *The Plant Journal*, *104*(3), 768–780. https://doi.org/10.1111/tpj.14965

Porco, S., Pěnčík, A., Rashed, A., Voß, U., Casanova-Sáez, R., Bishopp, A., Golebiowska, A., Bhosale, R., Swarup, R., Swarup, K., Peňáková, P., Novák, O., Staswick, P., Hedden, P., Phillips, A. L., Vissenberg, K., Bennett, M. J., & Ljung, K. (2016). Dioxygenase-encoding AtDAO1 gene controls IAA oxidation and homeostasis in Arabidopsis. *Proceedings of the National Academy of Sciences*, *113*(39), 11016–11021. https://doi.org/10.1073/pnas.1604375113

Praena, J., van Veen, E., Henriques, R., & Benlloch, R. (2022). Assessing Flowering Time Under Different Photoperiods. *Methods in Molecular Biology (Clifton, N.J.)*, *2494*, 101–115. https://doi.org/10.1007/978-1-0716-2297-1_7

Putterill, J., Robson, F., Lee, K., Simon, R., & Coupland, G. (1995). The CONSTANS gene of arabidopsis promotes flowering and encodes a protein showing similarities to zinc finger transcription factors. *Cell*, *80*(6), 847–857. https://doi.org/10.1016/0092-8674(95)90288-0

Putterill, J., & Varkonyi-Gasic, E. (2016). FT and florigen long-distance flowering control in plants. *Current Opinion in Plant Biology*, *33*, 77–82. https://doi.org/10.1016/j.pbi.2016.06.008

Ralston-Hooper, K., Hopf, A., Oh, C., Zhang, X., Adamec, J., & Sepúlveda, M. S. (2008). Development of GCxGC/TOF-MS metabolomics for use in ecotoxicological

studies with invertebrates. *Aquatic Toxicology*, *88*(1), 48–52. https://doi.org/10.1016/j.aquatox.2008.03.002

Razzaq, A., Sadia, B., Raza, A., Khalid Hameed, M., & Saleem, F. (2019). Metabolomics: A Way Forward for Crop Improvement. *Metabolites*, *9*(12), 303. https://doi.org/10.3390/metabo9120303

Riboni, M., Galbiati, M., Tonelli, C., & Conti, L. (2013). GIGANTEA Enables Drought Escape Response via Abscisic Acid-Dependent Activation of the Florigens and SUPPRESSOR OF OVEREXPRESSION OF CONSTANS1. *Plant Physiology*, *162*(3), 1706–1719. https://doi.org/10.1104/pp.113.217729

Riboni, M., Robustelli Test, A., Galbiati, M., Tonelli, C., & Conti, L. (2016). ABA-dependent control of *GIGANTEA* signalling enables drought escape via up-regulation of *FLOWERING LOCUS T* in *Arabidopsis thaliana*. *Journal of Experimental Botany*, *67*(22), 6309–6322. https://doi.org/10.1093/jxb/erw384

Rieu, I., Eriksson, S., Powers, S. J., Gong, F., Griffiths, J., Woolley, L., Benlloch, R., Nilsson, O., Thomas, S. G., Hedden, P., & Phillips, A. L. (2008). Genetic Analysis Reveals That C19-GA 2-Oxidation Is a Major Gibberellin Inactivation Pathway in Arabidopsis. *The Plant Cell*, *20*(9), 2420–2436. https://doi.org/10.1105/tpc.108.058818

Rigal, A., Ma, Q., & Robert, S. (2014). Unraveling plant hormone signaling through the use of small molecules. *Frontiers in Plant Science*, *5*, 373. https://doi.org/10.3389/fpls.2014.00373

Robert, S., Chary, S. N., Drakakaki, G., Li, S., Yang, Z., Raikhel, N. V., & Hicks, G. R. (2008). Endosidin1 defines a compartment involved in endocytosis of the brassinosteroid receptor BRI1 and the auxin transporters PIN2 and AUX1.

Proceedings of the National Academy of Sciences, *105*(24), 8464–8469. https://doi.org/10.1073/pnas.0711650105

Robert, S., Raikhel, N. V., & Hicks, G. R. (2009). Powerful Partners: Arabidopsis and Chemical Genomics. *The Arabidopsis Book / American Society of Plant Biologists*, *7*, e0109. https://doi.org/10.1199/tab.0109

Roberts, L. D., Souza, A. L., Gerszten, R. E., & Clish, C. B. (2012). Targeted Metabolomics. *Current Protocols in Molecular Biology*, *98*(1), 30.2.1-30.2.24. https://doi.org/10.1002/0471142727.mb3002s98

Romera-Branchat, M., Andrés, F., & Coupland, G. (2014). Flowering responses to seasonal cues: What's new? *Current Opinion in Plant Biology*, *21*, 120–127. https://doi.org/10.1016/j.pbi.2014.07.006

Ruijter, N. C. A., Verhees, J., Leeuwen, W., & Krol, A. R. (2003). Evaluation and Comparison of the *GUS*, *LUC* and *GFP* Reporter System for Gene Expression Studies in Plants. *Plant Biology*, *5*(2), 103–115. https://doi.org/10.1055/s-2003-40722

Rupasinghe, T. W. T., & Roessner, U. (2018). Extraction of Plant Lipids for LC-MS-Based Untargeted Plant Lipidomics. In C. António (Ed.), *Plant Metabolomics: Methods and Protocols* (pp. 125–135). Springer. https://doi.org/10.1007/978-1-4939-7819-9_9

Salvi, P., Kamble, N. U., & Majee, M. (2020). Ectopic over-expression of ABA-responsive Chickpea *GALACTINOL SYNTHASE* (Ca*GOLS*) gene results in improved tolerance to dehydration stress by modulating ROS scavenging. *Environmental and Experimental Botany*, *171*, 103957. https://doi.org/10.1016/j.envexpbot.2019.103957

Samach, A., Onouchi, H., Gold, S. E., Ditta, G. S., Schwarz-Sommer, Z., Yanofsky, M. F., & Coupland, G. (2000). Distinct Roles of CONSTANS Target Genes in Reproductive Development of *Arabidopsis*. *Science*, *288*(5471), 1613–1616. https://doi.org/10.1126/science.288.5471.1613

Santner, A., Calderon-Villalobos, L. I. A., & Estelle, M. (2009). Plant hormones are versatile chemical regulators of plant growth. *Nature Chemical Biology*, *5*(5), 301–307. https://doi.org/10.1038/nchembio.165

Sauer, M., Robert, S., & Kleine-Vehn, J. (2013). Auxin: Simply complicated. *Journal of Experimental Botany*, *64*(9), 2565–2577. https://doi.org/10.1093/jxb/ert139

Sawa, M., & Kay, S. A. (2011). GIGANTEA directly activates *FLOWERING LOCUS T* in *Arabidopsis thaliana*. *Proceedings of the National Academy of Sciences*, *108*(28), 11698–11703. https://doi.org/10.1073/pnas.1106771108

Schauer, N., Steinhauser, D., Strelkov, S., Schomburg, D., Allison, G., Moritz, T., Lundgren, K., Roessner-Tunali, U., Forbes, M. G., Willmitzer, L., Fernie, A. R., & Kopka, J. (2005). GC–MS libraries for the rapid identification of metabolites in complex biological samples. *FEBS Letters*, *579*(6), 1332–1337. https://doi.org/10.1016/j.febslet.2005.01.029

Selvaraj, M. G., Ishizaki, T., Valencia, M., Ogawa, S., Dedicova, B., Ogata, T., Yoshiwara, K., Maruyama, K., Kusano, M., Saito, K., Takahashi, F., Shinozaki, K., Nakashima, K., & Ishitani, M. (2017). Overexpression of an *Arabidopsis thaliana GALACTINOL SYNTHASE* gene improves drought tolerance in transgenic rice and increased grain yield in the field. *Plant Biotechnology Journal*, *15*(11), 1465–1477. https://doi.org/10.1111/pbi.12731

Sengupta, S., Mukherjee, S., Basak, P., & Majumder, A. L. (2015). Significance of galactinol and raffinose family oligosaccharide synthesis in plants. *Frontiers in Plant Science*, *6*, 656. https://doi.org/10.3389/fpls.2015.00656

Sengupta, S., Mukherjee, S., Parween, S., & Majumder, A. L. (2012). Galactinol synthase across evolutionary diverse taxa: Functional preference for higher plants? *FEBS Letters*, *586*(10), 1488–1496. https://doi.org/10.1016/j.febslet.2012.04.003

Serrano, M., Kombrink, E., & Meesters, C. (2015). Considerations for designing chemical screening strategies in plant biology. *Frontiers in Plant Science*, *6*. https://doi.org/10.3389/fpls.2015.00131

Sharma, V., Gupta, P., Priscilla, K., SharanKumar, Hangargi, B., Veershetty, A., Ramrao, D. P., Suresh, S., Narasanna, R., Naik, G. R., Kumar, A., Guo, B., Zhuang, W., Varshney, R. K., Pandey, M. K., & Kumar, R. (2021). Metabolomics Intervention Towards Better Understanding of Plant Traits. *Cells*, *10*(2), 346. https://doi.org/10.3390/cells10020346

Shu, K., Chen, Q., Wu, Y., Liu, R., Zhang, H., Wang, S., Tang, S., Yang, W., & Xie, Q. (2016). ABSCISIC ACID-INSENSITIVE 4 negatively regulates flowering through directly promoting Arabidopsis *FLOWERING LOCUS C* transcription. *Journal of Experimental Botany*, *67*(1), 195–205. https://doi.org/10.1093/jxb/erv459

Shu, K., Luo, X., Meng, Y., & Yang, W. (2018). Toward a Molecular Understanding of Abscisic Acid Actions in Floral Transition. *Plant and Cell Physiology*, *59*(2), 215–221. https://doi.org/10.1093/pcp/pcy007

Shu, K., Zhou, W., Chen, F., Luo, X., & Yang, W. (2018). Abscisic Acid and Gibberellins Antagonistically Mediate Plant Development and Abiotic Stress Responses.

Frontiers in Plant Science, *9*. https://www.frontiersin.org/article/10.3389/fpls.2018.00416

Silvestre Vañó, M. (2020). *Identificación de dianas e interactores de TFL1, un regulador clave en la floración y la arquitectura de la inflorescencia*. https://roderic.uv.es/handle/10550/77996

Simon, R., Igeño, M. I., & Coupland, G. (1996). Activation of floral meristem identity genes in Arabidopsis. *Nature*, *384*(6604), 59–62. https://doi.org/10.1038/384059a0

Soneson, C., Love, M. I., & Robinson, M. D. (2015). Differential analyses for RNA-seq: Transcript-level estimates improve gene-level inferences. *F1000Research*, *4*, 1521. https://doi.org/10.12688/f1000research.7563.2

Song, J. T., Lu, H., & Greenberg, J. T. (2004). Divergent Roles in Arabidopsis thaliana Development and Defense of Two Homologous Genes, *ABERRANT GROWTH AND DEATH2* and *AGD2-LIKE DEFENSE RESPONSE PROTEIN1*, Encoding Novel Aminotransferases. *The Plant Cell*, *16*(2), 353–366. https://doi.org/10.1105/tpc.019372

Song, Y. H., Estrada, D. A., Johnson, R. S., Kim, S. K., Lee, S. Y., MacCoss, M. J., & Imaizumi, T. (2014). Distinct roles of FKF1, GIGANTEA, and ZEITLUPE proteins in the regulation of CONSTANS stability in Arabidopsis photoperiodic flowering. *Proceedings of the National Academy of Sciences*, *111*(49), 17672–17677. https://doi.org/10.1073/pnas.1415375111

Song, Y. H., Ito, S., & Imaizumi, T. (2013). Flowering time regulation: Photoperiod- and temperature-sensing in leaves. *Trends in Plant Science*, *18*(10), 575–583. https://doi.org/10.1016/j.tplants.2013.05.003

Song, Y. H., Kubota, A., Kwon, M. S., Covington, M. F., Lee, N., Taagen, E. R., Laboy Cintrón, D., Hwang, D. Y., Akiyama, R., Hodge, S. K., Huang, H., Nguyen, N. H., Nusinow, D. A., Millar, A. J., Shimizu, K. K., & Imaizumi, T. (2018). Molecular basis of flowering under natural long-day conditions in Arabidopsis. *Nature Plants*, *4*(10), 824–835. https://doi.org/10.1038/s41477-018-0253-3

Song, Y. H., Smith, R. W., To, B. J., Millar, A. J., & Imaizumi, T. (2012). FKF1 Conveys Timing Information for CONSTANS Stabilization in Photoperiodic Flowering. *Science*, *336*(6084), 1045–1049. https://doi.org/10.1126/science.1219644

Spoel, S. H., & Dong, X. (2012). How do plants achieve immunity? Defence without specialized immune cells. *Nature Reviews Immunology*, *12*(2), 89–100. https://doi.org/10.1038/nri3141

Srikanth, A., & Schmid, M. (2011). Regulation of flowering time: All roads lead to Rome. *Cellular and Molecular Life Sciences*, *68*(12), 2013–2037.

Stokes, M. E., & McCourt, P. (2014). Towards personalized agriculture: What chemical genomics can bring to plant biotechnology. *Frontiers in Plant Science*, *5*. https://www.frontiersin.org/article/10.3389/fpls.2014.00344

Suárez-López, P., Wheatley, K., Robson, F., Onouchi, H., Valverde, F., & Coupland, G. (2001). CONSTANS mediates between the circadian clock and the control of flowering in Arabidopsis. *Nature*, *410*(6832), 1116–1120.

Subramanian, A., Tamayo, P., Mootha, V. K., Mukherjee, S., Ebert, B. L., Gillette, M. A., Paulovich, A., Pomeroy, S. L., Golub, T. R., Lander, E. S., & Mesirov, J. P. (2005). Gene set enrichment analysis: A knowledge-based approach for interpreting genome-wide expression profiles. *Proceedings of the National Academy of Sciences*, *102*(43), 15545–15550. https://doi.org/10.1073/pnas.0506580102

Sui, X., Meng, F., Wang, H., Wei, Y., Li, R., Wang, Z., Hu, L., Wang, S., & Zhang, Z. (2012). Molecular cloning, characteristics and low temperature response of raffinose synthase gene in *Cucumis sativus* L. *Journal of Plant Physiology*, *169*(18), 1883–1891. https://doi.org/10.1016/j.jplph.2012.07.019

Sumner, L. W., Mendes, P., & Dixon, R. A. (2003). Plant metabolomics: Large-scale phytochemistry in the functional genomics era. *Phytochemistry*, *62*(6), 817–836. https://doi.org/10.1016/S0031-9422(02)00708-2

Sun, T., & Zhang, Y. (2021). Short- and long-distance signaling in plant defense. *The Plant Journal*, *105*(2), 505–517. https://doi.org/10.1111/tpj.15068

Sun, Z., Qi, X., Wang, Z., Li, P., Wu, C., Zhang, H., & Zhao, Y. (2013). Overexpression of Ts*GOLS2*, a galactinol synthase, in *Arabidopsis thaliana* enhances tolerance to high salinity and osmotic stresses. *Plant Physiology and Biochemistry*, *69*, 82–89. https://doi.org/10.1016/j.plaphy.2013.04.009

Sundaresan, V., Springer, P., Volpe, T., Haward, S., Jones, J. D., Dean, C., Ma, H., & Martienssen, R. (1995). Patterns of gene action in plant development revealed by enhancer trap and gene trap transposable elements. *Genes & Development*, *9*(14), 1797–1810. https://doi.org/10.1101/gad.9.14.1797

Susila, H., Jurić, S., Liu, L., Gawarecka, K., Chung, K. S., Jin, S., Kim, S.-J., Nasim, Z., Youn, G., Suh, M. C., Yu, H., & Ahn, J. H. (2021). Florigen sequestration in cellular membranes modulates temperature-responsive flowering. *Science*, *373*(6559), 1137–1142. https://doi.org/10.1126/science.abh4054

Susila, H., Nasim, Z., & Ahn, J. H. (2018). Ambient Temperature-Responsive Mechanisms Coordinate Regulation of Flowering Time. *International Journal of Molecular Sciences*, *19*(10), 3196. https://doi.org/10.3390/ijms19103196

Taji, T., Ohsumi, C., Iuchi, S., Seki, M., Kasuga, M., Kobayashi, M., Yamaguchi-Shinozaki, K., & Shinozaki, K. (2002). Important roles of drought- and cold-inducible genes for galactinol synthase in stress tolerance in Arabidopsis thaliana. *The Plant Journal*, *29*(4), 417–426. https://doi.org/10.1046/j.0960-7412.2001.01227.x

Takada, S., & Goto, K. (2003). TERMINAL FLOWER2, an Arabidopsis Homolog of HETEROCHROMATIN PROTEIN1, Counteracts the Activation of *FLOWERING LOCUS T* by CONSTANS in the Vascular Tissues of Leaves to Regulate Flowering Time. *The Plant Cell*, *15*(12), 2856–2865. https://doi.org/10.1105/tpc.016345

Takimoto, A., Kaihara, S., Hirai, N., Koshimizu, K., Hosoi, Y., Oda, Y., Sakakibara, N., & Nagakura, A. (1989). Flower-Inducing Activity of Water Extract of Lemna. *Plant and Cell Physiology*, *30*(7), 1017–1021. https://doi.org/10.1093/oxfordjournals.pcp.a077831

Taoka, K., Ohki, I., Tsuji, H., Furuita, K., Hayashi, K., Yanase, T., Yamaguchi, M., Nakashima, C., Purwestri, Y. A., Tamaki, S., Ogaki, Y., Shimada, C., Nakagawa, A., Kojima, C., & Shimamoto, K. (2011). 14-3-3 proteins act as intracellular receptors for rice Hd3a florigen. *Nature*, *476*(7360), 332–335. https://doi.org/10.1038/nature10272

Tessadori, F., Schulkes, R. K., Driel, R. van, & Fransz, P. (2007). Light-regulated large-scale reorganization of chromatin during the floral transition in Arabidopsis. *The Plant Journal*, *50*(5), 848–857. https://doi.org/10.1111/j.1365-313X.2007.03093.x

The Arabidopsis Genome Initiative. (2000). Analysis of the genome sequence of the flowering plant Arabidopsis thaliana. *Nature*, *408*(6814), 796–815. https://doi.org/10.1038/35048692

Thomas, B. (2006). Light signals and flowering. *Journal of Experimental Botany*, *57*(13), 3387–3393. https://doi.org/10.1093/jxb/erl071

Tóth, R., & Van der Hoorn, R. A. (2010). Emerging principles in plant chemical genetics. *Trends in Plant Science*, *15*(2), 81–88.

Toubiana, D., Sade, N., Liu, L., Rubio Wilhelmi, M. del M., Brotman, Y., Luzarowska, U., Vogel, J. P., & Blumwald, E. (2020). Correlation-based network analysis combined with machine learning techniques highlight the role of the GABA shunt in *Brachypodium sylvaticum* freezing tolerance. *Scientific Reports*, *10*(1), 4489. https://doi.org/10.1038/s41598-020-61081-4

Trovato, M., Forlani, G., Signorelli, S., & Funck, D. (2019). Proline Metabolism and Its Functions in Development and Stress Tolerance. In M. A. Hossain, V. Kumar, D. J. Burritt, M. Fujita, & P. S. A. Mäkelä (Eds.), *Osmoprotectant-Mediated Abiotic Stress Tolerance in Plants: Recent Advances and Future Perspectives* (pp. 41–72). Springer International Publishing. https://doi.org/10.1007/978-3-030-27423-8_2

Umezawa, T., Okamoto, M., Kushiro, T., Nambara, E., Oono, Y., Seki, M., Kobayashi, M., Koshiba, T., Kamiya, Y., & Shinozaki, K. (2006). CYP707A3, a major ABA 8′-hydroxylase involved in dehydration and rehydration response in *Arabidopsis thaliana*. *The Plant Journal*, *46*(2), 171–182. https://doi.org/10.1111/j.1365-313X.2006.02683.x

Valverde, F., Mouradov, A., Soppe, W., Ravenscroft, D., Samach, A., & Coupland, G. (2004). Photoreceptor regulation of CONSTANS protein in photoperiodic flowering. *Science*, *303*(5660), 1003–1006.

van Meer, G. (2005). Cellular lipidomics. *The EMBO Journal*, *24*(18), 3159–3165. https://doi.org/10.1038/sj.emboj.7600798

Veit, M., & Pauli, G. F. (1999). Major flavonoids from Arabidopsis thaliana leaves. *Journal of Natural Products*, *62*(9), 1301–1303. https://doi.org/10.1021/np990080o

Velten, J., Pogson, B. J., & Cazzonelli, C. I. (2008). *Luciferase as a Reporter of Gene Activity in Plants*. 13.

Verslues, P. E., & Juenger, T. E. (2011). Drought, metabolites, and Arabidopsis natural variation: A promising combination for understanding adaptation to water-limited environments. *Current Opinion in Plant Biology*, *14*(3), 240–245. https://doi.org/10.1016/j.pbi.2011.04.006

Vidershaîn, G. I., & Beîer, E. M. (1976). [Interrelation of alpha-D-fucosidase and alpha-D-galactosidase activities in man and animals]. *Doklady Akademii nauk SSSR*, *231*(2), 486–488.

Vinaixa, M., Samino, S., Saez, I., Duran, J., Guinovart, J. J., & Yanes, O. (2012). A Guideline to Univariate Statistical Analysis for LC/MS-Based Untargeted Metabolomics-Derived Data. *Metabolites*, *2*(4), 775–795. https://doi.org/10.3390/metabo2040775

Vinaixa, M., Schymanski, E. L., Neumann, S., Navarro, M., Salek, R. M., & Yanes, O. (2016). Mass spectral databases for LC/MS- and GC/MS-based metabolomics: State of the field and future prospects. *TrAC Trends in Analytical Chemistry*, *78*, 23–35. https://doi.org/10.1016/j.trac.2015.09.005

Vranova, V., Lojkova, L., Rejsek, K., & Formanek, P. (2013). Significance of the Natural Occurrence of L- Versus D-Pipecolic Acid: A Review. *Chirality*, *25*(12), 823–831. https://doi.org/10.1002/chir.22237

Wahl, V., Ponnu, J., Schlereth, A., Arrivault, S., Langenecker, T., Franke, A., Feil, R., Lunn, J. E., Stitt, M., & Schmid, M. (2013). Regulation of flowering by trehalose-6-phosphate signaling in Arabidopsis thaliana. *Science*, *339*(6120), 704–707.

Wang, D., Liu, H., Wang, H., Zhang, P., & Shi, C. (2020). A novel sucrose transporter gene IbSUT4 involves in plant growth and response to abiotic stress through the ABF-dependent ABA signaling pathway in Sweetpotato. *BMC Plant Biology*, *20*(1), 157. https://doi.org/10.1186/s12870-020-02382-8

Wang, H., Blakeslee, J. J., Jones, M. L., Chapin, L. J., & Dami, I. E. (2020). Exogenous abscisic acid enhances physiological, metabolic, and transcriptional cold acclimation responses in greenhouse-grown grapevines. *Plant Science*, *293*, 110437. https://doi.org/10.1016/j.plantsci.2020.110437

Wang, J.-W. (2014). Regulation of flowering time by the miR156-mediated age pathway. *Journal of Experimental Botany*, *65*(17), 4723–4730. https://doi.org/10.1093/jxb/eru246

Wang, R., Farrona, S., Vincent, C., Joecker, A., Schoof, H., Turck, F., Alonso-Blanco, C., Coupland, G., & Albani, M. C. (2009). PEP1 regulates perennial flowering in *Arabis alpina*. *Nature*, *459*(7245), 423–427.

Wang, Y., Li, L., Ye, T., Lu, Y., Chen, X., & Wu, Y. (2013). The inhibitory effect of ABA on floral transition is mediated by ABI5 in Arabidopsis. *Journal of Experimental Botany*, *64*(2), 675–684.

Weckwerth, W. (2003). Metabolomics in Systems Biology. *Annual Review of Plant Biology*, *54*(1), 669–689. https://doi.org/10.1146/annurev.arplant.54.031902.135014

Weigel, D., & Glazebrook, J. (2009). Quick Miniprep for Plant DNA Isolation. *Cold Spring Harbor Protocols*, *2009*(3), pdb.prot5179. https://doi.org/10.1101/pdb.prot5179

Welti, R. (2007). Plant lipidomics: Discerning biological function by profiling plant complex lipids using mass spectrometry. *Frontiers in Bioscience*, *12*(1), 2494. https://doi.org/10.2741/2250

Wickland, D. P., & Hanzawa, Y. (2015). The F*LOWERING LOCUS T/TERMINAL FLOWER 1* Gene Family: Functional Evolution and Molecular Mechanisms. *Molecular Plant*, *8*(7), 983–997. https://doi.org/10.1016/j.molp.2015.01.007

Wigge, P. A., Kim, M. C., Jaeger, K. E., Busch, W., Schmid, M., Lohmann, J. U., & Weigel, D. (2005). Integration of Spatial and Temporal Information During Floral Induction in Arabidopsis. *Science*, *309*(5737), 1056–1059. https://doi.org/10.1126/science.1114358

Wilson, R. N., Heckman, J. W., & Somerville, C. R. (1992). Gibberellin Is Required for Flowering in Arabidopsis thaliana under Short Days 1. *Plant Physiology*, *100*(1), 403–408. https://doi.org/10.1104/pp.100.1.403

Wingler, A. (2018). Transitioning to the Next Phase: The Role of Sugar Signaling throughout the Plant Life Cycle. *Plant Physiology*, *176*(2), 1075–1084. https://doi.org/10.1104/pp.17.01229

Winkel-Shirley, B. (2002). Biosynthesis of flavonoids and effects of stress. *Current Opinion in Plant Biology*, *5*(3), 218–223. https://doi.org/10.1016/s1369-5266(02)00256-x

Woodward, A. W., & Bartel, B. (2005). Auxin: Regulation, Action, and Interaction. *Annals of Botany*, *95*(5), 707–735. https://doi.org/10.1093/aob/mci083

Woodward, A. W., & Bartel, B. (2018). Biology in Bloom: A Primer on the Arabidopsis thaliana Model System. *Genetics*, *208*(4), 1337–1349. https://doi.org/10.1534/genetics.118.300755

Xia, J., & Wishart, D. S. (2010). MSEA: A web-based tool to identify biologically meaningful patterns in quantitative metabolomic data. *Nucleic Acids Research*, *38*(suppl_2), W71–W77. https://doi.org/10.1093/nar/gkq329

Xiao, J. F., Zhou, B., & Ressom, H. W. (2012). Metabolite identification and quantitation in LC-MS/MS-based metabolomics. *TrAC Trends in Analytical Chemistry*, *32*, 1–14. https://doi.org/10.1016/j.trac.2011.08.009

Yadav, U. P., Ivakov, A., Feil, R., Duan, G. Y., Walther, D., Giavalisco, P., Piques, M., Carillo, P., Hubberten, H.-M., Stitt, M., & Lunn, J. E. (2014). The sucrose–trehalose 6-phosphate (Tre6P) nexus: Specificity and mechanisms of sucrose signalling by Tre6P. *Journal of Experimental Botany*, *65*(4), 1051–1068. https://doi.org/10.1093/jxb/ert457

Yamaguchi, A., Wu, M.-F., Yang, L., Wu, G., Poethig, R. S., & Wagner, D. (2009). The MicroRNA-Regulated SBP-Box Transcription Factor SPL3 Is a Direct Upstream Activator of LEAFY, FRUITFULL, and APETALA1. *Developmental Cell*, *17*(2), 268–278. https://doi.org/10.1016/j.devcel.2009.06.007

Yang, L., Xu, M., Koo, Y., He, J., & Poethig, R. S. (2013). Sugar promotes vegetative phase change in Arabidopsis thaliana by repressing the expression of MIR156A and MIR156C. *ELife*, *2*, e00260. https://doi.org/10.7554/eLife.00260

Yanovsky, M. J., & Kay, S. A. (2002). Molecular basis of seasonal time measurement in Arabidopsis. *Nature*, *419*(6904), 308–312. https://doi.org/10.1038/nature00996

Yildiz, I., Mantz, M., Hartmann, M., Zeier, T., Kessel, J., Thurow, C., Gatz, C., Petzsch, P., Köhrer, K., & Zeier, J. (2021). The mobile SAR signal N-hydroxypipecolic acid induces NPR1-dependent transcriptional reprogramming and immune priming. *Plant Physiology*, *186*(3), 1679–1705. https://doi.org/10.1093/plphys/kiab166

Yildizli, A., Çevik, S., & Ünyayar, S. (2018). Effects of exogenous myo-inositol on leaf water status and oxidative stress of Capsicum annuum under drought stress. *Acta Physiologiae Plantarum*, *40*(6), 122. https://doi.org/10.1007/s11738-018-2690-z

Yonekura-Sakakibara, K., Tohge, T., Niida, R., & Saito, K. (2007). Identification of a Flavonol 7-O-Rhamnosyltransferase Gene Determining Flavonoid Pattern in Arabidopsis by Transcriptome Coexpression Analysis and Reverse Genetics * ♦. *Journal of Biological Chemistry*, *282*(20), 14932–14941. https://doi.org/10.1074/jbc.M611498200

Yoo, S. K., Chung, K. S., Kim, J., Lee, J. H., Hong, S. M., Yoo, S. J., Yoo, S. Y., Lee, J. S., & Ahn, J. H. (2005). CONSTANS Activates *SUPPRESSOR OF OVEREXPRESSION OF CONSTANS 1* through FLOWERING LOCUS T to Promote Flowering in Arabidopsis. *Plant Physiology*, *139*(2), 770–778. https://doi.org/10.1104/pp.105.066928

Yoshida, N., Yanai, Y., Chen, L., Kato, Y., Hiratsuka, J., Miwa, T., Sung, Z. R., & Takahashi, S. (2001). EMBRYONIC FLOWER2, a Novel Polycomb Group Protein Homolog, Mediates Shoot Development and Flowering in Arabidopsis. *The Plant Cell*, *13*(11), 2471–2481. https://doi.org/10.1105/tpc.010227

Yu, S., Cao, L., Zhou, C.-M., Zhang, T.-Q., Lian, H., Sun, Y., Wu, J., Huang, J., Wang, G., & Wang, J.-W. (2013). Sugar is an endogenous cue for juvenile-to-adult phase transition in plants. *ELife*, *2*, e00269. https://doi.org/10.7554/eLife.00269

Zeier, J. (2021). Metabolic regulation of systemic acquired resistance. *Current Opinion in Plant Biology*, *62*, 102050. https://doi.org/10.1016/j.pbi.2021.102050

Zhang, Z., Li, Q., Li, Z., Staswick, P. E., Wang, M., Zhu, Y., & He, Z. (2007). Dual Regulation Role of GH3.5 in Salicylic Acid and Auxin Signaling during Arabidopsis-Pseudomonas syringae Interaction. *Plant Physiology*, *145*(2), 450–464. https://doi.org/10.1104/pp.107.106021

Zheng, Z., Guo, Y., Novák, O., Chen, W., Ljung, K., Noel, J. P., & Chory, J. (2016). Local auxin metabolism regulates environment-induced hypocotyl elongation. *Nature Plants*, *2*(4), 1–9. https://doi.org/10.1038/nplants.2016.25

Zuther, E., Büchel, K., Hundertmark, M., Stitt, M., Hincha, D. K., & Heyer, A. G. (2004). The role of raffinose in the cold acclimation response of *Arabidopsis thaliana*. *Febs Letters*, *576*(1–2), 169–173.

GLOSSARY OF ABBREVIATURES

ABA: Abscisic Acid

Abr: Abbreviature

ACN: Acetonitrile

AGAL1: ALPHA-GALACTOSIDASE 1

AGAL2: ALPHA-GALACTOSIDASE 2

AGAL3: ALPHA-GALACTOSIDASE 3

ALD1: AGD2-LIKE DEFENSE RESPONSE PROTEIN 1

ANOVA: Analysis of Variance

AP1: APETALA 1

AP2: APETALA 2

APL: ALTERED PHLOEM DEVELOPMENT

APSE: B-L-ARABINOPYRANOSIDASE

BFT: BROTHER OF FT AND TFL1

C1B1: CRYPTOCHROME-INTERACTING BASIC-HELIX-LOOP-HELIX 1

CCA1: CIRCADIAN CLOCK ASSOCIATED 1

CDF: CYCLING DOF FACTOR

CF: Candidate Flowering

CF1: 4-tert-butyl-N'-(2-pyridinylmethylene)benzohydrazide

CF11: 3-[(4-chloro-1H-pyrazol-1-yl)methyl]-N-(pentafluorophenyl)benzamide

CF2: N'-[(2-methyl-1H-indol-3-yl)methylene]-2-(2-methylphenoxy)acetohydrazide

CF3: 3-chloro-N'-(2-pyridinylmethylene)-1-benzothiophene-2-carbohydrazide

CF4: 2,4,6-trimethyl-N-(5-methyl-1,3,4-thiadiazol-2-yl)benzenesulfonamide

CF5: 1-(2-chloro-6-fluorobenzyl)-2-methyl-1H-benzimidazole

CO: CONSTANS

Col-0: Columbia-0

COL1: CONSTANS-LIKE 1

CYP707A1: CYTOCHROME P450, FAMILY 707, SUBFAMILY A, POLYPEPTIDE 1

CYP707A2: CYTOCHROME P450, FAMILY 707, SUBFAMILY A, POLYPEPTIDE 2

CYP707A3: CYTOCHROME P450, FAMILY 707, SUBFAMILY A, POLYPEPTIDE 3

Da: Dalton

DE: Drought Response

DEGS: Differentially Expressed Genes

Dexa: Dexamethasone

DIG-ab: Digoxigenin antibodies

DMSO: Dimethyl sulfoxide

EF: Early flowering

ELF3: EARLY FLOWERING 3

ELF4: EARLY FLOWERING 4

ESI: Electrospray ionization

FA: Fatty Acids

FAE: 50% ethanol, 3.7% (v/v) formaldehyde, 5% glacial acetic acid.

FBH4: FLOWERING BHLH 4

FD: FLOWERING LOCUS D

FDR: False Discovery Rate

FKF1: FLAVIN-BINDING, KELCH REPEAT, F- BOX PROTEIN1

FMO1: FLAVIN-DEPENDENT MONOOXYGENASE 1

FT: FLOWERING LOCUS T

FTIP1: FLOWERING LOCUS T INTERACTIN PROTEIN

FUL: FRUITFULL

G1D1A: GA INSENSITIVE DWARF 1A

GA: GIBERELIN

GA2OX7: GIBBERELLIN 2- OXIDASE 2

GALK/GAL1: GALACTOKINASE 1

GC: Gas chromatography

GH27: Glycoside Hydrolase Family 27

GH3.4: GRETCHEN HAGEN 3.4

GI: GIGANTEA

GIPCs: glycosyl-inositol phosphorylceramides

GL: Glycerolipids

gluCER: glycosyl-CERamides

GO: Gene Ontology

GOLS: GALACTINOL SYNTHASE

GOLS1: GALACTINOL SYNTHASE 1

GOLS2: GALACTINOL SYNTHASE 2

GOLS3: GALACTINOL SYNTHASE 3

GOLS4: GALACTINOL SYNTHASE 4

GP: Glycerophospholipids

GR: Rat Glucocorticoid Receptor

GSEA: Gene Set Enrichment Analysis

GUS: β-GLUCURONIDASE

HPLC: High Performance Liquid Chromatography

HSD: Honestly Significant Difference

IAA: Indole-3-acetic acid

IBMCP: Institute of Plant Molecular and Cell Biology

ID: Identification Number

IPP2: Isopentenyl-diphosphate Delta-isomerase II

IS: Internal Standard

JA: Jasmonic Acid

Kan: Kanamycin

KEGG: as Kyoto Encyclopedia of Genes and Genomes

LB: Luria-Bertani

LC: Liquid Chromatography

LD: Long Day

Ler: Landsberg erecta

LF: Late Flowering

LFY: LEAFY

LHY: LATE ELONGATED HYPOCOTYL

LIPEA: Lipid Pathway Enrichment Analysis

LPC: Lysophosphatidylcholine

LUC: LUCIFERASE

LUX: LUX ARRYTHMO

MES: 4-Morpholineethanesulfonic acid

MIOX: MYO-INOSITOL OXYGENASE

MS: Mass Spectrometry

MSTFA: N-Trimethylsilyl-N-methyl trifluoroacetamide

MW: Molecular weight

NASC: Eurasian Arabidopsis Stock Center

ND: Neutral Day

NHP: N-hydroxypipecolic acid

NIST: National Institute of Standards and Technology

ORA: Over Representation Analysis

PA: Phosphatidic Acid

PC: Phosphatidylcholine,

PCA: Principal Component Analysis

PE: Phosphatidylethanolamine

PEBP: Phosphatidyl-Ethanolamine-Binding Protein

PG: Phosphatidylglycerol

PI: Phosphatidylinositol

Pip: Pipecolic acid

PK: Polyketides

PMN: Plant Metabolomic Network

PPKR1: PEP CARBOXYLASE KINASE-RELATED KINASE 1

PR: Prenol Lipids

PRC2: POLYCOMB REPRESSIVE COMPLEX 2

PRR5: PSEUDO RESPONSE REGULATOR 5

PRR7: PSEUDO RESPONSE REGULATOR 7

PRR9: PSEUDO RESPONSE REGULATOR 9

PS: Phosphatidylserine

QA: Quality Assessment

QC: Quality control

QEA: Quantitative enrichment analysis

Q-TOF: Quadrupole time of flight

Ref: Reference

RFOs: Raffinose Family of Oligosaccharides

RLU: Relative Luminescence units

rpm: revolutions per minute

RS1: RAFFINOSE SYNTHASE 1

RS2: RAFFINOSE SYNTHASE 2

RS4: RAFFINOSE SYNTHASE 4

RS5: RAFFINOSE SYNTHASE 5

RS6: RAFFINOSE SYNTHASE 6

RT: Retention Time

RT-qPCR: Reverse Transcription-Quantitative Real-Time Polymerase Chain Reaction.

RVE2: REVEILLE 2

SA: Salicylic Acid

SAM: Shoot Apical Meristem

SAR: Systemic Acquired Resistance

SARD4: SAR DEFICIENT 4

SD: Short day

SDS: Sodium dodecyl sulfate

SEM: Standard Error of the Mean

SL: Saccharolipids

SMZ: SCHLAFMUTZE

SNZ: SCHNARCHZAPFEN

SOC1: SUPPRESSOR OF OVEEXPRESSION OF CO 1

SP: Sphingolipids

SPE: Solid phase extraction

Spec: Spectinomycin

SPL: SQUAMOSA PROMOTER BINDING PROTEIN-LIKE

SPL3: SQUAMOSA PROMOTER BINDING PROTEIN-LIKE 3

SPL4: SQUAMOSA PROMOTER BINDING PROTEIN-LIKE 4

SPL5: SQUAMOSA PROMOTER BINDING PROTEIN-LIKE 5

SPL9: SQUAMOSA PROMOTER BINDING PROTEIN-LIKE 9

sPLS-DA: Sparse Partial Least Square-Discriminant Analysis

SSC: Saline-sodium citrate

ST: sterol lipids

SUC2: SUCROSE-PROTON SYMPORTER 2

T6P: Trehalose-6-phosphate

TBE: Tris 44.5mM (pH 8.0), boric acid 44.5mM, EDTA 1.25mM

TBS: 50 mM Tris-Cl, pH 7.5

TEM1: TEMPRANILLO 1

TEM2: TEMPRANILLO 2

TFL1: TERMINAL FLOWER 1

TIP41: TAP42 INTERACTING PROTEIN OF 41 KDA

TMCS: Trimethylchlorosilane

TOC1: TIMING OF CAB EXPRESSION 1

TOE1: TARGET OF EAT1

TOE2: TARGET OF EAT2

TOE3: TARGET OF EAT3

TOF: Time of flight

TPL: TOPLESS

TPPs: TREHALOSE PHOSPHATE PHOSPHATASES

TPS1: TREHALOSE PHOSPHATE SYNTHASE 1

TSF: TWIN SISTER OF FT

UDP: Uridine diphosphate

UGT73B2: UDP-GLUCOSYL TRANSFERASE 73B2

UGT73B3: UDP-GLUCOSYL TRANSFERASE 73B3

UGT78C1: UDP-GLUCOSYL TRANSFERASE 78C1

UGT89D1: UDP-GLUCOSYL TRANSFERASE 89D1

UHPLC: Ultra High Performance Liquid Chromatography

UPLC: Ultra Performance Liquid Chromatography

UPSC: Umeå Plant Science Centre

UV: Ultraviolet

VAS2: VAS2/GRETCHEN HAGEN 3.17

WES1: WES1/ GRETCHEN HAGEN 3.5 (WES1)

ZT: Zeitgeber time

Δ^1-P2C: Δ^1-piperideine-2-carboxylic acid

OTHERS INDICES

1. FIGURES INDEX

INTRODUCTION

RESULTS

Chapter 1: The search for new candidates to regulate flowering time by chemical genetics.

Chapter 2: Effect of Pipecolic acid on plant development.

Chapter 3: A multi-omics approach to decipher the metabolic changes during the floral transition in Arabidopsis.

DISCUSSION

2. TABLES INDEX

MATERIALS AND METHODS

RESULTS

Chapter 1: The search for new candidates to regulate flowering time by chemical genetics.

Chapter 2: Effect of Pipecolic acid on plant development.

Chapter 3: A multi-omics approach to decipher the metabolic changes during the floral transition in Arabidopsis.